Adverse Outcome Pathway on Substance interaction with the pulmonary resident cell membrane components leading to pulmonary fibrosis

Series on Adverse Outcome Pathways No. 33

AOP No. 173 in the AOP-Wiki platform

Foreword

This Adverse Outcome Pathway (AOP) on Substance interaction with the pulmonary resident cell membrane components leading to pulmonary fibrosis has been developed under the auspices of the OECD AOP Development Programme, overseen by the Extended Advisory Group on Molecular Screening and Toxicogenomics (EAGMST), formerly an advisory group under the Working Party of the National Coordinators for the Test Guidelines Programme (WNT) and the Working Party on Hazard Assessment (WPHA).

The AOP has been reviewed for compliance with the AOP development principles. The scientific review was subsequently conducted by experts nominated by the WNT. This AOP was endorsed by the WNT and the WPHA on 17 October 2023.

Through endorsement of this AOP, the WNT and the WPHA express confidence in the scientific review process that the AOP has undergone and accept the recommendation of the EAGMST that the AOP be disseminated publicly. Endorsement does not necessarily indicate that the AOP is now considered a tool for direct regulatory application.

The OECD's Chemicals and Biotechnology Committee agreed to declassification of this AOP on 30 November 2023.

This document is being published under the responsibility of the OECD's Chemicals and Biotechnology Committee.

The outcome of the scientific review is publicly available at the following link: [scientific review] and the AOP corresponding [discussion page] of the AOP-Wiki includes follow-up comments, revisions and discussions.

Authors:

Sabina Halappanavar[1], Monita Sharma[2], Silvia Solorio-Rodriguez[1], Hakan Wallin[3], Ulla Vogel[3], Kristie Sullivan[4], Amy J. Clippinger[2]

[1]Environmental Health Science and Research Bureau, Health Canada, Ottawa, Canada.

[2]PETA International Science Consortium Ltd., London, United Kingdom.

[3]National Research Centre for the Working Environment, Copenhagen, Denmark.

[4]Physicians Committee for Responsible Medicine, Washington, DC, USA.

Abstract

This AOP describes the qualitative linkages between interactions of substances (e.g. physical, chemical or, receptor-mediated) with the membrane components (e.g. receptors, lipids) of pulmonary (lung) cells leading to pulmonary fibrosis. The terms 'lung' and 'pulmonary' mean the same and are used throughout the AOP description in an interchangeable manner. This AOP represents a pro-fibrotic mechanism that involves a strong inflammatory component. It demonstrates the applicability of the AOP framework for nanotoxicology and describes a mechanism that is common to both chemical and nanomaterial-induced lung fibrosis. Lung fibrosis is a dysregulated or exaggerated tissue repair process. It denotes the presence of scar tissue in the localised alveolar capillary region of the lung where gas exchange occurs; it can be localised or more diffuse involving, bronchi and pleura. It involves the presence of sustained or repeated exposure to a stressor and intricate dynamics between several inflammatory and immune response cells, and the microenvironment of the alveolar-capillary region consisting of both immune and non-immune cells, and the lung interstitium. The interaction between the substance and components of the cellular membrane leading to release of danger signals/alarmins marks the first event, which is a molecular initiating event (MIE; Event 1495) in the process of tissue repair. As a consequence, a myriad of pro-inflammatory mediators are secreted (Key Event (KE) 1; Event 1496) that signal the recruitment of pro-inflammatory cells into the lungs (KE2; Event 1497). The MIE, KE1 and KE2 represent the same functional changes that are collectively known as inflammation. In the presence of continuous stimulus or persistent stressor, non-resolving inflammation and ensuing tissue injury, leads to the alveolar capillary membrane integrity loss (KE3; Event 1498) and activation of adaptive immune response, T helper type 2 cell signalling (KE4;Event 1499), during which anti-inflammatory and pro-repair/fibrotic molecules are secreted. The repair and healing process stimulates fibroblast proliferation and myofibroblast differentiation (KE5;Event 1500), leading to synthesis and accumulation of extracellular matrix or collagen (KE6; Event 68). Excessive collagen deposition culminates in alveolar septa thickening, decrease in total lung volume, and pulmonary fibrosis (Adverse Outcome (AO);Event 1458). At the individual level, pulmonary fibrosis will lead to death, which is the ultimate AO (Mortality, increased); however, it is not discussed in the AOP description. Thus, for this AOP, pulmonary fibrosis is the final AO (Event 1458).

Lung fibrosis is frequently observed in miners and welders exposed to metal dusts, making this AOP relevant to occupational exposures. Other stressors include pharmacological products, fibres, chemicals, microorganisms or overexpression of specific inflammatory mediators. Novel technology-enabled stressors, such as nanomaterials possess properties that promote fibrosis via this mechanism. Lung fibrosis occurs in humans and the key biological events involved are the same as the ones observed in experimental animals. Thus, this AOP is applicable to a broad group of stressors of diverse properties and provides a detailed mechanistic account of the process of lung fibrosis across species.

Acknowledgements: The lead author would like to acknowledge the able assistance of Andrey Boyadzhiev of Health Canada, Ottawa, Ontario, Canada, in formatting the response document and preparing some responses to external reviewers' comments and questions, and Professor Carole Yauk for her expert advice and kind support throughout the development and review process of AOP173. Lastly, the author acknowledges the funding received through the Genomics Research and Development Initiative and the Chemicals Management Plan of Health Canada.

Table of contents

Adverse Outcome Pathway on Substance interaction with the pulmonary resident cell membrane components leading to pulmonary fibrosis **1**

Foreword **2**

Abstract **4**

Background **6**

AOP Development Strategy **8**

Graphical representation **9**

Summary of the AOP **10**

Events 10
Key Event Relationships 10
Prototypical Stressors 11

Overall Assessment of the AOP **13**

Appendix 1 - MIE, KEs and AO **38**

List of MIEs in this AOP 38
List of Key Events in the AOP 46
Event: 1496: Increased, secretion of proinflammatory mediators 46
Event: 1497: Increased, recruitment of inflammatory cells 51
Event: 1498: Loss of alveolar capillary membrane integrity 55
Event: 1499: Increased, activation of T (T) helper (h) type 2 cells 61
Event: 1500: Increased, fibroblast proliferation and myofibroblast differentiation 64
Event: 68: Accumulation, Collagen 69
List of Adverse Outcomes in this AOP 73
Event: 1458: Pulmonary fibrosis 73

Appendix 2 – Key Event Relationships **78**

List of Key Event Relationships in the AOP 78
List of Adjacent Key Event Relationships 78
Relationship: 1702: Interaction with the lung cell membrane leads to Increased proinflammatory mediators 78
Relationship: 1703: Increased proinflammatory mediators leads to Recruitment of inflammatory cells 88
Relationship: 1704: Recruitment of inflammatory cells leads to Loss of alveolar capillary membrane integrity 110
Relationship: 1705: Loss of alveolar capillary membrane integrity leads to Activation of Th2 cells 123
Relationship: 1706: Activation of Th2 cells leads to Increased cellular proliferation and differentiation 131
Relationship: 2652: Increased cellular proliferation and differentiation leads to Accumulation, Collagen 142
Relationship: 1629: Accumulation, Collagen leads to Pulmonary fibrosis 154

Background

There is a high potential for inhalation exposure to toxicants in various occupational settings and polluted environments. Extensive investigation of pulmonary toxicity following inhalation of chemical and particulate stressors have demonstrated that these toxicants mount an exuberant inflammatory response early after exposure that, when unresolved, lays the foundation for later pathologies. Although inflammation is a normal immune reaction of the organism designed to effectively eliminate the invading threat, chronic and unresolved tissue inflammation is detrimental. Unresolved lung inflammation in humans plays a causative role in many debilitating and even lethal adverse health effects, such as decreased lung function, emphysema, fibrosis, and cancer. The various pathways, mechanisms, and biological processes associated with the pulmonary inflammatory process are well characterized in experimental animals and, to a great extent, in humans. Here, a mechanism underlying stressor-induced pulmonary fibrosis that involves a pro-inflammatory component is described.

Pulmonary fibrosis is a chronic lung pathology, which when not treated, results in lethality. It is characterized by the excessive extracellular matrix (ECM) and collagen deposition and restructuring. Numerous respiratory diseases, such as pneumoconiosis, silicosis, asbestosis, bronchiolitis obliterans (BO) (‘popcorn lung’), and chronic beryllium disease have pulmonary fibrosis as a main or secondary symptom. In addition, exposure to pharmaceuticals and environmental contaminants such as bleomycin and arsenic via inhalation, oral or intravenous routes also induces the adverse outcome (AO) of pulmonary fibrosis. Idiopathic pulmonary fibrosis (IPF) is the most common type of pulmonary fibrosis in humans and involves alveolar regions of the lung consisting of type 2 alveolar epithelial cells (AEC2s), type 1 alveolar epithelial cells (AEC1s) and mesenchymal cells. AEC1s are responsible for gas exchange and AEC2s synthesise surfactant. The AEC2s are capable of self-renewal and differentiate to AEC1s regularly during normal tissue maintenance (Barkauskas and Noble, 2014). In pro-fibrotic conditions, AEC2s fail to regenerate AEC1s lost by injury and do not respond normally to epithelial injury, undergoing hyperplasia. As a result, human patients suffering from IPF have dysregulated levels of surfactant proteins normally secreted by AEC2s (Barlo et al.,2009; Phelps et al., 2004). Genetic studies have associated mutations in genes encoding surfactant proteins and the development of a familial type of lung fibrosis. Furthermore, immunohistochemical staining of human IPF lung slices shows AEC death as well as proliferation adjacent to fibrotic foci (Uhal et al., 1998). AEC2s are hyperplastic and are located on top of the fibrotic lesions in the lung in human specimens (Katzenstein and Myers, 1998). In animal models of bleomycin-induced pulmonary fibrosis, abnormal AEC2s are incapable of protecting the basement membrane destroyed by cell death, leading to aberrant repair and deposition of ECM, resulting in fibrosis (Rock et al., 2011). Targeted removal of AEC2s in mouse lungs results in full manifestation of the fibrotic disease (Sisson et al., 2010). In certain infectious conditions, epithelial cell stress and dysfunction leading to inefficient repair capacity or transcriptional reprogramming of epithelial cells to secrete pro-fibrotic and pro-inflammatory factors leads to lung fibrosis (Lawson et al., 2008; Lawson et al., 2011). Mesenchymal cells are the other main type of cell, which contribute to fibrosis development. The dysregulated proliferation of fibroblasts and myofibroblast differentiation leading to excessive ECM deposition in the fibrotic scar is the result of disrupted cross-talk between epithelial and mesenchymal cells (Barkauskas and Noble 2014). Myofibroblasts exhibiting contractile properties of smooth muscle cells and expressing Alpha-smooth muscle actin (α-SMA) and vimentin, are the types of mesenchymal cells that are most commonly associated with excessive collagen secretion in pro-fibrotic phenotypes (Todd et al., 2012). Myofibroblasts can arise mainly from

differentiation of tissue resident fibroblasts, translocation of bone marrow (BM) derived fibrocytes into the lung, or from epithelial-to-mesenchymal transformation (EMT; a type of trans-differentiation) (Hung, 2020; Todd et al., 2012). These cells are critical to the normal process of wound healing, and are the main cells contributing to collagen deposition in both normal wear-and-tear repair processes and in disease promoting conditions. Following successful wound healing, myofibroblasts de-differentiate and disappear (Friedman, 2012). Myofibroblasts persistence is suggested to play a key role in progressive pulmonary fibrosis in humans. There is evidence for both EMT derived myofibroblasts and BM derived fibrocytes in human pulmonary fibrotic conditions. Air epithelial biopsies from human patients suffering from BO following lung transplant show significantly increased staining for mesenchymal markers (Vimentin and α-SMA), decreased staining for e-cadherin, and co-localization of epithelial and mesenchymal markers as compared to stable patients (Borthwick et al., 2009). With respect to BM derived fibrocytes, these cells have been proposed as an indicator for poor prognosis in human IPF patients, and research has shown that the amount of fibrocytes in the human IPF lung correlates with the amount of fibroblastic foci (Andersson-Sjöland et al., 2008; Moeller et al., 2009). Additional cell types involved in fibrotic process include endothelial cells and immune cells such as macrophages, neutrophils, and T helper (Th) cells. Endothelial cells contribute to the fibrotic process through EMT, as evidenced in bleomycin model systems in which endothelial cells in fibrotic conditions take on the characteristics of myofibroblasts (Kato et al., 2018). Macrophages present in the alveolar space as well as macrophages recruited to the lung during the fibrotic process also contribute to the inflammatory environment and potentiate the AO of pulmonary fibrosis. Direct interaction of fibrotic stressors, such as multi-walled carbon nanotubes (MWCNTs), silica, and asbestos, with the macrophage cell membrane can occur through scavenger receptors as well as through receptors such as Macrophage receptor with collagenous structure (MARCO) (Li and Cao, 2018; Murphy et al., 2015). This can induce macrophage cell injury through frustrated or incomplete phagocytosis which leads to the production of alarmins such as Interleukin (IL)-1β and reactive oxygen species (ROS), and profibrotic mediators such as Tumour necrosis factor alpha (TNF-α), Transforming growth factor beta (TGF-β), and Platelet derived growth factor (PDGF) (Dong and Ma, 2016; Li and Cao, 2018). The injured resident macrophages contribute to the initial acute phase pro-inflammatory response leading to recruitment of additional immune cells to the lung. Depending on the fibrotic stressor, different populations of immune cells can be initially recruited to the site of action. The recruitment of neutrophils into the lung space potentiates the inflammatory response and tissue damage. Furthermore, in conditions of acute lung injury, which can precede the development of a fibrotic phenotype, neutrophil recruitment to the lung through trans-epithelial migration can induce the formation of lesions in the epithelium and contribute to the loss of alveolar capillary membrane (ACM) integrity (Zemans et al., 2009). Finally, Th cells recruited to the lung potentiate the inflammatory environment, and through the induction of a Th type 2 (Th2) response, stimulate the proliferation of fibroblasts and differentiation of myofibroblasts driving the development of a fibrotic phenotype (Shao et al., 2008; Wynn, 2004).

Although this AOP is applicable to a broad group of stressors, the AOP was specifically assembled keeping in mind, a novel class of engineered nanomaterials (NMs) exhibiting sophisticated properties that have been shown to induce lung fibrosis via this mechanism. Specifically, nanomaterial properties such as aspect ratio, tube/fiber rigidity, crystallinity and persistence are suggested to play a role in the induction of pulmonary fibrosis. Thus, it demonstrates the applicability of the AOP framework to nanotoxicology.

Given the fundamental role of inflammation in organ homeostasis, well characterized AOPs targeting the pathological outcomes of unregulated inflammatory responses are

important and will guide the development of appropriate assays to measure the key events that are predictive of inflammation-mediated chronic health impacts, and aid in screening a large array of inhalation toxicants that are inflammogenic, for their potential to induce lung diseases.

AOP Development Strategy

The development of AOP173 was initiated in 2014, mostly focusing on the available literature. Since then, the first representation of the AOP and its components including KEs have undergone several changes, mainly because of the results of the specific KE validation experiments conducted in the primary author's laboratory and the evolving literature. The KE titles were also changed to keep the KE ontology consistent across all AOPs, as well as to allow their use by the other AOP developers.

The AOP173 is written in a narrative review fashion, as the quantitative literature supporting all KERs is limited. Also, more targeted experiments are planned and being conducted currently to validate the AOP.

Graphical representation

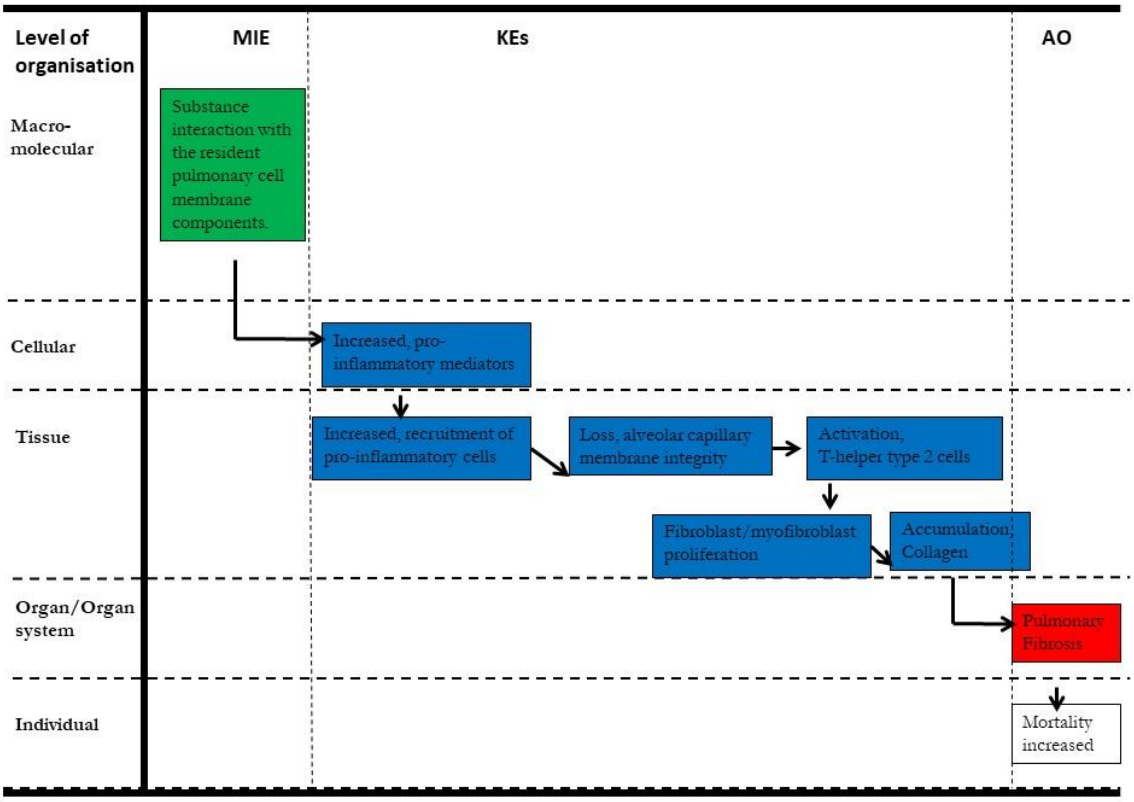

Summary of the AOP

Events

Molecular Initiating Events (MIE), Key Events (KE), Adverse Outcomes (AO)

Type	Event ID	Title	Short name
MIE	1495	Substance interaction with the lung resident cell membrane components	Interaction with the lung cell membrane
KE	1496	Increased, secretion of proinflammatory mediators	Increased proinflammatory mediators
KE	1497	Increased, recruitment of inflammatory cells	Recruitment of inflammatory cells
KE	1498	Loss of alveolar capillary membrane integrity	Loss of alveolar capillary membrane integrity
KE	1499	Increased, activation of T (T) helper (h) type 2 cells	Activation of Th2 cells
KE	1500	Increased, fibroblast proliferation and myofibroblast differentiation	Increased cellular proliferation and differentiation
KE	68	Accumulation, Collagen	Accumulation, Collagen
AO	1458	Pulmonary fibrosis	Pulmonary fibrosis

Key Event Relationships

Upstream Event	Relationship Type	Downstream Event	Evidence	Quantitative Understanding
Substance interaction with the lung resident cell membrane components	adjacent	Increased, secretion of proinflammatory mediators	Moderate	Moderate
Increased, secretion of proinflammatory mediators	adjacent	Increased, recruitment of inflammatory cells	Moderate	Low
Increased, recruitment of inflammatory cells	adjacent	Loss of alveolar capillary membrane integrity	Moderate	Moderate
Loss of alveolar capillary membrane integrity	adjacent	Increased, activation of T (T) helper (h) type 2 cells	Moderate	Low
Increased, activation of T (T) helper (h) type 2 cells	adjacent	Increased, fibroblast proliferation and myofibroblast differentiation	High	Low
Increased, fibroblast proliferation and myofibroblast differentiation	adjacent	Accumulation, Collagen	High	High
Accumulation, Collagen	adjacent	Pulmonary fibrosis	High	Low

Prototypical Stressors

Name	Evidence
Bleomycin	High
Carbon nanotubes, Multi-walled carbon nanotubes, single-walled carbon nanotubes, carbon nanofibres	High

Bleomycin

Bleomycin is a potent anti-tumour drug, routinely used for treating various types of human cancers (Umezawa et al., 1967; Adamson, 1976). Lung injury and lung fibrosis are the major adverse effects of this drug in humans (Hay J et al., 1991). Bleomycin is shown to induce lung fibrosis in experimental animals - in dogs (Fleischman et al., 1971), mice (Adamson IY and Bowden DH, 1974), hamsters (Snider GL et al., 1978) and is widely used as a model chemical to study the mechanisms of fibrosis in humans (reviewed in **Moeller** et al., **2008;** Gilhodes et al., 2017).

1. Adamson, I. (1976). Pulmonary Toxicity of Bleomycin. Environmental Health Perspectives, 16, p.119.
2. Adamson, IYR. and Bowden, DH. (1974). The Pathogenesis of Bleomycin-Induced Pulmonary Fibrosis in Mice. *The American Journal of Pathology*. 77(2), pp185-198.
3. Fleischman, R., Baker, J., Thompson, G., Schaeppi, U., Illievski, V., Cooney, D. and Davis, R. (1971). Bleomycin-induced interstitial pneumonia in dogs. Thorax, 26(6), pp.675-682.
4. Gilhodes, J., Julé, Y., Kreuz, S., Stierstorfer, B., Stiller, D. and Wollin, L. (2017). Quantification of Pulmonary Fibrosis in a Bleomycin Mouse Model Using Automated Histological Image Analysis. PLOS ONE, 12(1), p.e0170561.
5. Hay, J., Shahzeidi, S. and Laurent, G. (1991). Mechanisms of bleomycin-induced lung damage. Archives of Toxicology, 65(2), pp.81-94.
6. Moeller, A., Ask, K., Warburton, D., Gauldie, J. and Kolb, M. (2008). The bleomycin animal model: A useful tool to investigate treatment options for idiopathic pulmonary fibrosis?. The International Journal of Biochemistry & Cell Biology, 40(3), pp.362-382.
7. Snider GL., Celli, BR., Goldstein, RH., O'Brien, JJ. and Lucey, EC. (1978). Chronic interstitial pulmonary fibrosis produced in hamsters by endotracheal bleomycin. Lung volumes, volume-pressure relations, carbon monoxide uptake, and arterial blood gas studied. *Am Rev Respir Dis.* Feb; 117(2). pp289-97.
8. Umezawa, H., Ishizuka, M., Maeda, K. and Takeuchi, T. (1967). Studies on bleomycin. Cancer, 20(5), pp.891-895.

Carbon nanotubes, Multi-walled carbon nanotubes, single-walled carbon nanotubes, carbon nanofibres

CNTs are high aspect ratio materials and cause lung fibrosis in experimental animals (Muller et al., 2005; Porter DW et al., 2010). In an intelligence bulletin published by NIOSH on ‘Occupational exposure to carbon nanotubes and nanofibers’, NIOSH reviewed 54 individual animal studies investigating the pulmonary toxicity induced by CNTs and reported that half of those studies consistently showed lung fibrosis (NIOSH bulletin, 2013). Multiwalled carbon nanotubes induce lung fibrosis in mice (Nikota et al., 2017; Rahman et al., 2017). However, the evidence is inconsistent and the occurrence of fibrotic

pathology is influenced by the specific physical-chemical properties of CNTs (length, rigidity), their dispersion in exposure vehicle, and the mode of exposure.

1. Muller, J., Huaux, F., Moreau, N., Misson, P., Heilier, J., Delos, M., Arras, M., Fonseca, A., Nagy, J. and Lison, D. (2005). Respiratory toxicity of multi-wall carbon nanotubes. Toxicology and Applied Pharmacology, 207(3), pp.221-231.
2. NIOSH (2013). Occupational exposure to carbon nanotubes and nanofibers: current intelligence bulletin 65.
3. Porter, D., Hubbs, A., Mercer, R., Wu, N., Wolfarth, M., Sriram, K., Leonard, S., Battelli, L., Schwegler-Berry, D. and Friend, S. (2010). Mouse pulmonary dose- and time course-responses induced by exposure to multi-walled carbon nanotubes. Toxicology, 269(2-3), pp.136-147.
4. Nikota, J., Banville, A., Goodwin, L., Wu, D., Williams, A., Yauk, C., Wallin, H., Vogel, U. and Halappanavar, S. (2017). Stat-6 signaling pathway and not Interleukin-1 mediates multi-walled carbon nanotube-induced lung fibrosis in mice: insights from an adverse outcome pathway framework. *Particle and Fibre Toxicology*, 14(1).
5. Rahman L, Jacobsen NR, Aziz SA, Wu D, Williams A, Yauk CL, White P, Wallin H, Vogel U, Halappanavar S. Multi-walled carbon nanotube-induced genotoxic, inflammatory and pro-fibrotic responses in mice: Investigating the mechanisms of pulmonary carcinogenesis. Mutat Res. 2017 Nov;823:28-44.

Overall Assessment of the AOP

Pulmonary fibrosis is the thickening and scarring of lung tissue, caused by excessive deposition of collagen/ECM. The most common fibrotic disease of the lung in humans is IPF, a complex, progressive disease of unknown etiology with often poor prognosis. Pulmonary fibrosis in humans is also observed following exposure to pharmacological agents such as bleomycin, following inhalation of silica, asbestos, cigarette smoke (CS), coal dust and following exposure to microbials and allergens. Regardless of the etiology, lung fibrosis in humans is characterized by the presence of inflammatory lesions, excessive ECM/collagen deposition, and reduced lung volume and function. Mechanistically, using animals, it has been shown that key biological events that play a critical role in the onset and progression of the disease are similar in humans and animals. The main differences are limited to anatomical and physiological aspects of lung and its functions.

Some other considerations of relevance to this AOP:

This AOP represents a fibrotic mechanism that involves a strong inflammatory component. Exposure to pro-fibrotic stressors such as, bleomycin, silica, asbestos, carbon nanotubes (CNTs), radiation or models of cytokine overexpression involve a profound inflammatory response. IPF in humans is more commonly observed in male subjects. A study in mice showed that male mice developed lung fibrosis more readily following exposure to bleomycin compared to female mice and that age is a risk factor, with aged male mice showing exuberant fibrosis (Redente et al., 2011). Scar formation is reduced in fetal wounds (Yates et al., 2012). Asbestosis and silicosis, (two types of fibrotic disease) are clinically manifested in aged humans. Thus, the AOP presented here is applicable to lung fibrosis observed in adults predominantly.

Different animal species have been used to study the pathology of fibrotic disease; with mice being the most common and rats the second most used. Australian sheep, horse, dogs, cats, donkeys, pigs and other animals have been studied to investigate different types of fibrosis. There are some limitations, however, in these animal systems with respect to modelling human pulmonary fibrosis. The most commonly used model, the bleomycin mouse model, presents a rapidly developing fibrotic phenotype which undergoes at least partial resolution following 28 days (Tashiro et al., 2017). Higher order organisms, like dogs, cats, and horses offer a chance to examine naturally occurring pulmonary fibrosis, with closer resemblance to human IPF, with a natural cough reflex (Williams and Roman, 2015). However, inherent limitations in these models, such as their outbred nature and lack of systematic characterization (Williams and Roman, 2015) make them poor candidates for routine fibrosis research. Regardless of the species or the type of fibrosis investigated, the key characteristic events that define the disease process are the same with few species-specific anatomical, physiological and histological differences. Thus, cross-species applicability for this AOP is strong.

Domain of Applicability

Life Stage Applicability

Life stage	Evidence
Adult	High

Taxonomic Applicability

Term	Scientific Term	Evidence	Link
human	Homo sapiens	High	NCBI
mouse	Mus musculus	High	NCBI
rat	Rattus norvegicus	High	NCBI

Sex Applicability

Sex	Evidence
Unspecific	High

Sex/Gender and Age:

IPF in humans is more commonly observed in male subjects. Male mice develop lung fibrosis more readily following exposure to bleomycin compared to female mice and that age is a risk factor, with aged male mice showing exuberant fibrosis (Redente et al., 2011). Scar formation is reduced in fetal wounds (Yates et al., 2012). Asbestosis and silicosis, forms of fibrotic disease are clinically manifested in aged humans. This may be due to the fact that in humans, the disease progression is rather slow and takes time to manifest. Thus, the AOP presented here is applicable to lung fibrosis observed in adult males predominantly.

Taxonomy:

Different animal species have been used to study the pathology of fibrotic disease; with mice being the most common and rats the second most used. Australian sheep, horse, dogs, cats, donkeys, pigs and other animals have been studied to investigate different types of fibrosis. There are some limitations, however, in these animal systems with respect to modelling human pulmonary fibrosis. The most commonly used model, the bleomycin mouse model, presents a rapidly developing fibrotic phenotype which undergoes at least partial resolution following 28 days post-exposure (Tashiro et al., 2017). Higher order organisms, like dogs, cats, and horses offer a chance to examine naturally occurring pulmonary fibrosis, with closer resemblance to human IPF in animals with a natural cough reflex (Williams and Roman, 2015). However, inherent limitations in these models, such as their outbred nature and lack of systematic characterization (Williams and Roman, 2015) make them poor candidates for routine fibrosis research. Regardless of the species or the type of fibrosis investigated, the key characteristic events that define the disease process are the same with few species-specific anatomical, physiological and histological differences. Thus, cross-species applicability for this AOP is strong.

Types of Stressors:

Persistent and soluble stressors can induce fibrotic pathologies in humans (as well as in model animals) in concordance with the AOP presented. Asbestos exposure in humans has long been known to induce pulmonary fibrosis (asbestosis) due to chronic inflammation induced from persistent fibres deposited within the lung (Kamp and Weitzman 1997). Similarly, human exposure to silica (crystalline silica dust) leads to the development of silicosis in concordance with the AOP presented (Ding *et al.*, 2002). Furthermore, the soluble chemotherapeutic compound bleomycin has long been known to induce pulmonary fibrosis in humans (in line with this AOP) as a side effect of intravenous administration (Froudarakis et al., 2013). In addition to these model stressors, exposure to various metals including uranium, arsenic, cadmium, and soluble copper can lead to fibrotic outcomes in humans (Assad et al., 2019). Occupational exposure to cobalt can induce interstitial lung disease in humans, which can progress to fibrotic outcomes (Adams et al., 2017). In male

mice exposed via inhalation to cadmium oxide nanoparticles (NPs), increases in the pro-fibrotic and pro-inflammatory mediators IL-1β, TNF-α , and Interferon gamma (IFN-γ) were noted one day post-exposure, with accompanying pulmonary inflammation (Blum et al., 2014). In another study, intratracheal instillation of cadmium chloride ($CdCl_2$) in mice induced peribronchiolar fibrosis through activation of myofibroblasts via the Suppressor of mothers against decapentaplegic **(**SMAD) signalling (Li et al., 2017). As with the aforementioned cadmium NPs, murine animals exhibit pronounced acute inflammation and immune cell infiltration after pulmonary exposure to copper oxide NPs (Gosens et al., 2016), which can progress to a fibrotic phenotype in some model systems after 28 days with marked increases of TGF-β1 detected in the bronchoalveolar lavage fluid (BALF), activation of myofibroblasts, and pronounced deposition of ECM (Lai et al., 2018). In mice, intratracheal instillation of cobalt NPs results in pronounced infiltration of neutrophils and macrophages into the alveolar and interstitial space, and increased amounts of C-X-C motif chemokine ligand (CXCL)1 in the BALF 1-7 days post-exposure; pronounced pulmonary fibrosis was detected at 4 months post-exposure marked by increased collagen deposition and bronchiolization of the alveolar epithelium (Wan et al., 2017).

Essentiality of the Key Events

The essentiality of the MIE; Event 1495 was rated as moderate. Molecular interaction is an essential step but it is dynamic in nature. The interaction can be specific, non-specific or both depending on the stressor. Also, NMs, one type of stressors may adopt a molecular corona in biological environments, which can mediate cellular interactions. Efforts are currently made to develop each individual interaction described in MIE as group MIEs and the associated KERs.

The essentiality of KE1; Event 1496 and KE2; Event 1497 was rated as moderate, due to the redundant nature of the inflammatory response and the inherent challenges in abrogating this response without inducing another pathology in the model system.

For KE3; Event 1498, the essentiality was also listed as moderate, due to the fact that attenuation or abrogation of this response isn't practical, and as such the supporting evidence is indirect.

For KE4; Event 1499 and KE6; Event 68, the essentiality was rated as high due to the plethora of experimental evidence showing that modulation of these responses modifies the AO and downstream KEs. For additional information, please consult the Evidence Assessment Call Table below.

Weight of Evidence Summary

Concordance of Dose-Response Relationships:

The AOP presented here is qualitative. There is some evidence on dose-response relationships; however, dose-response relationships for each individual KE are not available. In Labib et al., 2016, Benchmark Dose (BMD) analysis of MWCNT-induced gene expression changes in lungs of mice and canonical pathways associated with each of the KEs identified in this AOP was conducted and the resulting BMD values were correlated with BMD values derived for the apical endpoints that measured histologically manifested fibrotic lesions in rodents (National Institute for Occupational Safety and Health, 2013). The study showed that low doses of MWCNTs induce early KEs of inflammation and immune response at the acute post-exposure timepoints, and histological manifestation of fibrosis required higher MWCNT doses and was only evident at the later

timepoints. Similarly, in another study, the meta-analyses of transcriptomics data gathered from mouse lungs (over 2000 microarrays) exposed individually to a variety of pro-fibrotic agents showed that the gene expression profiles from the high dose MWCNT-exposed samples collected at sub-chronic timepoints were strongly associated with the Th2 response signalling observed in mouse fibrotic disease models compared to the low dose early timepoint MWCNT samples (Nikota et al., 2016). These studies showed temporal and dose-response relationships between KEs.

In another study, pharyngeal aspiration of 10, 20, 40, or 80 µg/mouse MWCNTs induced lung fibrosis in a dose-dependent manner, which became apparent as early as 7 days post-exposure at 40 µg/mouse dose and persisted up to 56 days post-exposure (Porter et al., 2010). Pharyngeal aspiration of 10, 20, 40, or 80 µg/mouse MWCNTs induced significant alveolar septa thickness over time (1, 7, 28, and 56 days post-exposure) in 40 and 80 µg dose groups (Mercer et al., 2011). Similarly, inhalation of MWCNTs (10 mg/m^3, 5h/day) for 2, 4, 8, or 12 days showed dose-dependent lung inflammation and lung injury with the development of lung fibrosis in mice (Porter et al., 2013). Lung inflammation and fibrosis were observed in mice intratracheally instilled with 162 µg/mouse MWCNTs at 28 days post-exposure (Nikota et al., 2017). The above studies involving CNTs showed elevated levels of pro-inflammatory mediators, pro-inflammatory cells and cytotoxicity in BALF.

Strength, Consistency, and Specificity of Association of AO and Initiating Event:

This AOP describes a non-specific MIE. Typically, in an experimental setting, the MIE itself is not assessed. Rather, the outcomes of MIE engagement or MIE trigger are assessed. Depending on the type of stressor and its physical-chemical property, the type of interactions between the stressor and the lung resident cells differ. High aspect ratio fibres such as asbestos and CNTs induce frustrated phagocytosis, acute cell injury (Boyles et al., 2015; Brown et al., 2007; Dörger et al., 2001; Kim et al., 2010; Poland et al., 2008), leading to inflammation, immune responses and fibrosis. Asbestos and silica crystals engage scavenger receptors present on the macrophages (Murthy et al., 2015), resulting in acute cell injury and inflammatory cascade, leading eventually to the AO. Bleomycin binds high affinity bleomycin binding sites present on rat alveolar macrophage surfaces, leading to macrophage activation (Denholm and Phan, 1990). Asbestos fibres also bind directly to cellular macromolecules including proteins and membrane lipids, which is influenced by their surface properties such as surface charge (reviewed in Agency for Toxic Substances and Disease Registry 2001). These studies demonstrate the types of interactions between cells and the pro-fibrotic stressors, which are often not measured in animal or cell culture experiments. Instead, the consequences or outcomes of triggering the MIE are measured, which are the release of danger associated molecular patterns (DAMPs) or alarmins from cells.

The alarmin High mobility group box 1 (HMGB1) is released from damaged or necrotic cells in cell culture models and in animals following exposure to asbestos and is involved in the inflammatory events elicited by asbestos (Yang et al., 2010), which plays a critical role in asbestosis. CNTs interact with HMGB1-Receptor for advanced glycation end-products (RAGE), which is implicated in pro-inflammatory and genotoxic effects of CNTs (Hiraku et al., 2016). Mechanical stress and membrane damage following cellular uptake of long and stiff CNTs by lysosomes results in cell injury and consequent adverse effects (Zhu, et al., 2016). CNT-induced inflammatory response *in vitro* is mediated by IL-1, absence of which negatively impacts gap junctional intercellular communication (Arnoldussen et al., 2016). The levels of IL-1α are increased in BALF of mice immediately after exposure to MWCNT doses that induce fibrosis (Nikota et al., 2017).

Although there is enough empirical evidence to suggest the occurrence of the MIE; Event 1495 following exposure to pro-fibrogenic substances, there is incongruence in supporting

its essentiality to the eventual AO. The inconsistency could be due to the fact that early defence mechanisms involving DAMPs is fundamental for the organism's survival, which may necessitate multifaceted signalling pathways. As a result, inhibition of a single biological pathway of the innate immune response may not be sufficient to completely abrogate the lung fibrotic response. For example, MWCNTs induce IL-1α secretion in BALF of mice (Nikota et al., 2017) and thus, IL-1α mediated signalling is involved in MWCNT-induced lung inflammation and fibrosis (Rydman et al., 2015). Inhibition of IL-1α signalling alone does not alter the MWCNT-induced fibrotic response in mice (Nikota et al., 2017). This study further showed that simultaneous inhibition of both acute inflammatory events (KE1; Event 1496 and KE2; Event 1497) and Th2–mediated signalling (KE4; Event 1499) is required to suppress lung fibrosis induced by MWCNTs (Nikota et al., 2017). Disengagement between innate immune responses (MIE; Event 1495, KE1; Event 1496 and KE2; Event 1497) and lung fibrosis is shown in mice following exposure to silica (Re et al., 2014). In this study, the role of innate immune responses in lung fibrosis were characterized in 11 separate knockout (KO) mouse models lacking individual members of the IL-1 family. The study supported the earlier hypothesis of Nikota et al., 2017 that inhibition of a single pathway may not be sufficient to attenuate the fibrotic response. On the contrary, IL-1α and IL-1 receptor (IL1-R)1 mediated signalling are shown to be involved in bleomycin-induced lung inflammation and fibrosis; inhibition of IL1-R1 signalling attenuated the bleomycin pathology (Gasse et al, 2007).

Biological Plausibility, Coherence, and Consistency of the Experimental Evidence:

As described above, there is significant evidence to support the occurrence of the MIE and individual KEs, and thus, evidence supporting the KEs involved in this AOP is strong. However, there is inconsistency in empirical evidence supporting the KERs. Again, this may be due to the redundancy in pathways involved in the early immune responses to injury and repair. Despite the incongruences, AOP presented is coherent and logical.

Alternative Mechanisms:

The AOP as presented is the most agreed upon sequence of biological events occurring in the process of lung fibrosis that involves robust inflammation following exposure to a variety of stressors of different physical-chemical properties. However, in a recent study, using ToxCast data, a different MIE that involves inhibition of Peroxisome proliferator-activated receptor gamma (PPAR-γ) resulting in lung fibrosis was proposed (Jeong et al., 2019). This alternate AOP for fibrosis placed activation of TGF-β1 upstream of inflammatory events (KE2; Event 1497, KE3; Event 1498), which is contrary to its perceived role in downstream events leading to fibroblast proliferation and differentiation, and ECM deposition. The stressors identified in this study were also different, suggesting the PPAR-γ inhibition may be selective to a group of chemicals. The other alternative mechanisms may involve bypassing of the initial inflammatory KEs that directly trigger activation of fibroblast proliferation and differentiation leading to ECM deposition. For example, overexpression of TGF-β1 can promote excessive ECM deposition and fibrosis in rodents independent of inflammation (Hardie et al., 2004)

Further mechanisms may involve the targeted inhibition of receptor tyrosine kinases by compounds like Gefitinib, Imatinib, and Sorafenib, as well as some monoclonal antibodies which affect receptors for growth factors like Platelet derived growth factor (PDGF), Endothelial growth factor (EGF), and Vascular endothelial growth factor (VEGF). This is thought to directly impair the regenerative capacity of lung epithelial cells (MIE; Event 1495 to KE3; Event 1497), resulting in an aberrant wound healing response (Li et al., 2018). Finally, one more alternative mechanism involves pulmonary fibrosis in the context of BO. In this condition, the fibrotic phenotype is brochiolocentric and not alveolocentric – with the main insult involving the bronchiolar epithelium and an inability of the basal

cells to replace lost bronchio epithelial cells. Stressors, such as soluble diacetyl used in popcorn flavoring and e-cigarette vape liquids, can cause BO in humans. A recent human case study of a Canadian youth admitted to hospital with BO following vaping flavored liquid containing diacetyl, as well as tetrahydrocannabinol, shows septal thickening, type II pneumocyte hyperplasia, immune cell infiltration and myofibroblast proliferation & incorporation into pulmonary septa (Landmann et al., 2019). Pulmonary exposures in murine model systems indicate that diacetyl induces pronounced damage to the airway epithelium, and that repair processes result in a compositionally different epithelium (Reviewed in Brass and Palmer, 2017). In a study using rat models, inhalation of 200 ppm of diacetyl resulted in bronchiolar fibrosis, with chronic inflammation accompanying the fibrotic outcomes (Morgan et al., 2016).

Evidence Assessment Summary:

The MIE; Event 1495 and KE1; Event 1496 – KE2; Event 1497 occur in sequence, however most *in vivo* and *in vitro* experiments are not designed to measure these events separately. This is an area of focus for future pulmonary fibrosis research.

Support for Essentiality of KEs		
MIE; Event 1495: Interaction with the lung resident cell membrane components	Persistent fibres like CNTs and asbestos are known to induce frustrated or incomplete phagocytosis in resident lung cells following respiratory exposure. Particles such as silica, as well as asbestos fibers engage scavenger receptors on the surface of macrophages leading to activation and inflammation. The soluble pro-fibrotic compound bleomycin binds to as-of-yet uncharacterised sites on macrophages, leading to similar activation.	Essentiality: Moderate. While the specific receptors involved vary depending on the stressor, and there is evidence of compensation in the context of KO models, over 20 years of research has shown that interaction between the fibrotic stressor and the resident lung cells is crucial for downstream responses. (Behzadi et al., 2017; Denholm and Phan 1990; Mossman and Churg 1998).
KE 1; Event 1496: Increased, secretion of proinflammatory mediators	Injured and activated resident lung cells release pro-inflammatory and fibrotic mediators, such as cytokines, chemokines, growth factors and ROS, into the surrounding environment.	Essentiality: Moderate. It is accepted that one of the main mechanisms underlying pulmonary fibrosis involves a profound inflammatory component. This has been shown in animal models exposed to fibrotic stressors such as bleomycin, MWCNTs, silica, and asbestos. The exact nature of the secreted mediators, and the essentiality of specific mediators requires further research. (Park and Im, 2019; Rabolli et al., 2014; Rahman et al., 2017).
KE 2; Event 1497: Increased, recruitment of inflammatory cells	Inflammatory cells migrate into the lung according to the pro-inflammatory stimuli released.	Essentiality: High. The migration of inflammatory immune cells relies upon secretion of chemotactic stimuli in response to a stressor. KO models have shown reduced recruitment of immune cells to the lung in response to fibrotic stressors such as bleomycin. However, compensation has been noted due to the redundant nature of these molecules. (Gasse et al., 2007; Girtsman et al., 2014; Rabolli et al., 2014)
KE 3; Event 1498: Loss of alveolar capillary membrane integrity	Significant alveolar damage from the inflammatory environment (including chronic inflammation and oxidative stress) results in the loss of ACM integrity.	Essentiality: Moderate. While it is generally recognized that damage to the ACM is integral to the development of fibrosis, evidence from KO models is lacking. Indirect evidence using bleomcyin has shown that animals deficient in Nuclear factor erythroid 2-related factor 2 (Nrf2),and

		therefore presenting a weakened antioxidant response, have higher levels of ACM injury and more pronounced fibrosis as compared to Nrf2 competent mice. This was assessed by proxy, using lactate dehydrogenase release into the BALF and the presence of pulmonary injury markers as a proxy for ACM injury. (Cho et al., 2004; Kikuchi et al., 2010)
KE 4; Event 1499: Increased, activation of T (T) helper (h) type 2 cells	Th cells present in, and recruited to the lung environment commit to Th2 differentiation, which then release cytokines like IL-4, IL-5, and IL-13 and potentiate a Th2 driven response.	Essentiality: High. Induction of a Th2 response stimulates fibroblast proliferation and pulmonary fibrogenesis. Overexpression of Th2 type cytokine IL-13 stimulates pulmonary fibrosis in the absence of external stressors. IL-13 can directly activate TGF-○ and initiates fibroblast proliferation and differentiation in pulmonary fibrosis. In mice deficient in Signal transducer and activator of transcription 6 (STAT6) with reduced Th2 response, MWCNT-induced fibrotic response involving fibroblast proliferation, and eventual formation of fibrotic lesions, were reduced. There is some inconsistency, as IL-4 deficient mice had a lower fibrotic response compared to wild-type after bleomycin treatment, however with higher rate of mortality. This highlights that the timing of the Th2 response is important for the manifestation of fibrosis. (Huaux et al., 2003; Lee et al., 2001; Nikota et al., 2017; Sempowski et al., 1994; Zhu et al., 1999)
KE 5; Event 1500: Increased, fibroblast proliferation and myofibroblast differentiation	Fibroblasts originally present in the lung, and recruited to the lung, or which transdifferentiate from epithelial and endothelial cells proliferate and undergo differentiation into a collagen secreting myofibroblast phenotype which expresses a-SMA. This is the main effector cell responsible for secretion of ECM components in pulmonary fibrosis, and represents a nexus KE.	Essentiality: High. The proliferation of fibroblasts and differentiation into myofibroblasts is integral to the development of pulmonary fibrosis. Inhibition or attenuation of fibroblast proliferation and differentiation using TGF-Tantagonism attenuates fibrosis in bleomycin mice models. Targeted inhibition of the Wingless/integrated T(Wnt/ₛ-catenin pathway inhibited myofibroblasts transition and reduced the overall fibrotic phenotype. (Cao et al., 2018; Chen et al., 2013; Guan et al., 2016; Kuhn and McDonald, 1991)
KE 6; Event 68: Accumulation, collagen	The balance between ECM synthesis and destruction is disrupted, with a sustained increase in the deposition of ECM bearing compositional differences as compared to the native matrix.	Essentiality: High. A sustained imbalance between ECM synthesis and destruction is a prerequisite for the development of pulmonary fibrosis, and as such this KE is essential to the AO. (Bateman et al., 1981; McKleroy et al., 2013)
AO; Event 1458: Pulmonary fibrosis	Destruction of lung architecture and alveolar capillaries due to increased and aberrant deposition of ECM in the context of prolonged inflammation results in pulmonary fibrosis.	Essentiality: N/A. This is the AO of this AOP, and therefore, is essential.
Support for Biological Plausibility of KERs		
MIE --> KE1; Relationship 1702	Injury and activation resulting from the interaction of pro-fibrotic stressors with the membranes of resident lung cells results in the	Biological plausibility: High. There is a mechanistic relationship between the MIE and KE1 which has been evidenced

	secretion of pro-inflammatory cytokines, chemokines, growth factors, and ROS from the resident epithelial or immune cell.	in a number of both *in vitro* and *in vivo* model systems in response to stressors such as asbestos, silica, bleomycin, CNTs, and metal oxide NPs. (Behzadi et al., 2017; Denholm and Phan 1990; Mossman and Churg 1998)
KE1 --> KE2; Relationship 1703	The secreted pro-inflammatory and pro-fibrotic mediators induce chemotactic recruitment of immune cells to the lung, in a signal-specific manner. Increases in the presence of macrophages, neutrophils, and eosinophils within pulmonary air spaces is commonly seen in the process of fibrosis, depending on the fibrotic stressor in question.	Biological plausibility: High. There are very well established functional relationships between the secreted signalling molecules and the chemotactic effects on pro-inflammatory and pro-fibrotic cells. (Harris, 1954; Petri and Sanz, 2018)
KE2 --> KE3; Relationship 1704	Inflammatory cells recruited to the lung potentiate further injury to the ACM through ROS production and direct damage, persistent inflammation, or an insufficient wound healing response. AEC1s are lost, AEC2s exhibit enhanced proliferation, ECM changes are notable and alveoli collapse.	Biological plausibility: High. There is a mechanistic relationship between an increase in pro-inflammatory cells and mediators, and damage to the ACM. (Bhalla et al., 2009; Ward, 2003; Zemans et al., 2009)
KE3 --> KE4; Relationship 1705	Continued loss of ACM integrity, together with oxidative stress and chronic inflammation induce a Th2 response in the lung. Th cells differentiate into Th2 cells in response to stimuli such as IL-6 and IL-4, which increase the secretion of IL-4 and IL-13. Increased Th2 cells in the lung polarize macrophages to the M2 phenotype which further suppresses Th1 cell differentiation.	Biological Plausibility: High. There is a mechanistic relationship between ACM injury (tissue damage), and the induction of a Th2 response (responsible for wound healing). (Gieseck et al., 2018; Wynn, 2004)
KE4 --> KE5; Relationship 1706	The increased population of Th2 cells and M2 polarized macrophages increases secretion of pro-fibrotic mediators, like TGF-○˜, IL-4, and IL-13 which activate lung resident fibroblasts, as well as fibroblasts and fibrocytes recruited to the lung, and potentiate endo/epithelial to mesenchymal transition. This induces their proliferation and differentiation into a contractile myofibroblast phenotype capable of ECM synthesis and deposition.	Biological plausibility: High. There is a widely understood functional relationship between Th2 response related mediators, and their ability to induce proliferation and differentiation of fibroblasts. (Dong and Ma, 2018; Shao et al., 2008; Wynn, 2004; Wynn and Ramalingam, 2012)
KE5 --> KE6; Relationship 2625	Differentiated myofibroblasts represent the main effector cell responsible for the deposition of ECM during lung fibrosis. In the context of continuous stimuli and elevated levels of TGF-○˜myofibroblasts are persistently activated and deposit excessive amounts of collagen in the lung.	Biological plausibility: High. There is an accepted mechanistic relationship between activated myofibroblasts, and the capacity to secrete collagen. (Hinz, 2016ab; Hu and Phan, 2013)
KE6 --> AO; Relationship 1629	Persistent myofibroblast activation and continued deposition of ECM cause destruction of alveolar structures and normal lung architecture. Reductions in lung function are noted, and pulmonary fibrosis develops.	Biological plausibility: High. By definition, pulmonary fibrosis is characterized by excessive deposition of ECM and destruction of native lung architecture. Thus, the plausibility of this association is undisputed. (Fukuda et al., 1985; Richeldi et al., 2017; Thannickal et al., 2004)
Empirical Support for KERs		
MIE --> KE1; Relationship 1702	Direct interaction with the membrane is not a typically assessed endpoint in fibrosis research, except when dealing with fibrous stressors. Specific receptors involved in the initial immune cell activation are not wholly understood, even for model fibrotic stressors such as bleomycin.	Empirical Support: Moderate. There are limited *in vitro* studies which show a temporal and dose-dependent relationship between these two events, using the upregulation of specific surface receptors as a proxy for direct membrane interaction.

	Limited *in vitro* studies have shown toll-like receptors are involved in silica and zinc nanoparticle macrophage recognition, which stimulates secretion of inflammatory factors. Similarly, bleomycin has been shown to bind to high affinity sites on the surface of macrophages, which stimulates secretion of growth factors and monocyte chemotactic molecules.	(Chan et al., 2018; Denholm and Phan 1990; Roy et al., 2014)
KE1 --> KE2; Relationship 1703	There are many studies which have empirically shown a relationship between secreted mediators and recruitment of immune cells to the lung. A paper by Chen et al., 2016, showed that increases in the levels of CXCL1, CXCL2, and CXCL5 in the lung preceded neutrophil recruitment following *in vivo* treatment with carbon NPs. In an *in vitro* study, Schremmer et al., 2016 exposed rat alveolar macrophages to nano silica and noted increases in C-C motif chemokine ligand (CCL)4, CXCL1, CXCL3, and TNF-a in the supernatant. This supernatant was able to induce chemotaxis in unexposed macrophages.	Empirical Support: Moderate. There are many studies which show temporal and dose-dependent recruitment of immune cells following increases in pro-inflammatory mediators. However, these mediators exhibit pleiotropy, and knockdown or KO of a single pathway or mediator can result in compensation and recruitment of immune cells at a later time, as is seen in Nikota et al., 2017. (Chen et al., 2016; Nikota et al., 2017; Schremmer et al., 2016)
KE2 --> KE3; Relationship 1704	The chronic inflammatory environment and oxidative stress potentiated by an increase of immune cells in the lung is well known to precede significant alveolar damage. However, the variety of infiltrating leukocytes differs depending on the stressor in question. In a study with crystalline silica, Umbright et al., 2017, were able to show that increases in pulmonary leukocytes at 3 weeks, preceded increases in total albumin (loss of ACM integrity) at 6 weeks. In another publication by Zeidler-Erdely et al., 2011, mice exposed to stainless steel welding fumes had an increased amount of alveolar macrophages 1 day post-exposure, while alveolar damage (as measured by total protein) was not evident until 4 days post-exposure.	Empirical Support: Moderate. There is both temporal and dose-response evidence to suggest that an increased amount of pro-inflammatory immune cells potentiates alveolar capillary damage. However, few studies assessing these KEs include multiple concentrations and timepoints, and as such, these KEs are typically reported as occurring together (i.e. damage is detected along with an increase in cell abundance). (Umbright et al., 2017; Zeidler-Erdely et al., 2011)
KE3 --> KE4; Relationship 1705	Few studies have directly assessed the ACM integrity loss on the induction of a Th2 response. In one publication, He et al., 2016 showed that ROS induced by a specific superoxide dismutase induces M2 polarization in asbestosis, and inhibition of signalling by Jumonji domain-containing protein D3 (Jmjd3) reduces ROS, M2 polarization, and fibrosis. In another study using NRF2 KO mice, a significant Th2 bias is observed following bleomycin treatment, with enhanced fibrosis noted. Discrepancies are present, for instance where many groups have found that TNF-a receptor (TNF-R)1 and TNF-R2 are associated with fibrosis, and even though TNF-a is a therapeutic target for IPF and asbestosis in humans, other groups have reported the opposite and that its exogenous delivery can reduce the fibrotic burden.	Empirical Support: Moderate. There is limited *in vitro* and *in vivo* evidence to support a direct relationship between these two KEs, with some inconsistencies with respect to the specific mediators in question. (Ortiz et al., 1998; Piguet, 1989; Redente et al., 2014)
KE4 --> KE5; Relationship 1706	Activation of a Th2 response is known to activate lung fibroblasts. Research by Hashimoto et al. 2001, indicates that the Th2 cytokines IL-4 and IL-13 induce differentiation of human fibroblasts to myofibroblasts.	Empirical Support: High. There is a plethora of dose and time response evidence which shows that Th2 cytokines induce the activation and proliferation of fibroblasts. (Hashimoto et al., 2001; Lee et

	Furthermore, IL-13 has been shown to directly activate TGF-T*in vivo*, and lead to pulmonary fibrosis.	al., 2001)
KE5 --> KE6; Relationship 2625	While it is difficult to show the accumulation and incorporation of ECM *in vitro*, the levels of soluble collagen can be assessed. Many publications have reported secretion of soluble matrix components by activated myofibroblasts. For example, research by Li et al. 2017, has shown that soluble cadmium can induce fibrosis in mice, and that *in vitro* treatment of fibroblasts with cadmium induces expression of a-SMA (hallmark of myofibroblasts), as well as soluble collagen.	Empirical Support: High. It is generally accepted knowledge that activated myofibroblasts are collagen secreting cells. (Blaauboer et al., 2014; Hinz, 2016a; Li et al., 2017)
KE6 --> AO; Relationship 1629	Pulmonary fibrosis results from excessive accumulation of collagen and ECM in the lungs, in the context of prolonged inflammation, injury, and an aberrant healing response. IPF is the most common form in humans, with a poor prognosis overall.	Empirical Support: High. Excessive ECM deposition is the defining characteristic of pulmonary fibrosis, and the evidence to support this relationship is unequivocal. (Meyer, 2017; Thannickal et al., 2004; Williamson et al., 2015; Zisman et al., 2005)

Quantitative Consideration

The presented AOP is mostly qualitative and additional studies are needed to support the essentiality of the KEs and to build KERs. However, it is important to note that it is difficult to experimentally demonstrate the relevance of earlier KEs to the end outcome of fibrosis because of the redundancy in pathways involved. The mode or type of interactions between the resident cell membrane and a substance is dependent on the specific physical-chemical characteristics of the substance (e.g. for NMs, aspect ratio, crystallinity, persistence, surface charge, size, etc.). There has been an attempt to determine quantitatively the dose at which the events in AOP 173 are induced with respect to CNTs (Labib et al., 2016; reproduced below). In this manuscript, researchers applied global transcriptomic analysis and BMD modelling to determine the dose at which the MIE, KE1, KE2, KE4, KE5, and KE6 are induced using samples from three separate studies and compared the results to the apical BMD of the AO of pulmonary fibrosis. From the results shown, it can be seen that the BMD intervals of transcriptional pathway induction for each KE largely overlap but are representative of the BMD of AO induction. These results serve to highlight the parallel nature of the KEs in AOP 173, with many of the events occurring concurrently in addition to occurring sequentially.

Quantitative concordance table for AOP 173 KERs. Data is reproduced from Labib et al., 2016 (Figure 4., Additional file 4: Table S3). CNT: carbon nanotube. N/A: Not assessed

Stressor	Species	Time Point	MIEa (1495)	KE1a (1496)	KE2a (1497)	KE3 (1498)	KE4a (1499)	KE5a (1500)	KE6a (68)	AO (1458)
Mitsui 7 CNT	Mouse	24 Hr	4 – 9	3 - 7	9 – 13	N/A	5 – 11	10 – 21	9 – 13	N/A
Mitsui 7 CNT	Mouse	3 / 7 day	11 – 22	6 – 22	14 – 24	N/A	9 – 16	15 – 26	17 – 34	N/A
Mitsui 7 CNT	Mouse	28 day	No Effect	14 – 26	36 – 51	N/A	14 – 26	11 – 20	No Effect	N/A
Mitsui 7 CNT	Mouse	56 day	N/A	N/A	N/A	N/A	N/A	N/A	N/A	14 – 27b
NRCWE-026 CNT	Mouse	24 Hr	No effect	8 – 15	20 – 37	N/A	8 – 15	21 – 39	No Effect	N/A
CNT		3 / 7 day								
NRCWE-026	Mouse	28 day	No	No	No	N/A	12 – 20	No	No	N/A

CNT			Effect	Effect	Effect			Effect	Effect	
NM-401 CNT	Mouse	24 Hr	No Effect	3 – 20	8 – 22	N/A	8 – 22	13 – 22	18 – 29	N/A
NM-401 CNT	Mouse	3 / 7 day	11 - 17	12 - 19	12 - 20	N/A	7 - 20	14 - 22	13 – 21	N/A
NM-401 CNT	Mouse	28 day	20 - 37	17 - 28	No Effect	N/A	No Effect	13 - 21	18 – 31	N/A

[a]: BMD (Benchmark dose lower confidence (BMDL)) intervals in µg / lung based on transcriptional pathway induction.

[b]: BMDL – BMD interval in µg / lung based on alveolar thickness.

The MIE of substance interaction with the lung cell membrane is intentionally kept broad and vague, to reflect the many interactions pro-fibrotic substances can have with the plasma membrane of cells. The presented AOP, while applicable to both soluble and persistent stressors, is specifically applicable to substances which induce fibrosis through immune responses. NMs are a group of such substances, which interact with organisms and cells via a dynamic biomolecular corona that is dependent on the biological microenvironment. While great strides have been made in recent years to characterize and understand this corona and how it impacts cellular recognition, further research is needed in order to accurately describe the specific interactions necessary for the initiation of fibrosis pathogenesis. Indeed, this is also true for model soluble stressors such as bleomycin, for which cellular binding and uptake is incompletely understood.

The specific mediators involved in the first KE (KE1; Event 1496), and the threshold necessary for progression to subsequent KEs is incompletely understood. KO models have shown that ablation of alarmins, such as IL-1, changes the initial trajectory of pulmonary fibrosis, however, compensation from other pathways makes it difficult to determine its essentiality to the end pathogenesis.

In addition, other factors and events such as chronic lung inflammation, oxidative stress and macrophage polarization are suggested to play an important role in the progression of the disease trajectory. These events are not included as KEs in the main AOP because chronic lung inflammation defines temporality of the inflammation process and at present, sensitive markers that distinguish between acute and chronic inflammation are not available. Similarly, the role of ROS and oxidative stress in potentiating pulmonary fibrosis is also ambiguous. Many pro-fibrotic substances induce the formation of ROS and subsequent oxidative stress, as do many non-fibrotic stressors. While it is hard to deny that ROS and oxidative stress serve an important role in fibrosis by increasing cellular injury, potentiating an environment of chronic inflammation & damage, and activation of pro-fibrotic factors like TGF-β1, a causal relationship between the two has not been established. Furthermore, antioxidant treatment in IPF patients has been largely unsuccessful, indicating a lack of knowledge of the specific redox mechanisms involved. Recent research has indicated a potential role of specific redox mechanisms, such as mitochondrial ROS and nitrogen oxides derived ROS; however, further research is needed to elucidate their role in potentiating pulmonary fibrosis. The development of newer fibrosis model systems that can better capitulate the human condition will assist in clarifying this aspect. Lastly, many studies show influence of macrophage polarization in lung fibrosis; however, collective evidence supporting its inclusion as a main KE in the AOP is lacking.

Given their influence on the progression and prognosis of the disease, the three events are described in detail below and depicted in a schematic in relation to this AOP. As the new

data becomes available, these events will be used to connect multiple AOPs in a network and develop necessary KEs and KERs, respectively.

Chronic Inflammation:

In the presence of continuous stimulus (e.g., presence of biopersistent toxic fibres such as asbestos, MWCNTs) or following repeated stimulus (e.g., repeated exposure to silica or coal dust), the ensuing lung cell injury fuels the inflammatory mechanisms leading to accumulation of immune cells, prolonged inflammation and aggravated tissue damage. This sustained and perpetuated immunological response is termed as chronic inflammation. During this phase, active inflammation, tissue injury and destruction, and tissue repair processes proceed in tandem. Thus, the causative substance must contain unique physical-chemical properties that grant the material biopersistance in the pulmonary environment or the pulmonary system has to be repeatedly exposed to the same substance that perpetuates the tissue injury leading to loss of ACM. Although, increases in number of neutrophils are observed during chronic inflammation, mononuclear phagocytes (circulating monocytes, tissue macrophages) and lymphoid cells mark this phase. The macrophages, components of mononuclear phagocyte system, are the predominant cells in chronic inflammation. Activated macrophages release a variety of cytokines, chemokines, growth factors, and ROS that, which when uncontrolled, lead to extensive tissue injury. The other types of inflammatory cells involved in chronic inflammation include eosinophils in allergen-induced lung fibrosis, lymphocytes and epithelial cells. Chronic inflammation exists to potentiate the KEs associated with inflammation and tissue injury, rather than acting as a separate KE itself.

Knockdown and KO models have shown that attenuation of the inflammatory response also attenuates the downstream fibrotic phenotype. Compensation from other inflammatory pathways makes complete abrogation of this response difficult. Furthermore, the essentiality of chronic inflammation leading to fibrotic phenotypes like IPF is questionable, as treatment with anti-inflammatory agents like corticosteroids does not have substantial benefits for patients. (Strieter and Mehrad, 2009; Ueha et al., 2012; Wilson and Wynn, 2009).

Oxidative stress (KE1392)

In KE1392 (AOPwiki), ‘Oxidative stress’ is described as an imbalance in the production of ROS and antioxidant defenses. High levels of oxidizing free radicals can be very damaging to cells and molecules within the cell. As a result, the cell has important defense mechanisms to protect itself from ROS. For example, Nrf2 is a transcription factor and master regulator of the oxidative stress response. During periods of oxidative stress, Nrf2-dependent changes in gene expression are important in regaining cellular homeostasis (Nguyen, et al. 2009) and can be used as indicators of the presence of oxidative stress in the cell. In the context of pulmonary fibrosis, oxidative stress potentiates the inflammatory response (KE1-2) and injury to the respiratory epithelium (KE3), and contribute to the differentiation and activation of myofibroblasts (KE5). The exact species of ROS, the specific cell types, and the perturbed oxidative stress related pathways vary depending on the type of pulmonary fibrosis, and even among different human patients suffering from the same fibrosing disease (ex. IPF). Increased levels of ROS have been shown to activate TGF-β1 and induce apoptosis of AECs. Furthermore, oxidative stress induces secretion of pro-inflammatory mediators (mitochondrial DNA, Nalp3 inflammasome-related molecules) from the injured epithelium as well as from resident immune cells like macrophages. This potentiates additional recruitment of immune cells to the site of injury, further compounding the inflammatory response, and inducing further production of ROS by effector cells like neutrophils. Clinical studies in IPF patients have consistently found higher levels of ROS biomarkers in the BALF, serum, as well as in exhaled condensate.

Furthermore, increases in ROS and oxidative stress are associated with BO, a fibrosing disease of the bronchioles instead of the alveolar tissue. While there is strong evidence for the involvement of ROS in the pathogenesis of pulmonary fibrosis, it acts to potentiate multiple KEs rather than acting as a key event itself. Oxidative stress is both causative and the consequence of observed responses in a feedforward type mechanism.

Multiple studies using knockdown and KO mammalian models have shown that oxidative stress is involved in the development of pulmonary fibrosis. However, its essentiality in its pathogenesis is not conclusive, as antioxidant treatment offers no significant benefit in patients with IPF, the most common type of pulmonary fibrosis in humans. Furthermore, uncertainties remain concerning the exact molecular mechanisms underlying oxidative stress in the context of pulmonary fibrosis. (Checa and Aran, 2020; Cheresh et al., 2013; Dostert et al., 2008; Madill et al., 2009ab; Veith et al., 2019; https://aopwiki.org/aops/411; https://aopwiki.org/aops/424; https://aopwiki.org/aops/425).

Macrophage polarization

Depending on the lung microenvironment (damaged cells, microbial products, activated lymphocytes), the precursor monocytes differentiate into distinct types of macrophages. Classically activated (M1) macrophages and alternatively activated (M2) macrophages are the important ones to consider in the context of this AOP. The M1 macrophages produce high levels of pro-inflammatory cytokines, mediate resistance to pathogens, induce generation of high levels of ROS and reactive nitrogen species, and Th type 1 (Th1) responses. M1 macrophages produce IL-1, IL-12, IL-23 and induce Th1 cell infiltration and activation. The M2 macrophages secrete anti-inflammatory mediators, by which they play a role in regulation of inflammation. M2 polarization is mediated by Th2 cytokines such as IL-4 and IL-13, which in turn, promotes M2 activation. M2 macrophages express immunosuppressive molecules such as IL-10, Arginase (Arg)-1 and -2, which suppress the induction of Th1 cells that produce the anti-fibrotic cytokine IFN-γ The activity of M2 is associated with tissue remodelling, immune regulation, tumor promotion, tissue regeneration and effective phagocytic activity.

Inhibition of M2 polarization through genetic depletion of surface receptors such as MARCO, attenuates the fibrotic phenotype. Depletion of interstitial macrophages bearing the M2 phenotype has been shown to block radiation-induced lung fibrosis. (Meziani et al., 2018; Murthy et al., 2015; Stahl et al., 2013).

Schematic depicting how chronic inflammation, oxidative stress and macrophage polarization connect to the main KEs in the AOP 173 through feedback loop

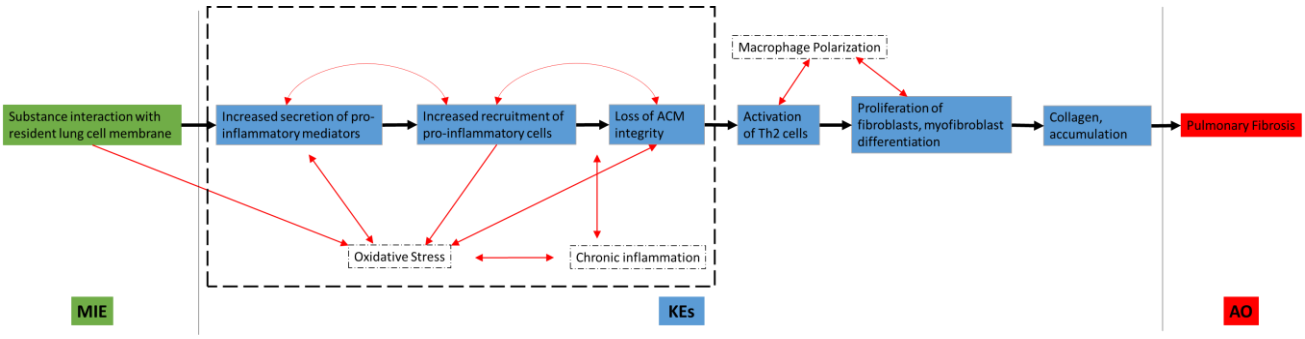

MIE: Molecular Initiating Event. KEs: Key Events. AO: Adverse Outcome.

Considerations for Potential Applications of the AOP

This AOP is applicable to occupational exposures as lung fibrosis is frequently observed in miners and welders exposed to metal dusts.

Pulmonary fibrosis is a progressive debilitating disease with no cure. A number of environmental and occupational agents, such as CS, agriculture or farming, wood dust, metal dust, stone and sand dust, play a causative role in the development of lung fibrosis. More recently, laboratory experiments in animals have shown that exposure to NMs, novel technology-enabled materials of sophisticated properties induce lung fibrosis. Fibrosis also develops in other organs (skin, liver, kidney, heart and pancreas) and the underlying mechanisms are similar. Thus, this AOP is applicable to screening of a broad group of suspected inhalation toxicants and allows the development of *in silico* and *in vitro* testing strategies for chemicals suspected to cause inhalation toxicity. Indeed, recent efforts aimed at collating all AOPs with potential relevance to NM risk assessment has led to the production of an AOP network which identified shared KEs of relevance to multiple AOs (Halappanavar et al., 2020). From this list, KE1 and KE2 from this AOP are among the most commonly shared between the various AOPs in the network. Shared KEs such as these can be prioritized for *in vitro* bio-assay development and tier-1 testing strategies. In a recent review, AOP 173 was used as a case study to define a testing strategy consisting of a slew of targeted bio-assay alternatives that can be used to screen for the *in vivo* occurrence of a number of the contained KEs (Halappanavar et al., 2021). These recent efforts serve to highlight the utility of AOP 173 in guiding the development of rapid screening strategies as well as research recommendations spanning across multiple AOPs with shared events.

This AOP is also currently being used by the various European Union nano research consortia to inform the design and development of relevant *in vitro* and *in silico* models for screening, prioritising, and assessing the potential of NMs to cause inhalation hazard. Specifically, this AOP has recently informed the development of a Nano Quantitative Structure Activity Relationship (NanoQSAR) model of CNT induced pulmonary inflammation, which found that the transcriptional response is associated with the aspect ratio of the nano fibres (Jagiello et al., 2021). Furthermore, this AOP can also inform the creation of biomarkers for fibrosis, such as the preliminary 17-gene pro-fibrotic biomarker panel, which was produced using global transcriptional datasets from mice exposed to CNTs (Rahman et al., 2020). Although in a preliminary stage, this signature composed of 17 genes can be used to assess the response of the MIE (Event 1495), KE1 (Event 1496), KE2 (Event 1497), KE4 (Event 1499), and KE5 (Event 1500), based on the differential expression of key bioinformatics-informed transcripts.

Given the fact that a number of pharmacological agents and allergens cause fibrosis via a similar mechanism; the mechanistic representation of the lung fibrotic process in an AOP format, clearly identifying the individual KEs potentially involved in the disease process, enables visualisation of the possible avenues for therapeutic interference in humans.

Confidence in the AOP

Mechanistically, there is enough evidence to support the occurrence of each individual KE in the process of lung fibrosis as described. There is also enough evidence to support each KERs. However, as mentioned earlier, the early KEs constitute an organism's defence system and thus exhibit high heterogeneity in the signalling pathways and biological networks involved. Therefore, the results of the essentiality experiments may show incongruence based on the individual protein, gene or pathway selected for intervention.

How well characterised is the AOP?

The AO is established and there is some quantitative data for some stressors.

How well are the initiating and other key events causally linked to the outcome?

The occurrence of each individual KE in the process leading to lung fibrosis is well accepted and established. However, individual studies mainly focus on a single KE and its relationship with the end AO. Quantitative data to support individual KERs is scarce.

What are the limitations in the evidence in support of the AOP?

As described earlier, attempts have been made to establish an *in vitro* model to predict the occurrence of fibrosis. However, the model has not been validated for screening the potential fibrogenic substances; the model has been used to identify drug targets that can effectively inhibit the progression to fibrosis (Chen et al., 2009). This is mainly due to the inability to accurately capture the responses induced by different cell types involved, and the intricate dynamics between the cell types, biological pathways and the biomolecules involved. Studies conducted to date have mainly focussed on the AO.

Is the AOP specific to certain tissues, life stages/age classes?

Fibrosis is a disease that affects several organ systems in an organism including lung, liver, heart, kidney, skin, and eye. The hallmark events preceding the end AO are similar to the one described here for lung fibrosis and involve similar cell types and biomolecules. Thus, the AOP can be extended to represent fibrosis in other organs. An AOP for liver fibrosis already exists and the KE 68 (collagen, accumulation) is shared by several fibrosis-related AOPs. The AOP is mainly applicable to adults as evidence to support applicability to different life stages is lacking. Lung fibrosis is thought to be a disease of male subjects. The early inflammatory KEs represented in this AOP constitute functional changes that describe inflammation in general. Several diseases are known to be mediated by inflammation and thus, early KEs in this AOP can be extended to any study investigating inflammation mediated AOs.

Are the initiating and key events expected to be conserved across taxa?

The events and pathways captured in this AOP are suggested to be conserved across different species and the process itself is influenced by the physical-chemical properties of the toxic substance.

References

1. Adams TN, Butt YM, Batra K, Glazer CS. Cobalt related interstitial lung disease. Respir Med. 2017 Aug;129:91-97. doi: 10.1016/j.rmed.2017.06.008.
2. Agency for Toxic Substances and Disease Registry. Toxicological Profile for Asbestos. *ATSDRs Toxicological Profiles*. 2001. doi:10.1201/9781420061888_ch34
3. Andersson-Sjöland A, de Alba CG, Nihlberg K, Becerril C, Ramírez R, Pardo A, Westergren-Thorsson G, Selman M. Fibrocytes are a potential source of lung fibroblasts in idiopathic pulmonary fibrosis. Int J Biochem Cell Biol. 2008;40(10):2129-40. doi: 10.1016/j.biocel.2008.02.012.
4. Arnoldussen YJ, Anmarkrud KH, Skaug V, Apte RN, Haugen A, Zienolddiny S. Effects of carbon nanotubes on intercellular communication and involvement of IL-1 genes. J Cell Commun Signal. 2016 Jun;10(2):153-62. doi: 10.1007/s12079-016-0323-0.

5. Assad N, Sood A, Campen MJ, Zychowski KE. Metal-Induced Pulmonary Fibrosis. Curr Environ Health Rep. 2018 Dec;5(4):486-498. doi: 10.1007/s40572-018-0219-7.

6. Barkauskas CE, Noble PW. Cellular mechanisms of tissue fibrosis. 7. New insights into the cellular mechanisms of pulmonary fibrosis. Am J Physiol Cell Physiol. 2014 Jun 1;306(11):C987-96. doi: 10.1152/ajpcell.00321.2013.

7. Barlo NP, van Moorsel CH, Ruven HJ, Zanen P, van den Bosch JM, Grutters JC. Surfactant protein-D predicts survival in patients with idiopathic pulmonary fibrosis. Sarcoidosis Vasc Diffuse Lung Dis. 2009 Jul;26(2):155-61.

8. Bateman ED, Turner-Warwick M, Adelmann-Grill BC. Immunohistochemical study of collagen types in human foetal lung and fibrotic lung disease. Thorax. 1981 Sep;36(9):645-53. doi: 10.1136/thx.36.9.645.

9. Behzadi S, Serpooshan V, Tao W, Hamaly MA, Alkawareek MY, Dreaden EC, Brown D, Alkilany AM, Farokhzad OC, Mahmoudi M. Cellular uptake of nanoparticles: journey inside the cell. Chem Soc Rev. 2017 Jul 17;46(14):4218-4244. doi: 10.1039/c6cs00636a.

10. Bhalla DK, Hirata F, Rishi AK, Gairola CG. Cigarette smoke, inflammation, and lung injury: a mechanistic perspective. J Toxicol Environ Health B Crit Rev. 2009 Jan;12(1):45-64. doi: 10.1080/10937400802545094.

11. Blaauboer ME, Boeijen FR, Emson CL, Turner SM, Zandieh-Doulabi B, Hanemaaijer R, Smit TH, Stoop R, Everts V. Extracellular matrix proteins: a positive feedback loop in lung fibrosis? Matrix Biol. 2014 Feb;34:170-8. doi: 10.1016/j.matbio.2013.11.002.

12. Blum JL, Rosenblum LK, Grunig G, Beasley MB, Xiong JQ, Zelikoff JT. Short-term inhalation of cadmium oxide nanoparticles alters pulmonary dynamics associated with lung injury, inflammation, and repair in a mouse model. Inhal Toxicol. 2014 Jan;26(1):48-58. doi: 10.3109/08958378.2013.851746.

13. Borthwick LA, Parker SM, Brougham KA, Johnson GE, Gorowiec MR, Ward C, Lordan JL, Corris PA, Kirby JA, Fisher AJ. Epithelial to mesenchymal transition (EMT) and airway remodelling after human lung transplantation. Thorax. 2009 Sep;64(9):770-7. doi: 10.1136/thx.2008.104133.

14. Boyles MS, Young L, Brown DM, MacCalman L, Cowie H, Moisala A, Smail F, Smith PJ, Proudfoot L, Windle AH, Stone V. Multi-walled carbon nanotube induced frustrated phagocytosis, cytotoxicity and pro-inflammatory conditions in macrophages are length dependent and greater than that of asbestos. Toxicol In Vitro. 2015 Oct;29(7):1513-28. doi: 10.1016/j.tiv.2015.06.012.

15. Brass DM, Palmer SM. Models of toxicity of diacetyl and alternative diones. Toxicology. 2017 Aug 1;388:15-20. doi: 10.1016/j.tox.2017.02.011.

16. Brown DM, Kinloch IA, Bangert U, Windle AH, Walter DM, Walker GS, et al. An in vitro study of the potential of carbon nanotubes and nanofibres to induce inflammatory mediators and frustrated phagocytosis. Carbon. 2007;45(9):1743-56. doi: https://doi.org/10.1016/j.carbon.2007.05.011.

17. Cao H, Wang C, Chen X, Hou J, Xiang Z, Shen Y, Han X. Inhibition of Wnt/β-catenin signaling suppresses myofibroblast differentiation of lung resident mesenchymal stem cells and pulmonary fibrosis. Sci Rep. 2018 Sep 11;8(1):13644. doi: 10.1038/s41598-018-28968-9.

18. Chan JYW, Tsui JCC, Law PTW, So WKW, Leung DYP, Sham MMK, Tsui SKW, Chan CWH. Regulation of TLR4 in silica-induced inflammation: An underlying mechanism of silicosis. Int J Med Sci. 2018 Jun 14;15(10):986-991. doi: 10.7150/ijms.24715.

19. Checa J, Aran JM. Airway Redox Homeostasis and Inflammation Gone Awry: From Molecular Pathogenesis to Emerging Therapeutics in Respiratory Pathology. Int J Mol Sci. 2020 Dec 7;21(23):9317. doi: 10.3390/ijms21239317.

20. Chen CZ, Peng YX, Wang ZB, Fish PV, Kaar JL, Koepsel RR, Russell AJ, Lareu RR, Raghunath M. The Scar-in-a-Jar: studying potential antifibrotic compounds from the epigenetic to extracellular level in a single well. Br J Pharmacol. 2009 Nov;158(5):1196-209. doi: 10.1111/j.1476-5381.2009.00387.x.

21. Chen YL, Zhang X, Bai J, Gai L, Ye XL, Zhang L, Xu Q, Zhang YX, Xu L, Li HP, Ding X. Sorafenib ameliorates bleomycin-induced pulmonary fibrosis: potential roles in the inhibition of epithelial-mesenchymal transition and fibroblast activation. Cell Death Dis. 2013 Jun 13;4(6):e665. doi: 10.1038/cddis.2013.154.

22. Chen S, Yin R, Mutze K, Yu Y, Takenaka S, Königshoff M, Stoeger T. No involvement of alveolar macrophages in the initiation of carbon nanoparticle induced acute lung inflammation in mice. Part Fibre Toxicol. 2016 Jun 21;13(1):33. doi: 10.1186/s12989-016-0144-6.

23. Cheresh P, Kim SJ, Tulasiram S, Kamp DW. Oxidative stress and pulmonary fibrosis. Biochim Biophys Acta. 2013 Jul;1832(7):1028-40. doi: 10.1016/j.bbadis.2012.11.021.

24. Cho HY, Reddy SP, Yamamoto M, Kleeberger SR. The transcription factor NRF2 protects against pulmonary fibrosis. FASEB J. 2004 Aug;18(11):1258-60. doi: 10.1096/fj.03-1127fje.

25. Denholm EM, Phan SH. Bleomycin binding sites on alveolar macrophages. J Leukoc Biol. 1990 Dec;48(6):519-23. doi: 10.1002/jlb.48.6.519.

26. Ding M, Chen F, Shi X, Yucesoy B, Mossman B, Vallyathan V. Diseases caused by silica: mechanisms of injury and disease development. Int Immunopharmacol. 2002 Feb;2(2-3):173-82. doi: 10.1016/s1567-5769(01)00170-9.

27. Dong J, Ma Q. Myofibroblasts and lung fibrosis induced by carbon nanotube exposure. Part Fibre Toxicol. 2016 Nov 4;13(1):60. doi: 10.1186/s12989-016-0172-2.

28. Dong J, Ma Q. Type 2 Immune Mechanisms in Carbon Nanotube-Induced Lung Fibrosis. Front Immunol. 2018 May 22;9:1120. doi: 10.3389/fimmu.2018.01120.

29. Dörger M, Münzing S, Allmeling AM, Messmer K, Krombach F. Differential responses of rat alveolar and peritoneal macrophages to man-made vitreous fibers in vitro. Environ Res. 2001 Mar;85(3):207-14. doi: 10.1006/enrs.2001.4234.

30. Dostert C, Pétrilli V, Van Bruggen R, Steele C, Mossman BT, Tschopp J. Innate immune activation through Nalp3 inflammasome sensing of asbestos and silica. Science. 2008 May 2;320(5876):674-7. doi: 10.1126/science.1156995.

31. Friedman SL. Fibrogenic cell reversion underlies fibrosis regression in liver. Proc Natl Acad Sci U S A. 2012 Jun 12;109(24):9230-1. doi: 10.1073/pnas.1206645109.

32. Froudarakis M, Hatzimichael E, Kyriazopoulou L, Lagos K, Pappas P, Tzakos AG, Karavasilis V, Daliani D, Papandreou C, Briasoulis E. Revisiting bleomycin from pathophysiology to safe clinical use. Crit Rev Oncol Hematol. 2013 Jul;87(1):90-100. doi: 10.1016/j.critrevonc.2012.12.003.

33. Fukuda Y, Ferrans VJ, Schoenberger CI, Rennard SI, Crystal RG. Patterns of pulmonary structural remodeling after experimental paraquat toxicity. The morphogenesis of intraalveolar fibrosis. Am J Pathol. 1985 Mar;118(3):452-75.

34. Gasse P, Mary C, Guenon I, Noulin N, Charron S, Schnyder-Candrian S, Schnyder B, Akira S, Quesniaux VF, Lagente V, Ryffel B, Couillin I. IL-1R1/MyD88 signaling and the inflammasome are essential in pulmonary inflammation and fibrosis in mice. J Clin Invest. 2007 Dec;117(12):3786-99. doi: 10.1172/JCI32285.

35. Gieseck RL 3rd, Wilson MS, Wynn TA. Type 2 immunity in tissue repair and fibrosis. Nat Rev Immunol. 2018 Jan;18(1):62-76. doi: 10.1038/nri.2017.90.

36. Girtsman TA, Beamer CA, Wu N, Buford M, Holian A. IL-1R signalling is critical for regulation of multi-walled carbon nanotubes-induced acute lung inflammation in C57Bl/6 mice. Nanotoxicology. 2014 Feb;8(1):17-27. doi: 10.3109/17435390.2012.744110.

37. Gosens I, Cassee FR, Zanella M, Manodori L, Brunelli A, Costa AL, Bokkers BG, de Jong WH, Brown D, Hristozov D, Stone V. Organ burden and pulmonary toxicity of nano-sized copper (II) oxide particles after short-term inhalation exposure. Nanotoxicology. 2016 Oct;10(8):1084-95. doi: 10.3109/17435390.2016.1172678.

38. Guan R, Wang X, Zhao X, Song N, Zhu J, Wang J, Wang J, Xia C, Chen Y, Zhu D, Shen L. Emodin ameliorates bleomycin-induced pulmonary fibrosis in rats by suppressing epithelial-mesenchymal transition and fibroblast activation. Sci Rep. 2016 Oct 24;6:35696. doi: 10.1038/srep35696.

39. Halappanavar S, van den Brule S, Nymark P, Gaté L, Seidel C, Valentino S, Zhernovkov V, Høgh Danielsen P, De Vizcaya A, Wolff H, Stöger T, Boyadziev A, Poulsen SS, Sørli JB, Vogel U. Adverse outcome pathways as a tool for the design of testing strategies to support the safety assessment of emerging advanced materials at the nanoscale. Part Fibre Toxicol. 2020 May 25;17(1):16. doi: 10.1186/s12989-020-00344-4.

40. Halappanavar S, Nymark P, Krug HF, Clift MJD, Rothen-Rutishauser B, Vogel U. Non-Animal Strategies for Toxicity Assessment of Nanoscale Materials: Role of Adverse Outcome Pathways in the Selection of Endpoints. Small. 2021 Apr;17(15):e2007628. doi: 10.1002/smll.202007628.

41. Hardie WD, Le Cras TD, Jiang K, Tichelaar JW, Azhar M, Korfhagen TR. Conditional expression of transforming growth factor-alpha in adult mouse lung causes pulmonary fibrosis. Am J Physiol Lung Cell Mol Physiol. 2004 Apr;286(4):L741-9. doi: 10.1152/ajplung.00208.2003.

42. HARRIS H. Role of chemotaxis in inflammation. Physiol Rev. 1954 Jul;34(3):529-62. doi: 10.1152/physrev.1954.34.3.529.

43. Hashimoto S, Gon Y, Takeshita I, Maruoka S, Horie T. IL-4 and IL-13 induce myofibroblastic phenotype of human lung fibroblasts through c-Jun NH2-terminal kinase-dependent pathway. J Allergy Clin Immunol. 2001 Jun;107(6):1001-8. doi: 10.1067/mai.2001.114702.

44. He C, Larson-Casey JL, Gu L, Ryan AJ, Murthy S, Carter AB. Cu,Zn-Superoxide Dismutase-Mediated Redox Regulation of Jumonji Domain Containing 3 Modulates Macrophage Polarization and Pulmonary Fibrosis. Am J Respir Cell Mol Biol. 2016 Jul;55(1):58-71. doi: 10.1165/rcmb.2015-0183OC.

45. Hinz B. Myofibroblasts. Exp Eye Res. 2016a Jan;142:56-70. doi: 10.1016/j.exer.2015.07.009.

46. Hinz B. The role of myofibroblasts in wound healing. Curr Res Transl Med. 2016b Oct-Dec;64(4):171-177. doi: 10.1016/j.retram.2016.09.003.

47. Hiraku Y, Guo F, Ma N, Yamada T, Wang S, Kawanishi S, Murata M. Multi-walled carbon nanotube induces nitrative DNA damage in human lung epithelial cells via HMGB1-RAGE

interaction and Toll-like receptor 9 activation. Part Fibre Toxicol. 2016 Mar 29;13:16. doi: 10.1186/s12989-016-0127-7.

48. Hu B, Phan SH. Myofibroblasts. Curr Opin Rheumatol. 2013 Jan;25(1):71-7. doi: 10.1097/BOR.0b013e32835b1352.
49. Huaux F, Liu T, McGarry B, Ullenbruch M, Phan SH. Dual roles of IL-4 in lung injury and fibrosis. J Immunol. 2003 Feb 15;170(4):2083-92. doi: 10.4049/jimmunol.170.4.2083.
50. Hung CF. Origin of Myofibroblasts in Lung Fibrosis. Current Tissue Microenvironment Reports. 2020;1(4):155-62. doi: 10.1007/s43152-020-00022-9.
51. Jagiello K, Halappanavar S, Rybińska-Fryca A, Willliams A, Vogel U, Puzyn T. Transcriptomics-Based and AOP-Informed Structure-Activity Relationships to Predict Pulmonary Pathology Induced by Multiwalled Carbon Nanotubes. Small. 2021 Apr;17(15):e2003465. doi: 10.1002/smll.202003465.
52. Jeong J, Garcia-Reyero N, Burgoon L, Perkins E, Park T, Kim C, Roh JY, Choi J. Development of Adverse Outcome Pathway for PPARγ Antagonism Leading to Pulmonary Fibrosis and Chemical Selection for Its Validation: ToxCast Database and a Deep Learning Artificial Neural Network Model-Based Approach. Chem Res Toxicol. 2019 Jun 17;32(6):1212-1222. doi: 10.1021/acs.chemrestox.9b00040.
53. Kamp DW, Weitzman SA. Asbestosis: clinical spectrum and pathogenic mechanisms. Proc Soc Exp Biol Med. 1997 Jan;214(1):12-26. doi: 10.3181/00379727-214-44065.
54. Kato S, Inui N, Hakamata A, Suzuki Y, Enomoto N, Fujisawa T, Nakamura Y, Watanabe H, Suda T. Changes in pulmonary endothelial cell properties during bleomycin-induced pulmonary fibrosis. Respir Res. 2018 Jun 26;19(1):127. doi: 10.1186/s12931-018-0831-y.
55. Katzenstein AL, Myers JL. Idiopathic pulmonary fibrosis: clinical relevance of pathologic classification. Am J Respir Crit Care Med. 1998 Apr;157(4 Pt 1):1301-15. doi: 10.1164/ajrccm.157.4.9707039.
56. Kikuchi N, Ishii Y, Morishima Y, Yageta Y, Haraguchi N, Itoh K, Yamamoto M, Hizawa N. Nrf2 protects against pulmonary fibrosis by regulating the lung oxidant level and Th1/Th2 balance. Respir Res. 2010 Mar 18;11(1):31. doi: 10.1186/1465-9921-11-31.
57. Kim JE, Lim HT, Minai-Tehrani A, Kwon JT, Shin JY, Woo CG, Choi M, Baek J, Jeong DH, Ha YC, Chae CH, Song KS, Ahn KH, Lee JH, Sung HJ, Yu IJ, Beck GR Jr, Cho MH. Toxicity and clearance of intratracheally administered multiwalled carbon nanotubes from murine lung. J Toxicol Environ Health A. 2010;73(21-22):1530-43. doi: 10.1080/15287394.2010.511578.
58. Kuhn C, McDonald JA. The roles of the myofibroblast in idiopathic pulmonary fibrosis. Ultrastructural and immunohistochemical features of sites of active extracellular matrix synthesis. Am J Pathol. 1991 May;138(5):1257-65.
59. Labib S, Williams A, Yauk CL, Nikota JK, Wallin H, Vogel U, Halappanavar S. Nano-risk Science: application of toxicogenomics in an adverse outcome pathway framework for risk assessment of multi-walled carbon nanotubes. Part Fibre Toxicol. 2016 Mar 15;13:15. doi: 10.1186/s12989-016-0125-9.
60. Lai X, Zhao H, Zhang Y, Guo K, Xu Y, Chen S, Zhang J. Intranasal Delivery of Copper Oxide Nanoparticles Induces Pulmonary Toxicity and Fibrosis in C57BL/6 mice. Sci Rep. 2018 Mar 14;8(1):4499. doi: 10.1038/s41598-018-22556-7.

61. Landman ST, Dhaliwal I, Mackenzie CA, Martinu T, Steel A, Bosma KJ. Life-threatening bronchiolitis related to electronic cigarette use in a Canadian youth. CMAJ. 2019 Dec 2;191(48):E1321-E1331. doi: 10.1503/cmaj.191402.

62. Lawson WE, Crossno PF, Polosukhin VV, Roldan J, Cheng DS, Lane KB, Blackwell TR, Xu C, Markin C, Ware LB, Miller GG, Loyd JE, Blackwell TS. Endoplasmic reticulum stress in alveolar epithelial cells is prominent in IPF: association with altered surfactant protein processing and herpesvirus infection. Am J Physiol Lung Cell Mol Physiol. 2008 Jun;294(6):L1119-26. doi: 10.1152/ajplung.00382.2007.

63. Lawson WE, Cheng DS, Degryse AL, Tanjore H, Polosukhin VV, Xu XC, Newcomb DC, Jones BR, Roldan J, Lane KB, Morrisey EE, Beers MF, Yull FE, Blackwell TS. Endoplasmic reticulum stress enhances fibrotic remodeling in the lungs. Proc Natl Acad Sci U S A. 2011 Jun 28;108(26):10562-7. doi: 10.1073/pnas.1107559108.

64. Lee CG, Homer RJ, Zhu Z, Lanone S, Wang X, Koteliansky V, Shipley JM, Gotwals P, Noble P, Chen Q, Senior RM, Elias JA. Interleukin-13 induces tissue fibrosis by selectively stimulating and activating transforming growth factor beta(1). J Exp Med. 2001 Sep 17;194(6):809-21. doi: 10.1084/jem.194.6.809.

65. Li FJ, Surolia R, Li H, Wang Z, Liu G, Liu RM, Mirov SB, Athar M, Thannickal VJ, Antony VB. Low-dose cadmium exposure induces peribronchiolar fibrosis through site-specific phosphorylation of vimentin. Am J Physiol Lung Cell Mol Physiol. 2017 Jul 1;313(1):L80-L91. doi: 10.1152/ajplung.00087.2017.

66. Li L, Mok H, Jhaveri P, Bonnen MD, Sikora AG, Eissa NT, Komaki RU, Ghebre YT. Anticancer therapy and lung injury: molecular mechanisms. Expert Rev Anticancer Ther. 2018 Oct;18(10):1041-1057. doi: 10.1080/14737140.2018.1500180.

67. Li Y, Cao J. The impact of multi-walled carbon nanotubes (MWCNTs) on macrophages: contribution of MWCNT characteristics. Sci China Life Sci. 2018 Nov;61(11):1333-1351. doi: 10.1007/s11427-017-9242-3.

68. Madill J, Aghdassi E, Arendt B, Hartman-Craven B, Gutierrez C, Chow CW, Allard J; University Health Network. Lung transplantation: does oxidative stress contribute to the development of bronchiolitis obliterans syndrome? Transplant Rev (Orlando). 2009a Apr;23(2):103-10. doi: 10.1016/j.trre.2009.01.003.

69. Madill J, Aghdassi E, Arendt BM, Gutierrez C, Singer L, Chow CW, Keshavjee S, Allard JP. Oxidative stress and nutritional intakes in lung patients with bronchiolitis obliterans syndrome. Transplant Proc. 2009b Nov;41(9):3838-44. doi: 10.1016/j.transproceed.2009.04.012.

70. McKleroy W, Lee TH, Atabai K. Always cleave up your mess: targeting collagen degradation to treat tissue fibrosis. Am J Physiol Lung Cell Mol Physiol. 2013 Jun 1;304(11):L709-21. doi: 10.1152/ajplung.00418.2012.

71. Mercer RR, Hubbs AF, Scabilloni JF, Wang L, Battelli LA, Friend S, Castranova V, Porter DW. Pulmonary fibrotic response to aspiration of multi-walled carbon nanotubes. Part Fibre Toxicol. 2011 Jul 22;8:21. doi: 10.1186/1743-8977-8-21.

72. Meyer KC. Pulmonary fibrosis, part I: epidemiology, pathogenesis, and diagnosis. Expert Rev Respir Med. 2017 May;11(5):343-359. doi: 10.1080/17476348.2017.1312346.

73. Meziani L, Mondini M, Petit B, Boissonnas A, Thomas de Montpreville V, Mercier O, Vozenin MC, Deutsch E. CSF1R inhibition prevents radiation pulmonary fibrosis by depletion of interstitial macrophages. Eur Respir J. 2018 Mar 1;51(3):1702120. doi: 10.1183/13993003.02120-2017.

74. Moeller A, Gilpin SE, Ask K, Cox G, Cook D, Gauldie J, Margetts PJ, Farkas L, Dobranowski J, Boylan C, O'Byrne PM, Strieter RM, Kolb M. Circulating fibrocytes are an indicator of poor prognosis in idiopathic pulmonary fibrosis. Am J Respir Crit Care Med. 2009 Apr 1;179(7):588-94. doi: 10.1164/rccm.200810-1534OC.

75. Morgan DL, Jokinen MP, Johnson CL, Price HC, Gwinn WM, Bousquet RW, Flake GP. Chemical Reactivity and Respiratory Toxicity of the α-Diketone Flavoring Agents: 2,3-Butanedione, 2,3-Pentanedione, and 2,3-Hexanedione. Toxicol Pathol. 2016 Jul;44(5):763-83. doi: 10.1177/0192623316638962.

76. Mossman BT, Churg A. Mechanisms in the pathogenesis of asbestosis and silicosis. Am J Respir Crit Care Med. 1998 May;157(5 Pt 1):1666-80. doi: 10.1164/ajrccm.157.5.9707141.

77. Murthy S, Larson-Casey JL, Ryan AJ, He C, Kobzik L, Carter AB. Alternative activation of macrophages and pulmonary fibrosis are modulated by scavenger receptor, macrophage receptor with collagenous structure. FASEB J. 2015 Aug;29(8):3527-36. doi: 10.1096/fj.15-271304.

78. Nguyen T, Nioi P, Pickett CB. The Nrf2-antioxidant response element signaling pathway and its activation by oxidative stress. J Biol Chem. 2009 May 15;284(20):13291-5. doi: 10.1074/jbc.R900010200.

79. Nikota J, Williams A, Yauk CL, Wallin H, Vogel U, Halappanavar S. Meta-analysis of transcriptomic responses as a means to identify pulmonary disease outcomes for engineered nanomaterials. Part Fibre Toxicol. 2016 May 11;13(1):25. doi: 10.1186/s12989-016-0137-5.

80. Nikota J, Banville A, Goodwin LR, Wu D, Williams A, Yauk CL, Wallin H, Vogel U, Halappanavar S. Stat-6 signaling pathway and not Interleukin-1 mediates multi-walled carbon nanotube-induced lung fibrosis in mice: insights from an adverse outcome pathway framework. Part Fibre Toxicol. 2017 Sep 13;14(1):37. doi: 10.1186/s12989-017-0218-0.

81. National Institute for Occupational Safety and Health. Current Intelligence Bulletin 65: Occupational Exposure to Carbon Nanotubes and Nanofibers. Publication No. 2013-145. Cincinnati, OH, USA: National Institute for Occupational Safety and Health, Centers for Disease Control and Prevention, Department of Health and Human Services (DHHS); 2013. http://www.cdc.gov/niosh/docs/2013-145/pdfs/2013-145.pdf.

82. Ortiz LA, Lasky J, Hamilton RF Jr, Holian A, Hoyle GW, Banks W, Peschon JJ, Brody AR, Lungarella G, Friedman M. Expression of TNF and the necessity of TNF receptors in bleomycin-induced lung injury in mice. Exp Lung Res. 1998 Nov-Dec;24(6):721-43. doi: 10.3109/01902149809099592.

83. Park SJ, Im DS. Deficiency of Sphingosine-1-Phosphate Receptor 2 (S1P2) Attenuates Bleomycin-Induced Pulmonary Fibrosis. Biomol Ther (Seoul). 2019 May 1;27(3):318-326. doi: 10.4062/biomolther.2018.131.

84. Petri B, Sanz MJ. Neutrophil chemotaxis. Cell Tissue Res. 2018 Mar;371(3):425-436. doi: 10.1007/s00441-017-2776-8.

85. Phelps DS, Umstead TM, Mejia M, Carrillo G, Pardo A, Selman M. Increased surfactant protein-A levels in patients with newly diagnosed idiopathic pulmonary fibrosis. Chest. 2004 Feb;125(2):617-25. doi: 10.1378/chest.125.2.617.

86. Piguet PF, Collart MA, Grau GE, Kapanci Y, Vassalli P. Tumor necrosis factor/cachectin plays a key role in bleomycin-induced pneumopathy and fibrosis. J Exp Med. 1989 Sep 1;170(3):655-63. doi: 10.1084/jem.170.3.655.

87. Poland CA, Duffin R, Kinloch I, Maynard A, Wallace WA, Seaton A, Stone V, Brown S, Macnee W, Donaldson K. Carbon nanotubes introduced into the abdominal cavity of mice show asbestos-like pathogenicity in a pilot study. Nat Nanotechnol. 2008 Jul;3(7):423-8. doi: 10.1038/nnano.2008.111.

88. Porter DW, Hubbs AF, Mercer RR, Wu N, Wolfarth MG, Sriram K, Leonard S, Battelli L, Schwegler-Berry D, Friend S, Andrew M, Chen BT, Tsuruoka S, Endo M, Castranova V. Mouse pulmonary dose- and time course-responses induced by exposure to multi-walled carbon nanotubes. Toxicology. 2010 Mar 10;269(2-3):136-47. doi: 10.1016/j.tox.2009.10.017.

89. Porter DW, Hubbs AF, Chen BT, McKinney W, Mercer RR, Wolfarth MG, Battelli L, Wu N, Sriram K, Leonard S, Andrew M, Willard P, Tsuruoka S, Endo M, Tsukada T, Munekane F, Frazer DG, Castranova V. Acute pulmonary dose-responses to inhaled multi-walled carbon nanotubes. Nanotoxicology. 2013 Nov;7(7):1179-94. doi: 10.3109/17435390.2012.719649.

90. Rabolli V, Badissi AA, Devosse R, Uwambayinema F, Yakoub Y, Palmai-Pallag M, Lebrun A, De Gussem V, Couillin I, Ryffel B, Marbaix E, Lison D, Huaux F. The alarmin IL-1α is a master cytokine in acute lung inflammation induced by silica micro- and nanoparticles. Part Fibre Toxicol. 2014 Dec 13;11:69. doi: 10.1186/s12989-014-0069-x.

91. Rahman L, Jacobsen NR, Aziz SA, Wu D, Williams A, Yauk CL, White P, Wallin H, Vogel U, Halappanavar S. Multi-walled carbon nanotube-induced genotoxic, inflammatory and pro-fibrotic responses in mice: Investigating the mechanisms of pulmonary carcinogenesis. Mutat Res Genet Toxicol Environ Mutagen. 2017 Nov;823:28-44. doi: 10.1016/j.mrgentox.2017.08.005.

92. Rahman L, Williams A, Gelda K, Nikota J, Wu D, Vogel U, Halappanavar S. 21st Century Tools for Nanotoxicology: Transcriptomic Biomarker Panel and Precision-Cut Lung Slice Organ Mimic System for the Assessment of Nanomaterial-Induced Lung Fibrosis. Small. 2020 Sep;16(36):e2000272. doi: 10.1002/smll.202000272.

93. Re SL, Giordano G, Yakoub Y, Devosse R, Uwambayinema F, Couillin I, Ryffel B, Marbaix E, Lison D, Huaux F. Uncoupling between inflammatory and fibrotic responses to silica: evidence from MyD88 knockout mice. PLoS One. 2014 Jul 22;9(7):e99383. doi: 10.1371/journal.pone.0099383.

94. Redente EF, Jacobsen KM, Solomon JJ, Lara AR, Faubel S, Keith RC, Henson PM, Downey GP, Riches DW. Age and sex dimorphisms contribute to the severity of bleomycin-induced lung injury and fibrosis. Am J Physiol Lung Cell Mol Physiol. 2011 Oct;301(4):L510-8. doi: 10.1152/ajplung.00122.2011.

95. Redente EF, Keith RC, Janssen W, Henson PM, Ortiz LA, Downey GP, Bratton DL, Riches DW. Tumor necrosis factor-α accelerates the resolution of established pulmonary fibrosis in mice by targeting profibrotic lung macrophages. Am J Respir Cell Mol Biol. 2014 Apr;50(4):825-37. doi: 10.1165/rcmb.2013-0386OC.

96. Richeldi L, Collard HR, Jones MG. Idiopathic pulmonary fibrosis. Lancet. 2017 May 13;389(10082):1941-1952. doi: 10.1016/S0140-6736(17)30866-8.

97. Rock JR, Barkauskas CE, Cronce MJ, Xue Y, Harris JR, Liang J, Noble PW, Hogan BL. Multiple stromal populations contribute to pulmonary fibrosis without evidence for epithelial to mesenchymal transition. Proc Natl Acad Sci U S A. 2011 Dec 27;108(52):E1475-83. doi: 10.1073/pnas.1117988108.

98. Roy R, Singh SK, Das M, Tripathi A, Dwivedi PD. Toll-like receptor 6 mediated inflammatory and functional responses of zinc oxide nanoparticles primed macrophages. Immunology. 2014 Jul;142(3):453-64. doi: 10.1111/imm.12276.

99. Rydman EM, Ilves M, Vanhala E, Vippola M, Lehto M, Kinaret PA, Pylkkänen L, Happo M, Hirvonen MR, Greco D, Savolainen K, Wolff H, Alenius H. A Single Aspiration of Rod-like Carbon Nanotubes Induces Asbestos-like Pulmonary Inflammation Mediated in Part by the IL-1 Receptor. Toxicol Sci. 2015 Sep;147(1):140-55. doi: 10.1093/toxsci/kfv112.

100. Schremmer I, Brik A, Weber DG, Rosenkranz N, Rostek A, Loza K, Brüning T, Johnen G, Epple M, Bünger J, Westphal GA. Kinetics of chemotaxis, cytokine, and chemokine release of NR8383 macrophages after exposure to inflammatory and inert granular insoluble particles. Toxicol Lett. 2016 Nov 30;263:68-75. doi: 10.1016/j.toxlet.2016.08.014.

101. Sempowski GD, Beckmann MP, Derdak S, Phipps RP. Subsets of murine lung fibroblasts express membrane-bound and soluble IL-4 receptors. Role of IL-4 in enhancing fibroblast proliferation and collagen synthesis. J Immunol. 1994 Apr 1;152(7):3606-14.

102. Shao DD, Suresh R, Vakil V, Gomer RH, Pilling D. Pivotal Advance: Th-1 cytokines inhibit, and Th-2 cytokines promote fibrocyte differentiation. J Leukoc Biol. 2008 Jun;83(6):1323-33. doi: 10.1189/jlb.1107782.

103. Sisson TH, Mendez M, Choi K, Subbotina N, Courey A, Cunningham A, Dave A, Engelhardt JF, Liu X, White ES, Thannickal VJ, Moore BB, Christensen PJ, Simon RH. Targeted injury of type II alveolar epithelial cells induces pulmonary fibrosis. Am J Respir Crit Care Med. 2010 Feb 1;181(3):254-63. doi: 10.1164/rccm.200810-1615OC.

104. Stahl M, Schupp J, Jäger B, Schmid M, Zissel G, Müller-Quernheim J, Prasse A. Lung collagens perpetuate pulmonary fibrosis via CD204 and M2 macrophage activation. PLoS One. 2013 Nov 20;8(11):e81382. doi: 10.1371/journal.pone.0081382.

105. Strieter RM, Mehrad B. New mechanisms of pulmonary fibrosis. Chest. 2009 Nov;136(5):1364-1370. doi: 10.1378/chest.09-0510.

106. Tashiro J, Rubio GA, Limper AH, Williams K, Elliot SJ, Ninou I, Aidinis V, Tzouvelekis A, Glassberg MK. Exploring Animal Models That Resemble Idiopathic Pulmonary Fibrosis. Front Med (Lausanne). 2017 Jul 28;4:118. doi: 10.3389/fmed.2017.00118.

107. Thannickal VJ, Toews GB, White ES, Lynch JP 3rd, Martinez FJ. Mechanisms of pulmonary fibrosis. Annu Rev Med. 2004;55:395-417. doi: 10.1146/annurev.med.55.091902.103810.

108. Todd NW, Luzina IG, Atamas SP. Molecular and cellular mechanisms of pulmonary fibrosis. Fibrogenesis Tissue Repair. 2012 Jul 23;5(1):11. doi: 10.1186/1755-1536-5-11.

109. Ueha S, Shand FH, Matsushima K. Cellular and molecular mechanisms of chronic inflammation-associated organ fibrosis. Front Immunol. 2012 Apr 10;3:71. doi: 10.3389/fimmu.2012.00071.

110. Uhal BD, Joshi I, Hughes WF, Ramos C, Pardo A, Selman M. Alveolar epithelial cell death adjacent to underlying myofibroblasts in advanced fibrotic human lung. Am J Physiol. 1998 Dec;275(6):L1192-9. doi: 10.1152/ajplung.1998.275.6.L1192.

111. Umbright C, Sellamuthu R, Roberts JR, Young SH, Richardson D, Schwegler-Berry D, McKinney W, Chen B, Gu JK, Kashon M, Joseph P. Pulmonary toxicity and global gene expression changes in response to sub-chronic inhalation exposure to crystalline silica in

rats. J Toxicol Environ Health A. 2017;80(23-24):1349-1368. doi: 10.1080/15287394.2017.1384773.

112. Veith C, Boots AW, Idris M, van Schooten FJ, van der Vliet A. Redox Imbalance in Idiopathic Pulmonary Fibrosis: A Role for Oxidant Cross-Talk Between NADPH Oxidase Enzymes and Mitochondria. Antioxid Redox Signal. 2019 Nov 10;31(14):1092-1115. doi: 10.1089/ars.2019.7742.

113. Wan R, Mo Y, Zhang Z, Jiang M, Tang S, Zhang Q. Cobalt nanoparticles induce lung injury, DNA damage and mutations in mice. Part Fibre Toxicol. 2017 Sep 18;14(1):38. doi: 10.1186/s12989-017-0219-z.

114. Ward PA. Acute lung injury: how the lung inflammatory response works. Eur Respir J Suppl. 2003 Sep;44:22s-23s. doi: 10.1183/09031936.03.00000703a.

115. Williams K, Roman J. Studying human respiratory disease in animals--role of induced and naturally occurring models. J Pathol. 2016 Jan;238(2):220-32. doi: 10.1002/path.4658.

116. Williamson JD, Sadofsky LR, Hart SP. The pathogenesis of bleomycin-induced lung injury in animals and its applicability to human idiopathic pulmonary fibrosis. Exp Lung Res. 2015 Mar;41(2):57-73. doi: 10.3109/01902148.2014.979516.

117. Wilson MS, Wynn TA. Pulmonary fibrosis: pathogenesis, etiology and regulation. Mucosal Immunol. 2009 Mar;2(2):103-21. doi: 10.1038/mi.2008.85.

118. Wynn TA. Fibrotic disease and the T(H)1/T(H)2 paradigm. Nat Rev Immunol. 2004 Aug;4(8):583-94. doi: 10.1038/nri1412.

119. Wynn TA, Ramalingam TR. Mechanisms of fibrosis: therapeutic translation for fibrotic disease. Nat Med. 2012 Jul 6;18(7):1028-40. doi: 10.1038/nm.2807.

120. Yang H, Rivera Z, Jube S, Nasu M, Bertino P, Goparaju C, Franzoso G, Lotze MT, Krausz T, Pass HI, Bianchi ME, Carbone M. Programmed necrosis induced by asbestos in human mesothelial cells causes high-mobility group box 1 protein release and resultant inflammation. Proc Natl Acad Sci U S A. 2010 Jul 13;107(28):12611-6. doi: 10.1073/pnas.1006542107.

121. Yates CC, Hebda P, Wells A. Skin wound healing and scarring: fetal wounds and regenerative restitution. Birth Defects Res C Embryo Today. 2012 Dec;96(4):325-33. doi: 10.1002/bdrc.21024.

122. Zeidler-Erdely PC, Battelli LA, Stone S, Chen BT, Frazer DG, Young SH, Erdely A, Kashon ML, Andrews R, Antonini JM. Short-term inhalation of stainless steel welding fume causes sustained lung toxicity but no tumorigenesis in lung tumor susceptible A/J mice. Inhal Toxicol. 2011 Feb;23(2):112-20. doi: 10.3109/08958378.2010.548838.

123. Zemans RL, Colgan SP, Downey GP. Transepithelial migration of neutrophils: mechanisms and implications for acute lung injury. Am J Respir Cell Mol Biol. 2009 May;40(5):519-35. doi: 10.1165/rcmb.2008-0348TR.

124. Zhu Z, Homer RJ, Wang Z, Chen Q, Geba GP, Wang J, Zhang Y, Elias JA. Pulmonary expression of interleukin-13 causes inflammation, mucus hypersecretion, subepithelial fibrosis, physiologic abnormalities, and eotaxin production. J Clin Invest. 1999 Mar;103(6):779-88. doi: 10.1172/JCI5909.

125. Zhu W, von dem Bussche A, Yi X, Qiu Y, Wang Z, Weston P, Hurt RH, Kane AB, Gao H. Nanomechanical mechanism for lipid bilayer damage induced by carbon nanotubes confined in intracellular vesicles. Proc Natl Acad Sci U S A. 2016 Nov 1;113(44):12374-12379. doi: 10.1073/pnas.1605030113.

126. Zisman DA, Keane MP, Belperio JA, Strieter RM, Lynch JP 3rd. Pulmonary fibrosis. Methods Mol Med. 2005;117:3-44. doi: 10.1385/1-59259-940-0:003.

Appendix 1 - MIE, KEs and AO

List of MIEs in this AOP

Event: 1495: Substance interaction with the lung resident cell membrane components

Short Name: Interaction with the lung cell membrane

Key Event Component

Process	Object	Action
pattern recognition receptor signaling pathway		increased
toll-like receptor signaling pathway	Toll-like receptor	increased
toll-like receptor 4 signaling pathway	Toll-like receptor 4	increased

AOPs Including This Key Event

AOP ID and Name	Event Type
Aop:173 - Substance interaction with the pulmonary resident cell membrane components leading to pulmonary fibrosis	Molecular Initiating Event
Aop:451 - Interaction with lung resident cell membrane components leads to lung cancer	Molecular Initiating Event
Aop:237 - Substance interaction with lung resident cell membrane components leading to atherosclerosis	Molecular Initiating Event

Biological context

Level of Biological Organization
Molecular

Cell term

Cell term
eukaryotic cell

Evidence for Perturbation by Stressor

Overview for Molecular Initiating Event

As stated earlier, there are many different ways by which pro-fibrotic stressors can interact with the components of cell membrane and often involve multiple interactions at the same time. Few studies investigate the exact interaction between the stressor and the cellular membrane components. Asbestos and silica crystals engage scavenger receptors present on the macrophages (Murthy et al., 2015). Bleomycin binds high affinity bleomycin binding sites present on rat alveolar macrophage surfaces, leading to macrophage activation (Denholm and Phan, 1990). However, the consequences of such interactions such as, the release of PRR agonists DAMPs (alarmins) from dying or injured cells, increased gene or protein synthesis downstream of receptor binding or in the case of NMs, their cellular uptake, are measured routinely as indicative of occurrence of such interactions (Nel et al., 2009; Cheng et al., 2013). Because of the phys-chem properties such as surface charge, NMs and asbestos like materials can bind to cellular macromolecules and cell surface/membrane components, which in turn, facilitate their uptake and intracellular sequestration by the cells (NIOSH, 2011a; Pascolo et al., 2013). Several DAMPs that can

be effectively measured in biological samples and cultured cells include High Mobility Group Binding 1 (HMGB1) protein, Heat Shock proteins (HSPs), uric acid, annexins, and S100 proteins (Bianchi, 2007). Of all DAMPs, interleukin (IL)-1α is the most commonly measured alarmin. IL-1α is the principal pro-inflammatory moiety and is a designated 'alarmin' in the cell that alerts the host to injury or damage (Di Paolo and Shayakhmetov, 2016). It is shown that administration of necrotic cells to mice results in neutrophilic inflammation that was entirely mediated by IL-1α released from the dying or necrosed cells and consequent activation of IL-1 Receptor 1 (IL-1R1) signalling (**Suwara** et al., 2014). IL-1α is released following exposure to MWCNTs (Nikota et al., 2017) and silica (Rabolli et al., 2014). Although IL1-b is not a designated alarmin, its secretion following exposure to stressors is routinely assessed and is linked to initiation of cell or tissue injury.

Other high aspect ratio fibres such as asbestos and CNTs induce frustrated phagocytosis and acute cell injury (Boyles et al., 2015; Dörger et al., 2001; Brown et al., 2007; Kim et al., 2010; Poland et al., 2008), leading to DAMP release (Nikota et al, 2017), inflammation and immune responses.

Domain of Applicability

Taxonomic Applicability

Term	Scientific Term	Evidence	Links
mouse	Mus musculus	High	NCBI
rat	Rattus norvegicus	High	NCBI
human	Homo sapiens	High	NCBI

Life Stage Applicability

Life Stage	Evidence
Adults	High

Sex Applicability

Sex	Evidence
Male	High

Human, mouse, rat.

Although the expression of DAMPs following exposure to pro-fibrotic substances is not assessed across species, it is known that alarmins are released after trauma or injury, and their release is important for initiating the inflammatory response in all species including humans. The immediate acute inflammatory response involving DAMP signalling is also observed in human idiopathic pulmonary fibrosis (IPF); however, anti-inflammatory drugs have proven ineffective for treating IPF. Danger signalling axis including uric acid, adenosine triphosphate and IL-33/ST2 has been proven to promote lung fibrosis in animals.

Key Event Description

The human lung consists of approximately 40 different resident cell types that play different roles during homeostasis, injury, repair and disease states (Franks et al., 2008; Luettich et al., 2021). Of these, resident airway epithelial cells, alveolar/interstitial macrophages and dendritic cells are well characterised for their ability to sense the danger upon interaction with harmful substances and relay the message to mount the necessary immune/inflammatory response. The resident macrophages are present in all tissues, and

in a steady state, macrophages contribute to epithelial integrity, survey the tissue for invading pathogens or chemicals and maintain an immunosuppressive environment. Their main function is to clear the incoming irritants and microbes. They are named differently based on the tissue type and their specific functions (Kierdorf et al., 2015).

Substance interactions:

The chemicals or pathogens interact with cellular membrane to gain access to the organisms' interior. A predominant interaction mechanism involves the recognition of innate immune response agonists by pattern recognition receptors (PRRs) present on resident cells such as epithelial and alveolar macrophages. PRRs are also present on other immune and parenchymal cells. PRRs can be activated by two classes of ligands. Pathogen associated molecular patterns (PAMPs) are microbial molecules derived from invading pathogens. PAMPs will not be discussed further as pathogens are not the focus for the AOP presented here. The other class of ligands are called danger associated molecular patterns (DAMPs) that include cellular fragments, nucleic acids, small molecules, proteins and even cytokines released from injured or dying cells (Bianchi, 2007). Most fibrogenic stressors discussed in this AOP act via DAMPs-driven PRR activation. High aspect ratio (HAR) materials such as asbestos or carbon nanotubes (CNTs) pierce the cellular membrane of epithelial cells or resident macrophages resulting in cell injury or non-programmed cellular death. Alveolar macrophages trying to engulf HAR fibres that are long and stiff undergo frustrated phagocytosis because of their inability to engulf the piercing fibres and subsequently lead to cell injury (Boyles et al., 2015; Brown et al., 2007; Donaldson K et al., 2010; Dörger et al., 2001; Mossman and Churg, 1998). The cellular debris from injured or dying cell then serves as ligands for PRRs (Nakayama, 2018), leading to cell activation. In case of pro-fibrotic insoluble particles such as silica, coal dust and nanomaterials (NMs), the particle adsorbed opsonins such as immunoglobulins, complement proteins, or serum proteins act as ligands to the receptors on the macrophage cell surface (Behzadi et al., 2017). The tissue response to these materials resembles that observed following foreign body invasion in lungs.

Toll-like receptors (TLRs) are highly conserved PRRs that are associated with fibrogenic stressors (Desai et al., 2018). Inhibition of TLR-4 is protective against bleomycin-induced fibrosis (Li et al., 2015). However, the exact role and mechanisms by which TLRs mediate lung fibrosis are yet to be uncovered and some studies have shown TLRs to be protective against lung fibrosis (Desai et al., 2018). Asbestos and silica crystals are suggested to engage scavenger receptors present on the macrophages. Mice deficient in class A scavenger macrophage receptor with collagenous structure (MARCO) are shown to induce reduced fibrogenic response following chrysotile asbestos exposure; although, the direct binding of MARCO by asbestos is not investigated in the study (Murthy et al., 2015). In case of soluble substances such as bleomycin, paraquat (Dinis-Oliveira et al., 2008) (N,N'-dimethyl-4, 4′-bipyridinium dichloride) and other soluble fibrogenic chemicals, direct damage of lung epithelial cells and resulting cellular debris or secreted cytokines (DAMPs) serve as triggers for downstream cascading pro-inflammatory events, tissue injury and fibrosis. Engagement of PRRs and consequent cell activation is observed in various organisms including flies and mammals (Denholm and Phan, 1990; Matzinger, 2002).

How it is Measured or Detected

Detection of DAMPs or homeostasis-altering molecular processes:

Cellular interaction with substances or particles can be measured by assessing the release of DAMPs from stressed, injured or dying cells - indicative of binding of PRRs on the cell surface. Release of DAMPs is reflective of substance interaction with resident cells and their activation, a key step in the process of inflammation.

The release of DAMPs can be measured by the techniques listed in the published literature (Nikota et al., 2017; Rabolli et al., 2014; Suwara et al., 2014).

Targeted enzyme-linked immunosorbent assays (ELISA) (routinely used and recommended):

ELISA – permits quantitative measurement of antigens in biological samples. For example, in a cytokine ELISA (sandwich ELISA), an antibody (capture antibody) specific to a cytokine is immobilised on microtitre wells (96-well, 386-well, etc.). Experimental samples or samples containing a known amount of the specific recombinant cytokine are then reacted with the immobilised antibody. Following removal of unbound antibody by thorough washing, plates are reacted with the secondary antibody (detection antibody) that is conjugated to an enzyme such as horseradish peroxidase, which when bound, will form a sandwich with the capture antibody and the cytokine (Amsen and De Visser, 2009). The secondary antibody can be conjugated to biotin, which is then detected by addition of streptavidin linked to horseradish peroxidase. A chromogenic substrate can also be added, which is the most commonly used method. Chromogenic substrate is chemically converted by the enzyme coupled to the detection antibody, resulting in colour change. The amount of colour detected is directly proportional to the amount of cytokine in the sample that is bound to the capture antibody. The results are read using a spectrophotometer and compared to the levels of cytokine in control samples where cytokine is not expected to be secreted or to the samples containing known recombinant cytokine levels.

Interleukin (IL)-1α and -1β is activated or secreted into the cytosol following stimulus (Di Paolo and Shayakhmetov, 2016). Targeted ELISA can be used to quantify IL-1α or IL-1β that is released in the culture supernatant of the cells exposed to toxicants, in bronchoalveolar lavage fluid and serum of exposed animals. The assay is also applicable to human serum, cerebrospinal fluid, and peritoneal fluids.

Similarly, other alarmins can also be quantified by ELISA. Western blot is another method that can be used to quantify the release of various alarmins using specific antibodies. ELISA or real-time reverse transcription-polymerase chain reaction (qRT-PCR) assays can also be used to quantify the expression of genes or proteins that are regulated by the receptor binding – e.g. downstream of TLR binding.

Frustrated phagocytosis and cellular uptake of NMs:

In vitro, interaction of NMs with the cellular membrane is investigated by assessing their uptake by lysosomes (Chen et al., 2013; Nel et al., 2009; Varela et al., 2012). Immunohistochemistry methods targeting lysosome specific proteins are regularly employed for this purpose. In co-localisation experiments, lysosomal marker Lysosomal-associated membrane protein 1 (LAMP1) antibody is used to detect particle co-localisation with lysosomes. A combination of Cytoviva hyperspectral microscope and immunolocalisation (Decan et al., 2016) or confocal microscopy to visualise co-localisation of fluorescence labelled nanoparticles with lysosomal markers have been used.

Frustrated phagocytosis is assessed using microscopic techniques such as time-lapse microscopy, backscatter electron microscopy and others (Donaldson et al., 2010; Murphy et al., 2012; Padmore et al., 2017; Pascolo et al., 2013; Schinwald et al., 2012). In addition, MIE 1668 of AOP303 notes other indirect methods for measuring frustrated phagocytosis.

Cellular co-culture models of the pulmonary epithelium:

Complex co-culture systems, such as those containing epithelial cells and immune cells, better model the environment of the lung epithelium and can be used to study the interaction of potentially pro-fibrotic fibres and particles with resident lung cells. This type of model has been used, alongside electron microscopy, to study lung cell interactions with CNTs

following 24 h *in vitro* exposure (Clift *et al.,* 2014). More recently, the EpiAlveolar model, which contains primary human alveolar epithelial cells, endothelial cells, as well as fibroblasts was assessed for its ability to predict fibrosis induced by CNTs (Barasova *et al.,* 2020). Using laser scanning, fluorescence, and enhanced darkfield microscopy, CNT interaction with the resident cells of the model was shown, and this interaction induced the formation of holes in the epithelial model (Barasova *et al.,* 2020). While new co-culture models are a better recapitulation of the native lung environment as compared to traditional mono-cultures, the increased complexity necessitates enhanced expertise in tissue culture techniques, and can make them less practical as compared to submerged mono culture methods.

Ex vivo model of the lung – Precision cut lung slices (PCLS):

Even closer to the *in vivo* condition than co-culture models, PCLS techniques capture the native lung architecture, cell-cell communication and cellularity of the lung. Advancement in culturing and cryopreservation techniques has increased accessibility and use of PCLS for longer term studies (Bai *et al*., 2016, Neuhaus *et al*., 2017). These slices can be cultured *ex vivo* for up to a week with minimal reduction in viability, and the technique has recently been assessed for its applicability to assess nanomaterial induced fibrosis *ex vivo* (Rahman *et al.,* 2020). Using multi-walled carbon nanotubes (MWCNTs) and darkfield microscopy, interaction between the nanofibers and the lung epithelium could be determined. The main downside of this technique is the animal requirement, which precludes their use in a first-pass screening context for the MIE.

References

1. Amsen D, de Visser KE, Town T. Approaches to determine expression of inflammatory cytokines. Methods Mol Biol. 2009;511:107-42. doi: 10.1007/978-1-59745-447-6_5.

2. Bai Y, Krishnamoorthy N, Patel KR, Rosas I, Sanderson MJ, Ai X. Cryopreserved Human Precision-Cut Lung Slices as a Bioassay for Live Tissue Banking. A Viability Study of Bronchodilation with Bitter-Taste Receptor Agonists. Am J Respir Cell Mol Biol. 2016 May;54(5):656-63. doi: 10.1165/rcmb.2015-0290MA.

3. Barosova H, Maione AG, Septiadi D, Sharma M, Haeni L, Balog S, O'Connell O, Jackson GR, Brown D, Clippinger AJ, Hayden P, Petri-Fink A, Stone V, Rothen-Rutishauser B. Use of EpiAlveolar Lung Model to Predict Fibrotic Potential of Multiwalled Carbon Nanotubes. ACS Nano. 2020 Apr 28;14(4):3941-3956. doi: 10.1021/acsnano.9b06860.

4. Behzadi S, Serpooshan V, Tao W, Hamaly MA, Alkawareek MY, Dreaden EC, Brown D, Alkilany AM, Farokhzad OC, Mahmoudi M. Cellular uptake of nanoparticles: journey inside the cell. Chem Soc Rev. 2017 Jul 17;46(14):4218-4244. doi: 10.1039/c6cs00636a.

5. Bianchi ME. DAMPs, PAMPs and alarmins: all we need to know about danger. J Leukoc Biol. 2007 Jan;81(1):1-5. doi: 10.1189/jlb.0306164.

6. Boyles MS, Young L, Brown DM, MacCalman L, Cowie H, Moisala A, Smail F, Smith PJ, Proudfoot L, Windle AH, Stone V. Multi-walled carbon nanotube induced frustrated phagocytosis, cytotoxicity and pro-inflammatory conditions in macrophages are length dependent and greater than that of asbestos. Toxicol In Vitro. 2015 Oct;29(7):1513-28. doi: 10.1016/j.tiv.2015.06.012.

7. Brown DM, Kinloch IA, Bangert U, Windle AH, Walter DM, Walker GS, et al. An in vitro study of the potential of carbon nanotubes and nanofibres to induce inflammatory mediators and frustrated phagocytosis. Carbon. 2007;45(9):1743-56. doi: https://doi.org/10.1016/j.carbon.2007.05.011.

8. Centers for Disease Control and Prevention, National Institute for Occupational Safety and Health. (2011). Current Intelligence Bulletin 62: Asbestos Fibers and Other Elongate Mineral Particles: State of the Science and Roadmap for Research. Retrieved from https://www.cdc.gov/niosh/docs/2011-159/.

9. Cheng LC, Jiang X, Wang J, Chen C, Liu RS. Nano-bio effects: interaction of nanomaterials with cells. Nanoscale. 2013 May 7;5(9):3547-69. doi: 10.1039/c3nr34276j.

10. Clift MJ, Endes C, Vanhecke D, Wick P, Gehr P, Schins RP, Petri-Fink A, Rothen-Rutishauser B. A comparative study of different in vitro lung cell culture systems to assess the most beneficial tool for screening the potential adverse effects of carbon nanotubes. Toxicol Sci. 2014 Jan;137(1):55-64. doi: 10.1093/toxsci/kft216.

11. Decan N, Wu D, Williams A, Bernatchez S, Johnston M, Hill M, Halappanavar S. Characterization of in vitro genotoxic, cytotoxic and transcriptomic responses following exposures to amorphous silica of different sizes. Mutat Res Genet Toxicol Environ Mutagen. 2016 Jan 15;796:8-22. doi: 10.1016/j.mrgentox.2015.11.011.

12. Denholm EM, Phan SH. Bleomycin binding sites on alveolar macrophages. J Leukoc Biol. 1990 Dec;48(6):519-23. doi: 10.1002/jlb.48.6.519.

13. Desai O, Winkler J, Minasyan M, Herzog EL. The Role of Immune and Inflammatory Cells in Idiopathic Pulmonary Fibrosis. Front Med (Lausanne). 2018 Mar 20;5:43. doi: 10.3389/fmed.2018.00043.

14. Di Paolo NC, Shayakhmetov DM. Interleukin 1α and the inflammatory process. Nat Immunol. 2016 Jul 19;17(8):906-13. doi: 10.1038/ni.3503.

15. Dinis-Oliveira RJ, Duarte JA, Sánchez-Navarro A, Remião F, Bastos ML, Carvalho F. Paraquat poisonings: mechanisms of lung toxicity, clinical features, and treatment. Crit Rev Toxicol. 2008;38(1):13-71. doi: 10.1080/10408440701669959.

16. Donaldson K, Murphy FA, Duffin R, Poland CA. Asbestos, carbon nanotubes and the pleural mesothelium: a review of the hypothesis regarding the role of long fibre retention in the parietal pleura, inflammation and mesothelioma. Part Fibre Toxicol. 2010 Mar 22;7:5. doi: 10.1186/1743-8977-7-5.

17. Dörger M, Münzing S, Allmeling AM, Messmer K, Krombach F. Differential responses of rat alveolar and peritoneal macrophages to man-made vitreous fibers in vitro. Environ Res. 2001 Mar;85(3):207-14. doi: 10.1006/enrs.2001.4234.

18. Franks TJ, Colby TV, Travis WD, Tuder RM, Reynolds HY, Brody AR, Cardoso WV, Crystal RG, Drake CJ, Engelhardt J, Frid M, Herzog E, Mason R, Phan SH, Randell SH, Rose MC, Stevens T, Serge J, Sunday ME, Voynow JA, Weinstein BM, Whitsett J, Williams MC. Resident cellular components of the human lung: current knowledge and goals for research on cell phenotyping and function. Proc Am Thorac Soc. 2008 Sep 15;5(7):763-6. doi: 10.1513/pats.200803-025HR.

19. Kierdorf K, Prinz M, Geissmann F, Gomez Perdiguero E. Development and function of tissue resident macrophages in mice. Semin Immunol. 2015 Dec;27(6):369-78. doi: 10.1016/j.smim.2016.03.017.

20. Kim JE, Lim HT, Minai-Tehrani A, Kwon JT, Shin JY, Woo CG, Choi M, Baek J, Jeong DH, Ha YC, Chae CH, Song KS, Ahn KH, Lee JH, Sung HJ, Yu IJ, Beck GR Jr,

Cho MH. Toxicity and clearance of intratracheally administered multiwalled carbon nanotubes from murine lung. J Toxicol Environ Health A. 2010;73(21-22):1530-43. doi: 10.1080/15287394.2010.511578.

21. Luettich K, Sharma M, Yepiskoposyan H, Breheny D, Lowe FJ. An Adverse Outcome Pathway for Decreased Lung Function Focusing on Mechanisms of Impaired Mucociliary Clearance Following Inhalation Exposure. Front Toxicol. 2021 Dec 14;3:750254. doi: 10.3389/ftox.2021.750254.

22. Li XX, Jiang DY, Huang XX, Guo SL, Yuan W, Dai HP. Toll-like receptor 4 promotes fibrosis in bleomycin-induced lung injury in mice. Genet Mol Res. 2015 Dec 21;14(4):17391-8. doi: 10.4238/2015.

23. Matzinger P. The danger model: a renewed sense of self. Science. 2002 Apr 12;296(5566):301-5. doi: 10.1126/science.1071059.

24. Mossman BT, Churg A. Mechanisms in the pathogenesis of asbestosis and silicosis. Am J Respir Crit Care Med. 1998 May;157(5 Pt 1):1666-80. doi: 10.1164/ajrccm.157.5.9707141.

25. Murphy FA, Schinwald A, Poland CA, Donaldson K. The mechanism of pleural inflammation by long carbon nanotubes: interaction of long fibres with macrophages stimulates them to amplify pro-inflammatory responses in mesothelial cells. Part Fibre Toxicol. 2012 Apr 3;9:8. doi: 10.1186/1743-8977-9-8.

26. Murthy S, Larson-Casey JL, Ryan AJ, He C, Kobzik L, Carter AB. Alternative activation of macrophages and pulmonary fibrosis are modulated by scavenger receptor, macrophage receptor with collagenous structure. FASEB J. 2015 Aug;29(8):3527-36. doi: 10.1096/fj.15-271304.

27. Nakayama M. Macrophage Recognition of Crystals and Nanoparticles. Front Immunol. 2018 Jan 29;9:103. doi: 10.3389/fimmu.2018.00103.

28. Nel AE, Mädler L, Velegol D, Xia T, Hoek EM, Somasundaran P, Klaessig F, Castranova V, Thompson M. Understanding biophysicochemical interactions at the nano-bio interface. Nat Mater. 2009 Jul;8(7):543-57. doi: 10.1038/nmat2442.

29. Neuhaus V, Schaudien D, Golovina T, Temann UA, Thompson C, Lippmann T, Bersch C, Pfennig O, Jonigk D, Braubach P, Fieguth HG, Warnecke G, Yusibov V, Sewald K, Braun A. Assessment of long-term cultivated human precision-cut lung slices as an ex vivo system for evaluation of chronic cytotoxicity and functionality. J Occup Med Toxicol. 2017 May 26;12:13. doi: 10.1186/s12995-017-0158-5.

30. Nikota J, Banville A, Goodwin LR, Wu D, Williams A, Yauk CL, Wallin H, Vogel U, Halappanavar S. Stat-6 signaling pathway and not Interleukin-1 mediates multi-walled carbon nanotube-induced lung fibrosis in mice: insights from an adverse outcome pathway framework. Part Fibre Toxicol. 2017 Sep 13;14(1):37. doi: 10.1186/s12989-017-0218-0.

31. Padmore T, Stark C, Turkevich LA, Champion JA. Quantitative analysis of the role of fiber length on phagocytosis and inflammatory response by alveolar macrophages. Biochim Biophys Acta Gen Subj. 2017 Feb;1861(2):58-67. doi: 10.1016/j.bbagen.2016.09.031.

32. Pascolo L, Gianoncelli A, Schneider G, Salomé M, Schneider M, Calligaro C, Kiskinova M, Melato M, Rizzardi C. The interaction of asbestos and iron in lung tissue revealed by synchrotron-based scanning X-ray microscopy. Sci Rep. 2013;3:1123. doi: 10.1038/srep01123.

33. Poland CA, Duffin R, Kinloch I, Maynard A, Wallace WA, Seaton A, Stone V, Brown S, Macnee W, Donaldson K. Carbon nanotubes introduced into the abdominal cavity of

mice show asbestos-like pathogenicity in a pilot study. Nat Nanotechnol. 2008 Jul;3(7):423-8. doi: 10.1038/nnano.2008.111.

34. Rabolli V, Badissi AA, Devosse R, Uwambayinema F, Yakoub Y, Palmai-Pallag M, Lebrun A, De Gussem V, Couillin I, Ryffel B, Marbaix E, Lison D, Huaux F. The alarmin IL-1α is a master cytokine in acute lung inflammation induced by silica micro- and nanoparticles. Part Fibre Toxicol. 2014 Dec 13;11:69. doi: 10.1186/s12989-014-0069-x.

35. Rahman L, Williams A, Gelda K, Nikota J, Wu D, Vogel U, Halappanavar S. 21st Century Tools for Nanotoxicology: Transcriptomic Biomarker Panel and Precision-Cut Lung Slice Organ Mimic System for the Assessment of Nanomaterial-Induced Lung Fibrosis. Small. 2020 Sep;16(36):e2000272. doi: 10.1002/smll.202000272.

36. Schinwald A, Donaldson K. Use of back-scatter electron signals to visualise cell/nanowires interactions in vitro and in vivo; frustrated phagocytosis of long fibres in macrophages and compartmentalisation in mesothelial cells in vivo. Part Fibre Toxicol. 2012 Aug 28;9:34. doi: 10.1186/1743-8977-9-34.

37. Suwara MI, Green NJ, Borthwick LA, Mann J, Mayer-Barber KD, Barron L, Corris PA, Farrow SN, Wynn TA, Fisher AJ, Mann DA. IL-1α released from damaged epithelial cells is sufficient and essential to trigger inflammatory responses in human lung fibroblasts. Mucosal Immunol. 2014 May;7(3):684-93. doi: 10.1038/mi.2013.87.

38. Varela JA, Bexiga MG, Åberg C, Simpson JC, Dawson KA. Quantifying size-dependent interactions between fluorescently labeled polystyrene nanoparticles and mammalian cells. J Nanobiotechnology. 2012 Sep 24;10:39. doi: 10.1186/1477-3155-10-39.

List of Key Events in the AOP

Event: 1496: Increased, secretion of proinflammatory mediators

Short Name: Increased proinflammatory mediators

Key Event Component

Process	Object	Action
cytokine production involved in inflammatory response	Cytokine	increased
chemokine secretion	Chemokine	increased
complement activation		increased
	Interleukin	increased

AOPs Including This Key Event

AOP ID and Name	Event Type
Aop:173 - Substance interaction with the pulmonary resident cell membrane components leading to pulmonary fibrosis	Key Event
Aop:320 - Binding of SARS-CoV-2 to ACE2 receptor leading to acute respiratory distress associated mortality	Key Event
Aop:382 - Angiotensin II type 1 receptor (AT1R) agonism leading to lung fibrosis	Key Event
Aop:392 - Decreased fibrinolysis and activated bradykinin system leading to hyperinflammation	Key Event
Aop:409 - Frustrated phagocytosis leads to malignant mesothelioma	Key Event
Aop:377 - Dysregulated prolonged Toll Like Receptor 9 (TLR9) activation leading to Multi Organ Failure involving Acute Respiratory Distress Syndrome (ARDS)	Key Event
Aop:39 - Covalent Binding, Protein, leading to Increase, Allergic Respiratory Hypersensitivity Response	Key Event
Aop:319 - Binding to ACE2 leading to lung fibrosis	Key Event
Aop:451 - Interaction with lung resident cell membrane components leads to lung cancer	Key Event
Aop:468 - Binding of SARS-CoV-2 to ACE2 leads to hyperinflammation (via cell death)	Key Event
Aop:237 - Substance interaction with lung resident cell membrane components leading to atherosclerosis	Key Event

Biological context

Level of Biological Organization
Cellular

Domain of Applicability

Taxonomic Applicability

Term	Scientific Term	Evidence	Links
mouse	Mus musculus	High	NCBI
rats	Rattus norvegicus	High	NCBI
human	Homo sapiens	High	NCBI

Life Stage Applicability

Life Stage	Evidence
Adults	High

Sex Applicability

Sex	Evidence
Male	High
Female	High

Human, mouse, rat

Cytokines are the common pro-inflammatory mediators secreted following inflammogenic stimuli. Cytokines can be defined as a diverse group of signaling protein molecules. They are secreted by different cell types in different tissues and in all mammalian species, irrespective of gender, age or sex. A lot of literature is available to support cross species, gender and developmental stage application for this KE. The challenge is the specificity; most cytokines exhibit redundant functions and many are pleotropic.

Key Event Description

Pro-inflammatory mediators are the chemical and biological molecules that initiate and regulate inflammatory reactions. Pro-inflammatory mediators are secreted following exposure to an inflammogen in a gender/sex or developmental stage independent manner. They are secreted during inflammation in all species. Different types of pro-inflammatory mediators are secreted during innate or adaptive immune responses across various species (Mestas and Hughes, 2004). Cell-derived pro-inflammatory mediators include cytokines, chemokines, and growth factors. Blood derived pro-inflammatory mediators include vasoactive amines, complement activation products and others. These modulators can be grouped based on the cell type that secrete them, their cellular localisation and also based on the type of immune response they trigger. For example, members of the interleukin (IL) family including IL-2, IL-4, IL-7, IL-9, IL-15, IL-21, IL-3, IL-5 and Granulocyte-macrophage colony stimulating factor (GM-CSF) are involved in the adaptive immune responses. The pro-inflammatory cytokines include IL-1 family (IL-1α, IL-1β, IL-1rα, IL-18, IL-36α, IL-36β, IL-36γ, IL-36Rα, IL-37), IL-6family, Tumor necrosis factor (TNF) family, IL-17, and Interferon gamma (IFN-γ) (Turner et al., 2014). While IL-4 and IL-5 are considered T helper (Th) cell type 2 response, IFN-γ is suggested to be Th1 type response.

Different types of pro-inflammatory mediators are secreted during innate or adaptive immune responses across various species (Mestas and Hughes, 2004). However, IL-1 family cytokines, IL-4, IL-5, IL-6, TNF-α, IFN-γ are the commonly measured mediators in experimental animals and in humans. Similar gene expression patterns involving inflammation and matrix remodelling are observed in human patients of pulmonary fibrosis and mouse lungs exposed to bleomycin (Kaminski, 2002).

Literature evidence for its perturbation:

Several studies show increased proinflammatory mediators in rodent lungs and bronchoalveolar lavage fluid, and in cell culture supernatants following exposure to a variety of carbon nanotube (CNT) types and other materials. Poland et al., 2008 showed that long and thin CNTs (>5 µm) can elicit asbestos-like pathogenicity through the continual release of pro-inflammatory cytokines and reactive oxygen species. Exposure to crystalline silica induces release of inflammatory cytokines (TNF-α, IL-1, IL-6), transcription factors (Nuclear factor kappa B [NF-κB], Activator protein-1 [AP-1]) and kinase signalling pathways in mice that contain NF-κB luciferase reporter (Hubbard et al., 2002). Boyles et al., 2015 found that lung responses to long multi-walled carbon nanotubes (MWCNTs) included high expression levels of pro-inflammatory mediators Monocyte chemoattractant protein 1 (MCP-1), Transforming growth factor beta 1 (TGF-β1), and TNF-α (Boyles et al., 2015). Bleomycin administration in rodents induces lung

inflammation and increased expression of pro-inflammatory mediators (Park et al., 2019). Inflammation induced by bleomycin, paraquat and CNTs is characterised by the altered expression of pro-inflammatory mediators. A large number of nanomaterials induce expression of cytokines and chemokines in lungs of rodents exposed via inhalation (Halappanavar et al., 2011; Husain et al., 2015a). Similarities are observed in gene programs involving pro-inflammatory event is observed in both humans and experimental mice (Zuo et al., 2002).

How it is Measured or Detected

The selection of pro-inflammatory mediators for investigation varies based on the expertise of the lab, cell types studied and the availability of the specific antibodies.

Real-time reverse transcription-polymerase chain reaction (qRT-PCR) – will measure the abundance of cytokine mRNA in a given sample. The method involves three steps: conversion of RNA into cDNA by reverse transcription method, amplification of cDNA using the PCR, and the real-time detection and quantification of amplified products (amplicons) (Nolan et al., 2006). Amplicons are detected using fluorescence, increase in which is directly proportional to the amplified PCR product. The number of cycles required per sample to reach a certain threshold of fluorescence (set by the user – usually set in the linear phase of the amplification, and the observed difference in samples to cross the set threshold reflects the initial amount available for amplification) is used to quantify the relative amount in the samples. The amplified products are detected by the DNA intercalating minor groove-binding fluorophore SYBR green, which produces a signal when incorporated into double-stranded amplicons. Since the cDNA is single stranded, the dye does not bind enhancing the specificity of the results. There are other methods such as nested fluorescent probes for detection, but SYBR green is widely used. RT-PCR primers specific to several pro-inflammatory mediators in several species including mouse, rat and humans, are readily available commercially.

Enzyme-linked immunosorbent assays (ELISA) – permit quantitative measurement of antigens in biological samples. The method is the same as described for the MIE. Both ELISA and qRT-PCR assays are used *in vivo* and are readily applicable to *in vitro* cell culture models, where cell culture supernatants or whole cell homogenates are used for ELISA or mRNA assays. Both assays are straight forward, quantitative and require relatively a small amount of input sample.

Apart from assaying single protein or gene at a time, cytokine bead arrays or cytokine PCR arrays can also be used to detect a whole panel of inflammatory mediators in a multiplex method (Husain et al., 2015b). This method is quantitative and especially advantageous when the sample amount available for testing is scarce. Lastly, immunohistochemistry can also be used to detect specific immune cell types producing the pro-inflammatory mediators and its downstream effectors in any given tissue (Costa et al., 2017). Immunohistochemistry results can be used as weight of evidence; however, the technique is not quantitative and depending on the specific antibodies used, the assay sensitivity may also become an issue (Amsen and De Visser, 2009).

Cell models - of varying complexity have been used to assess the expression of pro-inflammatory mediators. Two dimensional submerged monocultures of the main fibrotic effector cells – lung epithelial cells, macrophages, and fibroblasts – have routinely been used *in vitro* due to the large literature base, and ease of use, but do not adequately mimic the *in vivo* condition (Sharma *et al.*, 2016; Sundarakrishnan *et al.*, 2018). Recently, the EpiAlveolar *in vitro* lung model (containing epithelial cells, endothelial cells, and fibroblasts) was used to predict the fibrotic potential of MWCNTs, and researchers noted

increases in the pro-inflammatory molecules TNF-α, IL-1β, and the pro-fibrotic TGF-β using ELISA (Barasova *et al.*, 2020). A similar, but less complicated co-culture model of immortalized human alveolar epithelial cells and idiopathic pulmonary fibrosis patient derived fibroblasts was used to assess pro-fibrotic signalling, and noted enhanced secretion of Platelet derived growth factor (PDGF) and Basic fibroblast growth factor (bFGF), as well as evidence for epithelial to mesenchymal transition of epithelial cells in this system (Prasad et al., 2014). Models such as these better capitulate the *in vivo* pulmonary alveolar capillary, but have lower reproducibility as compared to traditional submerged mono-culture experiments.

References

1. Amsen D, de Visser KE, Town T. Approaches to determine expression of inflammatory cytokines. Methods Mol Biol. 2009;511:107-42. doi: 10.1007/978-1-59745-447-6_5.

2. Barosova H, Maione AG, Septiadi D, Sharma M, Haeni L, Balog S, O'Connell O, Jackson GR, Brown D, Clippinger AJ, Hayden P, Petri-Fink A, Stone V, Rothen-Rutishauser B. Use of EpiAlveolar Lung Model to Predict Fibrotic Potential of Multiwalled Carbon Nanotubes. ACS Nano. 2020 Apr 28;14(4):3941-3956. doi: 10.1021/acsnano.9b06860.

3. Boyles MS, Young L, Brown DM, MacCalman L, Cowie H, Moisala A, Smail F, Smith PJ, Proudfoot L, Windle AH, Stone V. Multi-walled carbon nanotube induced frustrated phagocytosis, cytotoxicity and pro-inflammatory conditions in macrophages are length dependent and greater than that of asbestos. Toxicol In Vitro. 2015 Oct;29(7):1513-28. doi: 10.1016/j.tiv.2015.06.012.

4. Costa PM, Gosens I, Williams A, Farcal L, Pantano D, Brown DM, Stone V, Cassee FR, Halappanavar S, Fadeel B. Transcriptional profiling reveals gene expression changes associated with inflammation and cell proliferation following short-term inhalation exposure to copper oxide nanoparticles. J Appl Toxicol. 2018 Mar;38(3):385-397. doi: 10.1002/jat.3548.

5. Halappanavar S, Jackson P, Williams A, Jensen KA, Hougaard KS, Vogel U, Yauk CL, Wallin H. Pulmonary response to surface-coated nanotitanium dioxide particles includes induction of acute phase response genes, inflammatory cascades, and changes in microRNAs: a toxicogenomic study. Environ Mol Mutagen. 2011 Jul;52(6):425-39. doi: 10.1002/em.20639.

6. Hubbard AK, Timblin CR, Shukla A, Rincón M, Mossman BT. Activation of NF-kappaB-dependent gene expression by silica in lungs of luciferase reporter mice. Am J Physiol Lung Cell Mol Physiol. 2002 May;282(5):L968-75. doi: 10.1152/ajplung.00327.2001.

7. Husain M, Kyjovska ZO, Bourdon-Lacombe J, Saber AT, Jensen KA, Jacobsen NR, Williams A, Wallin H, Halappanavar S, Vogel U, Yauk CL. Carbon black nanoparticles induce biphasic gene expression changes associated with inflammatory responses in the lungs of C57BL/6 mice following a single intratracheal instillation. Toxicol Appl Pharmacol. 2015a Dec 15;289(3):573-88. doi: 10.1016/j.taap.2015.11.003.

8. Husain M, Wu D, Saber AT, Decan N, Jacobsen NR, Williams A, Yauk CL, Wallin H, Vogel U, Halappanavar S. Intratracheally instilled titanium dioxide nanoparticles

translocate to heart and liver and activate complement cascade in the heart of C57BL/6 mice. Nanotoxicology. 2015b;9(8):1013-22. doi: 10.3109/17435390.2014.996192.

9. Kaminski N. Microarray analysis of idiopathic pulmonary fibrosis. Am J Respir Cell Mol Biol. 2003 Sep;29(3 Suppl):S32-6.

10. Mestas J, Hughes CC. Of mice and not men: differences between mouse and human immunology. J Immunol. 2004 Mar 1;172(5):2731-8. doi: 10.4049/jimmunol.172.5.2731.

11. Nolan T, Hands RE, Bustin SA. Quantification of mRNA using real-time RT-PCR. Nat Protoc. 2006;1(3):1559-82. doi: 10.1038/nprot.2006.236.

12. Park SJ, Im DS. Deficiency of Sphingosine-1-Phosphate Receptor 2 ($S1P_2$) Attenuates Bleomycin-Induced Pulmonary Fibrosis. Biomol Ther (Seoul). 2019 May 1;27(3):318-326. doi: 10.4062/biomolther.2018.131.

13. Poland CA, Duffin R, Kinloch I, Maynard A, Wallace WA, Seaton A, Stone V, Brown S, Macnee W, Donaldson K. Carbon nanotubes introduced into the abdominal cavity of mice show asbestos-like pathogenicity in a pilot study. Nat Nanotechnol. 2008 Jul;3(7):423-8. doi: 10.1038/nnano.2008.111.

14. Prasad S, Hogaboam CM, Jarai G. Deficient repair response of IPF fibroblasts in a co-culture model of epithelial injury and repair. Fibrogenesis Tissue Repair. 2014 Apr 29;7:7. doi: 10.1186/1755-1536-7-7.

15. Sharma M, Nikota J, Halappanavar S, Castranova V, Rothen-Rutishauser B, Clippinger AJ. Predicting pulmonary fibrosis in humans after exposure to multi-walled carbon nanotubes (MWCNTs). Arch Toxicol. 2016 Jul;90(7):1605-22. doi: 10.1007/s00204-016-1742-7.

16. Sundarakrishnan A, Chen Y, Black LD, Aldridge BB, Kaplan DL. Engineered cell and tissue models of pulmonary fibrosis. Adv Drug Deliv Rev. 2018 Apr;129:78-94. doi: 10.1016/j.addr.2017.12.013.

17. Turner MD, Nedjai B, Hurst T, Pennington DJ. Cytokines and chemokines: At the crossroads of cell signalling and inflammatory disease. Biochim Biophys Acta. 2014 Nov;1843(11):2563-2582. doi: 10.1016/j.bbamcr.2014.05.014.

18. Zuo F, Kaminski N, Eugui E, Allard J, Yakhini Z, Ben-Dor A, Lollini L, Morris D, Kim Y, DeLustro B, Sheppard D, Pardo A, Selman M, Heller RA. Gene expression analysis reveals matrilysin as a key regulator of pulmonary fibrosis in mice and humans. Proc Natl Acad Sci U S A. 2002 Apr 30;99(9):6292-7. doi: 10.1073/pnas.092134099.

Event: 1497: Increased, recruitment of inflammatory cells

Short Name: Recruitment of inflammatory cells

Key Event Component

Process	Object	Action
inflammatory response	inflammatory cell	increased
macrophage activation	macrophage	increased

AOPs Including This Key Event

AOP ID and Name	Event Type
Aop:173 - Substance interaction with the pulmonary resident cell membrane components leading to pulmonary fibrosis	Key Event
Aop:303 - Frustrated phagocytosis-induced lung cancer	Key Event
Aop:392 - Decreased fibrinolysis and activated bradykinin system leading to hyperinflammation	Key Event
Aop:409 - Frustrated phagocytosis leads to malignant mesothelioma	Key Event
Aop:377 - Dysregulated prolonged Toll Like Receptor 9 (TLR9) activation leading to Multi Organ Failure involving Acute Respiratory Distress Syndrome (ARDS)	Key Event
Aop:451 - Interaction with lung resident cell membrane components leads to lung cancer	Key Event
Aop:468 - Binding of SARS-CoV-2 to ACE2 leads to hyperinflammation (via cell death)	Key Event
Aop:493 - ERa inactivation alters AT expansion and functions and leads to insulin resistance and metabolically unhealthy obesity	Key Event

Biological context

Level of Biological Organization
Tissue

Domain of Applicability

Taxonomic Applicability

Term	Scientific Term	Evidence	Links
human	Homo sapiens	High	NCBI
mouse	Mus musculus	High	NCBI
rats	Rattus norvegicus	High	NCBI

Life Stage Applicability

Life Stage	Evidence
All life stages	High

Sex Applicability

Sex	Evidence
Mixed	High

Key Event Description

Pro-inflammatory cells originate in bone marrow and are recruited to the site of infection or injury via circulation following specific pro-inflammatory mediator (cytokine and chemokine) signalling. Pro-inflammatory cells are recruited to lungs to clear the invading pathogen or the toxic substance. Monocytes (dendritic cells, macrophages, and neutrophils) are subsets of circulating white blood cells that are involved in the immune responses to pathogen or toxicant stimuli (Kolaczkowska and Kubes, 2013; Kopf et al., 2015). They are derived from the bone marrow. They can differentiate into different macrophage types and dendritic cells. They can be categorised based on their size, the type of cell surface receptors and their ability to differentiate following external or internal stimulus such as increased expression of cytokines. Monocytes participate in tissue healing, clearance of toxic substance or pathogens, and in the initiation of adaptive immunity. Recruited monocytes can also influence pathogenesis (Ingersoll et al., 2011). Sensing or recognition of pathogens and harmful substances results in the recruitment of monocytes to lungs (Shi and Pamer, 2011). Activated immune cells secrete a variety of pro-inflammatory mediators, the purpose of which is to propagate the immune signalling and response, which when not controlled, leads to chronic inflammation, cell death and tissue injury. Thus, Event 1496 and Event 1497 act in a positive feedback loop mechanism and propagate the proinflammatory environment.

Literature evidence for its perturbation:

Macrophages accumulate in bronchoalveolar fluid (BALF) post-exposure to bleomycin (Phan et al., 1980; Smith et al., 1995). Nanomaterial (NM)-induced inflammation is predominantly neutrophilic (Poulsen et al., 2015; Rahman L et al., 2017a; Rahman et al., 2017b; Shvedova et al., 2005). An increased number of neutrophils (Reynolds et al., 1977) is observed in the BALF of patients with idiopathic pulmonary fibrosis. Eosinophils are a type of white blood cells and a type of granulocytes (contain granules and enzymes) that are recruited following exposure to allergens, during allergic reactions such as asthma or during fibrosis (Reynolds et al., 1977). Multi-walled carbon nanotubes (MWCNTs) induce increased eosinophil count in lungs (Køb ler C et al., 2015). MWCNTs act as allergens and induce lung infiltration of eosinophils and cause airway hypersensitivity (Beamer et al., 2013).

It is important to note that the stressor-induced Event 1495, Event 1496, and Event 1497 are part of the functional changes that we collectively consider as inflammation, and together, they mark the initiation of acute inflammatory phase. Event 1495 and Event 1496 occur at the cellular level. Event 1497 occurs at the tissue level.

How it is Measured or Detected

In vivo, recruitment of pro-inflammatory cells is measured using BALF cellularity assay. The fluid lining the lung epithelium is lavaged (BALF) and its composition is assessed as marker of lung immune response to the toxic substances or pathogens. BALF is assessed quantitatively for types of infiltrating cells, levels and types of cytokines and chemokines. Thus, BALF assessment can aid in developing dose-response of a substance, to rank a substances' potency and to set up no effect level of exposure for the regulatory decision making. For NMs, *in vivo* BALF assessment is recommended as a mandatory test (discussed in ENV/JM/MONO(2012)40 and also in OECD inhalation test guideline for NMs). Temporal changes in the BALF composition can be prognostic of initiation and progression of lung immune disease (Cho et al., 2010).

In vitro, it is difficult to assess the recruitment of pro-inflammatory cells. Thus, a suit of pro-inflammatory mediators specific to cell types are assessed using the same techniques mentioned above (real-time reverse transcription-polymerase chain reaction [qRT-PCR], enzyme-linked immunosorbent assays [ELISA], immunohistochemistry) in cell culture models, as indicative of recruitment of cells into the lungs. Alternatively, the use of precision cut lung slices can allow for limited assessment of recruitment of tissue resident inflammatory cells, based on the repertoire of cells remaining in the specific slice following harvesting. This method was used to show that there is a histological increase in inflammatory foci following treatment with bleomycin and MWCNTs (Rahman et al., 2020). Finally, more complicated microfluidic lung-on-a-chip devices can be used to assess the migration of select immune cells and fibroblasts toward a simulated epithelium following treatment with a pro-fibrotic compound (He et al., 2017). However, this method is limited to two cell types, and it lacks the reservoirs of immune cells present in the body *in vivo*.

References

1. Beamer CA, Girtsman TA, Seaver BP, Finsaas KJ, Migliaccio CT, Perry VK, Rottman JB, Smith DE, Holian A. IL-33 mediates multi-walled carbon nanotube (MWCNT)-induced airway hyper-reactivity via the mobilization of innate helper cells in the lung. Nanotoxicology. 2013 Sep;7(6):1070-81. doi: 10.3109/17435390.2012.702230.

2. Cho WS, Duffin R, Poland CA, Howie SE, MacNee W, Bradley M, Megson IL, Donaldson K. Metal oxide nanoparticles induce unique inflammatory footprints in the lung: important implications for nanoparticle testing. Environ Health Perspect. 2010 Dec;118(12):1699-706. doi: 10.1289/ehp.1002201.

3. He J, Chen W, Deng S, Xie L, Feng J, Geng J, et al. Modeling alveolar injury using microfluidic co-cultures for monitoring bleomycin-induced epithelial/fibroblastic cross-talk disorder. RSC Advances. 2017 7(68):42738-49. doi: 10.1039/C7RA06752F.

4. Ingersoll MA, Platt AM, Potteaux S, Randolph GJ. Monocyte trafficking in acute and chronic inflammation. Trends Immunol. 2011 Oct;32(10):470-7. doi: 10.1016/j.it.2011.05.001.

5. Køble C, Poulsen SS, Saber AT, Jacobsen NR, Wallin H, Yauk CL, Halappanavar S, Vogel U, Qvortrup K, Mølhave K. Time-dependent subcellular distribution and effects of carbon nanotubes in lungs of mice. PLoS One. 2015 Jan 23;10(1):e0116481. doi: 10.1371/journal.pone.0116481.

6. Kolaczkowska E, Kubes P. Neutrophil recruitment and function in health and inflammation. Nat Rev Immunol. 2013 Mar;13(3):159-75. doi: 10.1038/nri3399.

7. Kopf M, Schneider C, Nobs SP. The development and function of lung-resident macrophages and dendritic cells. Nat Immunol. 2015 Jan;16(1):36-44. doi: 10.1038/ni.3052.

8. Phan SH, Thrall RS, Ward PA. Bleomycin-induced pulmonary fibrosis in rats: biochemical demonstration of increased rate of collagen synthesis. Am Rev Respir Dis. 1980 Mar;121(3):501-6. doi: 10.1164/arrd.1980.121.3.501.

9. Poulsen SS, Saber AT, Williams A, Andersen O, Køble C, Atluri R, Pozzebon ME, Mucelli SP, Simion M, Rickerby D, Mortensen A, Jackson P, Kyjovska ZO, Mølhave K,

Jacobsen NR, Jensen KA, Yauk CL, Wallin H, Halappanavar S, Vogel U. MWCNTs of different physicochemical properties cause similar inflammatory responses, but differences in transcriptional and histological markers of fibrosis in mouse lungs. Toxicol Appl Pharmacol. 2015 Apr 1;284(1):16-32. doi: 10.1016/j.taap.2014.12.011.

10. Rahman L, Wu D, Johnston M, William A, Halappanavar S. Toxicogenomics analysis of mouse lung responses following exposure to titanium dioxide nanomaterials reveal their disease potential at high doses. Mutagenesis. 2017a Jan;32(1):59-76. doi: 10.1093/mutage/gew048.

11. Rahman L, Jacobsen NR, Aziz SA, Wu D, Williams A, Yauk CL, White P, Wallin H, Vogel U, Halappanavar S. Multi-walled carbon nanotube-induced genotoxic, inflammatory and pro-fibrotic responses in mice: Investigating the mechanisms of pulmonary carcinogenesis. Mutat Res Genet Toxicol Environ Mutagen. 2017b Nov;823:28-44. doi: 10.1016/j.mrgentox.2017.08.005.

12. Rahman L, Williams A, Gelda K, Nikota J, Wu D, Vogel U, Halappanavar S. 21st Century Tools for Nanotoxicology: Transcriptomic Biomarker Panel and Precision-Cut Lung Slice Organ Mimic System for the Assessment of Nanomaterial-Induced Lung Fibrosis. Small. 2020 Sep;16(36):e2000272. doi: 10.1002/smll.202000272.

13. Reynolds HY, Fulmer JD, Kazmierowski JA, Roberts WC, Frank MM, Crystal RG. Analysis of cellular and protein content of broncho-alveolar lavage fluid from patients with idiopathic pulmonary fibrosis and chronic hypersensitivity pneumonitis. J Clin Invest. 1977 Jan;59(1):165-75. doi: 10.1172/JCI108615.

14. Shi C, Pamer EG. Monocyte recruitment during infection and inflammation. Nat Rev Immunol. 2011 Oct 10;11(11):762-74. doi: 10.1038/nri3070.

15. Shvedova AA, Kisin ER, Mercer R, Murray AR, Johnson VJ, Potapovich AI, Tyurina YY, Gorelik O, Arepalli S, Schwegler-Berry D, Hubbs AF, Antonini J, Evans DE, Ku BK, Ramsey D, Maynard A, Kagan VE, Castranova V, Baron P. Unusual inflammatory and fibrogenic pulmonary responses to single-walled carbon nanotubes in mice. Am J Physiol Lung Cell Mol Physiol. 2005 Nov;289(5):L698-708. doi: 10.1152/ajplung.00084.2005.

16. Smith RE, Strieter RM, Zhang K, Phan SH, Standiford TJ, Lukacs NW, Kunkel SL. A role for C-C chemokines in fibrotic lung disease. J Leukoc Biol. 1995 May;57(5):782-7. doi: 10.1002/jlb.57.5.782.

Event: 1498: Loss of alveolar capillary membrane integrity

Short Name: Loss of alveolar capillary membrane integrity

AOPs Including This Key Event

AOP ID and Name	Event Type
Aop:173 - Substance interaction with the pulmonary resident cell membrane components leading to pulmonary fibrosis	Key Event
Aop:302 - Lung surfactant function inhibition leading to decreased lung function	Key Event

Biological context

Level of Biological Organization
Tissue

Organ terms

Organ term
lung

Domain of Applicability

Taxonomic Applicability

Term	Scientific Term	Evidence	Links
mouse	Mus musculus	High	NCBI
human	Homo sapiens	Not Specified	NCBI

Life Stage Applicability

Life Stage	Evidence
Adult	High

Sex Applicability

Sex	Evidence
Male	High
Female	Not Specified

Key Event Description

The alveolar-capillary membrane (ACM) is the gas exchange surface of the lungs that is only ~0.3µm thick and is the largest surface area within the lung that separates the interior of the body from the environment. It is comprised of the microvascular endothelium, interstitium, and alveolar epithelium. As a consequence of its anatomical position, and the large surface area, it is the first point of contact for any inhaled pathogen, particles or toxic substances. Thus, ACM is subjected to injury constantly and rapidly repaired following the external insults without formation of fibrosis or scar tissue. The extent of ACM injury or how rapidly its integrity is restored is a pivotal determinant of whether the lung restores its normal functioning following an injury or is replaced by fibrotic lesion or scar tissue (Fukuda et al., 1987; Schwarz et al., 2001). Significant loss of endothelium and epithelium of the ACM results in loss of the barrier and membrane integrity. Increased membrane permeability leading to efflux of protein-rich fluid into the peribronchovascular interstitium

and the distal airspaces of the lung, disruption of normal fluid transport via downregulated Na^+ channels or malfunctioning Na^+/K^+ATPase pumps, loss of surfactant production, increased expression of epithelial or endothelial cell markers such as Intercellular adhesion molecule-1 (ICAM-1) or decreased expression of surfactant protein D (SP-D) are few of the markers of decreasing lung compliance arising from the lost integrity of ACM (Johnson and Matthay, 2010).

Literature evidence for its perturbation:

Bleomycin exposure causes alveolar barrier dysfunction (Miyoshi et al., 2013). Cigarette smoke impairs tight junction proteins and leads to altered permeability of the epithelial barrier (Schamberger et al., 2014). Exposure to bleomycin destroys the structural architecture of tight junctions, increases permeability, epithelial death and loss of specialised repair proteins such as claudins. Thoracic radiation and bleomycin induced lung injury results in decreased expression of E-cadherin and Aquaporin-5 (AQP5) expression (Almeida et al., 2013; Gabazza et al., 2004).

Repeated exposure to biopersistent toxic substances, pathogens or lung irritants initiate non-resolving inflammation and ACM injury (Costabel et al., 2012). Chronic inflammation mediated by overexpression of cytokines such as Interleukine (IL)-1 (Kolb et al., 2001), Tumor necrosis factor alpha (TNF-α) (Sime et al., 1998), T helper type 2 cytokine IL-13 or exposure to specific proteinases initiate ACM injury, leading to significant loss of the epithelium and endothelium of the ACM resulting loss of barrier integrity. In patients diagnosed with idiopathic pulmonary fibrosis (IPF), both type 1 pneumocyte & endothelial cell injury with ACM barrier loss is observed.

Bleomycin and silica exposure generate persistent inflammation and lung damage (Chua et al., 2005; Thrall and Scaliso, 1995). Exposure to single-walled carbon nanotubes (SWCNTs) induces persistent inflammation, granuloma formation and diffuse intestinal fibrosis in mice after pharyngeal aspiration (Shvedova *et al.,* 2005). Multi-walled carbon nanotubes act as allergens and induce lung infiltration of eosinophils and cause airway hypersensitivity (Beamer *et al.,* 2013). Inhaled particles induce chronic inflammation (Ernst *et al.,* 2002; Hamilton et al., 2008; Thakur et al., 2008). Increased numbers of alveolar macrophages, neutrophils and eosinophils are observed in the bronchoalveolar lavage fluid (BALF) of patients suffering from IPF and chronic inflammation is associated with decreased survival (Parra *et al.,* 2007; Schwartz *et al.,* 1991; Yasuoka *et al.,* 1985).

The BALF of patients diagnosed with interstitial diseases contains increased levels of 8-isoprostane (Psathakis *et al.,* 2006) and carbonyl-modified proteins (Lenz et al., 1996), markers of oxidative modification of lipids and proteins. *In vivo*, increased reactive oxygen species (ROS) levels in rodents (Ghio *et al.,* 1998) and enzymatic production of nitric oxide in rat alveolar macrophages is observed after asbestos exposure (Quinlan *et al.,* 1998). Some nanoparticles induce oxidative stress that contributes to cellular toxicity (Shi *et al.,* 2012). Nicotinamide adenine dinucleotide phosphate (NADPH) oxidase derived ROS is a critical determinant of the pulmonary response to SWCNTs in mice (Shvedova *et al.,* 2008). Oxidative lipidomics analysis of the lungs of carbon nanotube (CNT)-exposed mice showed, phospholipid oxidation (Tyurina *et al.,* 2011). ROS synthesis is suggested to be important for inflammosome activation involving NLR-related protein 3 complex, activated caspase-1 and IL-1β, which is observed following exposure to a variety of pro-inflammatory stimuli including, asbestos and crystalline silica (Cassel *et al.,* 2008; Dostert *et al.,* 2008) and long needle-like CNTs. In the case of asbestos, frustrated phagocytosis triggered ROS synthesis leads to inflammosome activation, which is associated with asbestos induced pathology (Dostert *et al.,* 2008).

How it is Measured or Detected

Proteinosis, BALF protein content:

Compromised ACM barrier integrity *in vivo* can be measured by measuring total protein or total albumin content in the BALF derived from experimental animals exposed to lung toxicants or in human patients suffering from lung fibrosis. In addition to albumin, the total urea in BALF is also a good indicator of the ACM integrity loss (Schmekel et al., 1992).

Cell type considerations:

ACM loss is a tissue level event. *In vitro*, assays with human cells are desired; however, the use of cells derived from experimental animals including alveolar macrophages, dendritic cells, epithelial cells, and neutrophils are routinely used. Primary cells are preferred over immortalised cell types that are in culture for a long period of time. *In vitro*, studies often assess the altered expression of pro-inflammatory mediators, increased ROS synthesis or oxidative stress and cytotoxicity events, an interplay between these three biological events occurring following exposure to stressors, is suggested to induce cell injury, which is reflective of tissue injury or loss of ACM (Halappanavar *et al.,* 2019) *in vivo*.

Cytotoxicity assessment:

Cellular viability or cytotoxicity assays are the most commonly used endpoints to assess the leaky or compromised cell membrane. The most commonly employed method is the trypan blue exclusion assay – a dye exclusion assay where cells with intact membrane do not permit entry of the dye into cells and thus remain clear, whereas the dye diffuses into cells with damaged membrane turning them to blue colour. Other high throughput assays that use fluorescent DNA stains such as ethidium bromide or propidium iodide can also be used and cells that have incorporated the dye can be scored using flow cytometry.

Lactate dehydrogenase (LDH) release assay is a very sensitive cytotoxicity assay that measures the amount of LDH released in the media following membrane injury. The assay is based on measuring the reduction of nicotinamide adenine dinucleotide (NAD) and conversion of a tetrazolium dye that is measured at a wavelength of 490 nm.

The Calcein AM assay depends on the hydrolysis of calcein AM (a non-fluorescent hydrophobic compound that permeates live cells by simple diffusion) by non-specific intracellular esterases resulting in production of calcein, a hydrophilic and strongly fluorescent compound that is readily released into the cell culture media by the damaged cells.

Although the above mentioned assays work for almost all chemicals, insoluble substances such as nanomaterials can confound the assay by inhibiting the enzyme activity or interfering with the absorbance reading. Thus, care must be taken to include appropriate controls in the assays.

Transepithelial/transendothelial electrical resistance (TEER):

TEER is an accepted quantitative technique that measures the integrity of tight junctions in cell culture models of endothelial and epithelial cell monolayers. They are based on measuring ohmic resistance or measuring impedance across a wide range of frequencies.

Other:

The other methods include targeted reverse transcription polymerase chain reaction (RT-PCR) or enzyme-linked immunosorbent assays (ELISA) for tight junction proteins, cell

adhesion molecules and inflammatory mediators such as Interferon gamma (IFN-γ), IL-10, and IL-13. Advanced *in vitro* co-culture models, like the EpiAlveolar model system, and other similar systems present an intact capillary membrane that can be used to assess loss in the membrane integrity (via TEER) after exposure to pro-fibrotic stressors like crystalline silica and Transforming growth factor beta (TGF-β) (Barasova *et al.*, 2020, Kasper *et al.*, 2011).

References

1. Almeida C, Nagarajan D, Tian J, Leal SW, Wheeler K, Munley M, Blackstock W, Zhao W. The role of alveolar epithelium in radiation-induced lung injury. PLoS One. 2013;8(1):e53628. doi: 10.1371/journal.pone.0053628.

2. Barosova H, Maione AG, Septiadi D, Sharma M, Haeni L, Balog S, O'Connell O, Jackson GR, Brown D, Clippinger AJ, Hayden P, Petri-Fink A, Stone V, Rothen-Rutishauser B. Use of EpiAlveolar Lung Model to Predict Fibrotic Potential of Multiwalled Carbon Nanotubes. ACS Nano. 2020 Apr 28;14(4):3941-3956. doi: 10.1021/acsnano.9b06860.

3. Beamer CA, Girtsman TA, Seaver BP, Finsaas KJ, Migliaccio CT, Perry VK, Rottman JB, Smith DE, Holian A. IL-33 mediates multi-walled carbon nanotube (MWCNT)-induced airway hyper-reactivity via the mobilization of innate helper cells in the lung. Nanotoxicology. 2013 Sep;7(6):1070-81. doi: 10.3109/17435390.2012.702230.

4. Cassel SL, Eisenbarth SC, Iyer SS, Sadler JJ, Colegio OR, Tephly LA, Carter AB, Rothman PB, Flavell RA, Sutterwala FS. The Nalp3 inflammasome is essential for the development of silicosis. Proc Natl Acad Sci U S A. 2008 Jul 1;105(26):9035-40. doi: 10.1073/pnas.0803933105.

5. Chua F, Gauldie J, Laurent GJ. Pulmonary fibrosis: searching for model answers. Am J Respir Cell Mol Biol. 2005 Jul;33(1):9-13. doi: 10.1165/rcmb.2005-0062TR.

6. Costabel U, Bonella F, Guzman J. Chronic hypersensitivity pneumonitis. Clin Chest Med. 2012 Mar;33(1):151-63. doi: 10.1016/j.ccm.2011.12.004.

7. Dostert C, Pétrilli V, Van Bruggen R, Steele C, Mossman BT, Tschopp J. Innate immune activation through Nalp3 inflammasome sensing of asbestos and silica. Science. 2008 May 2;320(5876):674-7. doi: 10.1126/science.1156995.

8. Ernst H, Rittinghausen S, Bartsch W, Creutzenberg O, Dasenbrock C, Görlitz BD, Hecht M, Kairies U, Muhle H, Müller M, Heinrich U, Pott F. Pulmonary inflammation in rats after intratracheal instillation of quartz, amorphous SiO2, carbon black, and coal dust and the influence of poly-2-vinylpyridine-N-oxide (PVNO). Exp Toxicol Pathol. 2002 Aug;54(2):109-26. doi: 10.1078/0940-2993-00241.

9. Fukuda Y, Ishizaki M, Masuda Y, Kimura G, Kawanami O, Masugi Y. The role of intraalveolar fibrosis in the process of pulmonary structural remodeling in patients with diffuse alveolar damage. Am J Pathol. 1987 Jan;126(1):171-82.

10. Gabazza EC, Kasper M, Ohta K, Keane M, D'Alessandro-Gabazza C, Fujimoto H, Nishii Y, Nakahara H, Takagi T, Menon AG, Adachi Y, Suzuki K, Taguchi O. Decreased expression of aquaporin-5 in bleomycin-induced lung fibrosis in the mouse. Pathol Int. 2004 Oct;54(10):774-80. doi: 10.1111/j.1440-1827.2004.01754.x.

11. Ghio AJ, Kadiiska MB, Xiang QH, Mason RP. In vivo evidence of free radical formation after asbestos instillation: an ESR spin trapping investigation. Free Radic Biol Med. 1998 Jan 1;24(1):11-7. doi: 10.1016/s0891-5849(97)00063-4.

12. Halappanavar S, van den Brule S, Nymark P, Gaté L, Seidel C, Valentino S, Zhernovkov V, Høgh Danielsen P, De Vizcaya A, Wolff H, Stöger T, Boyadziev A, Poulsen SS, Sørli JB, Vogel U. Adverse outcome pathways as a tool for the design of testing strategies to support the safety assessment of emerging advanced materials at the nanoscale. Part Fibre Toxicol. 2020 May 25;17(1):16. doi: 10.1186/s12989-020-00344-4.

13. Hamilton RF Jr, Thakur SA, Holian A. Silica binding and toxicity in alveolar macrophages. Free Radic Biol Med. 2008 Apr 1;44(7):1246-58. doi: 10.1016/j.freeradbiomed.2007.12.027.

14. Johnson ER, Matthay MA. Acute lung injury: epidemiology, pathogenesis, and treatment. J Aerosol Med Pulm Drug Deliv. 2010 Aug;23(4):243-52. doi: 10.1089/jamp.2009.0775.

15. Kasper J, Hermanns MI, Bantz C, Maskos M, Stauber R, Pohl C, Unger RE, Kirkpatrick JC. Inflammatory and cytotoxic responses of an alveolar-capillary coculture model to silica nanoparticles: comparison with conventional monocultures. Part Fibre Toxicol. 2011 Jan 27;8(1):6. doi: 10.1186/1743-8977-8-6.

16. Kolb M, Margetts PJ, Anthony DC, Pitossi F, Gauldie J. Transient expression of IL-1beta induces acute lung injury and chronic repair leading to pulmonary fibrosis. J Clin Invest. 2001 Jun;107(12):1529-36. doi: 10.1172/JCI12568.

17. Lenz AG, Costabel U, Maier KL. Oxidized BAL fluid proteins in patients with interstitial lung diseases. Eur Respir J. 1996 Feb;9(2):307-12. doi: 10.1183/09031936.96.09020307.

18. Miyoshi K, Yanagi S, Kawahara K, Nishio M, Tsubouchi H, Imazu Y, Koshida R, Matsumoto N, Taguchi A, Yamashita S, Suzuki A, Nakazato M. Epithelial Pten controls acute lung injury and fibrosis by regulating alveolar epithelial cell integrity. Am J Respir Crit Care Med. 2013 Feb 1;187(3):262-75. doi: 10.1164/rccm.201205-0851OC.

19. Parra ER, Kairalla RA, Ribeiro de Carvalho CR, Eher E, Capelozzi VL. Inflammatory cell phenotyping of the pulmonary interstitium in idiopathic interstitial pneumonia. Respiration. 2007;74(2):159-69. doi: 10.1159/000097133.

20. Psathakis K, Mermigkis D, Papatheodorou G, Loukides S, Panagou P, Polychronopoulos V, Siafakas NM, Bouros D. Exhaled markers of oxidative stress in idiopathic pulmonary fibrosis. Eur J Clin Invest. 2006 May;36(5):362-7. doi: 10.1111/j.1365-2362.2006.01636.x.

21. Quinlan TR, BeruBe KA, Hacker MP, Taatjes DJ, Timblin CR, Goldberg J, Kimberley P, O'Shaughnessy P, Hemenway D, Torino J, Jimenez LA, Mossman BT. Mechanisms of asbestos-induced nitric oxide production by rat alveolar macrophages in inhalation and in vitro models. Free Radic Biol Med. 1998 Mar 15;24(5):778-88. doi: 10.1016/s0891-5849(97)00357-2.

22. Schamberger AC, Mise N, Jia J, Genoyer E, Yildirim AÖ, Meiners S, Eickelberg O. Cigarette smoke-induced disruption of bronchial epithelial tight junctions is prevented by transforming growth factor-β. Am J Respir Cell Mol Biol. 2014 Jun;50(6):1040-52. doi: 10.1165/rcmb.2013-0090OC.

23. Schmekel B, Bos JA, Khan AR, Wohlfart B, Lachmann B, Wollmer P. Integrity of the alveolar-capillary barrier and alveolar surfactant system in smokers. Thorax. 1992 Aug;47(8):603-8. doi: 10.1136/thx.47.8.603.

24. Schwartz DA, Helmers RA, Dayton CS, Merchant RK, Hunninghake GW. Determinants of bronchoalveolar lavage cellularity in idiopathic pulmonary fibrosis. J Appl Physiol (1985). 1991 Nov;71(5):1688-93. doi: 10.1152/jappl.1991.71.5.1688.

25. Schwarz MA. Acute lung injury: cellular mechanisms and derangements. Paediatr Respir Rev. 2001 Mar;2(1):3-9. doi: 10.1053/prrv.2000.0095.

26. Shi J, Karlsson HL, Johansson K, Gogvadze V, Xiao L, Li J, Burks T, Garcia-Bennett A, Uheida A, Muhammed M, Mathur S, Morgenstern R, Kagan VE, Fadeel B. Microsomal glutathione transferase 1 protects against toxicity induced by silica nanoparticles but not by zinc oxide nanoparticles. ACS Nano. 2012 Mar 27;6(3):1925-38. doi: 10.1021/nn2021056.

27. Shvedova AA, Kisin ER, Mercer R, Murray AR, Johnson VJ, Potapovich AI, Tyurina YY, Gorelik O, Arepalli S, Schwegler-Berry D, Hubbs AF, Antonini J, Evans DE, Ku BK, Ramsey D, Maynard A, Kagan VE, Castranova V, Baron P. Unusual inflammatory and fibrogenic pulmonary responses to single-walled carbon nanotubes in mice. Am J Physiol Lung Cell Mol Physiol. 2005 Nov;289(5):L698-708. doi: 10.1152/ajplung.00084.2005.

28. Shvedova AA, Kisin ER, Murray AR, Kommineni C, Castranova V, Fadeel B, Kagan VE. Increased accumulation of neutrophils and decreased fibrosis in the lung of NADPH oxidase-deficient C57BL/6 mice exposed to carbon nanotubes. Toxicol Appl Pharmacol. 2008 Sep 1;231(2):235-40. doi: 10.1016/j.taap.2008.04.018.

29. Sime PJ, Marr RA, Gauldie D, Xing Z, Hewlett BR, Graham FL, Gauldie J. Transfer of tumor necrosis factor-alpha to rat lung induces severe pulmonary inflammation and patchy interstitial fibrogenesis with induction of transforming growth factor-beta1 and myofibroblasts. Am J Pathol. 1998 Sep;153(3):825-32. doi: 10.1016/s0002-9440(10)65624-6.

30. Thakur SA, Hamilton RF Jr, Holian A. Role of scavenger receptor a family in lung inflammation from exposure to environmental particles. J Immunotoxicol. 2008 Apr;5(2):151-7. doi: 10.1080/15476910802085863.

31. Thrall, R. S., & Scaliso, P. J. (1995). Bleomycin. Pulmonary Fibrosis. Edited by SH Phan, RS Thrall.

31. Tyurina YY, Kisin ER, Murray A, Tyurin VA, Kapralova VI, Sparvero LJ, Amoscato AA, Samhan-Arias AK, Swedin L, Lahesmaa R, Fadeel B, Shvedova AA, Kagan VE. Global phospholipidomics analysis reveals selective pulmonary peroxidation profiles upon inhalation of single-walled carbon nanotubes. ACS Nano. 2011 Sep 27;5(9):7342-53. doi: 10.1021/nn202201j.

32. Yasuoka S, Nakayama T, Kawano T, Ogushi F, Doi H, Hayashi H, Tsubura E. Comparison of cell profiles of bronchial and bronchoalveolar lavage fluids between normal subjects and patients with idiopathic pulmonary fibrosis. Tohoku J Exp Med. 1985 May;146(1):33-45. doi: 10.1620/tjem.146.33.

Event: 1499: Increased, activation of T (T) helper (h) type 2 cells

Short Name: Activation of Th2 cells

AOPs Including This Key Event

AOP ID and Name	Event Type
Aop:173 - Substance interaction with the pulmonary resident cell membrane components leading to pulmonary fibrosis	Key Event

Biological context

Level of Biological Organization
Tissue

Key Event Description

Naïve CD4+ T cells differentiate into four types of T helper (Th) cells – Th1, Th2, Th17 and inducible regulatory T cells following exposure to infectious agents. The differentiation process begins when antigen presenting cells (APCs) come in contact with toxic substances and is mainly driven by cytokines that make up the microenvironment. For example, increased concentrations of Interleukin (IL)-12 secreted by APCs in the environment may be biased towards Th1 type and increased IL-6 or IL-4 in the environment may commit to Th2 type differentiation. Th1 cytokines, Interferon gamma (IFN-γ) and IL-12 induce inflammation, aid in clearance of toxic substances, induce tissue damage and control the fibrotic responses. IFN-γ has suppressive effects on the production of extracellular matrix proteins including collagen and fibronectin. The Th2 response suppresses Th1 mediated response, which results in decreased Th1 cell-mediated tissue damage but at the same time contributing to the persistence of toxic substances leading to perpetuation of tissue damage, triggering uncontrolled healing response. The major sources of Th2 cytokines are Th2 cells themselves; however, mast cells, macrophages, epithelial cells and activated fibroblasts have shown to produce IL-4, IL-13 and IL-10 upon appropriate stimulation. Th2 cytokines IL-4 and IL-13 regulate wound healing.

Literature evidence for its perturbation in the context of pulmonary fibrosis:

For fibroplasia or fibrosis, the type of CD4+ T cell response that develops is crucial. Studies conducted in mice that do not express Th2 cytokines IL-4, IL-5 and IL-13 show complete attenuation of fibrosis despite the highly active Th1 response. Th2 cytokines IL-4 and IL-13 are elevated in fibrotic lungs; IL-13 activates Transforming growth factor beta 1 (TGF-β1) and initiates fibroblast proliferation and differentiation in lung fibrosis (Lee *et al.*, 2001). Overexpression of IL-13 induces sub-epithelial airway fibrosis in mice in the absence of any other external pro-inflammatory or pro-fibrotic stimulus (Zhu *et al.*, 1999). Both multi-walled carbon nanotubes (MWCNTs) and single-walled carbon nanotubes induce elevated expression of IL-4 and IL-13 in bronchoalveolar lavage fluid (BALF) of mouse lungs (Park *et al.*, 2011), and increased levels of IL-25 and IL- 33 in BALF and mouse lungs exposed to MWCNTs (Dong and Ma, 2018). In a rare human study, increased levels IL-4 and IL-5 were observed in the sputum of humans exposed to MWCNTs at an occupational setting (Fatkhutdinova *et al.*, 2016). Overexpression of IL-10 increases IL-4 and IL-13 production and lung fibrosis following exposure to silica (Barbarin *et al.*, 2005). Alveolar macrophages from asbestosis patients (a form of lung fibrosis) exhibit M2 phenotype (He et al., 2013). *Ex vivo* culture of alveolar macrophages obtained from BALF of patients suffering from idiopathic pulmonary fibrosis with collagen type I showed enhanced levels of M2 macrophage markers C-C motif chemokine ligand (CCL)-18, CCL-

2 and CD204 (Stahl *et al.*, 2013). Th2 response associated expression of IL-33 cytokine enhances polarization of M2 macrophages and inducing M2-mediated expression of IL-13 and TGF-β1 in mice (Dong and Ma, 2018). Cigarette smoke induces expression of genes associated with M2 sub-phenotypes, which is further enhanced in smokers presenting with chronic obstructive pulmonary disease (Shaykhiev *et al.*, 2009).

How it is Measured or Detected

Targeted enzyme-linked immunosorbent assays (ELISA) or real-time quantitative polymerase chain reaction (qRT-PCR) (routinely used and recommended):

The ELISA and qRT-PCR are routinely used to assess the levels of protein and mRNA of several Th1 and Th2 cytokines including IL-4, IL-5, IL- 13, IL-10, IL-12, IFN-γ. In addition, the levels of TGF-β is also assessed, expression of which is increased following induction of IL-13 synthesis. The other genes of relevance to Th2 response and eventual pro-fibrotic response include Arginine (Arg)-1 and Arg-2. BALF supernatant collected from lungs of animals exposed to toxic substances or human patients is used. Tissue homogenates or cell pellets can also be used. Expression of these genes and proteins can be assessed in *in vitro* cell cultures exposed to pro-fibrotic stimulus. Apart from assaying single protein or gene at a time, cytokine bead arrays or cytokine PCR arrays can be used to detect a whole panel of Th1 and/or Th2 cytokines using a multiplex method. This method is quantitative and especially advantageous when the sample amount available for testing is scarce. The details of ELISA and qRT-PCR are described under Event 1495. The details of BALF sample collection is described under Event 1497.

References

1. Barbarin V, Xing Z, Delos M, Lison D, Huaux F. Pulmonary overexpression of IL-10 augments lung fibrosis and Th2 responses induced by silica particles. Am J Physiol Lung Cell Mol Physiol. 2005 May;288(5):L841-8. doi: 10.1152/ajplung.00329.2004.

2. Dong J, Ma Q. Type 2 Immune Mechanisms in Carbon Nanotube-Induced Lung Fibrosis. Front Immunol. 2018 May 22;9:1120. doi: 10.3389/fimmu.2018.01120.

3. Fatkhutdinova LM, Khaliullin TO, Vasil'yeva OL, Zalyalov RR, Mustafin IG, Kisin ER, Birch ME, Yanamala N, Shvedova AA. Fibrosis biomarkers in workers exposed to MWCNTs. Toxicol Appl Pharmacol. 2016 May 15;299:125-31. doi: 10.1016/j.taap.2016.02.016.

4. He C, Ryan AJ, Murthy S, Carter AB. Accelerated development of pulmonary fibrosis via Cu,Zn-superoxide dismutase-induced alternative activation of macrophages. J Biol Chem. 2013 Jul 12;288(28):20745-57. doi: 10.1074/jbc.M112.410720.

5. Lee CG, Homer RJ, Zhu Z, Lanone S, Wang X, Koteliansky V, Shipley JM, Gotwals P, Noble P, Chen Q, Senior RM, Elias JA. Interleukin-13 induces tissue fibrosis by selectively stimulating and activating transforming growth factor beta(1). J Exp Med. 2001 Sep 17;194(6):809-21. doi: 10.1084/jem.194.6.809.

6. Park EJ, Roh J, Kim SN, Kang MS, Han YA, Kim Y, Hong JT, Choi K. A single intratracheal instillation of single-walled carbon nanotubes induced early lung fibrosis and subchronic tissue damage in mice. Arch Toxicol. 2011 Sep;85(9):1121-31. doi: 10.1007/s00204-011-0655-8.

7. Shaykhiev R, Krause A, Salit J, Strulovici-Barel Y, Harvey BG, O'Connor TP, Crystal RG. Smoking-dependent reprogramming of alveolar macrophage polarization: implication for pathogenesis of chronic obstructive pulmonary disease. J Immunol. 2009 Aug 15;183(4):2867-83. doi: 10.4049/jimmunol.0900473.

8. Stahl M, Schupp J, Jäger B, Schmid M, Zissel G, Müller-Quernheim J, Prasse A. Lung collagens perpetuate pulmonary fibrosis via CD204 and M2 macrophage activation. PLoS One. 2013 Nov 20;8(11):e81382. doi: 10.1371/journal.pone.0081382.

9. Zhu Z, Homer RJ, Wang Z, Chen Q, Geba GP, Wang J, Zhang Y, Elias JA. Pulmonary expression of interleukin-13 causes inflammation, mucus hypersecretion, subepithelial fibrosis, physiologic abnormalities, and eotaxin production. J Clin Invest. 1999 Mar;103(6):779-88. doi: 10.1172/JCI5909.

Event: 1500: Increased, fibroblast proliferation and myofibroblast differentiation

Short Name: Increased cellular proliferation and differentiation

AOPs Including This Key Event

AOP ID and Name	Event Type
Aop:173 - Substance interaction with the pulmonary resident cell membrane components leading to pulmonary fibrosis	Key Event

Biological context

Level of Biological Organization
Tissue

Domain of Applicability

Taxonomic Applicability

Term	Scientific Term	Evidence	Links
mouse	Mus musculus	High	NCBI
human	Homo sapiens	Moderate	NCBI

Life Stage Applicability

Life Stage	Evidence
Adult	High

Sex Applicability

Sex	Evidence
Male	High
Female	Not Specified

Key Event Description

Fibroblasts are non-hematopoietic, non-epithelial and non-endothelial cells. In steady state conditions, they are distributed throughout the mesenchyme. During the wound healing process, fibroblasts are rapidly recruited from mesenchymal cells or in case of exaggerated repair, and they can also be derived from fibrocytes in the bone marrow. They are not terminally differentiated. They synthesise structural proteins (fibrous collagen, elastin), adhesive proteins (laminin and fibronectins) and ground substance (glycosaminoglycans – hyaluronan and glycoproteins) proteins of the extracellular matrix (ECM) that provide structural support to tissue architecture and function. Fibroblasts play an important role in ECM maintenance and turnover, wound healing, inflammation and angiogenesis. They provide structural integrity to the newly formed wound. Fibroblasts with Alpha smooth muscle actin (α-SMA) expression are called myofibroblasts. It is thought that differentiating fibroblasts residing in the lung are the primary source of myofibroblast (CD45 Col I α-SMA) cells (Hashimoto et al., 2001; Serini and Gabbiani, 1999). Myofibroblasts can also originate from epithelial-mesenchymal transition (EMT) (Kim et al., 2006). The other sources of fibroblasts include fibrocytes that likely originate in the bone marrow and migrate to the site of injury upon cytokine signaling. Fibrocytes are capable of differentiating into fibroblasts or myofibroblasts, and comprise less than 1% of the circulating pool of leukocytes and express chemokines C-C motif chemokine receptor

(CCR)2, C-X-C chemokine receptor (CXCR)4 and CCR7 in addition to a characteristic pattern of biomarkers, including collagen I and III, CD34, CD43 and CD45 (Abe et al., 2001; Bucala *et al.*, 1994; Chesney et al., 1998). In bleomycin-induced lung fibrosis model, human CD34 CD45 collagen I CXCR4 cells (fibrocytes) are shown to migrate to the lungs in response to both bleomycin and C-X-C motif chemokine ligand (CXCL)12 (which is the only chemokine known to bind to CXCR4) (Phillips et al., 2004). Myofibroblasts exhibit features of both fibroblasts and smooth muscle cells. The myofibroblasts synthesise and deposit ECM components that eventually replace the provisional ECM. Because of their contractile properties, they play a major role in contraction and closure of the wound tissue. Apart from secreting ECM components, myofibroblasts also secrete proteolytic enzymes such as metalloproteinases and their inhibitors tissue inhibitor of metalloproteinases, which play a role in the final phase of the wound healing which is scar formation phase or tissue remodelling.

Literature evidence for its perturbation in the context of pulmonary fibrosis:

Idiopathic pulmonary fibrosis is characterised by progressive fibroblast and myofibroblast proliferation and excessive deposition of ECM (Kuhn and McDonald., 1991). High levels of α -SMA protein and increased number of α-SMA positive cells were observed in mouse lungs treated with multi-walled carbon nanotubes (MWCNTs) as early as day 1 post-exposure (Dong and Ma, 2016). Fibrotic lesions observed in mice treated with asbestos show proliferating fibroblasts and collagen deposition. The same study also demonstrated that bronchoalveolar lavage fluid supernatant derived from asbestos exposed lungs was sufficient to stimulate fibroblast proliferation *in vitro* (Lemaire et al., 1986). Fibrotic foci developed in rat lungs following exposure to bleomycin show α-SMA expressing myofibroblasts (Vyalov et al., 1993). Several *in vitro* studies have shown fibroblast proliferation following carbon nanotube treatment (Hussain et al., 2014; Wang et al., 2010a; Wang et al., 2010b).

How it is Measured or Detected

Immunohistochemistry (routinely used and recommended):

Proliferation of fibroblasts and activation of myofibroblasts is normally detected using individual antibodies against vimentin, procollagen 1 and α-SMA, specific markers of fibroblasts and myofibroblasts (Zhang, 1994). It is recommended to use more than one marker to confirm the activation of fibroblasts. The species-specific antibodies for all the markers are commercially available and the technique works in both *in vitro* and *in vivo* models as well as in human specimens. Immunohistochemistry is performed using immunoperoxidase technique. Formalin fixed and paraffin embedded lung sections are sliced in 3-5µm thin slices and reacted with diluted H_2O_2 for 10 min to block the endogenous peroxidase activity. The slices are then incubated with appropriate dilutions of primary antibody against the individual markers followed by incubation with the secondary antibody that is biotinylated. The slices are incubated for additional 30 minutes for avidin-biotin amplification and reacted with substrate 3’3’ diaminobenzidine before visualising the cells under the light microscope. Although only semiquantitative, morphometric analysis of the lung slices can be conducted to quantify the total number of cells expressing the markers against the control lung sections where expression of specific markers is expected to be low or nil. For the morphometric analysis, using ocular grids, images of 20-25 non-overlapping squares (0.25 mm) from 2-3 random lung section are taken under 20x magnification. Minimum of three animals per treatment group are assessed. Some researchers include only those cells that are positive for both procollagen I and α-SMA markers.

The limitation of the technique is that the antibodies have to be of high quality and specific. Background noise due to non-specific reactions can yield false-positive results.

In vitro, expression of type-1 collagen, Thy-1 cell surface antigen (Thy-1), cyclooxygenase-2 (COX2) and caveolin-1 (CAV1) are used as markers of homogeneous population of fibroblasts. Increased expression of Transforming growth factor beta (TGF-β) and α-SMA is used as markers of differentiated myofibroblasts. Transcription factor SMAD family member 3 (Smad3) is the other marker measured *in vitro* to assess the fibroblast proliferation and differentiation. Several *in vitro* studies using lung epithelial cells (e.g. A549 cells) have shown that asbestos induces markers of EMT (Tamminen et al., 2012), which is mediated by the activation of TGF-β-p-Smad2 (Kim et al., 2006).

Hydrogels:

Hydrogels are water-swollen crosslinked polymer networks. They are used to mimic the original ECM. Hydrogels consist of collagen, fibrin, hyaluronic acid or synthetic materials such as polyacrylamide enriched with ECM proteins, etc. Hydrogels can be prepared to express inherent biological signals, mechanical properties (e.g., modulus) and biochemical properties (e.g., proteins) of the ECM. Fibroblasts are usually cultured in fibrin and type-1 collagen that represent the matrix of the wound healing. Thus, the well-constructed hydrogel can be used to assess cell proliferation, activation and matrix synthesis as reflective of fibroblast activation. For naturally derived hydrogen scaffolds, cells derived directly from animal or human tissues can be used (Smithmyer et al., 2014).

Fibroblast proliferation assay:

Several primary and immortalised fibroblast types can be used for the assay. Proliferation assays such as water-soluble tetrazolium salts (WST)-1 and propidium iodide staining of cells have been used to show dose-dependent increase in MWCNT-induced increase in fibroblast proliferation that is in alignment with *in vivo* mouse fibrogenic response (Azad et al., 2013; Vietti et al., 2013) to the same material.

Advanced co-culture models (myofibroblast differentiation):

Co-culture models that mimic the alveolar capillary membrane (such as those listed for Event 1496 & Event 1498) can be used to assess myofibroblast differentiation in response to pro-fibrotic stressors using immunofluorescent staining for α-SMA. More complex *in vitro* microfluidic lung-on-a-chip models (such as the one listed for Event 1497) can be used to assess myofibroblast differentiation in the same stead. These provide a more realistic exposure model as opposed to a submerged monoculture of fibroblasts, however they require a higher degree of technical skill and advanced fabrication which may not be suitable for all labs.

References

1. Abe R, Donnelly SC, Peng T, Bucala R, Metz CN. Peripheral blood fibrocytes: differentiation pathway and migration to wound sites. J Immunol. 2001 Jun 15;166(12):7556-62. doi: 10.4049/jimmunol.166.12.7556.

2. Azad N, Iyer AK, Wang L, Liu Y, Lu Y, Rojanasakul Y. Reactive oxygen species-mediated p38 MAPK regulates carbon nanotube-induced fibrogenic and angiogenic responses. Nanotoxicology. 2013 Mar;7(2):157-68. doi: 10.3109/17435390.2011.647929.

3. Bucala R, Spiegel LA, Chesney J, Hogan M, Cerami A. Circulating fibrocytes define a new leukocyte subpopulation that mediates tissue repair. Mol Med. 1994 Nov;1(1):71-81.

4. Chesney J, Metz C, Stavitsky AB, Bacher M, Bucala R. Regulated production of type I collagen and inflammatory cytokines by peripheral blood fibrocytes. J Immunol. 1998 Jan 1;160(1):419-25.

5. Dong J, Ma Q. Myofibroblasts and lung fibrosis induced by carbon nanotube exposure. Part Fibre Toxicol. 2016 Nov 4;13(1):60. doi: 10.1186/s12989-016-0172-2.

6. Hashimoto S, Gon Y, Takeshita I, Maruoka S, Horie T. IL-4 and IL-13 induce myofibroblastic phenotype of human lung fibroblasts through c-Jun NH2-terminal kinase-dependent pathway. J Allergy Clin Immunol. 2001 Jun;107(6):1001-8. doi: 10.1067/mai.2001.114702.

7. Hussain S, Sangtian S, Anderson SM, Snyder RJ, Marshburn JD, Rice AB, Bonner JC, Garantziotis S. Inflammasome activation in airway epithelial cells after multi-walled carbon nanotube exposure mediates a profibrotic response in lung fibroblasts. Part Fibre Toxicol. 2014 Jun 10;11:28. doi: 10.1186/1743-8977-11-28.

8. Kim KK, Kugler MC, Wolters PJ, Robillard L, Galvez MG, Brumwell AN, Sheppard D, Chapman HA. Alveolar epithelial cell mesenchymal transition develops in vivo during pulmonary fibrosis and is regulated by the extracellular matrix. Proc Natl Acad Sci U S A. 2006 Aug 29;103(35):13180-5. doi: 10.1073/pnas.0605669103.

9. Kuhn C, McDonald JA. The roles of the myofibroblast in idiopathic pulmonary fibrosis. Ultrastructural and immunohistochemical features of sites of active extracellular matrix synthesis. Am J Pathol. 1991 May;138(5):1257-65.

10. Lemaire I, Beaudoin H, Massé S, Grondin C. Alveolar macrophage stimulation of lung fibroblast growth in asbestos-induced pulmonary fibrosis. Am J Pathol. 1986 Feb;122(2):205-11.

11. Phillips RJ, Burdick MD, Hong K, Lutz MA, Murray LA, Xue YY, Belperio JA, Keane MP, Strieter RM. Circulating fibrocytes traffic to the lungs in response to CXCL12 and mediate fibrosis. J Clin Invest. 2004 Aug;114(3):438-46. doi: 10.1172/JCI20997.

12. Serini G, Gabbiani G. Mechanisms of myofibroblast activity and phenotypic modulation. Exp Cell Res. 1999 Aug 1;250(2):273-83. doi: 10.1006/excr.1999.4543.

13. Smithmyer ME, Sawicki LA, Kloxin AM. Hydrogel scaffolds as in vitro models to study fibroblast activation in wound healing and disease. Biomater Sci. 2014 May 1;2(5):634-650. doi: 10.1039/C3BM60319A.

14. Tamminen JA, Myllärniemi M, Hyytiäinen M, Keski-Oja J, Koli K. Asbestos exposure induces alveolar epithelial cell plasticity through MAPK/Erk signaling. J Cell Biochem. 2012 Jul;113(7):2234-47. doi: 10.1002/jcb.24094.

15. Vietti G, Ibouraadaten S, Palmai-Pallag M, Yakoub Y, Bailly C, Fenoglio I, Marbaix E, Lison D, van den Brule S. Towards predicting the lung fibrogenic activity of

nanomaterials: experimental validation of an in vitro fibroblast proliferation assay. Part Fibre Toxicol. 2013 Oct 10;10:52. doi: 10.1186/1743-8977-10-52.

16. Vyalov SL, Gabbiani G, Kapanci Y. Rat alveolar myofibroblasts acquire alpha-smooth muscle actin expression during bleomycin-induced pulmonary fibrosis. Am J Pathol. 1993 Dec;143(6):1754-65.

17. Wang L, Mercer RR, Rojanasakul Y, Qiu A, Lu Y, Scabilloni JF, Wu N, Castranova V. Direct fibrogenic effects of dispersed single-walled carbon nanotubes on human lung fibroblasts. J Toxicol Environ Health A. 2010a;73(5):410-22. doi: 10.1080/15287390903486550.

18. Wang X, Xia T, Ntim SA, Ji Z, George S, Meng H, Zhang H, Castranova V, Mitra S, Nel AE. Quantitative techniques for assessing and controlling the dispersion and biological effects of multiwalled carbon nanotubes in mammalian tissue culture cells. ACS Nano. 2010b Dec 28;4(12):7241-52. doi: 10.1021/nn102112b.

19. Zhang K, Rekhter MD, Gordon D, Phan SH. Myofibroblasts and their role in lung collagen gene expression during pulmonary fibrosis. A combined immunohistochemical and in situ hybridization study. Am J Pathol. 1994 Jul;145(1):114-25.

Event: 68: Accumulation, Collagen

Short Name: Accumulation, Collagen

Key Event Component

Process	Object	Action
collagen biosynthetic process	collagen	increased

AOPs Including This Key Event

AOP ID and Name	Event Type
Aop:38 - Protein Alkylation leading to Liver Fibrosis	Key Event
Aop:241 - Latent Transforming Growth Factor beta1 activation leads to pulmonary fibrosis	Key Event
Aop:144 - Endocytic lysosomal uptake leading to liver fibrosis	Key Event
Aop:319 - Binding to ACE2 leading to lung fibrosis	Key Event
Aop:382 - Angiotensin II type 1 receptor (AT1R) agonism leading to lung fibrosis	Key Event
Aop:173 - Substance interaction with the pulmonary resident cell membrane components leading to pulmonary fibrosis	Key Event

Biological context

Level of Biological Organization
Tissue

Organ term

Organ term
connective tissue

Domain of Applicability

Taxonomic Applicability

Term	Scientific Term	Evidence	Links
human	Homo sapiens	High	NCBI
Rattus norvegicus	Rattus norvegicus	High	NCBI
mouse	Mus musculus	High	NCBI

Life Stage Applicability

Life Stage	Evidence
All life stages	

Sex Applicability

Sex	Evidence
Unspecific	

Humans: Bataller and Brenner, 2005; Decaris et al., 2015.
Mice: Dalton et al., 2009; Leung et al., 2008; Nan et al., 2013.
Rats: Hamdy and El-Demerdash, 2012; Li et al., 2012; Luckey and Petersen, 2001; Natajaran et al., 2006.

Key Event Description

Collagen is mostly found in fibrous tissues such as tendons, ligaments and skin. It is also abundant in corneas, cartilage, bones, blood vessels, the gut, intervertebral discs, and the dentin in teeth. In muscle tissue, it serves as a major component of the endomysium. Collagen is the main structural protein in the extracellular space in the various connective tissues, making up from 25% to 35% of the whole-body protein content. In normal tissues, collagen provides strength, integrity, and structure. When tissues are disrupted following injury, collagen is needed to repair the defect. If too much collagen is deposited, normal anatomical structure is lost, function is compromised, and fibrosis results.

The fibroblast is the most common collagen producing cell. Collagen-producing cells may also arise from the process of transition of differentiated epithelial cells into mesenchymal cells. This has been observed e.g. during renal fibrosis (transformation of tubular epithelial cells into fibroblasts) and in liver injury (transdifferentiation of hepatocytes and cholangiocytes into fibroblasts) (Henderson and Iredale, 2007).

There are close to 20 different types of collagen found with the predominant form being type I collagen. This fibrillar form of collagen represents over 90 percent of our total collagen and is composed of three very long protein chains which are wrapped around each other to form a triple helical structure called a collagen monomer. Collagen is produced initially as a larger precursor molecule called procollagen. As the procollagen is secreted from the cell, procollagen proteinases remove the extension peptides from the ends of the molecule. The processed molecule is referred to as collagen and is involved in fiber formation. In the extracellular spaces the triple helical collagen molecules line up and begin to form fibrils and then fibers. Formation of stable crosslinks within and between the molecules is promoted by the enzyme lysyl oxidase and gives the collagen fibers tremendous strength (Diegelmann,2001). The overall amount of collagen deposited by fibroblasts is a regulated balance between collagen synthesis and collagen catabolism. Disturbance of this balance leads to changes in the amount and composition of collagen. Changes in the composition of the extracellular matrix initiate positive feedback pathways that increase collagen production.

Normally, collagen in connective tissues has a slow turn over; degradating enzymes are collagenases, belonging to the family of matrix metalloproteinases. Other cells that can synthesize and release collagenase are macrophages, neutrophils, osteoclasts, and tumor cells (Di Lullo et al., 2002; Kivirikko and Risteli, 1976; Miller and Gay, 1987; Prockop and Kivirikko, 1995).

How it is Measured or Detected

Determination of the amount of collagen produced *in vitro* can be done in a variety of ways ranging from simple colorimetric assays to elaborate chromatographic procedures using radioactive and non-radioactive material. What most of these procedures have in common is the need to destroy the cell layer to obtain solubilized collagen from the pericellular matrix. Rishikof et al. describe several methods to assess the *in vitro* production of type I collagen: Western immunoblotting of intact alpha1(I) collagen using antibodies directed to alpha1(I) collagen amino and carboxyl propeptides, the measurement of alpha1(I) collagen mRNA levels using real-time polymerase chain reaction, and methods to determine the transcriptional regulation of alpha1(I) collagen using a nuclear run-on assay (Rishikof et al., 2005).

Histological staining with stains such as Masson Trichrome, Picro-sirius red are used to identify the tissue/cellular distribution of collagen, which can be quantified using

morphometric analysis both *in vivo* and *in vitro*. The assays are routinely used and are quantitative.

Sircol Collagen Assay for collagen quantification:

The Serius dye has been used for many decades to detect collagen in histology samples. The Serius Red F3BA selectively binds to collagen and the signal can be read at 540 nm (Chen and Raghunath, 2009; Nikota et al., 2017).

Hydroxyproline assay:

Hydroxyproline is a non-proteinogenic amino acid formed by the prolyl-4-hydroxylase. Hydroxyproline is only found in collagen and thus, it serves as a direct measure of the amount of collagen present in cells or tissues. Colorimetric methods are readily available and have been extensively used to quantify collagen using this assay (Chen and Raghunath, 2009; Nikota et al., 2017).

Ex vivo precision cut tissue slices

Precision cut tissue slices mimic the whole organ response and allow histological assessment, an endpoint of interest in regulatory decision making. While this technique uses animals, the number of animals required to conduct a dose-response study can be reduced to $1/4^{th}$ of what will be used in whole animal exposure studies (Rahman et al., 2020).

References

1. Bataller R, Brenner DA. Liver fibrosis. J Clin Invest. 2005 Feb;115(2):209-18. doi: 10.1172/JCI24282.
2. Chen CZ, Raghunath M. Focus on collagen: in vitro systems to study fibrogenesis and antifibrosis state of the art. Fibrogenesis Tissue Repair. 2009 Dec 15;2:7. doi: 10.1186/1755-1536-2-7.
3. Dalton SR, Lee SM, King RN, Nanji AA, Kharbanda KK, Casey CA, McVicker BL. Carbon tetrachloride-induced liver damage in asialoglycoprotein receptor-deficient mice. Biochem Pharmacol. 2009 Apr 1;77(7):1283-90. doi: 10.1016/j.bcp.2008.12.023.
4. Decaris ML, Emson CL, Li K, Gatmaitan M, Luo F, Cattin J, Nakamura C, Holmes WE, Angel TE, Peters MG, Turner SM, Hellerstein MK. Turnover rates of hepatic collagen and circulating collagen-associated proteins in humans with chronic liver disease. PLoS One. 2015 Apr 24;10(4):e0123311. doi: 10.1371/journal.pone.0123311.
5. Di Lullo GA, Sweeney SM, Korkko J, Ala-Kokko L, San Antonio JD. Mapping the ligand-binding sites and disease-associated mutations on the most abundant protein in the human, type I collagen. J Biol Chem. 2002 Feb 8;277(6):4223-31. doi: 10.1074/jbc.M110709200.
6. Diegelmann R. Collagen Metabolism. Wounds. 2001;13:177-82. Available at www.medscape.com/viewarticle/423231 (accessed on 20 January 2016).
7. Hamdy N, El-Demerdash E. New therapeutic aspect for carvedilol: antifibrotic effects of carvedilol in chronic carbon tetrachloride-induced liver damage. Toxicol Appl Pharmacol. 2012 Jun 15;261(3):292-9. doi: 10.1016/j.taap.2012.04.012.

8. Henderson NC, Iredale JP. Liver fibrosis: cellular mechanisms of progression and resolution. Clin Sci (Lond). 2007 Mar;112(5):265-80. doi: 10.1042/CS20060242.

9. Kivirikko KI, Risteli L. Biosynthesis of collagen and its alterations in pathological states. Med Biol. 1976 Jun;54(3):159-86.

10. Leung TM, Tipoe GL, Liong EC, Lau TY, Fung ML, Nanji AA. Endothelial nitric oxide synthase is a critical factor in experimental liver fibrosis. Int J Exp Pathol. 2008 Aug;89(4):241-50. doi: 10.1111/j.1365-2613.2008.00590.x.

11. Li L, Hu Z, Li W, Hu M, Ran J, Chen P, Sun Q. Establishment of a standardized liver fibrosis model with different pathological stages in rats. Gastroenterol Res Pract. 2012;2012:560345. doi: 10.1155/2012/560345.

12. Luckey SW, Petersen DR. Activation of Kupffer cells during the course of carbon tetrachloride-induced liver injury and fibrosis in rats. Exp Mol Pathol. 2001 Dec;71(3):226-40. doi: 10.1006/exmp.2001.2399.

13. Miller EJ, Gay S. The collagens: an overview and update. Methods Enzymol. 1987;144:3-41. doi: 10.1016/0076-6879(87)44170-0.

14. Nan YM, Kong LB, Ren WG, Wang RQ, Du JH, Li WC, Zhao SX, Zhang YG, Wu WJ, Di HL, Li Y, Yu J. Activation of peroxisome proliferator activated receptor alpha ameliorates ethanol mediated liver fibrosis in mice. Lipids Health Dis. 2013 Feb 6;12:11. doi: 10.1186/1476-511X-12-11.

15. Natarajan SK, Thomas S, Ramamoorthy P, Basivireddy J, Pulimood AB, Ramachandran A, Balasubramanian KA. Oxidative stress in the development of liver cirrhosis: a comparison of two different experimental models. J Gastroenterol Hepatol. 2006 Jun;21(6):947-57. doi: 10.1111/j.1440-1746.2006.04231.x.

16. Nikota J, Banville A, Goodwin LR, Wu D, Williams A, Yauk CL, Wallin H, Vogel U, Halappanavar S. Stat-6 signaling pathway and not Interleukin-1 mediates multi-walled carbon nanotube-induced lung fibrosis in mice: insights from an adverse outcome pathway framework. Part Fibre Toxicol. 2017 Sep 13;14(1):37. doi: 10.1186/s12989-017-0218-0.

17. Prockop DJ, Kivirikko KI. Collagens: molecular biology, diseases, and potentials for therapy. Annu Rev Biochem. 1995;64:403-34. doi: 10.1146/annurev.bi.64.070195.002155.

18. Rahman L, Williams A, Gelda K, Nikota J, Wu D, Vogel U, Halappanavar S. 21st Century Tools for Nanotoxicology: Transcriptomic Biomarker Panel and Precision-Cut Lung Slice Organ Mimic System for the Assessment of Nanomaterial-Induced Lung Fibrosis. Small. 2020 Sep;16(36):e2000272. doi: 10.1002/smll.202000272.

19. Rishikof DC, Kuang PP, Subramanian M, Goldstein RH. Methods for measuring type I collagen synthesis in vitro. Methods Mol Med. 2005;117:129-40. doi: 10.1385/1-59259-940-0:129.

List of Adverse Outcomes in this AOP

Event: 1458: Pulmonary fibrosis

Short Name: Pulmonary fibrosis

AOPs Including This Key Event

AOP ID and Name	Event Type
Aop:241 - Latent Transforming Growth Factor beta1 activation leads to pulmonary fibrosis	Adverse Outcome
Aop:173 - Substance interaction with the pulmonary resident cell membrane components leading to pulmonary fibrosis	Adverse Outcome
Aop:347 - Toll-like receptor 4 activation and peroxisome proliferator-activated receptor gamma inactivation leading to pulmonary fibrosis	Adverse Outcome
Aop:481 - AOPs of amorphous silica nanoparticles: ROS-mediated oxidative stress increased respiratory dysfunction and diseases.	Key Event

Stressors

Name
Bleomycin
Carbon nanotubes, Multi-walled carbon nanotubes, single-walled carbon nanotubes, carbon nanofibres

Biological context

Level of Biological Organization
Organ

Organ term

Organ term
lung

Evidence for Perturbation by Stressor

Bleomycin

Bleomycin is a potent anti-tumour drug, routinely used for treating various types of human cancers (Umezawa H et al., 1967; Adamson IY, 1976). Lung injury and lung fibrosis are the major adverse effects of this drug in humans (Hay J et al., 1991). Bleomycin is shown to induce lung fibrosis in animals – such as dogs (Fleischman RW et al., 1971), mice (Adamson IY and Bowden DH, 1974), and hamsters (Snider GL et al., 1978) and is widely used as a model to study the mechanisms of fibrosis (reviewed in **Moeller** A et al., **2008;** Gilhodes J-C et al., 2017).

1. Umezawa H, Ishizuka M, Maeda K, Takeuchi T. Studies on bleomycin. *Cancer*. 1967 May;20(5):891-5.
2. Adamson IY. Pulmonary toxicity of bleomycin. *Environ Health Perspect*. 1976 Aug;16:119-26.

3. Hay J, Shahzeidi S, Laurent G Mechanisms of bleomycin induced lung damage. 1991 *Arch Toxicol* 65:81–94.

4. Fleischman RW, Baker JR, Thompson GR, et al. Bleomycin-induced interstitial pneumonia in dogs. *Thorax*. 1971;26(6):675-682.

5. Adamson IYR, Bowden DH. The Pathogenesis of Bleomycin-Induced Pulmonary Fibrosis in Mice. *The American Journal of Pathology*. 1974;77(2):185-198.

6. Snider GL, Celli BR, Goldstein RH, O'Brien JJ, Lucey EC. Chronic interstitial pulmonary fibrosis produced in hamsters by endotracheal bleomycin. Lung volumes, volume-pressure relations, carbon monoxide uptake, and arterial blood gas studied. *Am Rev Respir Dis.* 1978 Feb; 117(2):289-97.

7. Moeller A, Ask K, Warburton D, Gauldie J, Kolb M. The bleomycin animal model: a useful tool to investigate treatment options for idiopathic pulmonary fibrosis? *The international journal of biochemistry & cell biology*. 2008;40(3):362-382.

8. Gilhodes J-C, Julé Y, Kreuz S, Stierstorfer B, Stiller D, Wollin L (2017) Quantification of Pulmonary Fibrosis in a Bleomycin Mouse Model Using Automated Histological Image Analysis. *PLoS ONE* 12(1): e0170561.

Carbon nanotubes, Multi-walled carbon nanotubes, single-walled carbon nanotubes, carbon nanofibres

Carbon nanotubes (CNTs) are allotropes of carbon, are made of rolled up sheet of graphene (single-walled carbon nanotubes) and are tubular in shape. A multi-walled carbon nanotube (MWCNT) is a multi-layered concentric cylinder of graphene sheets stacked one inside the other (N. Saifuddin et al., 2013). CNTs exhibit a combination of unique mechanical, thermal, and electronic properties and are highly desired commercially. They are light weight but their tensile strength is 50 times higher than that of steel, and they are stable chemically as well as in the environment. Consequently, they are produced in massive amounts and are increasingly incorporated in several industrial products.

CNTs are high aspect ratio materials and are shown to cause lung fibrosis in animals (Muller J et al., 2005; Porter DW et al., 2010; Dong and Ma 2016; Vietti, et al., 2016). In an intelligence bulletin published by NIOSH on ‘Occupational exposure to carbon nanotubes and nanofibers’, NIOSH reviewed 54 individual animal studies investigating the pulmonary toxicity induced by CNTs and reported that half of those studies consistently showed lung fibrosis (NIOSH bulletin, 2013). However, the evidence is inconsistent and the occurrence of fibrotic pathology is influenced by the specific physical-chemical properties of CNTs (i.e. length, rigidity), their dispersion in exposure vehicle, and the mode of exposure (Duke and Bonner 2018).

1. Dong, J., & Ma, Q. (2016). Myofibroblasts and lung fibrosis induced by carbon nanotube exposure. Particle and fibre toxicology, 13(1), 60.

2. Duke, K. S., & Bonner, J. C. (2018). Mechanisms of carbon nanotube-induced pulmonary fibrosis: a physicochemical characteristic perspective. Wiley interdisciplinary reviews. Nanomedicine and nanobiotechnology, 10(3), e1498.

3. Muller, J., Huaux, F., Moreau, N., Misson, P., Heilier, J. F., Delos, M., Arras, M., Fonseca, A., Nagy, J. B., & Lison, D. (2005). Respiratory toxicity of multi-wall carbon nanotubes. Toxicology and applied pharmacology, 207(3), 221–231.

4. NIOSH: Occupational exposure to carbon nanotubes and nanofibers: current intelligence bulletin 65. 2013.

5. Porter, D. W., Hubbs, A. F., Mercer, R. R., Wu, N., Wolfarth, M. G., Sriram, K., Leonard, S., Battelli, L., Schwegler-Berry, D., Friend, S., Andrew, M., Chen, B. T., Tsuruoka, S., Endo, M., & Castranova, V. (2010). Mouse pulmonary dose- and time course-responses induced by exposure to multi-walled carbon nanotubes. Toxicology, 269(2-3), 136–147.

6. N. Saifuddin, A. Z. Raziah, and A. R. Junizah. Carbon Nanotubes: A Review on Structure and Their Interaction with Proteins. Journal of Chemistry, vol. 2013, Article ID 676815, 18 pages, 2013.

7. Vietti, G., Lison, D., & van den Brule, S. (2016). Mechanisms of lung fibrosis induced by carbon nanotubes: towards an Adverse Outcome Pathway (AOP). Particle and fibre toxicology, 13, 11.

Domain of Applicability

Taxonomic Applicability

Term	Scientific Term	Evidence	Links
humans	Homo sapiens	High	NCBI
mouse	Mus musculus	High	NCBI
rat	Rattus norvegicus	High	NCBI

Life Stage Applicability

Life Stage	Evidence
Adults	High

Sex Applicability

Sex	Evidence
Unspecific	High

Key Event Description

Pulmonary fibrosis is broadly defined as the thickening or scarring of lung tissue, due to excessive deposition of extracellular matrix. In the normal human lung, the nasopharynx and the conducting airways are mainly covered by epithelium composed of ciliated, mucous secreting cells in direct contact with the basement membrane with submucosal glands containing goblet, duct, and serous cells also contributing to the fluid balance and mucous production (Koval and Sidhaye, 2017). Within this epithelium, basal cells are found which are stimulated to proliferate and differentiate in response to injury (Koval and Sidhaye, 2017). Further down the lung, in the terminal bronchiole region, the epithelium does not contain submucosal glands, but instead contains club cells which produce pulmonary surfactant and can differentiate into bronchiolar or alveolar epithelial cells (AECs). Finally, in the terminal airspaces, the epithelium is made up entirely of type I and type II AECs. In between the two adjacent alveoli are two layers of alveolar epithelium resting on basement membrane, which consists of interstitial space, pulmonary capillaries, elastin and collagen fibres. Thus, the alveolar capillary membrane (ACM), where gas exchange takes place, is made up of the alveolar epithelium and alveolar endothelium (Gracey et al, 1968). In pulmonary fibrosis, damage to the pulmonary epithelium results in excessive deposition of collagen by constitutively activated myofibroblasts during the wound healing response. This causes a pronounced decrease in

the number of capillaries within the alveolar septa with asymmetric deposition of collagen and cells between part of the surface of a capillary and the nearby alveolar lining. In areas where capillaries are not present, the ACM is occupied with collagen and cells.

How it is Measured or Detected

In vivo, histopathological analysis is used for assessing fibrotic lung disease. Morphometric analysis of the diseased area versus total lung area is used to quantitatively stage the fibrotic disease. Although, some inconsistencies can be introduced during the analysis due to the experience of the individual scoring the disease, the histological stain, etc., a numerical scale with grades from 0 to 8, originally developed by Ashcroft et al., 1988 is assigned to indicate the amount of fibrotic tissue in histological samples. This scale is applied to diagnose lung fibrosis in both human and animal samples. Modifications to this scoring system were proposed (Hubner et al., 2008), which enables morphological distinctions thus enabling a better grading of the disease. Using the modified scoring system, bleomycin induced lung fibrosis in rats was scored as follows: Grade 0 – normal lung, Grade 1 – isolated alveolar septa with gentle fibrotic changes, Grade 2 – knot like formation in fibrotic areas in alveolar septa, Grade 3 – contiguous fibrotic walls of alveolar septa, Grade 4 – single fibrotic masses, Grade 5 – confluent fibrotic masses, Grade 6 – large contiguous fibrotic masses, Grade 7 – air bubbles and Grade 8 – fibrotic obliteration. Further morphometric analysis can be conducted to quantify the total disease area (Nikota et al., 2017).

Lungs are formalin fixed and paraffin embedded such that an entire cross section of lung can be presented on a slide. The entire cross section is captured in a series of images using wide field light microscope. Areas of alveolar epithelium thickening and consolidated air space are identified. ImageJ software (freely available) is used to trace the total area (green line) and the diseased area (red line) imaged and quantified. The diseased area is equal to disease area/total area (Nikota et al., 2017).

In vitro, there is no single assay that can measure the alveolar thickness. However, a combination of assays spanning various KEs described above provide a measure of the extent of fibrogenesis potential of tested substances. Real-time reverse transcription-polymerase chain reaction (qRT-PCR) and enzyme-linked immunosorbent assays (ELISA) measuring increased collagen, Transforming growth factor beta 1 (TGF-β1) and various pro-inflammatory mediators are used as sensitive markers of potential of substances to induce the adverse outcome of lung fibrosis.

References

1. Ashcroft T, Simpson JM, Timbrell V. Simple method of estimating severity of pulmonary fibrosis on a numerical scale. J Clin Pathol. 1988 Apr;41(4):467-70. doi: 10.1136/jcp.41.4.467.

2. Gracey DR, Divertie MB, Brown AL Jr. Alveolar-capillary membrane in idiopathic interstitial pulmonary fibrosis. Electron microscopic study of 14 cases. Am Rev Respir Dis. 1968 Jul;98(1):16-21. doi: 10.1164/arrd.1968.98.1.16.

3. Hübner RH, Gitter W, El Mokhtari NE, Mathiak M, Both M, Bolte H, Freitag-Wolf S, Bewig B. Standardized quantification of pulmonary fibrosis in histological samples. Biotechniques. 2008 Apr;44(4):507-11, 514-7. doi: 10.2144/000112729.

4. Koval M, Sidhaye VK. Introduction: The Lung Epithelium. In: Sidhaye VK, Koval M, editors. Lung Epithelial Biology in the Pathogenesis of Pulmonary Disease. Boston: Academic Press; 2017. p. xiii-xviii. Elsevier.

5. Nikota J, Banville A, Goodwin LR, Wu D, Williams A, Yauk CL, Wallin H, Vogel U, Halappanavar S. Stat-6 signaling pathway and not Interleukin-1 mediates multi-walled carbon nanotube-induced lung fibrosis in mice: insights from an adverse outcome pathway framework. Part Fibre Toxicol. 2017 Sep 13;14(1):37. doi: 10.1186/s12989-017-0218-0.

Appendix 2 – Key Event Relationships

List of Key Event Relationships in the AOP

List of Adjacent Key Event Relationships

Relationship: 1702: Interaction with the lung cell membrane leads to Increased proinflammatory mediators

AOPs Referencing Relationship

AOP Name	Adjacency	Weight of Evidence	Quantitative Understanding
Substance interaction with the pulmonary resident cell membrane components leading to pulmonary fibrosis	adjacent	Moderate	Moderate
Interaction with lung resident cell membrane components leads to lung cancer	adjacent	Moderate	Moderate
Substance interaction with lung resident cell membrane components leading to atherosclerosis	adjacent		

Key Event Relationship Description

Innate immune response is the first line of defence in any organism against invading infectious pathogens and toxic substances. It involves tissue triggered startle response to cellular stress and is described by a complex set of interactions between the toxic stimuli, soluble macromolecules and cells (reviewed in Nathan, 2002). The process culminates in a functional change defined as inflammation, purpose of which is to resolve infection and promote healing. In lungs, the interaction of toxic substances with resident cells results in cellular stress, death or necrosis (Pouwels et al., 2016) leading to release of intracellular components such as alarmins (Damage associated molecular patterns [DAMPs], Interleukin (IL)-1α, High mobility group box 1 [HMGB1]). Released alarmins (danger sensors) bind cell surface receptors such as Interleukin 1 Receptor 1 (IL-1R1), Toll Like Receptors (TLRs) or others leading to activation of innate immune response signalling.

For example, binding of IL-1α to IL-1R1 can release Nuclear factor kappa B (NF-κB) resulting in its translocation to nucleus and transactivation of pro-inflammatory genes including cytokines, growth factors and acute phase genes. The signalling also stimulates secretion of a variety of pro-inflammatory mediators. Overexpression of IL-1α in cells induces increased secretion of pro-inflammatory mediators. Products of necrotic cells are shown to stimulate the immune system in an IL-1R1-dependent manner (Chen et al., 2007).

The secreted alarmins activate resident cells pre-stationed in the tissues such as mast cells or macrophages leading to propagation of the already initiated immune response by releasing more eicosanoids, cytokines, chemokines and other pro-inflammatory mediators. Thus, secreted mediators signal the recruitment of neutrophils, which are the first cell types to be recruited in acute inflammatory conditions. Neutrophil influx in sterile inflammation is driven mainly by IL-1α (Rider P, 2011). IL-1 mediated signalling regulates neutrophil influx in silica-induced acute lung inflammation (Hornung et al., 2008). IL-1 signalling also mediates neutrophil influx in other tissues and organs including liver and peritoneum. Other types of cells including macrophages, eosinophils, and lymphocytes are also recruited in a signal-specific manner. Recruitment of leukocytes induces critical cytokines

associated with the T helper type 2 immune response, including Tumor necrosis factor alpha (TNF-α), IL-1β, and IL-13.

Evidence Supporting this KER

Biological Plausibility

The biological plausibility of this relationship is high. There is a mechanistic relationship between the MIE (Event 1495) and KE1 (Event 1496) which has been evidenced in a number of both *in vitro* and *in vivo* model systems in response to stressors such as, asbestos, silica, bleomycin, carbon nanotubes, and metal oxide nanoparticles (NPs) (Behzadi *et al.*, 2017; Denholm & Phan 1990; Dostert et al., 2008; Mossman & Churg 1998).

Increased expression of IL-1α or IL-1β following lung exposure to multi-walled carbon nanotubes (MWCNTs), bleomycin, micro silica particles, silica crystals, and polyhexamethylene guanidine phosphate has been shown to be associated with neutrophil influx in rodents (Gasse et al., 2007; Girtsman et al., 2014; Hornung et al., 2008; Nikota et al., 2017; Rabolli et al., 2014; Suwara et al., 2014). Inhibition of IL-1 function by knocking out the expression of IL-1R1 using IL-1R1 knockout mice or via treatment with IL-1α or IL-1β neutralising antibodies results in complete abrogation of lung neutrophilic influx following exposure to MWCNTs (Nikota et al, 2017), cigarette smoke (CS) (Halappanavar et al., 2013), silica crystals (Rabolli et al., 2014) and bleomycin (Gasse et al., 2007). IL1-R1, Myeloid differentiation primary response protein (Myd88) or the IL-33/St2 signaling are involved in pulmonary fibrosis induced by bleomycin (Gasse et al., 2007; Xu et al., 2016).

Empirical Evidence

Empirical support for this KER is moderate. There are limited *in vitro* studies, which show a temporal and dose-dependent relationship between these two events, using the upregulation of specific surface receptors as a proxy for direct membrane interaction (Chan et al., 2018; Denholm & Phan, 1990; Roy et al., 2014). There are also studies that provide general support for the idea that an interaction with the lung resident cell membrane components leads to increased, secretion of pro-inflammatory and pro-fibrotic mediators (Table 1).

Table 1. Studies providing empirical evidence for the relationship between MIE (Event 1495) and KE1 (Event 1496). +: Severity of Response. References available in main KER page.

Stressor (Reference)	***In vitro/ in vivo/ ex vivo***	**Species/cell line**	**Exposure conditions**	**MEI (Event 1495) Interaction with the lung resident cell membrane components**		**KE1 (Event 1496) Increased, secretion of pro-inflammatory and pro-fibrotic mediators**
Silica (Chan et al., 2018)	*In vitro*	U937-differentiated macrophages	2.5 µg/cm^2 for 0 - 24 h	TLR4 mRNA expression level 0 h: 0.5 h: 2 h: 8 h: 16 h: + 24 h: ++ TLR4 Protein expression level 24 h: + MyD88, TIRAP protein expression level 24 h: +		An increase in the release of IL-1β, IL-6, IL-10, and TNF-α 24 h: +
Zinc oxide nanoparticles (Roy et al., 2014)	*In vitro*	Primary mice macrophages	2.5 µg/ml for 0.5 - 24 h	TLR6 mRNA expression level, MyD88, TRAF mRNA, and protein expression level 0.5 h: + 3 h: + 6 h: ++ 12 h: +++ 24 h: +++		Increased mRNA and protein expression of IL-1β, IL-6, and TNF-α 24 h: +
Crystalline silica (Brown et al., 2007)	*In vitro*	Mouse bone marrow-derived mast cells	6.25 - 50 µg/cm^2 for 0.5 - 24 h	Scavenger receptor MSR2 mRNA expression increased (2 h) µg/cm^2 6.25: + 12.5: + 25: ++ 50: +++	Scavenger receptor MSR2 mRNA expression increased (50 µg/cm^2) 30 min: + 1 h: ++ 2 h: +++	Increased TNF-α, IL-13, MCP-1 (24 h) µg/cm^2 6.25: + 12.5: ++ 25: +++ 50: ++++
Thapsigargin (Suwara M et al., 2014)	*In vitro*	Primary human bronchial epithelial cells (16HBE14o)	Conditioned medium obtained from 6HBE14o treated with thapsigargin 20 µM for 2 h	16HBE14o cells Release IL-1α (alarmin)		MRC5 treated with conditioned medium from 16HBE14o cells. Increased IL-6, IL-8, MCP-1 and GM-

		Human lung fibroblast (MRC5)	MRC5 treated with conditioned medium for 5 h.		CSF gene expression
Cigarette smoke (Heijink I et al., 2015)	*In vitro*	Human peripheral blood neutrophils Normal human bronchial epithelial cells	Cell-free supernatant collected from smoke-treated neutrophils (bubbled 1 min with cigarette smoke, rested 2 h). Normal human bronchial epithelial cells treated with conditioned medium for 24 h.	Neutrophils Released HMGB1	Normal human bronchial epithelial cells treated with conditioned medium from neutrophils Released CXCL8
Acetaminophen (Martin-Murphy et al., 2010)	*In vivo*/*in vitro*	C57BL/6J mice RAW 264.7 cells	350 mg/Kg intraperitoneal injection for 3 and 6 h (Mice) (Liver perfusate) RAW 264.7 cells treated for 3 h with liver perfusate (6 h acetaminophen treated mice)	Increased HSP-70 and HMGB1 levels in liver perfusate	Increased mRNA expression in RAW 264.7 cells treated with liver perfusate
				3 h: + 6 h: +	MCP-1: + IL-1β: +
Silica (Rabolli et al., 2014)	*In vivo*	Female C57BL/6 mice	Instillation 2.5 mg/mouse Evaluation: 1 – 24 h post-exposure	Release IL-1α (alarmin)	Increased mRNA expression pro IL-1β
				1 h: ++ 3 h: +++ 6 h: +++ 12 h: ++ 24 h: +	1 h: 3 h: 6 h: ++ 12 h: ++ 24 h: +++
Bleomycin (Xu J. et al., 2016)	*In vivo*	Kunming strain mice	5 mg/Kg intratracheal instillation Evaluation: 3 – 28 days post-exposure	Release of IL-33	Release of IL-4 and IL-13
				Day 3: ++ Day 7: ++ Day 14: + Day 28: +	Day 3: Day 7: + Day 14: ++ Day 28: ++

CXCL: C-X-C motif chemokine ligand.
GM-CSF: Granulocyte-macrophage colony-stimulating factor.
HMGB1: High mobility group box 1.
HSP: Heat shock protein.
IL: Interleukin.
MCP-1: Monocyte chemoattractant protein-1.
MSR2: Macrophage scavenger receptor.
MyD88: Myeloid differentiation primary response 88.
TIRAP: Toll-interleukin-1 receptor domain containing adaptor protein.
TLR: Toll-Like Receptor.
TNF: Tumor necrosis factor alpha.
TRAF: TNF receptor-associated factor

Dose-Response Evidence:

There are a few studies which provide evidence for a dose-response relationship in this KER. An *in vitro* study demonstrated a concentration-response relationship, in which silica exposure induced increases in pro-inflammatory cytokines through scavenger receptors in cultured bone marrow-derived murine mast cells. Cells were exposed to 6.25, 12.5, 25 or 50 µg/cm^2 silica dioxide (SiO_2) for 24 h. Macrophage scavenger receptor (MSR2) expression increased over time at 50 µg/cm^2 and in a concentration-dependent relationship. Moreover, Tumor necrosis factor alpha (TNF-α), IL-13 and Monocyte chemoattractant protein-1 (MCP-1) increased in a concentration-dependent manner (Brown et al., 2007). This provides indications that at higher concentrations of the stressor, the interaction with the lung resident cell membrane components (Event 1495) leads to an increased secretion of pro-inflammatory mediators (Event 1496).

Temporal Evidence:

In vitro and *in vivo* studies have demonstrated temporal concordance of the KEs.

TLR4 signal pathway was evaluated in differentiated macrophages exposed to silica at 2.5 µg/cm^2. After 16 and 24 h, the mRNA expression level of TLR4 increased. Moreover, the protein expression level of TLR-4 and related MyD88/Toll-interleukin-1 receptor domain containing adaptor protein (TIRAP) pathway increased at 24 h. Release of IL-1β, IL-6, IL-10, and TNF-α was induced by silica exposure at 24 h. Pre-treatment with resatorvid (TAK-242), an inhibitor of TLR4 signaling, suppressed the release of the cytokines (Chan et al., 2018).

Macrophages exposed to zinc oxide (ZnO) NPs at 2.5 µg/mL for 24 h increased the expression level of TLR6 and MyD88, TNF receptor-associated factor (TRAF), and IL-1 receptor-associated kinase (IRAK). At 24 h, they also observed an increase in the mRNA and protein levels of the pro-inflammatory cytokines IL-1β, IL-6, and TNF-α. These results demonstrated that ZnO NPs induced pro-inflammatory mediators by TLR stimulation and Mitogen-activated protein kinases (MAPKs) activation (Roy et al., 2014).

The pro-inflammatory IL-1β induced granulocyte migration and can be produced as a result of cellular detection of pathogen associated molecular patterns (PAMPs). Mice exposed to 2.5 mg/mouse of silica by instillation showed an increase of mRNA expression of pro-IL-1β in bronchoalveolar lavage fluid (BALF) at 6, 12, and 24 h post-exposure in a time-dependent manner. At early time points (1 h, 3 h, 6 h), there was an increase in the release of an alarmin (IL-1α) which indicates that the alarmin was released due to cell damage leading to cytokine production and an inflammatory reaction. Moreover, at 24 h, the levels of mature IL-1β and neutrophil accumulation in BALF increased. Neutralization or deletion of IL-1α reduced the observed responses (Rabolli et al., 2014).

Epithelial damage can lead to the release of alarmins. In this stead, conditioned media from primary human bronchial epithelial cells (PBECs) exposed to thapsigargin was able to induce a pro-inflammatory response in primary human lung fibroblasts. PBECs were exposed to thapsigargin (a tumor promoter in mammalian cells) 20 µM for 2 h. After that, the cell culture medium was replaced, and cells were incubated for 24 h. At this time, the medium was recovered and used to culture lung fibroblast for 5 h. This conditioned media from epithelial cell damage contains the alarmin IL-1α, which induced increased gene expression of IL-6, IL-8, MCP-1, and Granulocyte-macrophage colony-stimulating factor (GM-CSF) in fibroblasts. These responses were reduced with anti-IL-1α treatment (Suwara et al., 2014).

Heijink et al. 2015 conducted a similar strategy to identify the relationship between DAMPs and pro-inflammatory mediator release after exposure to CS. Neutrophils treated with CS bubbled for 1 min, released high levels of HMGB1 as a consequence of necrotic cell death. The cell-free supernatant, which contains HMGB1, was used to culture human bronchial epithelial cells, and after 24 h it promoted the production of the C-X-C motif chemokine ligand (CXCL)8 or IL-8 by lung epithelial cells. Pharmacological inhibitors, such as 1-palmitoyl-2-arachidonyl-sn-glycero-3-phosphorylcholine (OxPAPC) and Receptor for advanced glycation endproducts (RAGE) antagonist peptide (RAP), reduced the effect of CXCL8 release.

HMGB1 and Heat shock protein 70 (HSP-70) can be released by damaged hepatocytes. In a study, mice were treated with acetaminophen 350 mg/Kg for 3 and 6 h. At these time points, the liver perfusate was obtained and an increase in HSP-70 and HMGB1 protein levels was observed. RAW 264.7 cells (a macrophage cell line) treated with the liver perfusate exhibited increased mRNA expression levels of MCP-1 and IL-1β (Martin-Murphy et al. 2010).

Female mice were intratracheally administered with bleomycin at 5 mg/kg to represent idiopathic pulmonary fibrosis. IL-33, a molecule that can act as a DAMP, increased in lungs after 3 and 7 days of treatment. In serum, at 7-, 14- and 28-days post-exposure, IL-4 and IL-13 increased. It was concluded that IL-33/ST2 signaling pathway is involved in pulmonary fibrosis by bleomycin (Xu et al., 2016).

Uncertainties and Inconsistencies

Attenuation or complete abrogation of KE1 (Event 1496) and KE2 (Event 1497) following inflammogenic stimuli is observed in rodents lacking functional IL-1R1 or other cell surface receptors that engage innate immune response upon stimulation. However, following exposure to MWCNTs, it has been shown that absence of IL-1R1 signalling is compensated for eventually and neutrophil influx is observed at a later post-exposure time point (Nikota et al., 2017). In another study, acute neutrophilic inflammation induced by MWCNTs was suppressed at 24 h in mice deficient in IL-1R1 signalling; however, these mice showed exacerbated neutrophilic influx and fibrotic response at 28 days post-exposure (Girtsman et al., 2014). The early defence mechanisms involving DAMPs is fundamental for survival, which may necessitate activation of compensatory signaling pathways. As a result, inhibition of a single biological pathway mediated by an individual cell surface receptor may not be sufficient to completely abrogate the lung inflammatory response. Forced suppression of pro-inflammatory and immune responses early after exposure to substances that cannot be effectively cleared from lungs, may enhance the injury and initiate other pathways leading to exacerbated response.

Quantitative Understanding of the Linkage

A majority of the *in vivo* studies are conducted with only one dose and thus, it is difficult to derive quantitative dose-response relationships based on the existing data. However, it is clear from the studies referenced above that greater concentrations or doses of pro-fibrotic substances result in higher release of alarmins, and consequently, higher pro-inflammatory signalling. The above studies also demonstrate strong temporal relationships between the individual KEs.

Response-response relationship

One study has demonstrated a response-response relationship for this KER.

Human intervertebral disc cells were treated with 0, 0.5, 1, or 2 mg/ml of recombinant HMGB1 for 24 h. Protein levels were determined in cell medium supernatant by enzyme-linked immunosorbent assay (ELISA). HMGB1 stimulates the expression of IL-6 and Matrix metalloproteinase 1 (MMP-1) in a response-response relationship. A strong correlation was observed by Spearman's rank correlation coefficient between HMGB1 treatment and IL-6 or MMP-1 levels (Shah et al., 2019).

Other reports have studied both KEs, but they do not indicate if the response-response relationship was linear or not (coefficient or correlation is not shown) (Chakraborty et al., 2017; Fukuda et al. 2017; Kim et al., 2020, Piazza et al., 2013; Yang et al., 2012;).

Time-scale

Some studies have described how long after a change in the MIE (Event 1495; interaction substance and components), KE1 (Event 1496; pro-inflammatory mediators are secreted) is impacted (Table 2.).

Table 2. Time-scale related studies relevant to the MIE (Event 1495) - KE1 (Event 1496) relationship.

Reference	***In vitro*/*in vivo*/population study**	**Design**	**MIE (Event 1495)**	**KE1 (Event 1496)**
			Timepoint	**Timepoint**
Xu et al., 2016	*In vivo*	40 Female Kunming strain mice Bleomycin was intratracheally administered 5 mg/Kg.	IL-33 3, 7 days	IL-4, IL-13 7, 14, and 28 days
Roy et al., 2014	*In vitro*	Primary mice macrophages exposed to 2.5 mg/ml ZnO for 24 hrs.	Increased TLR6 expression 0.5, 3, 6, 12, and 24 h	Increased IL-6, TNF-α 24 h
Rabollli et al., 2014	*In vivo*	Female C57BL/6 mice Exposed to silica 2.5 mg/mouse by instillation	Increased the release of IL-1α 1, 3, and 6 h	Increased mRNA expression of pro-IL-1β 6, 12, and 24 h

Known Feedforward/Feedback loops influencing this KER

Pancreatic cancer cells stimulated with S100 calcium-binding protein A8 (S100A8) and S100 calcium-binding protein A9 (S100A9) released pro-inflammatory cytokines IL-8, TNF-α, and Fibroblast growth factor (FGF). Cancer cell-derived conditioned media and the individual cytokines (TNF-α and Transforming growth factor beta [TGF-β]) induced the protein expression of S100A8 and S100A9 in HL-60 monocytic cell line and primary human monocytes (Nedjadi et al. 2018).

References

1. Behzadi S, Serpooshan V, Tao W, Hamaly MA, Alkawareek MY, Dreaden EC, Brown D, Alkilany AM, Farokhzad OC, Mahmoudi M. Cellular uptake of nanoparticles: journey inside the cell. Chem Soc Rev. 2017 Jul 17;46(14):4218-4244. doi: 10.1039/c6cs00636a.
2. Brown JM, Swindle EJ, Kushnir-Sukhov NM, Holian A, Metcalfe DD. Silica-directed mast cell activation is enhanced by scavenger receptors. Am J Respir Cell Mol Biol. 2007 Jan;36(1):43-52. doi: 10.1165/rcmb.2006-0197OC.
3. Chakraborty D, Zenker S, Rossaint J, Hölscher A, Pohlen M, Zarbock A, Roth J, Vogl T. Alarmin S100A8 Activates Alveolar Epithelial Cells in the Context of Acute Lung Injury in a TLR4-Dependent Manner. Front Immunol. 2017 Nov 13;8:1493. doi: 10.3389/fimmu.2017.01493.
4. Chan JYW, Tsui JCC, Law PTW, So WKW, Leung DYP, Sham MMK, Tsui SKW, Chan CWH. Regulation of TLR4 in silica-induced inflammation: An underlying mechanism of silicosis. Int J Med Sci. 2018 Jun 14;15(10):986-991. doi: 10.7150/ijms.24715.
5. Chen CJ, Kono H, Golenbock D, Reed G, Akira S, Rock KL. Identification of a key pathway required for the sterile inflammatory response triggered by dying cells. Nat Med. 2007 Jul;13(7):851-6. doi: 10.1038/nm1603.
6. Denholm EM, Phan SH. Bleomycin binding sites on alveolar macrophages. J Leukoc Biol. 1990 Dec;48(6):519-23. doi: 10.1002/jlb.48.6.519.
7. Dostert C, Pétrilli V, Van Bruggen R, Steele C, Mossman BT, Tschopp J. Innate immune activation through Nalp3 inflammasome sensing of asbestos and silica. Science. 2008 May 2;320(5876):674-7. doi: 10.1126/science.1156995.
8. Fukuda K, Ishida W, Miura Y, Kishimoto T, Fukushima A. Cytokine expression and barrier disruption in human corneal epithelial cells induced by alarmin released from necrotic cells. Jpn J Ophthalmol. 2017 Sep;61(5):415-422. doi: 10.1007/s10384-017-0528-7.
9. Gasse P, Mary C, Guenon I, Noulin N, Charron S, Schnyder-Candrian S, Schnyder B, Akira S, Quesniaux VF, Lagente V, Ryffel B, Couillin I. IL-1R1/MyD88 signaling and the inflammasome are essential in pulmonary inflammation and fibrosis in mice. J Clin Invest. 2007 Dec;117(12):3786-99. doi: 10.1172/JCI32285.
10. Girtsman TA, Beamer CA, Wu N, Buford M, Holian A. IL-1R signalling is critical for regulation of multi-walled carbon nanotubes-induced acute lung inflammation in C57Bl/6 mice. Nanotoxicology. 2014 Feb;8(1):17-27. doi: 10.3109/17435390.2012.744110.
11. Halappanavar S, Nikota J, Wu D, Williams A, Yauk CL, Stampfli M. IL-1 receptor regulates microRNA-135b expression in a negative feedback mechanism during cigarette smoke-induced inflammation. J Immunol. 2013 Apr 1;190(7):3679-86. doi: 10.4049/jimmunol.1202456.
12. Heijink IH, Pouwels SD, Leijendekker C, de Bruin HG, Zijlstra GJ, van der Vaart H, ten Hacken NH, van Oosterhout AJ, Nawijn MC, van der Toorn M. Cigarette smoke-induced damage-associated molecular pattern release from necrotic neutrophils triggers proinflammatory mediator release. Am J Respir Cell Mol Biol. 2015 May;52(5):554-62. doi: 10.1165/rcmb.2013-0505OC.

13. Hornung V, Bauernfeind F, Halle A, Samstad EO, Kono H, Rock KL, Fitzgerald KA, Latz E. Silica crystals and aluminum salts activate the NALP3 inflammasome through phagosomal destabilization. Nat Immunol. 2008 Aug;9(8):847-56. doi: 10.1038/ni.1631.

14. Kim DH, Gu A, Lee JS, Yang EJ, Kashif A, Hong MH, Kim G, Park BS, Lee SJ, Kim IS. Suppressive effects of S100A8 and S100A9 on neutrophil apoptosis by cytokine release of human bronchial epithelial cells in asthma. Int J Med Sci. 2020 Feb 4;17(4):498-509. doi: 10.7150/ijms.37833.

15. Martin-Murphy BV, Holt MP, Ju C. The role of damage associated molecular pattern molecules in acetaminophen-induced liver injury in mice. Toxicol Lett. 2010 Feb 15;192(3):387-94. doi: 10.1016/j.toxlet.2009.11.016.

16. Mossman BT, Churg A. Mechanisms in the pathogenesis of asbestosis and silicosis. Am J Respir Crit Care Med. 1998 May;157(5 Pt 1):1666-80. doi: 10.1164/ajrccm.157.5.9707141.

17. Nathan C. Points of control in inflammation. Nature. 2002 Dec 19-26;420(6917):846-52. doi: 10.1038/nature01320.

18. Nedjadi T, Evans A, Sheikh A, Barerra L, Al-Ghamdi S, Oldfield L, Greenhalf W, Neoptolemos JP, Costello E. S100A8 and S100A9 proteins form part of a paracrine feedback loop between pancreatic cancer cells and monocytes. BMC Cancer. 2018 Dec 17;18(1):1255. doi: 10.1186/s12885-018-5161-4.

19. Nikota J, Banville A, Goodwin LR, Wu D, Williams A, Yauk CL, Wallin H, Vogel U, Halappanavar S. Stat-6 signaling pathway and not Interleukin-1 mediates multi-walled carbon nanotube-induced lung fibrosis in mice: insights from an adverse outcome pathway framework. Part Fibre Toxicol. 2017 Sep 13;14(1):37. doi: 10.1186/s12989-017-0218-0.

20. Piazza O, Leggiero E, De Benedictis G, Pastore L, Salvatore F, Tufano R, De Robertis E. S100B induces the release of pro-inflammatory cytokines in alveolar type I-like cells. Int J Immunopathol Pharmacol. 2013 Apr-Jun;26(2):383-91. doi: 10.1177/039463201302600211.

21. Pouwels SD, Zijlstra GJ, van der Toorn M, Hesse L, Gras R, Ten Hacken NH, Krysko DV, Vandenabeele P, de Vries M, van Oosterhout AJ, Heijink IH, Nawijn MC. Cigarette smoke-induced necroptosis and DAMP release trigger neutrophilic airway inflammation in mice. Am J Physiol Lung Cell Mol Physiol. 2016 Feb 15;310(4):L377-86. doi: 10.1152/ajplung.00174.2015.

22. Rabolli V, Badissi AA, Devosse R, Uwambayinema F, Yakoub Y, Palmai-Pallag M, Lebrun A, De Gussem V, Couillin I, Ryffel B, Marbaix E, Lison D, Huaux F. The alarmin IL-1α is a master cytokine in acute lung inflammation induced by silica micro- and nanoparticles. Part Fibre Toxicol. 2014 Dec 13;11:69. doi: 10.1186/s12989-014-0069-x.

23. Rider P, Carmi Y, Guttman O, Braiman A, Cohen I, Voronov E, White MR, Dinarello CA, Apte RN. IL-1α and IL-1β recruit different myeloid cells and promote different stages of sterile inflammation. J Immunol. 2011 Nov 1;187(9):4835-43. doi: 10.4049/jimmunol.1102048.

24. Roy R, Singh SK, Das M, Tripathi A, Dwivedi PD. Toll-like receptor 6 mediated inflammatory and functional responses of zinc oxide nanoparticles primed macrophages. Immunology. 2014 Jul;142(3):453-64. doi: 10.1111/imm.12276.

25. Shah BS, Burt KG, Jacobsen T, Fernandes TD, Alipui DO, Weber KT, Levine M, Chavan SS, Yang H, Tracey KJ, Chahine NO. High mobility group box-1 induces pro-inflammatory signaling in human nucleus pulposus cells via toll-like receptor 4-dependent pathway. J Orthop Res. 2019 Jan;37(1):220-231. doi: 10.1002/jor.24154.

26. Suwara MI, Green NJ, Borthwick LA, Mann J, Mayer-Barber KD, Barron L, Corris PA, Farrow SN, Wynn TA, Fisher AJ, Mann DA. IL-1α released from damaged epithelial cells is sufficient and essential to trigger inflammatory responses in human lung fibroblasts. Mucosal Immunol. 2014 May;7(3):684-93. doi: 10.1038/mi.2013.87.

27. Xu J, Zheng J, Song P, Zhou Y, Guan S. IL-33/ST2 pathway in a bleomycin-induced pulmonary fibrosis model. Mol Med Rep. 2016 Aug;14(2):1704-8. doi: 10.3892/mmr.2016.5446.

28. Yang D, Postnikov YV, Li Y, Tewary P, de la Rosa G, Wei F, Klinman D, Gioannini T, Weiss JP, Furusawa T, Bustin M, Oppenheim JJ. High-mobility group nucleosome-binding protein 1 acts as an alarmin and is critical for lipopolysaccharide-induced immune responses. J Exp Med. 2012 Jan 16;209(1):157-71. doi: 10.1084/jem.20101354.

Relationship: 1703: Increased proinflammatory mediators leads to Recruitment of inflammatory cells

AOPs Referencing Relationship

AOP Name	Adjacency	Weight of Evidence	Quantitative Understanding
Substance interaction with the pulmonary resident cell membrane components leading to pulmonary fibrosis	adjacent	Moderate	Low
Decreased fibrinolysis and activated bradykinin system leading to hyperinflammation	adjacent		
Frustrated phagocytosis leads to malignant mesothelioma	adjacent	High	Not Specified
Interaction with lung resident cell membrane components leads to lung cancer	adjacent	Moderate	Low
Binding of SARS-CoV-2 to ACE2 leads to hyperinflammation (via cell death)	adjacent	High	High

Key Event Relationship Description

Pro-inflammatory mediators are the chemical and biological molecules that initiate and regulate inflammatory reactions. They are secreted following inflammation or exposure to an inflammogen. Commonly measured pro-inflammatory mediators include Interleukin (IL)-1 family cytokines, IL-4,IL-5, IL-6, Tumor necrosis factor alpha (TNF-α), Interferon gamma (IFN-γ) (KE1496)

Proinflammatory mediator increase is caused when there's increased inflammation. This can be found in many ways, including bradykinin system activation or hypofibrinolysis (Hofman et al., 2016). With more proinflammatory mediators, this causes increased signaling from proinflammatory cytokines, which promotes leukocyte recruitment, which will differentiate into proinflammatory cells (Villeneuve et al., 2018). Increased proinflammatory mediators means this process happens more, which means increase recruitment of inflammatory cells.

Evidence Supporting this KER

Biological Plausibility

The biological plausibility of this KER is high. There are very well established functional relationships between the secreted signalling molecules and the chemotactic effects on pro-inflammatory cells (Harris, 1954; Petri and Sanz 2018).

Increased proinflammatory mediators means more pro-inflammatory cytokines, chemokines, vasoactive amines, and lipid mediators (Villeneuve et al., 2018). Increased signaling from these Cytokines and Chemokines promote leukocyte recruitment to areas of infection, including monocytes and neutrophils (Khatri et al., 2017; Leick et al., 2014; Marchini et al., 2016). The leukocytes will differentiate into mature pro-inflammatory cells, in response to mediators they encounter in the local tissue microenvironment (Villeneuve et al., 2018). With higher levels of leukocytes from increased pro-inflammatory mediators, it causes an increase in pro-inflammatory cells (Libby, 2015).

Empirical Evidence

The empirical support for this KER is moderate. There are many studies which show temporal and dose-dependent recruitment of immune cells following increases in pro-inflammatory mediators. However, these mediators exhibit pleiotropy, and knockdown or knockout of a single pathway or mediator can result in compensation and recruitment of immune cells at a later time, as is seen in Nikota et al.,. 2017. (Chen et al., 2016; Nikota et al., 2017; Schremmer et al., 2016) (Additional studies available in Table 1).

Table 1. Studies providing empirical evidence for the relationship between KE1 (Event 1496) and KE2 (Event 1497). +: Severity of Response. References available in main KER page.

Stressor (Reference)	***In vitro/ in vivo/ ex vivo***	**Species/cell line**	**Exposure Conditions**	**KE1 (Event 1496) Increased, secretion of pro-inflammatory and pro-fibrotic mediators**	**KE2 (Event 1497) Increased, recruitment of pro-inflammatory cells**	
Nanosized silica (Schremmer et al., 2016)	*In vitro*	NR8383 rat alveolar macrophages	16 µg/cm^2 for 1, 4, 16 h	Pro-inflammatory mediators using the supernatants obtained at different time points. (CCL4, CXCL1, CXCL3, TNF-α)	Chemotaxis using the supernatants obtained at different time points.	
				1 h: 4 h: + 16 h: ++	1 h: 4 h: + 16 h: ++	
Particulate matter $PM_{2.5}$ (Wang et al., 2019)	*In vitro*	Co-culture: A549 +THP-1+EA.hy926 cells	20, 60, 180 µg/ml for 24 h	Increased IL-6, IL-8 and TNF-α	Increased MMP9, ICAM-1, and CAV-1 mRNA expression	
				60: ++ 180: +++	20: + 60: ++ 180: +++	
Multi-walled carbon nanotubes (Ma et al., 2016)	*In vivo*	Male BALB/c mice	0.5, 1, 2, 4 mg/Kg intravenous injection Evaluation: 2 days post-exposure	Increased IL-6 and TNF-α	Increased the number of white blood cells, lymphocytes, and neutrophils	
				0.5: + 1: ++ 2: ++ 4: +++	0.5: 1: 2: 4: +++	
Multi-walled carbon nanotubes (Porter et al., 2020)	*In vivo*	Male C57BL/6J mice	2.5, 10, 40 µg/mouse oropharyngeal aspiration Evaluation: 1, 7 days post-exposure	Increased cathepsin, IL-1β, IL-18 (Day 1)	Increased number of polymorphonuclear cells (Day 1, Day 7)	
				40: Increased cathepsin, IL-1β, IL-18	Day 1 2.5: + 10: ++ 40: +++	Day 7 2.5: 10: +++ 40: ++++

Oleoresin C Spray (Patowary et al., 2020)	*In vivo*	Female Wistar rats	2%, 6%, 10% spray via whole body inhalation (single 20 min exposure) Evaluation: 1, 3, 24 h post-exposure	1 h TNF-α 2%: +++ IL-1 10%: +	3 h TNF-α 6%: ++ IL-1 10%: +	24 h TNF-α 10%: + IL-1 10%: +	Total cells in BALF:		
							1 h 2%: +	3 h 2%: + 6%: ++ 10%: ++	24 h 2%: + 6%: ++ 10%: ++
Carbon nanoparticles (Chen et al., 2016)	*In vivo*	Female C57BL/6J mice	20 µg/mouse intratracheal instillation Evaluation: 3-24 h post-exposure	Increase cytokine release			Total cell numbers in BALF		
				CXCL1 3 h: + 6 h: + 12 h: +++ 18 h: ++ 24 h: +	CXCL2 3 h: ++ 12 h: ++ 24 h: +	CXCL2 12 h: +++ 18 h: +++	6 h: + 12 h: ++ 24 h: +++		
Nickel oxide nanoparticles (Lee et al., 2016)	*In vivo*	Female Wistar rats	200 cm^2/rat intratracheal instillation Evaluation: 24-96 h post-exposure	24 h: Increased CINC3 48 h: 72 h: Increased eotaxin 96 h:			24 h: + neutrophils 48 h: ++ neutrophils 72 h: ++ neutrophils/eosinophils 96 h: +++ neutrophils/eosinophils/macrophages		
Crystalline silica (Porter et al., 2002)	*In vivo*	Male Fischer 344 rats	15 mg/m^3 inhalation (6h/day, 5 days/week) Evaluation: 5 - 116 days post-exposure	Increased BALF inflammatory mediators (IL-1; TNF-α) Day 10: IL-1 + Day 16: Day 20: Day 30: TNF-α + /IL-1 ++ Day 41: IL-1 + Day 79: TNF-α ++/IL-1 +++ Day 116: TNF-α ++/IL-1 ++++			Polymorphonuclear cells in BALF: Day 5: + Day 10: + Day 16: + Day 20: + Day 30: + Day 41: ++ Day 79: +++ Day 116: ++++	Neutrophils in BALF: Day 5: + Day 10: + Day 16: + Day 20: + Day 30: + Day 41: + Day 79: + Day 116: +	
Carbon black nanoparticles	*In vivo*	Female C57BL/6 mice	162 µg/mouse intratracheal instillation	Increased gene expression 3 h: IL-6, Ccl2			Recruitment of cells 3 h: + Neutrophils		

(Husain et al., 2015)			Evaluation: 3h – 42 days post-exposure	Day 1: Cxcl2, Ccl2 Day 2: Day 3: IL-17, IL-33 Day 4: Day 5: Day 14: Cd2 Day 42: Cxcl5	Day 1: + Neutrophils Day 2: + Neutrophils Day 3: + Neutrophils Day 4: +++ Neutrophils, eosinophils, lymphocytes and macrophages Day 5: ++++ Neutrophils, macrophages and lymphocytes Day 14: + Neutrophils Day 42: + Neutrophils, macrophages
Multi-walled carbon nanotubes (Poulsen et al., 2013)	*In vivo*	Female C57BL/6 mice	18 – 162 µg/mouse Intratracheal instillation Evaluation: 24 h post-exposure	Increased gene expression (Cxcl1, IL-6, Mt2, Saa1, Saa3)	Increased pro-inflammatory cells
				18: + 54: ++ 162: +++	18: + Neutrophils 54: ++ Neutrophils 162: +++ Neutrophils
Coated zinc oxide nanoparticles (Hadrup et al., 2019)	*In vivo*	Female C57BL/6J mice	11, 33, 100 µg/Kg intratracheal instillation Evaluation: 1-28 days post-exposure	Saa3 mRNA levels in lung	Neutrophils in BALF
				Day 1	Day 3 33: +++ 100: +++	Day 28	Day 1	Day 3 100: +++	Day 28 11: + 33: ++ 100: +++
Titanium dioxide nanoparticles (Rahman et al., 2017)	*In vivo*	Female C57BL/6 mice	18, 54, 162, 486 µg/mouse intratracheal instillation Evaluation: 1-28 days post-exposure	Increased gene expression associated with inflammation		BALF cell counts	
				Day 1 18: ++ 54: ++ 162: ++ 468: ++	Day 28 18: + 54: + 162: + 468: +	Day 1 18: + 54: ++ 162: +++ 468: ++++	Day 28 18: + 54: ++ 162: +++ 468: ++++
Polyhexamethyl guanidine phosphate (Song et al., 2014)	*In vivo*	Male C57BL/7 mice	0.3, 0.9, 1.5 mg/Kg Single intratracheal instillation 7-14 days post-exposure	Increased IL-1β, IL-6, CXCL1 levels		Increased MCP-1, MMP2, MMP12 mRNA expression	
				Day 7 0.9: ++ 1.5: +++	Day 14 0.9: ++ 1.5: +++	Day 7 0.3: + 0.9: ++ 1.5: ++	Day 14 0.3: + 0.9: ++ 1.5: ++

Carbon black nanoparticles (Bourdon et al., 2012)	*In vivo*	Female C57BL/6 mice	0.018, 0.054, 0.162 mg intratracheal instillation Evaluation: 1-28 days post-exposure	Saa3 mRNA expression						BALF cell counts				
				Day 1 0.018: +++ 0.054: ++++ 0.162: +++++	Day 3 0.018: ++ 0.054: +++ 0.162: ++++	Day 28 0.018: + 0.054: ++ 0.162: +++				Day 1 0.018: + 0.054: ++ 0.162: +++	Day 3 0.018: + 0.054: ++ 0.0162: +++	Day 28 0.018: + 0.054: ++ 0.0162: ++		
Quantum dot 705 (PEG or COOH coated) (Ho et al., 2013)	*In vivo*	Male ICR mice	12 and 60 µg/mouse intratracheal instillation of QD705-PEG or QD705-COOH Evaluation: 2, 17 and 90 days post-exposure	mRNA levels of gene expression (TNF-α, IL-1β, IL-6, CXCL1, CCL2, CCL1, CCL17, CXCL13)						BALF cell counts				
				Day 2 60: +	Day 17 12: ++ 60: +++	Day 90 60: ++				Day 2 60: +	Day 17 12: + 60: ++	Day 90 60: ++		
Nickel oxide (Morimoto et al., 2010)	*In vivo*	Male Wistar Rats	0.33, 0.66 mg/Kg intratracheal instillation Evaluation: 3 days, 1 week, 3 months, 6 months post-exposure	Concentration of MCP-1 (BALF) and IL-1β						Alveolar macrophage cells in BALF				
				Day 3 0.33: ++	Week 1 0.33: ++ 0.66: +	Month 1 0.33: ++ 0.66: +++	Month 3 0.33: +	Month 6		Day 3 0.33: + 0.66: +	Week 1 0.33: + 0.66: +	Month 1 0.33: + 0.66: ++	Month 3 0.33: ++ 0.66: +++	Month 6
Bleomycin and carbon black nanoparticles (Kamata et al., 2011)	*In vivo*	Female C57BL/6J mice	Bleomycin 20 µg/mouse and carbon black nanoparticles 10 µg/mouse intratracheal instillation Evaluation: 2 – 21 days post-exposure	Concentration of IL-6 and CCL2 in BALF						Total cells, macrophages, and lymphocytes in BALF				
				Day 2 ++	Day 7 +++	Day 14 +	Day 21			Day 2 +	Day 7 ++	Day 14 +++	Day 21 ++	

BALF: Bronchoalveolar lavage fluid.
CAV-1: Caveolin 1.
CCL: C-C motif chemokine ligand.
CINC3: Cytokine-Induced neutrophil chemoattractant 3.
CXCL: C-X-C motif chemokine ligand.

IL: Interleukin.
ICAM-1: Intercellular adhesion molecule 1.
MCP: Monocyte chemoattractant protein.
MMP: Matrix metalloproteinase.
Mt2: Metallothionein-2.
Saa: Serum Amyloid A3.
TNF-α: Tumor necrosis factor alpha.

Dose-Response Evidence:

Many studies provide dose-response evidence of this KER. For example, *in vitro* and *in vivo* studies testing stressors at different doses/concentrations have demonstrated a dose-response relationship; at the higher dose of the stressor, the pro-inflammatory mediators increased, leading to an increase of pro-inflammatory cell recruitment.

Ma et al. (2016) studied inflammatory responses in male BALB/c mice exposed to multi-walled carbon nanotubes (MWCNTs) administered intravenously at different doses (0.5-4 mg/kg) for 2 days. A dose-dependent relationship was found between the levels of the inflammatory mediators IL-6 and TNF-α and the MWCNT dose. At the highest dose, 4 mg/Kg, white blood cells, lymphocytes, and neutrophils levels increased.

Porter et al. (2020) have demonstrated that MWCNTs caused dose-dependent and time-dependent pulmonary inflammation in male C57BL/6J mice. Animals received a single dose of 2.5, 10, or 40 µg/mouse. At 40 µg/mouse, IL-1β and IL-18 increased at one day post-exposure. Moreover, polymorphonuclear leukocytes increased on day 1, and after 7 days the number of inflammatory cells was higher.

Zinc oxide (ZnO) nanoparticles (NPs) can induce metal fume fever and acute inflammation. Female C57BL/6J mice were intratracheally instilled once at 11, 33, and 100 µg/kg with coated ZnO NPs. Inflammatory responses were evaluated after 1, 3, and 28 days of exposure. An increase in Serum Amyloid A3 (Saa3) mRNA in lung tissue was observed at 33 and 100 µg/kg. Neutrophils accumulated in bronchoalveolar lavage fluid (BALF) after 28 days of exposure in a dose-dependent manner (Hadrup et al., 2019).

Polyhexamethylene guanidine phosphate (PHMG-P) is used as a disinfectant. PHMG-P at 0.3, 0.9, and 1.5 mg/kg was instilled into the lungs of mice. At 7- and 14-days post-exposure an increase in the levels of pro-inflammatory markers (IL-1β, IL-6, and C-X-C motif chemokine ligand [CXCL]1) and an increase in mRNA levels of Monocyte chemoattractant protein (MCP)1, Matrix metalloproteinase (MMP)2, and MMP12 was seen. Moreover, on day 7, neutrophils were recruited to the inflamed site. These changes were observed in a dose-response manner (Song et al., 2014).

Bourdon et al. 2012 evaluated the toxicity of carbon black nanoparticles (CBNPs) in mouse lung and liver. C57BL/6 mice were exposed to Printex 90 CBNPs with 0.018, 0.054, or 0.162 mg, and after 1, 3, and 28 days of the single instillation, BALF was analyzed. Polymorphonuclear cell counts in BALF increased in a dose-dependent manner with the strongest recruitment 1- and 3-days post-exposure and remained elevated at day 28. CBNPs also increased the expression of Saa3 mRNA levels in lung tissue on days 1, 3, and 28 in a dose-dependent manner. Although this response decreased over time, the expression of Saa3 mRNA increased at all time points, which indicates a persistent acute phase response.

A study evaluated the mechanisms of toxicity after exposure to particulate matter (PM2.5) in a tri-culture system: A549 cells (alveolar epithelial cells) and THP-1 differentiated macrophages in the apical chamber; meanwhile, EA.hy926 endothelial cells were cultured in the basolateral chamber. The system was exposed to PM2.5 at three different concentrations 20, 60, and 180 µg/ml for 24 h. An increase in the pro-inflammatory mediators IL-6, IL-8, and TNF-α was observed, as well an increase in mRNA expression of MMP9, Intercellular adhesion molecule 1 (ICAM-1), and caveolin 1 (CAV-1). These genes are involved in the movement and recruitment of leukocytes in sites of inflammation. Changes were observed in a concentration-dependent manner (Wang et al., 2019).

In another study, female C57BL/6 mice were exposed to 18, 54, or 162 µg of MWCNT/mouse via single intratracheal instillation. An increased gene expression of Cxcl1, IL-6, Metallothionein-2 (Mt2), Saa1, and Saa2 was observed in a dose-

dependent manner at 24 h post-exposure. Moreover, an increase in the recruitment of pro-inflammatory cells was observed in a dose-dependent manner (Poulsen et al., 2013).

Temporal Evidence:

There is significant evidence of the temporal relationship between the two KES. *In vitro* and *in vivo* studies have demonstrated that pro-inflammatory mediators (Event 1496) increased prior to the recruitment of pro-inflammatory cells (Event 1497).

Female C57BL/6J mice were exposed to carbon NPs at 20 µg/mouse via intratracheal instillation. An increase in the levels of cytokines CXCL1, CXCL2, and CXCL5 at 3 h post-exposure was observed, with peaks after 12 and 18 h post-exposure. These pro-inflammatory mediators preceded neutrophil recruitment (12 and 24 h post-exposure) (Chen et al., 2016). Alveolar macrophages (AM) were isolated from lungs 3 to 12 h after instillation, but they did not show a pro-inflammatory response. The authors suggest that AM are not involved in the initiation of the inflammatory response. Meanwhile, alveolar epithelial type II cells induced the highest CXCL levels and acute neutrophilic inflammation.

Nickel oxide (NiO) NPs intratracheally instilled at one single dose 200 cm^2/rat into female Wistar rats induced an increase of pro-inflammatory cytokines in BALF, at 24 and 74 h for Cytokine-Induced neutrophil chemoattractant 3 (CINC-3) and eotaxin, respectively. At 24 h and 48 h, neutrophils were observed, and after 72 h, the levels of neutrophils, eosinophils, and macrophages increased (Lee et al., 2016).

Porter et al. (2002) have shown pulmonary inflammation in rats exposed to crystalline silica aerosol at a concentration of 15 mg/m^3 (6h/day, 5 days/week) for 116 days. Lung disease was linked to TNF-α and IL-10 production in a timely response (10-116 days). The number of polymorphonuclear cells in the BALF increased progressively from day 41 - 116.

One study has demonstrated a dose-response and temporal relationship for these two KEs (Patowary et al., 2020). Female Wistar rats were exposed to oleoresin capsicum sprays at 2, 6, and 10%, and after 1, 3, and 24 h post-exposure, blood cell and BALF cytokines were evaluated. The pro-inflammatory cytokine TNF-α increased in a dose-dependent manner, and polymorphonuclear cells increased in a time-dependent manner.

Schremmer et al. (2016) have reported the time course of chemotaxis *in vitro* in response to the challenge of biopersistent particles and their relation to inflammatory mediators. NR8383 rat alveolar macrophages were challenged with different types of particles for 1, 4, and 16 h. The cell supernatants obtained from different time points were used to evaluate the chemotaxis of unexposed NR8383 macrophages. They found that nanosized silica at 16 µg/cm^2 induced an elevated transcription of C-C motif chemokine ligand (CCL)4, CXCL1, CXCL3, and TNF-α in a time-dependent manner. The pro-inflammatory cytokines present in the supernatants induced chemotaxis of unexposed macrophages at 4 and 16 h post-exposure.

Husain et al. (2015) found increased expression of genes related to chemotactic recruitment of pro-inflammatory cells at 3 h and 1 day after exposure to 162 µg/mouse CBNPs in female C57BL/6 mice. They observed an increase in the gene expression of pro-inflammatory mediators at day 1 (CXCL2, Ccl2), day 3 (IL-17, IL-33), day 14 (Cd2), and day 42 (Cxcl) post-exposure. The KE2 (Event 1497) increased over time with the maximum levels of neutrophils, macrophages, eosinophils, and lymphocytes at 4- and 5-days post-exposure. This response suggests chronic inflammation occurs because of an incomplete resolution of acute inflammation.

Rahman et al. (2017) evaluated whether different titanium dioxide (TiO_2) NPs induce lung inflammation. C57BL/6 mice were exposed to 18, 54, 162, or 486 µg/mouse of TiO_2 NPs

via single intratracheal instillation. At 1-day post-exposure, gene expression analysis showed more changes in genes associated with inflammation and fibrosis. Moreover, after 1- and 28 days post-exposure, an increase in cell counts in BALF was observed in a dose-dependent manner.

Ho et al. (2013) evaluated the inflammatory response in mice exposed to coated quantum dots, cadmium-based NPs, (QD705-poly(ethylene glycol[PEG], QD705-COOH) at 12 or 60 µg/mouse. At 2-, 17- and 90-days post-exposure, an increase in the level of TNF-α, IL-1b, IL-6, CXCL1, CCL2, CCL1, CCL17, and CXCL13 mRNA levels in lungs was observed and the amount of polymorphonuclear cells in BALF increased in a dose-dependent manner at day 7 post-exposure. The inflammatory response increased on days 2 and 17, but on day 90 decreased. QD705-COOH induced granulomas persistently presented from 2 to 90 days.

Morimoto et al. (2010) examined the different kinds of cytokines related to lung inflammation by NiO exposure. Rats were intratracheally exposed to 0.33 mg/Kg and 0.66 mg/kg NiO NPs and were sacrificed at day 3, after 1 week, 1, 3, and 6 months post-exposure. Infiltration of alveolar macrophages in lung tissue and BALF was observed from day 3 to 3 months post-exposure, with higher levels after 1 and 3 months. Before the recruitment of inflammatory cells, an increase in the level of pro-inflammatory cells such as MCP-1 and IL-1β in BALF was observed. NiO NPs induced a persistent inflammatory effect.

Kamata et al. (2011) studied the impact of CBNPs on susceptible subjects with predisposing lung disease and the effects of nanoparticles on inflammation and fibrotic changes. To achieve this goal, female C57BL/6J mice were intratracheally administered with bleomycin 20 µg/mouse and CBNPs 10 µg/mouse. Evaluations were performed post-exposure at different time points. An increase of IL-6 and CCL2 in BALF was observed at days 2 and 7. After 7- and 14 days, a recruitment of pro-inflammatory cells was observed. Oxidant injury (evaluated as nitrotyrosine expression) was observed after 7 days and 14 days. The levels of Transforming growth factor beta (TGF-β) increased over time with the highest level at day 14. Finally, they observed an increase in lung collagen deposition and a decrease in lung compliance at day 21.

Uncertainties and Inconsistencies

Attenuation or complete abrogation of KE1 (KE1496) and KE2 (KE1497) following inflammogenic stimuli is observed in rodents lacking functional Interleukin 1 receptor type 1 (IL-1R1) or other cell surface receptors that engage innate immune response upon stimulation (Gasse et al., 2007; Halappanavar et al., 2013). However, following exposure to MWCNTs, it has been shown that absence of IL-1R1 signalling is compensated for eventually and neutrophil influx is observed at a later post-exposure time point (Nikota et al., 2017). In another study, acute neutrophilic inflammation induced by MWCNTs was suppressed at 24 h in mice deficient in IL-1R1 signalling; however, these mice showed exacerbated neutrophilic influx and fibrotic response at 28 days post-exposure (Girtsman et al., 2014). The early defence mechanisms involving damage-associated molecular patterns is fundamental for survival, which may necessitate activation of compensatory signalling pathways. As a result, inhibition of a single biological pathway mediated by an individual cell surface receptor may not be sufficient to completely abrogate the lung inflammatory response. Forced suppression of pro-inflammatory and immune responses early after exposure to substances that cannot be effectively cleared from lungs, may enhance the injury and initiate other pathways leading to exacerbated response.

Most of the studies evaluate one dose at different time points or one-time point at different concentrations. Moreover, some studies have demonstrated that a stressor can lead to the

recruitment of pro-inflammatory cells, but the presence of pro-inflammatory mediators was not determined (Westphal et al., 2015).

Recruitment of pro-inflammatory cells is a key event that is complicated to replicate *in vitro* conditions as cell migration is induced by cooperative chemotactic mediators (Gouwy et al., 2015) which are produced and released from different cells. Therefore, more kinetics studies in co-culture techniques are needed to fill this gap.

Quantitative Understanding of the Linkage

A majority of the *in vivo* studies are conducted with only one dose and thus, it is difficult to derive quantitative dose-response relationships based on the existing data. However, it is clear from the studies referenced above that greater concentrations or doses of pro-fibrotic substances results in higher release of alarmins, and consequently, higher pro-inflammatory signalling. The above studies also demonstrate strong temporal relationships between the individual KEs.

Known modulating factors

Modulating Factor (MF)	MF Specification	Effect(s) on the KER	Reference(s)
Air pollution		Air pollution primes immunity; increases the levels of circulating IL-1β, IL-6 and TNF-α; impairs the normal functions of macrophages and alveolar cells. Exposure to particulate air pollution, such as PM2.5, is associated with pulmonary inflammation [1,2]. Both short term and chronic exposures to fine particulate matter (PM) have been shown to increase levels of circulating IL-1β, IL-6 and TNF-α [3-5]. Air pollution works as a priming factor that exacerbates the inflammatory phenotype of COVID-19 and further dysregulates immune cell activity. Dysregulation of the immune cell functions, on the other hand, plays a role in tissue damage and the ability of the immune system to fight pathogens, which increases the susceptibility to concomitant bacterial superinfection, for instance [6-9].	[1] Zhao et al., 2013 [2] Jia et al., 2021 [3] Tsai et al., 2012 [4] Ljungman et al., 2009 [5] Kido et al., 2011 [6] Knoll et al., 2021 [7] Glencross et al., 2020 [8] Yamasaki and Eeden, 2018 9) Signorini et al., 2018
Chemicals (weak evidence)	Per- and polyfluoroalkyl substances (PFAS) (Perfluorooctane sulfonate [PFOS], perfluorooctanoic acid [PFOA], perfluorobutane sulfonic acid [PFBS], perfluorooctane sulfonamide [PFOSA], and perfluorodecanoic acid [PFDA])	Several *in vitro* studies in human-derived cells have shown that PFAS can modify the secretion of pro-inflammatory mediators in a dose-dependent manner [1]. PFOS exposure significantly induced IL-1 IL-4, IL-6, and IL-8 in human lymphocytes and reduced chemokines CXCL8 and CXCL10 secretion in human bronchial epithelial cells while increasing of IL-1α release [2]; both PFOS and PFOA enhanced IL-1β release in response to Poly I:C [3]; PFOS, PFOA, PFBS, PFOSA, and PFDA exposure decreased PHA-induced release of IL-4, IL-10, and IL-6 and PFOS, PFOSA, and PFDA decreased IFN-γ release in human leukocytes with PFOS as a more potent inhibitor of cytokine production than other PFAS, and leukocytes obtained from female donors appeared to be more sensitive to the in vitro immunomodulating effects of PFAS, compared to leukocytes from male donors [4]. In a rat study exposed to PFOS, increased serum levels of TNF-α and IL-6 were observed. Kupffer cells exposed to PFOS showed cell activation, which was mostly inhibited by anti-TNF-α or anti-IL-6 treatment. Moreover, NF-κB inhibitor and JNK inhibitor significantly inhibited the production of IL-6 [5,6].	[1] Tian et al., 2021 [2] Li et al., 2020 [3] Sørli et al., 2020 [4] Corsini et al., 2012 [5] Han et al., 2018 [6] EFSA CONTAM Panel, 2020
Sex	Female sex (XX chromosomes)	Females produce higher amounts of the antiviral infection cytokine IFN-α than men [1]. Estrogens are critical regulators of gene expression and functions in innate immune cells, including monocytes, macrophages, and dendritic cells, as well as lymphocytes such as T helper 1/2 (TH1/2) cells, regulatory T-cells (Treg cells), and B cells. One of the major forms of estrogen, estradiol, has been shown to dampen the production of excessive innate inflammatory cytokines by monocytes and macrophages [2]. In the presence of progesterone, CD4+ Th cells skew from Th-1 to Th-2 in the production of anti-inflammatory cytokines, specifically IL-4 and IL-10 [3]. The cellular types involved in male and female immune responses to SARS-CoV-2 are distinct and immune response in females is enriched with activated T-cells [1]. In lactating women, higher SARS-CoV-2 reactive memory B-cells and antibody titers have been associated with the hormone prolactin [4]. Poor T-cell response to SARS-CoV-2 correlates with worse disease progression in female patients.	[1] Takahashi et al., 2020 [2] Scully et al., 2020 [3] Mauvais-Jarvis et al., 2020 [4] Gonçalves et al., 2021
	Male sex (XY chromosomes)	Males display a higher innate immune response to SARS-CoV-2 than females, which conditions their cytokine profile. Men have higher levels	[5] Bastard et al., 2020 [6] Agrawal et al., 2021

Modulating Factor (MF)	MF Specification	Effect(s) on the KER	Reference(s)
Air pollution		Air pollution primes immunity; increases the levels of circulating IL-1β, IL-6 and TNF-α; impairs the normal functions of macrophages and alveolar cells. Exposure to particulate air pollution, such as PM2.5, is associated with pulmonary inflammation [1,2]. Both short term and chronic exposures to fine particulate matter (PM) have been shown to increase levels of circulating IL-1β, IL-6 and TNF-α [3-5]. Air pollution works as a priming factor that exacerbates the inflammatory phenotype of COVID-19 and further dysregulates immune cell activity. Dysregulation of the immune cell functions, on the other hand, plays a role in tissue damage and the ability of the immune system to fight pathogens, which increases the susceptibility to concomitant bacterial superinfection, for instance [6-9].	[1] Zhao et al., 2013 [2] Jia et al., 2021 [3] Tsai et al., 2012 [4] Ljungman et al., 2009 [5] Kido et al., 2011 [6] Knoll et al., 2021 [7] Glencross et al., 2020 [8] Yamasaki and Eeden, 2018 9) Signorini et al., 2018
		of the innate immune cytokines IL-8 and IL-18 in circulation [1]. Moreover, elderly men in particular display autoantibodies against IFN-α more frequently [5]. The cellular types involved in male and female immune responses to SARS-CoV-2 are distinct. Men display higher circulating levels of non-classical monocytes [1]. Higher innate immune activation in men leads to higher plasma levels of the inflammatory cytokines IFN-α [6], IL-8 and IL-18 [1], driving hyperinflammation and more pronounced lymphopenia in males.	
Age	Old people	During aging, a subclinical chronic inflammatory response develops leading to an immune senescent state, where pathogen protective immune responses are impaired, but the production of inflammatory cytokines, such as IL-6, is increased. This process is called inflammaging. The persistent IL-6 elevation can induce lung tissue inflammation and mortality. The rate of inflammaging is higher in men and accelerated inflammaging is believed to worsen COVID-19 outcomes [1]. The chronic inflammatory status is associated with a dramatic depletion of B lymphocyte-driven acquired immunity. Aging also attenuates the upregulation of co-stimulatory molecules critical for T-cell priming and reduces antiviral IFN production by alveolar macrophages and dendritic cells in response to infection with the influenza virus [2].	[1] Bonafè et al., 2020 [2] Kovacs et al., 2017
Lipids	Atherogenic dyslipidemia	Lipids impact innate and adaptive immune responses [1,2]. **In COVID-19.** The atherogenic dyslipidemia associated with COVID-19 severity (high tryglycerides and low total, low density lipoprotein and high density lipoprotein cholesterol) was inversely correlated with inflammatory biomarkers such as increased levels of serum C-reactive protein (CRP), IL-6, IL-8, and IL-10 [3,4].	[1] Hubler and Kennedy, 2016 [2] Bernardi et al., 2018 [3] Henry et al., 2021 [4] Caterino et al., 2021 [5] Hubler and Kennedy, 2016 [6] Winer et al., 2009 [7] Im et al., 2011 [8] Muscogiuri et al., 2020
	Obesity	In obesity, immune cells interact with various classes of lipids, which can control the plasticity of macrophages and T lymphocytes. **In COVID-19.** Altered lipid homeostasis is associated with severe COVID-19 outcomes and, at the same time, with chronic inflammation and inflammatory polarization of macrophages and T lymphocytes [5]. Th1 lymphocytes are more prevalent in adipose tissue of obese patients [6]. In the same way, Th1 lymphocytes are elevated in visceral fat [6]. Both macrophages and T lymphocytes interact with lipids that influence their proliferation, differentiation, polarization [7] and transcriptional regulation, which is tightly controlled by Sterol regulatory element-binding protein (SREBP) and Liver X receptors (LXRs), expressed in macrophages and known regulators of cytokine release. Adipose tissue produces many pro-inflammatory adipokines and cytokines, which lead to low-grade inflammation and the recruitment of immune cells which may clarify the connection between obesity and COVID-19 severity [8].	
Gut microbiota	Gut dysbiosis (alteration of gut microbiota)	The gut microbiota is increasingly acknowledged to play a central role in human health and disease, notably by shaping the immune response. Notably some bacteria living in the gut produce short-chain fatty acids (SCFA), recognized as mediators of the intestinal inflammatory response [1]. SCFAs modulate inflammation by regulating immune cell cytokine production such as TNF-α, IL-12, IL-6 [2]. For example, butyrate decreased the lipopolysaccharide (LPS)-induced TNF-α expression in monocytes [4] and activated Treg cells, blocking an excessive inflammatory response [1,3]. **In COVID-19.** In a COVID-19 cohort, the depletion of several bacterial species (*B. adolescentis*, *E. rectale* and *F. prausnitzii*, known to play immunomodulatory roles in the human gastrointestinal system) was linked to increased plasma concentrations of TNF-α, CXCL10, CCL2 and IL-10 [4]. Conversely, two species enriched in the COVID-19 cohort, *B. dorei* and *Akkermansia muciniphila,* were positively correlated with IL-1β, IL-6 and CXCL8. Using a machine learning model [5], it was reported that the disruption of gut microbiota significantly correlated with pro-inflammatory cytokines and may predispose normal individuals to severe COVID-19. Decreases in the abundance of butyrate-producing bacteria and a decline in SCFA were observed in severe COVID-19 [4,6,7,8]. Reduced relative proportion of bacteria producing SCFA was observed in Syrian hamsters infected with SARS-CoV-2, compared to non-infected controls, with a transient decrease in systemic SCFA	[1] Yoo et al., 2020 [2] Vinolo et al., 2011 [3] Atarashi et al., 2013 [4] Yeo et al., 2021 [5] Gou et al., 2021 [6] Zuo et al., 2020 [7] Gu et al., 2020 [8] Grenga et al., 2022 [9] Sencio et al., 2022 [10] Zhang et al., 2022

Modulating Factor (MF)	MF Specification	Effect(s) on the KER	Reference(s)
Air pollution		Air pollution primes immunity; increases the levels of circulating IL-1β, IL-6 and TNF-α; impairs the normal functions of macrophages and alveolar cells. Exposure to particulate air pollution, such as PM2.5, is associated with pulmonary inflammation [1,2]. Both short term and chronic exposures to fine particulate matter (PM) have been shown to increase levels of circulating IL-1β, IL-6 and TNF-α [3-5]. Air pollution works as a priming factor that exacerbates the inflammatory phenotype of COVID-19 and further dysregulates immune cell activity. Dysregulation of the immune cell functions, on the other hand, plays a role in tissue damage and the ability of the immune system to fight pathogens, which increases the susceptibility to concomitant bacterial superinfection, for instance [6-9].	[1] Zhao et al., 2013 [2] Jia et al., 2021 [3] Tsai et al., 2012 [4] Ljungman et al., 2009 [5] Kido et al., 2011 [6] Knoll et al., 2021 [7] Glencross et al., 2020 [8] Yamasaki and Eeden, 2018 9) Signorini et al., 2018
		amounts [9]. However, SCFA supplementation in hamsters during infection had no effect on inflammatory parameters. Targeted analysis of fecal metabolites showed significantly lower fecal concentrations of SCFAs in COVID-19 patients, which correlated with disease severity and increased plasma concentrations of CXCL-10 and CRP [10].	
Vitamin D (low evidence)	Vitamin D deficiency	There is a complex interplay between vitamin D and the immune response to viral infections. Low vitamin D status is proposed to induce upregulation of the TNF-α and downstream of Nuclear Factor Kappa B Subunit 1 (NF–κB1) signaling pathway, which regulates inflammatory reactions toward viral infection in macrophages [1,2]. Vitamin D was shown as a potent suppressor of IFN-γ mediated macrophages response, preventing the release of inflammatory cytokines and chemokines [3]. Thus, release of pro-inflammatory cytokines might be exacerbated in COVID-19 patients with vitamin D deficiency [4].	[1] Hassan et al., 2022 [2] Książek et al., 2021 [3] Helming et al., 2005 [4] Munshi et al., 2021
Genetic factors		The inflammatory response manifested by increased cytokine levels results in inhibition of heme oxygenase (HO-1), with a subsequent loss of cytoprotection. In the 50-non-coding regions of the HO-1 gene, there are two polymorphic sites, namely the (GT)n dinucleotide and T (-413) A sites, which regulate the transcriptional activity of HO-1. These polymorphisms have been shown to be associated with the occurrence and progression of numerous diseases, including COVID-19 [1]. The timing of the IFN response to SARS-CoV-2 infection can vary with viral load and genetic differences in host response. When the viral load is low, IFN responses are engaged and contribute to viral clearance, resulting in mild infection. When viral load is high and/or genetic factors slow antiviral responses, virus replication can delay the IFN response and cytokine storm can occur before adaptive responses clear the virus, resulting in severe disease including multisystem inflammatory syndrome in Children (MIS-C) [2].	[1] Singh et al., 2020 [2] Rowley, 2020
Therapeutic intervention against COVID-19	Tocilizumab and Sarilumab	Are anti-IL-6 receptor monoclonal antibodies, which reduce inflammation [1] by attaching to the IL-6 receptor (as IL-6 receptor inhibitors) [2]. Tocilizumab, a biological drug approved for rheumatoid arthritis, is currently being evaluated for its efficacy against the effects of systemic IL-6 elevation (ClinicalTrial.gov accessed on March 2022, NCT04317092, NCT04320615, NCT04306705) [3].	[1] WHO, 2021. [2] European Medicines Agency, 2021 [3] Bonafè et al., 2020
	Baricitinib	Is an immunosuppressant that blocks the action of enzymes known as Janus kinases (JK), which play an important role in inflammatory processes (JAK inhibitor) [1–4].	[1] Jorgensen et al., 2020 [2] Bekerman et al., 2017 [3] Neveu et al., 2015 [4] Richardson et al., 2020
	Low molecular weight heparins (LMWHs)	Have anti-inflammatory effects by blocking pro-inflammatory mediators (TNF-α, IL-6 and Leukotriene [LTB4]) [1].	[1] Buijsers et al., 2020
Pre-existing heart failure		Dysregulation of renin angiotensin system due to pre-existing heart failure can have detrimental inflammatory effects both locally (in the heart) and systematically. The Angiotensin converting enzyme 2 (ACE2)/Angiotensin (Ang) (1-7) pathway is associated with the attenuation of a wide range of pro-inflammatory cytokines and chemokines, such as IL-1, IL-5, IL-6, IL-12, CCL2, TNF-α and MCP-1 [1].	[1] Rodrigues Prestes et al., 2017.
Diet	Dietary elements linked to pro-inflammatorymediators	High-fat diets have been linked—in multiple studies—to promote an “inflammatory status” in the gut and subsequently other organs [1]. Compounds found in many plant foods may affect COVID-19 prognosis by blocking inflammatory mediators and pathways. Bousquet et al. [2,3] identified bioactive compounds contained in spices and fermented vegetables, including capsaicin, cinnamaldehyde, curcumin, genistein, gingerol, mustard oil, piperine, wasabi, and sulforaphane, that upregulate the signaling of nuclear factor (erythroid-derived 2)-like 2 (Nrf2), a potent endogenous antioxidant which blocks oxidative stress from the Angiotensin type I receptor (AT1R) axis, inhibits overproduction of proinflammatory cytokines and chemokines (including IL-6), and limits	[1] Duan et al., 2018 [2] Bousquet et al., 2021a [3] Bousquet et al., 2020 [4] Bousquet et al., 2021b [5] Liu et al., 2022

Modulating Factor (MF)	MF Specification	Effect(s) on the KER	Reference(s)
Air pollution		Air pollution primes immunity; increases the levels of circulating IL-1β, IL-6 and TNF-α; impairs the normal functions of macrophages and alveolar cells. Exposure to particulate air pollution, such as PM2.5, is associated with pulmonary inflammation [1,2]. Both short term and chronic exposures to fine particulate matter (PM) have been shown to increase levels of circulating IL-1β, IL-6 and TNF-α [3-5]. Air pollution works as a priming factor that exacerbates the inflammatory phenotype of COVID-19 and further dysregulates immune cell activity. Dysregulation of the immune cell functions, on the other hand, plays a role in tissue damage and the ability of the immune system to fight pathogens, which increases the susceptibility to concomitant bacterial superinfection, for instance [6-9].	[1] Zhao et al., 2013 [2] Jia et al., 2021 [3] Tsai et al., 2012 [4] Ljungman et al., 2009 [5] Kido et al., 2011 [6] Knoll et al., 2021 [7] Glencross et al., 2020 [8] Yamasaki and Eeden, 2018 9) Signorini et al., 2018
		the activation of NF-κB. There is some *in vitro* evidence that Lactobacillus, found in many fermented foods, works through the same mechanism [4]. Finally, naringin, a compound found in citrus fruits, reduced LPS-induced IL-6 expression levels *in vitro* [5].	

Known Feedforward/Feedback loops influencing this KER

Activated pro-inflammatory cells secrete pro-inflammatory mediators, and those mediators' goal is to cause signalling and response, which can lead to chronic inflammation (KE1497). Chronic inflammation means proinflammatory mediators increase and increased recruitment of inflammatory cells acts in a positive feedback loop, which continues a pro-inflammatory environment.

References

1. Agrawal S, Salazar J, Tran TM, Agrawal A. Sex-Related Differences in Innate and Adaptive Immune Responses to SARS-CoV-2. Front Immunol. 2021 Oct 20;12:739757. doi: 10.3389/fimmu.2021.739757.
2. Atarashi K, Tanoue T, Oshima K, Suda W, Nagano Y, Nishikawa H, Fukuda S, Saito T, Narushima S, Hase K, Kim S, Fritz JV, Wilmes P, Ueha S, Matsushima K, Ohno H, Olle B, Sakaguchi S, Taniguchi T, Morita H, Hattori M, Honda K. Treg induction by a rationally selected mixture of Clostridia strains from the human microbiota. Nature. 2013 Aug 8;500(7461):232-6. doi: 10.1038/nature12331.
3. Bastard P, Rosen LB, Zhang Q, Michailidis E, Hoffmann HH, Zhang Y, Dorgham K, Philippot Q, Rosain J, Béziat V, Manry J, Shaw E, Haljasmägi L, Peterson P, Lorenzo L, Bizien L, Trouillet-Assant S, Dobbs K, de Jesus AA, Belot A, Kallaste A, Catherinot E, Tandjaoui-Lambiotte Y, Le Pen J, Kerner G, Bigio B, Seeleuthner Y, Yang R, Bolze A, Spaan AN, Delmonte OM, Abers MS, Aiuti A, Casari G, Lampasona V, Piemonti L, Ciceri F, Bilguvar K, Lifton RP, Vasse M, Smadja DM, Migaud M, Hadjadj J, Terrier B, Duffy D, Quintana-Murci L, van de Beek D, Roussel L, Vinh DC, Tangye SG, Haerynck F, Dalmau D, Martinez-Picado J, Brodin P, Nussenzweig MC, Boisson-Dupuis S, Rodríguez-Gallego C, Vogt G, Mogensen TH, Oler AJ, Gu J, Burbelo PD, Cohen JI, Biondi A, Bettini LR, D'Angio M, Bonfanti P, Rossignol P, Mayaux J, Rieux-Laucat F, Husebye ES, Fusco F, Ursini MV, Imberti L, Sottini A, Paghera S, Quiros-Roldan E, Rossi C, Castagnoli R, Montagna D, Licari A, Marseglia GL, Duval X, Ghosn J; HGID Lab; NIAID-USUHS Immune Response to COVID Group; COVID Clinicians; COVID-STORM Clinicians;

Imagine COVID Group; French COVID Cohort Study Group; Milieu Intérieur Consortium; CoV-Contact Cohort; Amsterdam UMC Covid-19 Biobank; COVID Human Genetic Effort; Tsang JS, Goldbach-Mansky R, Kisand K, Lionakis MS, Puel A, Zhang SY, Holland SM, Gorochov G, Jouanguy E, Rice CM, Cobat A, Notarangelo LD, Abel L, Su HC, Casanova JL. Autoantibodies against type I IFNs in patients with life-threatening COVID-19. Science. 2020 Oct 23;370(6515):eabd4585. doi: 10.1126/science.abd4585.

4. Bekerman E, Neveu G, Shulla A, Brannan J, Pu SY, Wang S, Xiao F, Barouch-Bentov R, Bakken RR, Mateo R, Govero J, Nagamine CM, Diamond MS, De Jonghe S, Herdewijn P, Dye JM, Randall G, Einav S. Anticancer kinase inhibitors impair intracellular viral trafficking and exert broad-spectrum antiviral effects. J Clin Invest. 2017 Apr 3;127(4):1338-1352. doi: 10.1172/JCI89857.

5. Bernardi S, Marcuzzi A, Piscianz E, Tommasini A, Fabris B. The Complex Interplay between Lipids, Immune System and Interleukins in Cardio-Metabolic Diseases. Int J Mol Sci. 2018 Dec 14;19(12):4058. doi: 10.3390/ijms19124058.

6. Bonafè M, Prattichizzo F, Giuliani A, Storci G, Sabbatinelli J, Olivieri F. Inflamm-aging: Why older men are the most susceptible to SARS-CoV-2 complicated outcomes. Cytokine Growth Factor Rev. 2020 Jun;53:33-37. doi: 10.1016/j.cytogfr.2020.04.005.

7. Bourdon JA, Saber AT, Jacobsen NR, Jensen KA, Madsen AM, Lamson JS, Wallin H, Møller P, Loft S, Yauk CL, Vogel UB. Carbon black nanoparticle instillation induces sustained inflammation and genotoxicity in mouse lung and liver. Part Fibre Toxicol. 2012 Feb 2;9:5. doi: 10.1186/1743-8977-9-5.

8. Bousquet J, Cristol JP, Czarlewski W, Anto JM, Martineau A, Haahtela T, Fonseca SC, Iaccarino G, Blain H, Fiocchi A, Canonica GW, Fonseca JA, Vidal A, Choi HJ, Kim HJ, Le Moing V, Reynes J, Sheikh A, Akdis CA, Zuberbier T; ARIA group. Nrf2-interacting nutrients and COVID-19: time for research to develop adaptation strategies. Clin Transl Allergy. 2020 Dec 3;10(1):58. doi: 10.1186/s13601-020-00362-7

9. Bousquet J, Czarlewski W, Zuberbier T, Mullol J, Blain H, Cristol JP, De La Torre R, Le Moing V, Pizarro Lozano N, Bedbrook A, Agache I, Akdis CA, Canonica GW, Cruz AA, Fiocchi A, Fonseca JA, Fonseca S, Gemicioğlu B, Haahtela T, Iaccarino G, Ivancevich JC, Jutel M, Klimek L, Kuna P, Larenas-Linnemann DE, Melén E, Okamoto Y, Papadopoulos NG, Pfaar O, Reynes J, Rolland Y, Rouadi PW, Samolinski B, Sheikh A, Toppila-Salmi S, Valiulis A, Choi HJ, Kim HJ, Anto JM. Spices to Control COVID-19 Symptoms: Yes, but Not Only…. Int Arch Allergy Immunol. 2021a;182(6):489-495. doi: 10.1159/000513538.

10. Bousquet J, Anto JM, Czarlewski W, Haahtela T, Fonseca SC, Iaccarino G, Blain H, Vidal A, Sheikh A, Akdis CA, Zuberbier T; ARIA group. Cabbage and fermented vegetables: From death rate heterogeneity in countries to candidates for mitigation strategies of severe COVID-19. Allergy. 2021b Mar;76(3):735-750. doi: 10.1111/all.14549.

11. Buijsers B, Yanginlar C, Maciej-Hulme ML, de Mast Q, van der Vlag J. Beneficial non-anticoagulant mechanisms underlying heparin treatment of COVID-19 patients. EBioMedicine. 2020 Sep;59:102969. doi: 10.1016/j.ebiom.2020.102969.

12. Caterino M, Gelzo M, Sol S, Fedele R, Annunziata A, Calabrese C, Fiorentino G, D'Abbraccio M, Dell'Isola C, Fusco FM, Parrella R, Fabbrocini G, Gentile I, Andolfo I, Capasso M, Costanzo M, Daniele A, Marchese E, Polito R, Russo R, Missero C, Ruoppolo M, Castaldo G. Dysregulation of lipid metabolism and pathological inflammation in patients with COVID-19. Sci Rep. 2021 Feb 3;11(1):2941. doi: 10.1038/s41598-021-82426-7.

13. Chen S, Yin R, Mutze K, Yu Y, Takenaka S, Königshoff M, Stoeger T. No involvement of alveolar macrophages in the initiation of carbon nanoparticle induced acute lung inflammation in mice. Part Fibre Toxicol. 2016 Jun 21;13(1):33. doi: 10.1186/s12989-016-0144-6.

14. Corsini E, Sangiovanni E, Avogadro A, Galbiati V, Viviani B, Marinovich M, Galli CL, Dell'Agli M, Germolec DR. In vitro characterization of the immunotoxic potential of several perfluorinated compounds (PFCs). Toxicol Appl Pharmacol. 2012 Jan 15;258(2):248-55. doi: 10.1016/j.taap.2011.11.004.

15. Duan Y, Zeng L, Zheng C, Song B, Li F, Kong X, Xu K. Inflammatory Links Between High Fat Diets and Diseases. Front Immunol. 2018 Nov 13;9:2649. doi: 10.3389/fimmu.2018.02649

16. EFSA Panel on Contaminants in the Food Chain (EFSA CONTAM Panel); Schrenk D, Bignami M, Bodin L, Chipman JK, Del Mazo J, Grasl-Kraupp B, Hogstrand C, Hoogenboom LR, Leblanc JC, Nebbia CS, Nielsen E, Ntzani E, Petersen A, Sand S, Vleminckx C, Wallace H, Barregård L, Ceccatelli S, Cravedi JP, Halldorsson TI, Haug LS, Johansson N, Knutsen HK, Rose M, Roudot AC, Van Loveren H, Vollmer G, Mackay K, Riolo F, Schwerdtle T. Risk to human health related to the presence of perfluoroalkyl substances in food. EFSA J. 2020 Sep 17;18(9):e06223. doi: 10.2903/j.efsa.2020.6223.

17. European Medicines Agency. RoActemra. 2021. Available online: https://www.ema.europa.eu/en/medicines/human/EPAR/roactemra (accessed 12 May 2022).

18. Gasse P, Mary C, Guenon I, Noulin N, Charron S, Schnyder-Candrian S, Schnyder B, Akira S, Quesniaux VF, Lagente V, Ryffel B, Couillin I. IL-1R1/MyD88 signaling and the inflammasome are essential in pulmonary inflammation and fibrosis in mice. J Clin Invest. 2007 Dec;117(12):3786-99. doi: 10.1172/JCI32285.

19. Girtsman TA, Beamer CA, Wu N, Buford M, Holian A. IL-1R signalling is critical for regulation of multi-walled carbon nanotubes-induced acute lung inflammation in C57Bl/6 mice. Nanotoxicology. 2014 Feb;8(1):17-27. doi: 10.3109/17435390.2012.744110.

20. Glencross DA, Ho TR, Camiña N, Hawrylowicz CM, Pfeffer PE. Air pollution and its effects on the immune system. Free Radic Biol Med. 2020 May 1;151:56-68. doi: 10.1016/j.freeradbiomed.2020.01.179.

21. Gonçalves J, Juliano AM, Charepe N, Alenquer M, Athayde D, Ferreira F, Archer M, Amorim MJ, Serrano F, Soares H. Secretory IgA and T cells targeting SARS-CoV-2 spike protein are transferred to the breastmilk upon mRNA vaccination. Cell Rep Med. 2021 Dec 21;2(12):100468. doi: 10.1016/j.xcrm.2021.100468.

22. Gou W, Fu Y, Yue L, Chen GD, Cai X, Shuai M, Xu F, Yi X, Chen H, Zhu Y, Xiao ML, Jiang Z, Miao Z, Xiao C, Shen B, Wu X, Zhao H, Ling W, Wang J, Chen YM, Guo T, Zheng JS. Gut microbiota, inflammation, and molecular signatures of host response to infection. J Genet Genomics. 2021 Sep 20;48(9):792-802. doi: 10.1016/j.jgg.2021.04.002.

23. Gouwy M, De Buck M, Pörtner N, Opdenakker G, Proost P, Struyf S, Van Damme J. Serum amyloid A chemoattracts immature dendritic cells and indirectly provokes monocyte chemotaxis by induction of cooperating CC and CXC chemokines. Eur J Immunol. 2015 Jan;45(1):101-12. doi: 10.1002/eji.201444818.

24. Grenga L, Pible O, Miotello G, Culotta K, Ruat S, Roncato MA, Gas F, Bellanger L, Claret PG, Dunyach-Remy C, Laureillard D, Sotto A, Lavigne JP, Armengaud J. Taxonomical and functional changes in COVID-19 faecal microbiome could be related to SARS-CoV-2

faecal load. Environ Microbiol. 2022 Sep;24(9):4299-4316. doi: 10.1111/1462-2920.16028.

25. Gu S, Chen Y, Wu Z, Chen Y, Gao H, Lv L, Guo F, Zhang X, Luo R, Huang C, Lu H, Zheng B, Zhang J, Yan R, Zhang H, Jiang H, Xu Q, Guo J, Gong Y, Tang L, Li L. Alterations of the Gut Microbiota in Patients With Coronavirus Disease 2019 or H1N1 Influenza. Clin Infect Dis. 2020 Dec 17;71(10):2669-2678. doi: 10.1093/cid/ciaa709.
26. Hadrup N, Rahmani F, Jacobsen NR, Saber AT, Jackson P, Bengtson S, Williams A, Wallin H, Halappanavar S, Vogel U. Acute phase response and inflammation following pulmonary exposure to low doses of zinc oxide nanoparticles in mice. Nanotoxicology. 2019 Nov;13(9):1275-1292. doi: 10.1080/17435390.2019.1654004.
27. Halappanavar S, Nikota J, Wu D, Williams A, Yauk CL, Stampfli M. IL-1 receptor regulates microRNA-135b expression in a negative feedback mechanism during cigarette smoke-induced inflammation. J Immunol. 2013 Apr 1;190(7):3679-86. doi: 10.4049/jimmunol.1202456.
28. Han R, Hu M, Zhong Q, Wan C, Liu L, Li F, Zhang F, Ding W. Perfluorooctane sulphonate induces oxidative hepatic damage via mitochondria-dependent and NF-κB/TNF-α-mediated pathway. Chemosphere. 2018 Jan;191:1056-1064. doi: 10.1016/j.chemosphere.2017.08.070.
29. HARRIS H. Role of chemotaxis in inflammation. Physiol Rev. 1954 Jul;34(3):529-62. doi: 10.1152/physrev.1954.34.3.529.
30. Hassan MH, Elsadek AAM, Mahmoud MA, Elsadek BEM. Vitamin D Receptor Gene Polymorphisms and Risk of Knee Osteoarthritis: Possible Correlations with TNF-α, Macrophage Migration Inhibitory Factor, and 25-Hydroxycholecalciferol Status. Biochem Genet. 2022 Apr;60(2):611-628. doi: 10.1007/s10528-021-10116-0.
31. Helming L, Böse J, Ehrchen J, Schiebe S, Frahm T, Geffers R, Probst-Kepper M, Balling R, Lengeling A. 1alpha,25-Dihydroxyvitamin D3 is a potent suppressor of interferon gamma-mediated macrophage activation. Blood. 2005 Dec 15;106(13):4351-8. doi: 10.1182/blood-2005-03-1029.
32. Henry BM, Szergyuk I, de Oliveira MHS, Abosamak MF, Benoit SW, Benoit JL, Lippi G. Alterations in the lipid profile associate with a dysregulated inflammatory, prothrombotic, anti-fibrinolytic state and development of severe acute kidney injury in coronavirus disease 2019 (COVID-19): A study from Cincinnati, USA. Diabetes Metab Syndr. 2021 May-Jun;15(3):863-868. doi: 10.1016/j.dsx.2021.04.011.
33. Ho CC, Chang H, Tsai HT, Tsai MH, Yang CS, Ling YC, Lin P. Quantum dot 705, a cadmium-based nanoparticle, induces persistent inflammation and granuloma formation in the mouse lung. Nanotoxicology. 2013 Feb;7(1):105-15. doi: 10.3109/17435390.2011.635814.
34. Hofman Z, de Maat S, Hack CE, Maas C. Bradykinin: Inflammatory Product of the Coagulation System. Clin Rev Allergy Immunol. 2016 Oct;51(2):152-61. doi: 10.1007/s12016-016-8540-0.
35. Hubler MJ, Kennedy AJ. Role of lipids in the metabolism and activation of immune cells. J Nutr Biochem. 2016 Aug;34:1-7. doi: 10.1016/j.jnutbio.2015.11.002.
36. Husain M, Kyjovska ZO, Bourdon-Lacombe J, Saber AT, Jensen KA, Jacobsen NR, Williams A, Wallin H, Halappanavar S, Vogel U, Yauk CL. Carbon black nanoparticles induce biphasic gene expression changes associated with inflammatory responses in the

lungs of C57BL/6 mice following a single intratracheal instillation. Toxicol Appl Pharmacol. 2015 Dec 15;289(3):573-88. doi: 10.1016/j.taap.2015.11.003.

37. Im SS, Yousef L, Blaschitz C, Liu JZ, Edwards RA, Young SG, Raffatellu M, Osborne TF. Linking lipid metabolism to the innate immune response in macrophages through sterol regulatory element binding protein-1a. Cell Metab. 2011 May 4;13(5):540-9. doi: 10.1016/j.cmet.2011.04.001

38. Jia H, Liu Y, Guo D, He W, Zhao L, Xia S. PM2.5-induced pulmonary inflammation via activating of the NLRP3/caspase-1 signaling pathway. Environmental Toxicology, 2021 Mar;36(3):298-307. doi: 10.1002/tox.23035.

39. Jorgensen SCJ, Tse CLY, Burry L, Dresser LD. Baricitinib: A Review of Pharmacology, Safety, and Emerging Clinical Experience in COVID-19. Pharmacotherapy. 2020 Aug;40(8):843-856. doi: 10.1002/phar.2438.

40. Kamata H, Tasaka S, Inoue K, Miyamoto K, Nakano Y, Shinoda H, Kimizuka Y, Fujiwara H, Ishii M, Hasegawa N, Takamiya R, Fujishima S, Takano H, Ishizaka A. Carbon black nanoparticles enhance bleomycin-induced lung inflammatory and fibrotic changes in mice. Exp Biol Med (Maywood). 2011 Mar;236(3):315-24. doi: 10.1258/ebm.2011.010180.

41. Khatri M, Bello D, Martin J, Bello A, Gore R, Demokritou P, et al. Chronic upper airway inflammation and systemic oxidative stress from nanoparticles in photocopier operators: Mechanistic insights. NanoImpact. 2017;5:133-45. doi: https://doi.org/10.1016/j.impact.2017.01.007.

42. Kido T, Tamagawa E, Bai N, Suda K, Yang HH, Li Y, Chiang G, Yatera K, Mukae H, Sin DD, Van Eeden SF. Particulate matter induces translocation of IL-6 from the lung to the systemic circulation. Am J Respir Cell Mol Biol. 2011 Feb;44(2):197-204. doi: 10.1165/rcmb.2009-0427OC.

43. Knoll R, Schultze JL, Schulte-Schrepping J. Monocytes and Macrophages in COVID-19. Front Immunol. 2021 Jul 21;12:720109. doi: 10.3389/fimmu.2021.720109.

44. Kovacs EJ, Boe DM, Boule LA, Curtis BJ. Inflammaging and the Lung. Clin Geriatr Med. 2017 Nov;33(4):459-471. doi: 10.1016/j.cger.2017.06.002.

45. Książek A, Zagrodna A, Bohdanowicz-Pawlak A, Lwow F, Słowińska-Lisowska M. Relationships between Vitamin D and Selected Cytokines and Hemogram Parameters in Professional Football Players-Pilot Study. Int J Environ Res Public Health. 2021 Jul 2;18(13):7124. doi: 10.3390/ijerph18137124.

46. Lee S, Hwang SH, Jeong J, Han Y, Kim SH, Lee DK, Lee HS, Chung ST, Jeong J, Roh C, Huh YS, Cho WS. Nickel oxide nanoparticles can recruit eosinophils in the lungs of rats by the direct release of intracellular eotaxin. Part Fibre Toxicol. 2016 Jun 9;13(1):30. doi: 10.1186/s12989-016-0142-8.

47. Leick M, Azcutia V, Newton G, Luscinskas FW. Leukocyte recruitment in inflammation: basic concepts and new mechanistic insights based on new models and microscopic imaging technologies. Cell Tissue Res. 2014 Mar;355(3):647-56. doi: 10.1007/s00441-014-1809-9.

48. Li R, Guo C, Lin X, Chan TF, Lai KP, Chen J. Integrative omics analyses uncover the mechanism underlying the immunotoxicity of perfluorooctanesulfonate in human lymphocytes. Chemosphere. 2020 Oct;256:127062. doi: 10.1016/j.chemosphere.2020.127062

49. Libby P. Fanning the flames: inflammation in cardiovascular diseases. Cardiovasc Res. 2015 Aug 1;107(3):307-9. doi: 10.1093/cvr/cvv188.

50. Liu W, Zheng W, Cheng L, Li M, Huang J, Bao S, Xu Q, Ma Z. Citrus fruits are rich in flavonoids for immunoregulation and potential targeting ACE2. Nat Prod Bioprospect. 2022 Feb 14;12(1):4. doi: 10.1007/s13659-022-00325-4.

51. Ljungman P, Bellander T, Schneider A, Breitner S, Forastiere F, Hampel R, Illig T, Jacquemin B, Katsouyanni K, von Klot S, Koenig W, Lanki T, Nyberg F, Pekkanen J, Pistelli R, Pitsavos C, Rosenqvist M, Sunyer J, Peters A. Modification of the interleukin-6 response to air pollution by interleukin-6 and fibrinogen polymorphisms. Environ Health Perspect. 2009 Sep;117(9):1373-9. doi: 10.1289/ehp.0800370.

52. Ma J, Li R, Qu G, Liu H, Yan B, Xia T, Liu Y, Liu S. Carbon nanotubes stimulate synovial inflammation by inducing systemic pro-inflammatory cytokines. Nanoscale. 2016 Oct 27;8(42):18070-18086. doi: 10.1039/c6nr06041b.

53. Marchini T, Wolf D, Michel NA, Mauler M, Dufner B, Hoppe N, Beckert J, Jäckel M, Magnani N, Duerschmied D, Tasat D, Alvarez S, Reinöhl J, von Zur Muhlen C, Idzko M, Bode C, Hilgendorf I, Evelson P, Zirlik A. Acute exposure to air pollution particulate matter aggravates experimental myocardial infarction in mice by potentiating cytokine secretion from lung macrophages. Basic Res Cardiol. 2016 Jul;111(4):44. doi: 10.1007/s00395-016-0562-5.

54. Mauvais-Jarvis F, Bairey Merz N, Barnes PJ, Brinton RD, Carrero JJ, DeMeo DL, De Vries GJ, Epperson CN, Govindan R, Klein SL, Lonardo A, Maki PM, McCullough LD, Regitz-Zagrosek V, Regensteiner JG, Rubin JB, Sandberg K, Suzuki A. Sex and gender: modifiers of health, disease, and medicine. Lancet. 2020 Aug 22;396(10250):565-582. doi: 10.1016/S0140-6736(20)31561-0.

55. Morimoto Y, Ogami A, Todoroki M, Yamamoto M, Murakami M, Hirohashi M, Oyabu T, Myojo T, Nishi K, Kadoya C, Yamasaki S, Nagatomo H, Fujita K, Endoh S, Uchida K, Yamamoto K, Kobayashi N, Nakanishi J, Tanaka I. Expression of inflammation-related cytokines following intratracheal instillation of nickel oxide nanoparticles. Nanotoxicology. 2010 Jun;4(2):161-76. doi: 10.3109/17435390903518479

56. Munshi R, Hussein MH, Toraih EA, Elshazli RM, Jardak C, Sultana N, Youssef MR, Omar M, Attia AS, Fawzy MS, Killackey M, Kandil E, Duchesne J. Vitamin D insufficiency as a potential culprit in critical COVID-19 patients. J Med Virol. 2021 Feb;93(2):733-740. doi: 10.1002/jmv.26360.

57. Muscogiuri G, Pugliese G, Barrea L, Savastano S, Colao A. Commentary: Obesity: The "Achilles heel" for COVID-19? Metabolism. 2020 Jul;108:154251. doi: 10.1016/j.metabol.2020.154251.

58. Neveu G, Ziv-Av A, Barouch-Bentov R, Berkerman E, Mulholland J, Einav S. AP-2-associated protein kinase 1 and cyclin G-associated kinase regulate hepatitis C virus entry and are potential drug targets. J Virol. 2015 Apr;89(8):4387-404. doi: 10.1128/JVI.02705-14.

59. Nikota J, Banville A, Goodwin LR, Wu D, Williams A, Yauk CL, Wallin H, Vogel U, Halappanavar S. Stat-6 signaling pathway and not Interleukin-1 mediates multi-walled carbon nanotube-induced lung fibrosis in mice: insights from an adverse outcome pathway framework. Part Fibre Toxicol. 2017 Sep 13;14(1):37. doi: 10.1186/s12989-017-0218-0.

60. Patowary P, Pathak MP, Zaman K, Dwivedi SK, Chattopadhyay P. Innate inflammatory response to acute inhalation exposure of riot control agent oleoresin capsicum in female rats: An interplay between neutrophil mobilization and inflammatory markers. Exp Lung Res. 2020 Apr-May;46(3-4):81-97. doi: 10.1080/01902148.2020.1733709.

61. Petri B, Sanz MJ. Neutrophil chemotaxis. Cell Tissue Res. 2018 Mar;371(3):425-436. doi: 10.1007/s00441-017-2776-8.

62. Porter DW, Ye J, Ma J, Barger M, Robinson VA, Ramsey D, McLaurin J, Khan A, Landsittel D, Teass A, Castranova V. Time course of pulmonary response of rats to inhalation of crystalline silica: NF-kappa B activation, inflammation, cytokine production, and damage. Inhal Toxicol. 2002 Apr;14(4):349-67. doi: 10.1080/08958370252870998.

63. Porter DW, Orandle M, Zheng P, Wu N, Hamilton RF Jr, Holian A, Chen BT, Andrew M, Wolfarth MG, Battelli L, Tsuruoka S, Terrones M, Castranova V. Mouse pulmonary dose- and time course-responses induced by exposure to nitrogen-doped multi-walled carbon nanotubes. Inhal Toxicol. 2020 Jan;32(1):24-38. doi: 10.1080/08958378.2020.1723746.

64. Poulsen SS, Jacobsen NR, Labib S, Wu D, Husain M, Williams A, Bøgelund JP, Andersen O, Købler C, Mølhave K, Kyjovska ZO, Saber AT, Wallin H, Yauk CL, Vogel U, Halappanavar S. Transcriptomic analysis reveals novel mechanistic insight into murine biological responses to multi-walled carbon nanotubes in lungs and cultured lung epithelial cells. PLoS One. 2013 Nov 19;8(11):e80452. doi: 10.1371/journal.pone.0080452.

65. Rahman L, Wu D, Johnston M, William A, Halappanavar S. Toxicogenomics analysis of mouse lung responses following exposure to titanium dioxide nanomaterials reveal their disease potential at high doses. Mutagenesis. 2017 Jan;32(1):59-76. doi: 10.1093/mutage/gew048.

66. Richardson P, Griffin I, Tucker C, Smith D, Oechsle O, Phelan A, Rawling M, Savory E, Stebbing J. Baricitinib as potential treatment for 2019-nCoV acute respiratory disease. Lancet. 2020 Feb 15;395(10223):e30-e31. doi: 10.1016/S0140-6736(20)30304-4.

67. Rodrigues Prestes TR, Rocha NP, Miranda AS, Teixeira AL, Simoes-E-Silva AC. The Anti-Inflammatory Potential of ACE2/Angiotensin-(1-7)/Mas Receptor Axis: Evidence from Basic and Clinical Research. Curr Drug Targets. 2017;18(11):1301-1313. doi: 10.2174/1389450117666160727142401

68. Rowley AH. Understanding SARS-CoV-2-related multisystem inflammatory syndrome in children. Nat Rev Immunol. 2020 Aug;20(8):453-454. doi: 10.1038/s41577-020-0367-5.

69. Schremmer I, Brik A, Weber DG, Rosenkranz N, Rostek A, Loza K, Brüning T, Johnen G, Epple M, Bünger J, Westphal GA. Kinetics of chemotaxis, cytokine, and chemokine release of NR8383 macrophages after exposure to inflammatory and inert granular insoluble particles. Toxicol Lett. 2016 Nov 30;263:68-75. doi: 10.1016/j.toxlet.2016.08.014.

70. Scully EP, Haverfield J, Ursin RL, Tannenbaum C, Klein SL. Considering how biological sex impacts immune responses and COVID-19 outcomes. Nat Rev Immunol. 2020 Jul;20(7):442-447. doi: 10.1038/s41577-020-0348-8.

71. Sencio V, Machelart A, Robil C, Benech N, Hoffmann E, Galbert C, Deryuter L, Heumel S, Hantute-Ghesquier A, Flourens A, Brodin P, Infanti F, Richard V, Dubuisson J, Grangette C, Sulpice T, Wolowczuk I, Pinet F, Prévot V, Belouzard S, Briand F, Duterque-Coquillaud M, Sokol H, Trottein F. Alteration of the gut microbiota following SARS-CoV-2 infection correlates with disease severity in hamsters. Gut Microbes. 2022 Jan-Dec;14(1):2018900. doi: 10.1080/19490976.2021.2018900.

72. Signorini C, Pignatti P, Coccini T. How Do Inflammatory Mediators, Immune Response and Air Pollution Contribute to COVID-19 Disease Severity? A Lesson to Learn. Life (Basel). 2021 Feb 25;11(3):182. doi: 10.3390/life11030182.

73. Singh D, Wasan H, Reeta KH. Heme oxygenase-1 modulation: A potential therapeutic target for COVID-19 and associated complications. Free Radic Biol Med. 2020 Dec;161:263-271. doi: 10.1016/j.freeradbiomed.2020.10.016.

74. Song JA, Park HJ, Yang MJ, Jung KJ, Yang HS, Song CW, Lee K. Polyhexamethyleneguanidine phosphate induces severe lung inflammation, fibrosis, and thymic atrophy. Food Chem Toxicol. 2014 Jul;69:267-75. doi: 10.1016/j.fct.2014.04.027.

75. Sørli JB, Låg M, Ekeren L, Perez-Gil J, Haug LS, Da Silva E, Matrod MN, Gützkow KB, Lindeman B. Per- and polyfluoroalkyl substances (PFASs) modify lung surfactant function and pro-inflammatory responses in human bronchial epithelial cells. Toxicol In Vitro. 2020 Feb;62:104656. doi: 10.1016/j.tiv.2019.104656.

76. Takahashi T, Ellingson MK, Wong P, Israelow B, Lucas C, Klein J, Silva J, Mao T, Oh JE, Tokuyama M, Lu P, Venkataraman A, Park A, Liu F, Meir A, Sun J, Wang EY, Casanovas-Massana A, Wyllie AL, Vogels CBF, Earnest R, Lapidus S, Ott IM, Moore AJ; Yale IMPACT Research Team; Shaw A, Fournier JB, Odio CD, Farhadian S, Dela Cruz C, Grubaugh ND, Schulz WL, Ring AM, Ko AI, Omer SB, Iwasaki A. Sex differences in immune responses that underlie COVID-19 disease outcomes. Nature. 2020 Dec;588(7837):315-320. doi: 10.1038/s41586-020-2700-3.

77. Tian J, Hong Y, Li Z, Yang Z, Lei B, Liu J, Cai Z. Immunometabolism-modulation and immunotoxicity evaluation of perfluorooctanoic acid in macrophage. Ecotoxicol Environ Saf. 2021 Jun 1;215:112128. doi: 10.1016/j.ecoenv.2021.112128.

78. Tsai DH, Amyai N, Marques-Vidal P, Wang JL, Riediker M, Mooser V, Paccaud F, Waeber G, Vollenweider P, Bochud M. Effects of particulate matter on inflammatory markers in the general adult population. Particle and Fibre Toxicolgy. 2012 Jul 6;9:24. doi: 10.1186/1743-8977-9-24

79. Villeneuve DL, Landesmann B, Allavena P, Ashley N, Bal-Price A, Corsini E, Halappanavar S, Hussell T, Laskin D, Lawrence T, Nikolic-Paterson D, Pallardy M, Paini A, Pieters R, Roth R, Tschudi-Monnet F. Representing the Process of Inflammation as Key Events in Adverse Outcome Pathways. Toxicol Sci. 2018 Jun 1;163(2):346-352. doi: 10.1093/toxsci/kfy047.

80. Vinolo MA, Rodrigues HG, Nachbar RT, Curi R. Regulation of inflammation by short chain fatty acids. Nutrients. 2011 Oct;3(10):858-76. doi: 10.3390/nu3100858.

81. Wang G, Zhang X, Liu X, Zheng J, Chen R, Kan H. Ambient fine particulate matter induce toxicity in lung epithelial-endothelial co-culture models. Toxicol Lett. 2019 Feb;301:133-145. doi: 10.1016/j.toxlet.2018.11.010.

82. Westphal GA, Schremmer I, Rostek A, Loza K, Rosenkranz N, Brüning T, Epple M, Bünger J. Particle-induced cell migration assay (PICMA): A new in vitro assay for inflammatory particle effects based on permanent cell lines. Toxicol In Vitro. 2015 Aug;29(5):997-1005. doi: 10.1016/j.tiv.2015.04.005.

83. World Health Organization, 2021. Therapeutics and COVID-19: Living Guideline. WHO/2019-NCoV/Therapeutics/2021.1'. IL-6 Receptor Blockers 2021. Available online: https://www.who.int/publications/i/item/WHO-2019-nCoV-therapeutics-2022.4 (accessed 12 May 2022).

84. Winer S, Chan Y, Paltser G, Truong D, Tsui H, Bahrami J, Dorfman R, Wang Y, Zielenski J, Mastronardi F, Maezawa Y, Drucker DJ, Engleman E, Winer D, Dosch HM. Normalization of obesity-associated insulin resistance through immunotherapy. Nat Med. 2009 Aug;15(8):921-9. doi: 10.1038/nm.2001

85. Yamasaki K, Eeden SFV. Lung Macrophage Phenotypes and Functional Responses: Role in the Pathogenesis of COPD. Int J Mol Sci. 2018 Feb 15;19(2):582. doi: 10.3390/ijms19020582.

86. Yeoh YK, Zuo T, Lui GC, Zhang F, Liu Q, Li AY, Chung AC, Cheung CP, Tso EY, Fung KS, Chan V, Ling L, Joynt G, Hui DS, Chow KM, Ng SSS, Li TC, Ng RW, Yip TC, Wong GL, Chan FK, Wong CK, Chan PK, Ng SC. Gut microbiota composition reflects disease severity and dysfunctional immune responses in patients with COVID-19. Gut. 2021 Apr;70(4):698-706. doi: 10.1136/gutjnl-2020-323020.

87. Yoo JY, Groer M, Dutra SVO, Sarkar A, McSkimming DI. Gut Microbiota and Immune System Interactions. Microorganisms. 2020 Oct 15;8(10):1587. doi: 10.3390/microorganisms8101587.

88. Zhang F, Wan Y, Zuo T, Yeoh YK, Liu Q, Zhang L, Zhan H, Lu W, Xu W, Lui GCY, Li AYL, Cheung CP, Wong CK, Chan PKS, Chan FKL, Ng SC. Prolonged Impairment of Short-Chain Fatty Acid and L-Isoleucine Biosynthesis in Gut Microbiome in Patients With COVID-19. Gastroenterology. 2022 Feb;162(2):548-561.e4. doi: 10.1053/j.gastro.2021.10.013.

89. Zhao J, Gao Z, Tian Z, Xie Y, Xin F, Jiang R, Kan H, Song W. The biological effects of individual-level PM(2.5) exposure on systemic immunity and inflammatory response in traffic policemen. Occup Environ Med. 2013 Jun;70(6):426-31. doi: 10.1136/oemed-2012-100864.

90. Zuo T, Zhang F, Lui GCY, Yeoh YK, Li AYL, Zhan H, Wan Y, Chung ACK, Cheung CP, Chen N, Lai CKC, Chen Z, Tso EYK, Fung KSC, Chan V, Ling L, Joynt G, Hui DSC, Chan FKL, Chan PKS, Ng SC. Alterations in Gut Microbiota of Patients With COVID-19 During Time of Hospitalization. Gastroenterology. 2020 Sep;159(3):944-955.e8. doi: 10.1053/j.gastro.2020.05.048.

Relationship: 1704: Recruitment of inflammatory cells leads to Loss of alveolar capillary membrane integrity

AOPs Referencing Relationship

AOP Name	Adjacency	Weight of Evidence	Quantitative Understanding
Substance interaction with the pulmonary resident cell membrane components leading to pulmonary fibrosis	adjacent	Moderate	Moderate

Key Event Relationship Description

Acute lung injury followed by normal repair of the alveolar capillary membrane (ACM) results in rapid resolution of the tissue injury and restoration of tissue integrity and function. The irreversible loss of ACM integrity occurs when 1) acute inflammation is not able to get rid of the toxic substance or invading pathogen (this happens following exposure to a toxic substance that is persistent or when the host is repeatedly exposed to the substance over a long period of time, 2) acute inflammation, originally incited to protect the host from external stimuli and to maintain normal homeostasis, by itself damages the host, resulting in tissue injury, and 3) the host fails to initiate a resolution response, which is essential to override the self-perpetuating inflammation response (Nathan, 2002). Loss of type-1 alveolar epithelial cells (AEC1s) and endothelial cells, the collapse of alveolar structures and fusion of basement membranes, and persistent proliferation of type II alveolar epithelial cells (AEC2s) on a damaged extracellular matrix, mark this phase (Barosova et al., 2020; Blum et al., 2014; Inoue et al., 2009; Janga et al., 2018; Marcus et al., 1997; Nemmar et al., 2016; Strieter and Mehrad, 2009). The lung tissues from patients diagnosed with idiopathic pulmonary fibrosis (IPF) show ultrastructural damage to the ACM with type-1 pneumocyte and endothelial cell injury (Strieter and Mehrad, 2009). In rodents treated with bleomycin, the damaged ACM resembles that seen in the fibrotic human lung (Grande *et al.*, 1998).

Evidence Supporting this KER

Biological Plausibility

The biological plausibility of this KER is high. There is a mechanistic relationship between an increase in pro-inflammatory cells and mediators, and damage to the ACM (Bhalla et al., 2009; Ward, 2003; Zemans et al., 2009).

Exposure to high doses of insoluble nanomaterials can impair the macrophage-mediated clearance process, initiating chronicity of inflammation characterized by cytokine release, reactive oxygen species (ROS) synthesis and the tissue damage cascade (Palecanda and Kobzik, 2001) and subsequently leading to tissue injury. For example, exposure to crystalline silica generates oxidative stress, increased release of pro-inflammatory cytokines (e.g. Tumor necrosis factor alpha [TNF-α], Interleukin [IL]-1, IL-6), activation of transcription factors (e.g. Nuclear factor kappa B [NF-κB], Activator protein [AP-1]), and other cell signalling pathways including Mitogen-activated protein kinases (MAPKs) and Extracellular signal-regulated kinases [ERKs] (Fubini and Hubbard 2003; Hubbard et al., 2001; Hubbard et al., 2002). In silicosis, TNF-α is suggested to play a critical role in the observed pathogenicity (Castranova et al., 2004), which in turn, is dependent on activation of NF-κB and ROS synthesis (Cassel et al.,2008; Kawasaki et al.,

2015; Shi et al.,1998). It has been proposed that IPF is a disorder of elevated oxidative stress, with the existence of an oxidant-antioxidant imbalance in distal alveolar air spaces (MacNee, 2001). Several studies have reported that antioxidant treatment attenuates the bleomycin-induced oxidative burden and subsequent pulmonary fibrosis (Punithavathi, et al., 2000; Serrano-Mollar et al., 2003; Wang et al., 2002).

Mice deficient in NLR family pyrin domain containing 3 (Nalp3) showed reduced inflammation, lower cytokine production and dampened fibrotic response following exposure to asbestos or silica (Dostert et al., 2008). Single-walled carbon nanotube exposure induces alveolar macrophage activation, enhanced oxidative stress, increased and persistent expression of pro-inflammatory mediators associated with chronic inflammation and severe granuloma formation in mice (Chou et al., 2008). Bleomycin treatment induces increased lung weight, epithelial cell death, inflammation, increased hydroxyproline content, collagen accumulation and fibrotic lesions in mice, all of which were elevated in mice deficient in Nuclear factor erythroid 2-related factor 2 (Nrf2) (Cho et al., 2004). Multi-walled carbon nanotube (MWCNT)-induced fibrotic response is the result of interplay between oxidative stress and inflammation, which determines the severity of the fibrotic pathology. Mice lacking Nrf2 that is associated with mounting antioxidant defense against oxidative stress, exhibit exuberant fibrotic responses to MWCNT (Dong and Ma, 2016).

Empirical Evidence

The empirical support for this KER is moderate. There is both temporal and dose-response evidence to suggest that an increased amount of pro-inflammatory immune cells potentiates ACM damage. However, few studies assessing these KEs include multiple concentrations and timepoints, and as such, these KEs are typically reported as occurring together (i.e. damage is detected along with an increase in cell abundance) (Umbright et al., 2017; Zeidler-Erdley et al., 2011; Additional references available in Table 1).

Table 1. Studies providing empirical evidence for the relationship between KE2 (Event 1497) and KE3 (Event 1498). +: Severity of Response. References available in main KER page

Stressor (Reference)	***In vitro/in vivo/ex vivo***	**Species/Cell line**	**Exposure conditions**	**KE2 (Event 1497) Increased, recruitment of pro-inflammatory cells**			**KE3 (Event 1498) Loss of alveolar capillary membrane integrity**	
Polyhexamethylene guanidine phosphate (Kim et al., 2016)	*In vitro*	Calu-3, THP-1 and HMC-1 cells (Bronquial ALI co-culture)	2.2, 4.4, 8.8, 17.6 mg/mL Incubation for 1, 6, 24 h	Chemoattractant cytokine IL-8			Disruption of the epithelial airway barrier (Paracellular flux %, transepithelial electrical resistance)	
				1 h 2.2: + 4.4: ++ 8.8: ++ 17.6: ++	6 h 2.2: + 4.4: ++ 8.8: +++ 17.6: ++++	24 h 2.2: + 4.4: ++ 8.8: ++++ 17.6: ++++	24 h 2.2: 4.4: 8.8: + 17.6: ++	
Silica nanoparticles (Kasper et al., 2011)	*In vitro*	Co-culture, microvascular endothelial cell line and the human lung adenocarcinoma cell line.	6, 60, 600, 6000 µg/mL 4 h exposure, 4 h exposure + 20 h recovery	Increased sICAM-1, IL-6, IL-8			Decreased transepithelial electrical resistance	
				4 h exposure + 20 h recovery 6: + 60: ++ 600: +++ 6000: +++			4 h exposure 6: + 60: ++ 600: +++ 6000: ++++	
fMLP (N-formylmethionyl-leucyl-phenylalanine) (Gautam et al., 1998)	*Ex vivo* Polymorphonuclear cells (PMN) isolated from human whole blood	Bovine aorta endothelial cells (BAEC)	10^{-7} M lower compartment for 0, 10, 20, 30, 40, 50 min	Transmigration of PMN			Albumin clearance	Decreased endothelial cells resistance
				0 min: + 10 min: + 20 min: ++ 30 min: ++ 40 min: +++ 50 min: +++			0 min: + 10 min: + 20 min: ++ 30 min: ++ 40 min: +++ 50 min: +++	0 min: + 10 min: ++ 20 min: ++ 30 min: ++
Multi-walled carbon nanotubes (Porter et al., 2013)	*In vivo*	Male mice C57BL/6J	10 mg/m^3 aerosol inhalation 5h/day for 2, 4, 8, 12 days	Increased PMN	Neutrophil chemoattractant		Whole lung fluid	

			Evaluation: post-exposure	Day 2: + Day 4: + Day 8: ++ Day 12: ++		Day 2: + Day 4: ++ Day 8: +++ Day 12: +++		Albumin concentration				LDH activity			
								Day 2: + Day 4: ++ Day 8: +++ Day 12: +++				Day 2: + Day 4: ++ Day 8: +++ Day 12: +++			
Crystalline silica (Umbright et al., 2017)	*In vivo*	Male Fischer 344 rats	15 mg/m^3 inhalation, 6h/day, 5 days/week for 3, 6, 12 weeks Evaluation: post-exposure	Increased PMN				Albumin concentration-BALF				BALF LDH activity			
				Week 3: + Week 6: ++ Week 12: +++				Week 3: Week 6: ++ Week 12: +				Week 3: ++ Week 6: ++ Week 12: ++			
Paraquat (Shinozaki et al., 1992)	*In vivo*	Sheep	5 mg/Kg intramuscular injection Evaluation: 1, 2, 3 weeks post-exposure	Number of granulocytes				Alveolar wall thickening				Lung malondialdehyde			
				Week 1: + Week 2: + Week 3: ++				Week 1: Week 2: Week 3: +++				Week 1: Week 2: Week 3: +++			
DQ12 particles (Arras et al., 2001)	*In vivo*	Transgenic Tg5 mice expressing high levels of IL-9. WT FVB mice C57BL6/J	1, 5 mg intratracheal instillation. Evaluation: 2, 4 months post-exposure	Increased PMN in BALF				LDH content in BALF				Proteins in BALF			
				Month 2 1: + 5: ++		Month 4 1: + 5: ++		Month 2 1: + 5: ++		Month 4 1: + 5: ++		Month 2 1: + 5: ++		Month 4 1: + 5: ++	
CeO_2 nanoparticles (Morimoto et al., 2015)	*In vivo*	Male Fischer 344 rats	0.2 mg (0.8 mg/kg), 1 mg (4 mg/Kg) intratracheal instillation Evaluation: 3 days (D), 1 week (W), 1, 3, 6 months (M) post-exposure	Total cell counts in BALF						LDH activity in BALF					
				3D 0.2: 1:	1W 0.2: 1: +++	1 M 0.2: 1: ++	3M 0.2: 1: ++	6M 0.2: 1:		3D 0.2: +++ 1: ++++	1W 0.2: ++ 1: +++	1 M 0.2: + 1: ++	3M 0.2: + 1: +	6M 0.2: + 1: +	
			2, 10 mg/m^3 Inhalation, 6h per day, 5 days/week, 4 weeks Evaluation: 3 days, 1, 3 months post-exposure	Total cell counts in BALF						LDH activity in BALF					
				Day 3 2: ++ 10: +++		Month 1 2: 10:		Month 3 2: 10: ++		Day 3 2: +++ 10: ++++		Month 1 2: ++ 10: +++		Month 3 2: + 10: ++	

Nickel nanoparticles (Mo et al., 2019)	*In vivo*	Male C57BL/6 mice	10, 20, 50, 100 µg/mouse intratracheal instillation Evaluation: 3 days post-exposure	Neutrophil count in BALF	TBARS 8-OHdG level	LDH activity	Total protein in BALF
				10: + 20: + 50: +++ 100: ++	10: 20: 50: 100:	10: + 20: + 50: +++ 100: ++	10: + 20: + 50: +++ 100: +
			50 µg/mouse intratracheal instillation Evaluation: 1, 3, 7, 14, 28, 42 days post-exposure	Neutrophil count in BALF	*3 days post-exposure	LDH activity	Total protein in BALF
				Day 1: ++ Day 3: +++ Day 7: + Day 14: + Day 28: + Day 42: +	Increased levels of TBARS and 8-OHdG in lung tissues	Day 1: + Day 3: +++ Day 7: ++ Day 14: + Day 28: + Day 42: +	Day 1: + Day 3: +++ Day 7: ++ Day 14: + Day 28: + Day 42: +
Radiation (Park et al., 2009)	*In vivo*	Sprague-Dawley rats	Right lung 20 Gray (Gy) of radiation Evaluation: 3, 7, 14, 28, 56 days post-exposure	Increase cell count in BALF	Total protein in BALF		
				Day 3: Day 7: Day 14: + Day 28: + Day 56: +++	Day 3: Day 7: - Day 14: + Day 28: ++++ Day 56: +		
Ricin (Sapoznikov et al., 2019)	*In vivo*	Female CD-1 mice	Crude ricin (50 µl; 7 µg/Kg diluted in PBS) administered intranasally Evaluation: 3, 6, 24, 48, 72 Hours post-exposure	Neutrophil count increase	Evans blue dye extravasation	Decrease Vascular Endothelial-cadherin, claudin 18, claudin 5, connexin 43 and occludin protein expression	
				24 h: + 48 h: ++ 72 h: +++	6 h: + 24 h: ++ 48 h: +++ 72 h: +++	3 h: +++ 6 h: +++ 24 h: +++ 48 h: +++ 72 h:	
Cobalt nanoparticles (Wan et al., 2017)	*In vivo*	Female or male gpt delta transgenic mice (C57BL/6 background)	50 µg/mouse intratracheal instillation Evaluation: 1, 3, 7, 28 days, 4 months post-exposure	CXCL1/KC In BALF	Neutrophils in BALF	LDH activity in BALF	Protein content in BALF	8-OHdG levels in lung tissue
				Day 1: +++ Day 3: +++ Day 7: +++ Day 28:	Day 1: +++ Day 3: +++ Day 7: ++ Day 28: +	Day 1: +++ Day 3: +++ Day 7: +++ Day 28: ++	Day 1: ++ Day 3: +++ Day 7: ++ Day 28: +	Month 4: ++

IL: Interleukin.
PMN: Polymorphonuclear cells.
sICAM: Soluble intercellular adhesion molecule 1.
BALF: Bronchoalveolar lavage fluid.
LDH: Lactate dehydrogenase.
TBARS: Thiobarbituric acid reactive substances.
8-OHdG: 8-hydroxy-2-deoxyguanosine.
CXCL1/KC: C-X-C motif chemokine ligand 1/keratinocyte-derived chemokine.

Dose-Response Evidence:

There are some studies that provide dose-response evidence of this KER. For example, *in vitro* and *in vivo* studies testing stressors at different doses/concentrations have demonstrated a dose-response relationship; at the higher dose/concentration of the stressor, the recruitment of pro-inflammatory cells increased leading to loss of ACM integrity.

Microvascular endothelial and the human lung adenocarcinoma cell lines in co-culture were exposed to 6-600 µg/ml silica nanoparticles (NPs). After 4 h of exposure and 20 h recovery, Soluble intercellular adhesion molecule-1 (sICAM-1), IL-6, and IL-8 increased in a concentration-dependent manner. These cytokines increased the recruitment and regulation of neutrophils. The study suggests that there is a crosstalk of both cell types in co-culture that leads to basolateral cytokine secretion. Moreover, transepithelial/transendothelial electrical resistance decreased in a concentration-dependent manner after 4 h exposure, and changes in the assembly of cell-cell junctions were observed (Kasper J et al. 2011).

Polyhexamethylene guanidine phosphate is used for the prevention of microorganism growth in humidifiers. To evaluate the inflammation response after the exposure to this chemical, three human lung cells (Calu-3, differentiated THP-1, and HMC-1 cells) were culture and exposed at the air-liquid interface at 2.2, 4.4, 8.8, and 17.6 mg/ml for 1, 6 and 24 h. An increase in chemoattractant cytokine IL-8 release was observed in a concentration- and time-dependent manner. This response preceded the ACM integrity loss, which occurred at 24 h at the highest concentration. These changes were followed by ROS generation, an increase in the levels of Matrix metalloproteinase (MMP)-2, Metalloproteinase inhibitor 1 (TIMP-1), MMP-9, TIMP-2 mRNA expression, and the release of TNF-α, IL-6 and Transforming growth factor beta 1 (TGF-β1). Moreover, inflammatory cell infiltration, fibrosis, and the release of cytokines was observed in lung sections in Sprague-Dawley rats following a 3 week exposure (Kim et al., 2016).

Arras et al. (2001) studied the effect of IL-9 on the development of lung fibrosis after crystalline silica particle (DQ12) exposure. Transgenic Tg5 mice expressing high levels of IL-9 and wild type (WT) FVB mice were exposed to DQ12 particles by intratracheal instillation at 1 or 5 mg, and mice were sacrificed 2, 4, and 6 months after instillation. Recruitment of pro-inflammatory cells and an increase in the level of Lactate dehydrogenase (LDH) and proteins were observed in bronchoalveolar lavage fluid (BALF) after 2 and 4 months at the highest exposure (5 mg). Hydroxyproline content in the lung increased over time with the highest levels seen 4 months after instillation. Moreover, IL-4 increased in a dose-dependent manner after 2 months of exposure. In contrast, Interferon gamma (IFN-γ) decreased after 2 months and 4 months after the highest exposure dose. In Tg5 mice, fibrosis was less severe than in WT mice. Moreover, intraperitoneal injection of IL-9 in C57BL/6 reduced the amplitude of silica-induced lung fibrosis associated with a recruitment of B lymphocytes in the lung parenchyma.

Morimoto et al. (2015) studied the inflammatory response of cerium oxide NPs in the acute and chronic phases. Male F344 rats were exposed once to 0.2 mg or 1 mg of NPs. Total cell counts in BALF increased at 1 mg after one week, and decreased after 1 and 3 months. Only neutrophils increased at the lowest dose at 3 days and 1 week after exposure and dropped after 1, 3, and 6 months. LDH activity in BALF increased after 3 days of exposure and decreased over time (1 week to 3 months). In the chronic phase, the total cell counts increased 3-days post-exposure, with no effects after 1 and 3 months. LDH increased after 3 days of administration and decreased in a time-dependent manner. The effects were more severe at the highest dose.

Temporal Evidence:

There is strong evidence of a temporal relationship between the two KES. *In vitro* and *in vivo* studies have demonstrated that the recruitment of pro-inflammatory cells increased prior to loss of ACM integrity.

Mice exposed to aerosolized multi-walled carbon nanotube (MWCNT) at 10 mg/m^3 (5 h per day for 2, 4, 8 or 12 days) developed pulmonary inflammation 1-day post-exposure. There was an increase in the recruitment of polymorphonuclear cells, neutrophil chemoattractant, albumin concentration, and LDH activity in the whole lung fluid in a time-dependent manner (Porter et al., 2013).

Research has shown that crystalline silica induces pulmonary toxicity. Rats exposed to this stressor at 15 mg/m^3, 6 h/day, 5 days/week for 3, 6, and 12 weeks, showed an accumulation of macrophages and neutrophils in BALF. Moreover, an increase in BALF LDH activity and albumin content was also observed (Umbright et al., 2017).

Gautam et al. (1998) studied the effect of a chemotactic stimulant, N-formylmethionine-leucyl-phenylalanine (fMLP), on polymorphonuclear cells resting on an endothelial cell monolayer in the upper compartment. Bovine aorta endothelial cells exposed to 10^{-7} M fMLP in the upper compartment induced adhesion of polymorphonuclear (PMN) cells followed by a decrease in transendothelial electrical resistance and an increase in protein permeability for 10-50 min in a time-dependent manner. The findings indicate that PMN are activated by fMLP and adhere to the endothelium which induces an increase in cytosolic free Ca^{2+}. This lead to a decrease in electrical resistance, leading to a structural rearrangement of endothelial cells which impairing their barrier integrity.

Paraquat is a herbicide that induces pulmonary toxicity. Chronic exposure to Paraquat results in inflammation, damage to AECs, and fibrosis. In sheep exposed to Paraquat at 5 mg/Kg (intramuscular), there was an increase in the number of granulocytes after 1, 2, and 3 weeks in a dose-dependent manner. After 3 weeks of paraquat administration alveolar wall thickening was observed, and the concentration of lung malondialdehyde increased as an indicator of lipid peroxidation. These results indicate that the recruitment of pro-inflammatory cells precedes alveolar damage (Shinozaki et al., 1992).

Exposure to nickel NPs can induce oxidative stress and lung inflammation. In a dose-response study, mice were intratracheally instilled with 0, 10, 20, 50, and 100 µg per mouse of nickel NPs and sacrificed at day 3 post-exposure. There was an increase in the neutrophil count in BALF, LDH activity, and total protein in BALF in a dose-dependent manner; the highest response was observed at 50 µg per mouse (Mo et al., 2019). Mice were intratracheally instilled with 50 µg per mouse of nickel NPs and sacrificed at days 1, 3, 7, 14, 28, and 42 post-instillation. The recruitment of neutrophils increased at day 1 and 3 post-exposure. The levels of thiobarbituric acid reactive substances (TBARS) and deoxyguanosine (8-OHdG), which are biomarkers for oxidative stress, increased after 3 days of instillation. LDH activity and total protein in BALF increased at day 3 and 7 post-exposure. These responses decreased after 14 days post-exposure. However, at 42-day post-exposure, an increase in the level of hydroxyproline content was observed in lung tissues exposed to NPs (Mo et al., 2019).

Park et al. (2009) used BALF indicators as a tool for evaluating radiation-induced lung damage. Sprague-Dawley rats received 20 Gray (Gy) of radiation to the right lung. At 3, 7, 14, 28, and 56 days after radiation, rats were sacrificed. Total cells in the BALF increased at 14 and 28 days, with the highest levels at day 56. Meanwhile, total protein in BALF increased after 7 days of radiation and peaked at 28 days post-radiation. The levels of TGF-β increase after 56 days of radiation.

Sapoznikov et al. (2019) studied the role of neutrophils in the early disruption of the alveolar-capillary barrier in a ricin-induced acute respiratory distress syndrome mouse model. Female CD-1 mice were administered intranasally with crude ricin (50 ml; 7 μg/Kg diluted in phosphate buffered saline), and after 3, 6, 24, 48, and 72 h animals were sacrificed. The neutrophil count increased at 24, 48, and 72 h post-exposure. ACM integrity loss was evaluated as Evans blue dye extravasation and the protein expression of Vascular endothelial cadherin (VE-cadherin), claudin 18, claudin 5, connexin 43, and occludin. After 6 h post-exposure, alveolar permeability increased in a time-dependent manner. From 3 h post-exposure, the decrease of junction proteins was evident. Animals treated with anti-ricin antibody, anti-Ly6G (neutrophil depletion), and marismat (MMP inhibition) showed less severity in alveolar membrane integrity loss.

Wan et al. (2017) studied the genotoxic effects of cobalt NPs and their capacity for causing oxidative stress and inflammation. Gpt delta transgenic mice were exposed to 50 μg/mouse of cobalt NPs by intratracheal instillation, and animals were sacrificed at days 1, 3, 7, and 28 post-exposure, as well as 4 months post-exposure. The levels of C-X-C motif chemokine ligand (CXCL)1/Keratinocyte chemoattractant (KC) and neutrophils increased at 1, 3, and 7 days post-exposure, but they decreased at day 28. LDH activity and protein content in BALF also increased, but their levels dropped after 28 days post-exposure. Four months after instillation, 8-OHdG levels were measured and were found at high levels. Moreover, histological changes were observed 7 days (infiltration of a large amount of neutrophils and macrophages in the alveolar space and septa, focal alveolar epithelial cell hyperplasia, and thickening of the alveolar wall) and 4 months (interstitial fibrosis, bronchiolization of the alveoli and collagen deposition in the alveolar septa) after the exposure.

Uncertainties and Inconsistencies

Although there is enough evidence to suggest a role for persistent inflammation and oxidative stress in ACM integrity loss, a direct relationship is hard to establish as studies involving inhibition of early pro-inflammatory cellular influx alter other immune cell types, thereby altering the end outcome.

Quantitative Understanding of the Linkage

In the context of lung fibrosis, data supporting quantitative dose-response relationships between the individual KEs is scarce. A majority of the mechanistic studies investigating the role of inflammation in lung fibrosis report acute neutrophilic inflammation and how altering neutrophil influx acutely after exposure to a toxic substance alters the end fibrotic outcome. However, these studies do not characterise the impact on immediate downstream KEs including the loss of ACM integrity or chronic inflammation in the absence of acute neutrophilia. Few studies have shown such concordance. For example, in mice exposed to different doses of bleomycin, total number of cells in BALF increased in a dose-dependent manner with predominant neutrophil phenotype at 7 days post-exposure and macrophage dominance at 24 days post-exposure (Kim et al., 2010). Other studies have shown that upon onset of chronic inflammation, secondary stimuli such as persisting toxic substance can make the injured tissue highly sensitive to acute inflammatory stimuli and may in turn fuel the ongoing chronic inflammation and affect the disease process (Ma et al., 2016).

Time-scale

One publication examined the timescale of KE induction with relation to this KER, in the context of AOP 173. Mo et al., 2019 found that KE2 (Event 1497) (1 and 3 days post-exposure) precedes KE3 (Event 1498) (3 and 7 days post-exposure) in mice exposed to 50 μg per mouse of nickel NPs by intratracheal instillation.

Reference	*In vitro*/*in vivo*/population study	Design	KE1 (Event 1496)	KE2 (Event 1497)	KE3 (Event 1498)	KE6 (Event 1501)
Mo Y et al., 2019	*In vivo*	Mice C57BL/6, 50 µg per mouse intratracheal instillation	C-X-C motif chemokine ligand 1/keratinocyte-derived chemokine (CXCL1/KC) **1- and 3-days** post-exposure	Neutrophil content **1 and 3 days** post-exposure	LDH activity, oxidative stress protein content **3- and 7-days** post-exposure	Hydroxyproline content **42 days** post-exposure

References

1. Arras M, Huaux F, Vink A, Delos M, Coutelier JP, Many MC, Barbarin V, Renauld JC, Lison D. Interleukin-9 reduces lung fibrosis and type 2 immune polarization induced by silica particles in a murine model. Am J Respir Cell Mol Biol. 2001 Apr;24(4):368-75. doi: 10.1165/ajrcmb.24.4.4249.
2. Barosova H, Maione AG, Septiadi D, Sharma M, Haeni L, Balog S, O'Connell O, Jackson GR, Brown D, Clippinger AJ, Hayden P, Petri-Fink A, Stone V, Rothen-Rutishauser B. Use of EpiAlveolar Lung Model to Predict Fibrotic Potential of Multiwalled Carbon Nanotubes. ACS Nano. 2020 Apr 28;14(4):3941-3956. doi: 10.1021/acsnano.9b06860.
3. Bhalla DK, Hirata F, Rishi AK, Gairola CG. Cigarette smoke, inflammation, and lung injury: a mechanistic perspective. J Toxicol Environ Health B Crit Rev. 2009 Jan;12(1):45-64. doi: 10.1080/10937400802545094.
4. Blum JL, Rosenblum LK, Grunig G, Beasley MB, Xiong JQ, Zelikoff JT. Short-term inhalation of cadmium oxide nanoparticles alters pulmonary dynamics associated with lung injury, inflammation, and repair in a mouse model. Inhal Toxicol. 2014 Jan;26(1):48-58. doi: 10.3109/08958378.2013.851746.
5. Cassel SL, Eisenbarth SC, Iyer SS, Sadler JJ, Colegio OR, Tephly LA, Carter AB, Rothman PB, Flavell RA, Sutterwala FS. The Nalp3 inflammasome is essential for the development of silicosis. Proc Natl Acad Sci U S A. 2008 Jul 1;105(26):9035-40. doi: 10.1073/pnas.0803933105.
6. Castranova V. Signaling pathways controlling the production of inflammatory mediators in response to crystalline silica exposure: role of reactive oxygen/nitrogen

species. Free Radic Biol Med. 2004 Oct 1;37(7):916-25. doi: 10.1016/j.freeradbiomed.2004.05.032.

7. Cho HY, Reddy SP, Yamamoto M, Kleeberger SR. The transcription factor NRF2 protects against pulmonary fibrosis. FASEB J. 2004 Aug;18(11):1258-60. doi: 10.1096/fj.03-1127fje.
8. Chou CC, Hsiao HY, Hong QS, Chen CH, Peng YW, Chen HW, Yang PC. Single-walled carbon nanotubes can induce pulmonary injury in mouse model. Nano Lett. 2008 Feb;8(2):437-45. doi: 10.1021/nl0723634.
9. Dong J, Ma Q. Suppression of basal and carbon nanotube-induced oxidative stress, inflammation and fibrosis in mouse lungs by Nrf2. Nanotoxicology. 2016 Aug;10(6):699-709. doi: 10.3109/17435390.2015.
10. Dostert C, Pétrilli V, Van Bruggen R, Steele C, Mossman BT, Tschopp J. Innate immune activation through Nalp3 inflammasome sensing of asbestos and silica. Science. 2008 May 2;320(5876):674-7. doi: 10.1126/science.1156995.
11. Fubini B, Hubbard A. Reactive oxygen species (ROS) and reactive nitrogen species (RNS) generation by silica in inflammation and fibrosis. Free Radic Biol Med. 2003 Jun 15;34(12):1507-16. doi: 10.1016/s0891-5849(03)00149-7.
12. Gautam N, Hedqvist P, Lindbom L. Kinetics of leukocyte-induced changes in endothelial barrier function. Br J Pharmacol. 1998 Nov;125(5):1109-14. doi: 10.1038/sj.bjp.0702186.
13. Grande NR, Peao MN, de Sa CM, Aguas AP. Lung Fibrosis Induced by Bleomycin: Structural Changes and Overview of Recent Advances. Scanning Microsc. 1998 12(3), 487–494.
14. Hubbard AK, Timblin CR, Rincon M, Mossman BT. Use of transgenic luciferase reporter mice to determine activation of transcription factors and gene expression by fibrogenic particles. Chest. 2001 Jul;120(1 Suppl):24S-25S. doi: 10.1378/chest.120.1_suppl.s24.
15. Hubbard AK, Timblin CR, Shukla A, Rincón M, Mossman BT. Activation of NF-kappaB-dependent gene expression by silica in lungs of luciferase reporter mice. Am J Physiol Lung Cell Mol Physiol. 2002 May;282(5):L968-75. doi: 10.1152/ajplung.00327.2001.
16. Inoue H, Shimada A, Kaewamatawong T, Naota M, Morita T, Ohta Y, Inoue K, Takano H. Ultrastructural changes of the air-blood barrier in mice after intratracheal instillation of lipopolysaccharide and ultrafine carbon black particles. Exp Toxicol Pathol. 2009 Jan;61(1):51-8. doi: 10.1016/j.etp.2007.10.001.
17. Janga H, Cassidy L, Wang F, Spengler D, Oestern-Fitschen S, Krause MF, Seekamp A, Tholey A, Fuchs S. Site-specific and endothelial-mediated dysfunction of the alveolar-capillary barrier in response to lipopolysaccharides. J Cell Mol Med. 2018 Feb;22(2):982-998. doi: 10.1111/jcmm.13421.
18. Kasper J, Hermanns MI, Bantz C, Maskos M, Stauber R, Pohl C, Unger RE, Kirkpatrick JC. Inflammatory and cytotoxic responses of an alveolar-capillary coculture model to silica nanoparticles: comparison with conventional monocultures. Part Fibre Toxicol. 2011 Jan 27;8(1):6. doi: 10.1186/1743-8977-8-6.
19. Kawasaki H. A mechanistic review of silica-induced inhalation toxicity. Inhal Toxicol. 2015;27(8):363-77. doi: 10.3109/08958378.2015.1066905.

20. Kim HR, Lee K, Park CW, Song JA, Shin DY, Park YJ, Chung KH. Polyhexamethylene guanidine phosphate aerosol particles induce pulmonary inflammatory and fibrotic responses. Arch Toxicol. 2016 Mar;90(3):617-32. doi: 10.1007/s00204-015-1486-9.

21. Kim SN, Lee J, Yang HS, Cho JW, Kwon S, Kim YB, Her JD, Cho KH, Song CW, Lee K. Dose-response Effects of Bleomycin on Inflammation and Pulmonary Fibrosis in Mice. Toxicol Res. 2010 Sep;26(3):217-22. doi: 10.5487/TR.2010.26.3.217.

22. Ma B, Whiteford JR, Nourshargh S, Woodfin A. Underlying chronic inflammation alters the profile and mechanisms of acute neutrophil recruitment. J Pathol. 2016 Nov;240(3):291-303. doi: 10.1002/path.4776.

23. MacNee W. Oxidative stress and lung inflammation in airways disease. Eur J Pharmacol. 2001 Oct 19;429(1-3):195-207. doi: 10.1016/s0014-2999(01)01320-6.

24. Marcus BC, Hynes KL, Gewertz BL. Loss of endothelial barrier function requires neutrophil adhesion. Surgery. 1997 Aug;122(2):420-6; discussion 426-7. doi: 10.1016/s0039-6060(97)90035-0.

25. Mo Y, Jiang M, Zhang Y, Wan R, Li J, Zhong CJ, Li H, Tang S, Zhang Q. Comparative mouse lung injury by nickel nanoparticles with differential surface modification. J Nanobiotechnology. 2019 Jan 7;17(1):2. doi: 10.1186/s12951-018-0436-0.

26. Morimoto Y, Izumi H, Yoshiura Y, Tomonaga T, Oyabu T, Myojo T, Kawai K, Yatera K, Shimada M, Kubo M, Yamamoto K, Kitajima S, Kuroda E, Kawaguchi K, Sasaki T. Pulmonary toxicity of well-dispersed cerium oxide nanoparticles following intratracheal instillation and inhalation. J Nanopart Res. 2015;17(11):442. doi: 10.1007/s11051-015-3249-1.

27. Nathan C. Points of control in inflammation. Nature. 2002 Dec 19-26;420(6917):846-52. doi: 10.1038/nature01320.

28. Nemmar A, Al-Salam S, Yuvaraju P, Beegam S, Yasin J, Ali BH. Chronic Exposure to Water-Pipe Smoke Induces Alveolar Enlargement, DNA Damage and Impairment of Lung Function. Cell Physiol Biochem. 2016;38(3):982-92. doi: 10.1159/000443050.

29. Palecanda A, Kobzik L. Receptors for unopsonized particles: the role of alveolar macrophage scavenger receptors. Curr Mol Med. 2001 Nov;1(5):589-95. doi: 10.2174/1566524013363384.

30. Park KJ, Oh YT, Kil WJ, Park W, Kang SH, Chun M. Bronchoalveolar lavage findings of radiation induced lung damage in rats. J Radiat Res. 2009 May;50(3):177-82. doi: 10.1269/jrr.08089.

31. Porter DW, Hubbs AF, Chen BT, McKinney W, Mercer RR, Wolfarth MG, Battelli L, Wu N, Sriram K, Leonard S, Andrew M, Willard P, Tsuruoka S, Endo M, Tsukada T, Munekane F, Frazer DG, Castranova V. Acute pulmonary dose-responses to inhaled multi-walled carbon nanotubes. Nanotoxicology. 2013 Nov;7(7):1179-94. doi: 10.3109/17435390.2012.719649.

32. Punithavathi D, Venkatesan N, Babu M. Curcumin inhibition of bleomycin-induced pulmonary fibrosis in rats. Br J Pharmacol. 2000 Sep;131(2):169-72. doi: 10.1038/sj.bjp.0703578.

33. Sapoznikov A, Gal Y, Falach R, Sagi I, Ehrlich S, Lerer E, Makovitzki A, Aloshin A, Kronman C, Sabo T. Early disruption of the alveolar-capillary barrier in a ricin-induced ARDS mouse model: neutrophil-dependent and -independent impairment of junction

proteins. Am J Physiol Lung Cell Mol Physiol. 2019 Jan 1;316(1):L255-L268. doi: 10.1152/ajplung.00300.2018.

34. Serrano-Mollar A, Closa D, Prats N, Blesa S, Martinez-Losa M, Cortijo J, Estrela JM, Morcillo EJ, Bulbena O. In vivo antioxidant treatment protects against bleomycin-induced lung damage in rats. Br J Pharmacol. 2003 Mar;138(6):1037-48. doi: 10.1038/sj.bjp.0705138.

35. Shi X, Castranova V, Halliwell B, Vallyathan V. Reactive oxygen species and silica-induced carcinogenesis. J Toxicol Environ Health B Crit Rev. 1998 Jul-Sep;1(3):181-97. doi: 10.1080/10937409809524551.

36. Shinozaki S, Kobayashi T, Kubo K, Sekiguchi M. Pulmonary hemodynamics and lung function during chronic paraquat poisoning in sheep. Possible role of reactive oxygen species. Am Rev Respir Dis. 1992 Sep;146(3):775-80. doi: 10.1164/ajrccm/146.3.775.

37. Strieter RM, Mehrad B. New mechanisms of pulmonary fibrosis. Chest. 2009 Nov;136(5):1364-1370. doi: 10.1378/chest.09-0510.

38. Umbright C, Sellamuthu R, Roberts JR, Young SH, Richardson D, Schwegler-Berry D, McKinney W, Chen B, Gu JK, Kashon M, Joseph P. Pulmonary toxicity and global gene expression changes in response to sub-chronic inhalation exposure to crystalline silica in rats. J Toxicol Environ Health A. 2017;80(23-24):1349-1368. doi: 10.1080/15287394.2017.1384773.

39. Wan R, Mo Y, Zhang Z, Jiang M, Tang S, Zhang Q. Cobalt nanoparticles induce lung injury, DNA damage and mutations in mice. Part Fibre Toxicol. 2017 Sep 18;14(1):38. doi: 10.1186/s12989-017-0219-z.

40. Wang HD, Yamaya M, Okinaga S, Jia YX, Kamanaka M, Takahashi H, Guo LY, Ohrui T, Sasaki H. Bilirubin ameliorates bleomycin-induced pulmonary fibrosis in rats. Am J Respir Crit Care Med. 2002 Feb 1;165(3):406-11. doi: 10.1164/ajrccm.165.3.2003149.

41. Ward PA. Acute lung injury: how the lung inflammatory response works. Eur Respir J Suppl. 2003 Sep;44:22s-23s. doi: 10.1183/09031936.03.00000703a.

42. Zeidler-Erdely PC, Battelli LA, Stone S, Chen BT, Frazer DG, Young SH, Erdely A, Kashon ML, Andrews R, Antonini JM. Short-term inhalation of stainless steel welding fume causes sustained lung toxicity but no tumorigenesis in lung tumor susceptible A/J mice. Inhal Toxicol. 2011 Feb;23(2):112-20. doi: 10.3109/08958378.2010.548838.

43. Zemans RL, Colgan SP, Downey GP. Transepithelial migration of neutrophils: mechanisms and implications for acute lung injury. Am J Respir Cell Mol Biol. 2009 May;40(5):519-35. doi: 10.1165/rcmb.2008-0348TR.

Relationship: 1705: Loss of alveolar capillary membrane integrity leads to Activation of Th2 cells

AOPs Referencing Relationship

AOP Name	Adjacency	Weight of Evidence	Quantitative Understanding
Substance interaction with the pulmonary resident cell membrane components leading to pulmonary fibrosis	adjacent	Moderate	Low

Key Event Relationship Description

During the tissue injury-mediated immune response, naïve CD4+ T helper (Th) cells differentiate into two major functional subsets: Th1 and Th2 type. Both Th1 and Th2 secrete distinct cytokines that promote proliferation and differentiation of their respective T cell population and inhibit proliferation and differentiation of the opposing subset. Th2 cytokines including pro-inflammatory and fibrotic mediators such as GATA binding protein 3 (GATA-3), Interleukin (IL)-13 and Arginase (Arg)-1 are increased in lung-irradiation induced fibrosis (Brush et al., 2007; Han et al., 2011; Wynn, 2004). Th2 immune response is implicated in allergen-mediated lung fibrosis. Meta-analysis of gene expression data collected from lungs of mice exposed to various fibrogenic substances including multi-walled carbon nanotubes (MWCNTs), showed that the expression and function of Th2 response associated genes and pathways are altered in fibrotic lungs (Nikota et al., 2016). Exposure of mice lacking Signal transducer and activator of transcription 6 (STAT6) to MWCNTs resulted in abrogated expression of Th2 genes and reduced lung fibrosis (Nikota et al., 2017). IL-4, the archetypal Th2 cytokine is a pro-fibrotic cytokine and is elevated in idiopathic pulmonary fibrosis (IPF) and lung fibrosis. Overexpression of pro-fibrotic Th2 cytokine IL-13 results in sub-epithelial fibrosis with eosinophilic inflammation (Wilson and Wynn, 2009). In silica-induced pulmonary fibrosis in mice, T regulatory lymphocytes are recruited to the lungs where they increase expression of Platelet-derived growth factor (PDGF) and Transforming growth factor beta (TGF-β) (Maggi et al., 2005). Chemokines associated with the Th2 response in airway epithelial cells include C-C motif chemokine ligand (CCL)1, CCL17, CCL20, and CCL22 (Lekkerkerker et al., 2012).

Evidence Supporting this KER

Biological Plausibility

The biological plasubility of this KER is high as there is a mechanistic relationship between alveolar capillary membrane (ACM) injury (tissue damage), and the induction of a Th2 response (responsible for wound healing) (Gieseck et al., 2018; Wynn, 2004).

Empirical Evidence

The empirical support for this KER is moderate. There is limited *in vitro* and *in vivo* evidence to support a direct relationship between these two KEs, with some inconsistencies with respect to the specific mediators in question (Ortiz et al., 1998; Piguet, 1989; Redente et al., 2014; Additional references can be found in Table 1).

Table 1. Studies providing empirical evidence for the relationship between KE3 (Event 1498) and KE4 (Event 1499). +: Severity of Response. References available in main KER page

Stressor (Reference)	***In vitro/in vivo/ex vivo***	**Species/Cell line**	**Exposure Conditions**	**KE3 (Event 1498) Loss of alveolar capillary membrane integrity**		**KE4 (Event 1499) Activation, T helper (Th) type 2 cells**			
Bleomycin (Kikuchi et al., 2010)	*In vivo*	Wild-type C57BL/6 and Nrf2-deficient mice	5 mg/Kg intratracheal instillation Evaluation: 1 - 28 days post-exposure	LDH in BALF	Antioxidant genes induction	Th2 cytokine expression	Expression GATA-3		
				Day 1: + Day 3: + Day 8:	Day 1: ++ Day 3: +	Day 7: + (IL-4, IL-13)	Day 7: +		
Aspergillus fumigatus extract (Haczku et al., 2006)	*In vivo*	Female BALB/c	Extract intraperitoneal injection on day 0 and day 14. Intranasal challenge on day 24. Evaluation: 12, 24, 48, 72 h post intranasal challenge.	Total BALF protein		Increased IL-4. IL-5, IL-13 in BALF			
				12 h: + 24 h: ++ 48 h: + 72 h: +		12 h: ++ 24 h: ++ 48 h: + 72 h:			
Nitrogen mustard (Venosa et al., 2016)	*In vivo*	Male Wistar rats	0.125 mg/kg intratracheal instillation Evaluation: 1, 3, 7, 28 days post-exposure.	Genes upregulated		Decreased resident macrophages	Increased infiltrating macrophages	M2 macrophages	Genes upregulated
				iNOS, IL-12α, COX-2, TNF-α, MMP9 and MMP10, CCR5, CCL2, CCL5 Day 1: +++ Day 3: ++ Day 7: ++ Day 28: +		CD11b-, CD43-, CD68+ Day 1: +++ Day 3: ++ Day 7: + Day 28: +++	CD11b+, CD43+ Day 1: + Day 3: ++ Day 7: + Day 28:	CD11b+, CD4- Day 1: + Day 3: ++ Day 7: +++ Day 28: +	IL-10, pentraxin-2, ApoE, CX3CR1, fractalkine Day 1: ++ Day 3: +++ Day 7: +++ Day 28: +
Exotoxin Pyocyanin (Caldwell et al., 2009)	*In vivo*	Wild-type FVBN mice Wild-type and STAT6-/- C57BL/6 mice	10, 25 µg intranasal challenge 3 times/ weeks, for 3, 6, 12 weeks. Evaluation: During week 3, 6, 12 of exposure.	Alveolar airspace destruction		Th2 cytokines	Decreased resident macrophages	Increased infiltrating macrophages	CD4 T cells/ml BALF
				25 µg Week 6: + Week 12: ++		25 µg IL-13, IL-4, TGF-β, IL-10	25 µg F4/80^{+}/CD 11b^{-}	25 µg F4/80^{+}/CD 11b^{+}	25 µg Week 3: +++

							Week 3: + (only IL-10) Week 6: + Week 12: +++	Week 3: Week 6: +++ Week 12: +	Week 3: Week 6: Week 12: +++	
Sodium arsenite $NaAsO_2$ (Li et al., 2017)	*In vivo*	Female C57BL/6 mice	2.5, 5, 10 mg/kg intragastrical single oral administration. Evaluation: 24 h post-exposure.	Total protein levels in BALF	MDA content in lung	Nrf2 relative protein levels in lung	Increase relative mRNA levels in lung Gata3, IL-4, Foxp3, IL-10		Decrease relative mRNA levels in lung T-bet, Ifn-γ, Ror-γt, IL-23	
				2.5: + 5: + 10: ++	2.5: + 5: ++ 10: +++	2.5: + 5: +++ 10: +++	2.5: + 5: ++ 10: +++		2.5: + 5: ++ 10: +++	
			100 mg/mL administered freely in drinking water for 2 months. Evaluation: post-exposure	Increase NF-κB, p-38, p-JNK, p-ERK relative mRNA levels			Increase IL-4, IL-23, IL-10, Ifn-γ, IL-1β mRNA levels			
NiO (Chang et al., 2017)	*In vivo*	Male Wistar rats	0.015, 0.06, 0.24 mg/Kg intratracheal instillation twice/ week, for 6 weeks Evaluation: post-exposure	Increase relative protein expression NFκ-B, IKK-α, NIK in lung tissue	Increase nitrative stress in rat lung tissue		Increase relative protein expression GATA-3		Decrease ratio of relative protein expression T-bet/GATA-3	
				0.015: 0.06: + 0.24: ++	0.015: 0.06: 0.014: +++		0.015: 0.06: + 0.024: ++		0.015: + 0.06: ++ 0.024: +++	

ApoE: Apolipoprotein E.
BALF: Bronchoalveolar lavage fluid.
CCL: C-C motif chemokine ligand.
CCR: C-C chemokine receptor.
CD: Cluster of differentiation.
COX-2: Cyclooxygenase-2.
CX3CR1: C-X3-C motif chemokine receptor 1.
Foxp3: Forkhead box P3.
Gata3: GATA binding protein 3.
Ifn-γ: Interferon gamma.
IL: Interleukin.
IKK-α: Inhibitor of NF-κB kinase subunit alpha.
iNOS: Inducible nitric oxide synthase.
LDH: Lactate dehydrogenase.
MDA: Malondialdehyde.

MMP: Matrix metalloproteinase.
NF-κB: Nuclear Factor Kappa B.
NIK: NF-κB-inducing kinase.
Nrf2: Nuclear factor erythroid 2-related factor 2.
p-38: A mitogen-activated protein kinase.
p-ERK: Phospho-extracellular signal-regulated kinase.
p-JNK: Phospho-c-Jun N-terminal kinase.
Ror-γt: Retinoic acid-related orphan receptor gamma t.
T-bet: T-box transcription factor.
TGF-β: Transforming growth factor beta.
Th: T helper.
TNF: Tumor necrosis factor.

In mice lacking both Tumor necrosis factor receptor 1 (TNF-R1) and receptor 2 (TNF-R2) or in wild-type (WT) mice treated with anti-TNFα, bleomycin-induced lung fibrosis is attenuated (Ortiz, 1998; Piguet, 1989). Persistent activation of TNF-α and IL-1β results in elevated secretion of pro-inflammatory cytokines that are tissue damaging. Overexpression of IL-1β induces acute lung injury and lung fibrosis in mice (Kolb, 2001). TNF-α and IL-1β are the therapeutic targets in IPF and asbestosis (Zhang et al., 1994). Overexpression of TNF-α induces spontaneous fibrosis in mouse lungs (Miyazaki et al., 1995). In cases of infestation with parasitic worm helminths, chronic injury activates a large immune response, resulting in secretion of pro-inflammatory mediators that can inflict cell and tissue damage. Effective treatment involves control of immune-response mediated damage (reviewed in Jackson et al., 2009).

Dose-Response Relationship:

There are some *in vivo* studies that provide dose-response evidence of this KER.

Li et al. (2017) studied the immunotoxic effects of the lung after arsenic exposure in an acute and a subchronic phase. Female C57BL/6 mice were exposed to 2.5, 5, and 10 mg/Kg sodium arsenite ($NaAsO_2$) via a single oral intragastric administration. After 24 h, bronchoalveolar lavage fluid (BALF) and lung tissue were collected. The induction of KE3 (Event 1498; ACM injury) was observed as an increase in the total protein levels in BALF, malondialdehyde content, and Nuclear factor erythroid 2-related factor 2 (Nrf2) protein expression in the lung. The induction of KE4 (Event 1499; Th2 activation) was determined as an increase in the levels of Gata3, IL-4, Forkhead box P3 (Foxp3), and IL-10 levels, as well as a decrease in the levels of T-box transcription factor (T-bet), Interferon gamma (Ifn-γ), Retinoic acid-related orphan receptor gamma t (Ror-γt), and IL-23. All these changes were observed in a dose-dependent manner. After a subchronic exposure (100 mg/mL $NaAsO_2$ administered freely in drinking water for 2 months), an increase in the levels of Nuclear Factor Kappa B (NF-κB), p-38 (a mitogen-activated protein kinase), Phospho-c-Jun N-terminal kinase (p-JNK), Phospho-extracellular signal-regulated kinase (p-ERK) mRNA and an increase in the levels of IL-4, IL-23, IL-10, Ifn-γ, IL-1β was observed.

Chang et al. (2017) studied the role of NF-κB activation and Th1/Th2 imbalance in pulmonary inflammation induced by Nickel oxide (NiO) nanoparticles (NPs). Male Wistar rats were exposed to 0.015, 0.06, and 0.24 mg/Kg by intratracheal instillation twice a week for 6 weeks. At the highest dose, an increase of nitrative stress in rat lung tissue was observed. TNF-α, IL-2, IL-10, and Cytokine-induced neutrophil chemoattractant (CINC) increased in a dose-response manner. Activation of the NF-κB signalling pathway (NF-κB, Inhibitor of NF-κB kinase subunit alpha [IKK-α] and NF-κB-inducing kinase [NIK]) also increased in a dose-response manner. An increase in the levels of GATA3 and a decrease in T-bet was observed, indicating a Th1/T2 imbalance after exposure to NiO NPs. NiO NPs the nitrative stress and inflammatory response in lung tissue, related to NF-κB and Th1/Th2 imbalance.

Temporal Evidence:

In vivo studies have demonstrated that the loss of ACM integrity precedes the activation of Th type 2 cells.

It has been described that oxidant and antioxidant Th1/Th2 balances are essential in the inflammatory response and fibrosis. To evaluate whether transcription factor Nrf2 is a mediator, WT C57BL/6 mice, and Nrf2-deficient mice were administered with 5 mg/kg bleomycin intratracheally, and the inflammatory response, antioxidant response, and fibrosis were evaluated at different time points post-exposure. The loss of ACM integrity was observed at days 1 and 3, as well as a decrease in the induction of antioxidant genes. On day 7, an increase in the level of Th2 cytokine production (IL-4 and IL-13) was

observed. The expression of GATA-3, a transcription factor that regulates the differentiation of Th1/Th2 cells, was also increased at this time point. These responses were more intense in Nrf2-deficient mice. Moreover, bleomycin administration increased the recruitment of cells at day 1 and 3, and fibrosis were observed after 28 days of treatment (Kikuchi et al., 2010).

Haczku et al. (2006) observed in mice sensitized and challenged with Aspergillus fumigatus extract (intraperitoneal injection at day 0 and day 14, intranasal challenge at day 24) an increase in the expression of surfactant protein D (SP-D) mRNA and protein levels in lungs in a time-dependent manner after allergen challenge. Total BALF protein increased over time at 12 and 24 h; after that, protein content decreased. IL-4, IL-5, and IL-13 increased at 12 h and 24 h, but decreased at later time points. They found that allergen exposure increased the expression of SP-D and IL-4/IL-13 in a time-dependent manner.

Venosa et al. (2016) evaluated the presence of classically activated (M1) macrophages and alternatively activated (M2) macrophages in lung after the exposure to nitrogen mustard. Rats were exposed to nitrogen mustard at 0.125 mg/kg, intratracheally, and the inflammatory response was evaluated 1, 3, 7- and 28-days post-exposure. A decrease in the levels of resident macrophages and an accumulation of infiltrating M1 and M2 macrophages was observed. M1 macrophages were prominent after 1- and 3-days of exposure; meanwhile, M2 macrophages were more prominent after 28 days of exposure. M1 and M2 genes were also upregulated. These events were in a time-dependent manner. M2 macrophages in early time points phagocytized cellular debris and counterbalanced M1 cell activation. At later time points, they promoted matrix deposition, tissue remodeling, and fibrosis.

Caldwell et al. (2009) studied the inflammatory response after exotoxin pyocyanin exposure in WT and FVBN mice. Mice were exposed to pyocyanin 10 or 25 µg intranasally inoculated chronically into the lungs three times a week for intervals of 3, 6, and 12 weeks. At 25 µg, after 6 and 12 weeks, alveolar airspace destruction was observed (KE3 (Event 1498)). The KE4 event (Event 1499) decreased resident macrophages and increased CDT cells/ml in BALF, changed in a time-dependent manner with maximum levels after 12 weeks. STAT6 mediated the induction of Th2 cytokines by pyocyanin.

Uncertainties and Inconsistencies

Exogenous delivery of TNF-α to mouse lungs with established fibrosis, reduced the fibrotic burden. Exogenous treatment with TNF-α slowed the M2 macrophage polarization. TNF-α deficient mice showed prolonged pro-fibrotic response and M2 polarization following bleomycin treatment (Redente et al., 2014).

References

1. Brush J, Lipnick SL, Phillips T, Sitko J, McDonald JT, McBride WH. Molecular mechanisms of late normal tissue injury. Semin Radiat Oncol. 2007 Apr;17(2):121-30. doi: 10.1016/j.semradonc.2006.11.008.
2. Caldwell CC, Chen Y, Goetzmann HS, Hao Y, Borchers MT, Hassett DJ, Young LR, Mavrodi D, Thomashow L, Lau GW. Pseudomonas aeruginosa exotoxin pyocyanin causes cystic fibrosis airway pathogenesis. Am J Pathol. 2009 Dec;175(6):2473-88. doi: 10.2353/ajpath.2009.090166.
3. Chang X, Zhu A, Liu F, Zou L, Su L, Li S, Sun Y. Role of NF-κB activation and Th1/Th2 imbalance in pulmonary toxicity induced by nano NiO. Environ Toxicol. 2017 Apr;32(4):1354-1362. doi: 10.1002/tox.22329.
4. Gieseck RL 3rd, Wilson MS, Wynn TA. Type 2 immunity in tissue repair and fibrosis. Nat Rev Immunol. 2018 Jan;18(1):62-76. doi: 10.1038/nri.2017.90.
5. Haczku A, Cao Y, Vass G, Kierstein S, Nath P, Atochina-Vasserman EN, Scanlon ST, Li L, Griswold DE, Chung KF, Poulain FR, Hawgood S, Beers MF, Crouch EC. IL-4 and IL-13 form a negative feedback circuit with surfactant protein-D in the allergic airway response. J Immunol. 2006 Mar 15;176(6):3557-65. doi: 10.4049/jimmunol.176.6.3557.
6. Han G, Zhang H, Xie CH, Zhou YF. Th2-like immune response in radiation-induced lung fibrosis. Oncol Rep. 2011 Aug;26(2):383-8. doi: 10.3892/or.2011.1300.
7. Jackson JA, Friberg IM, Little S, Bradley JE. Review series on helminths, immune modulation and the hygiene hypothesis: immunity against helminths and immunological phenomena in modern human populations: coevolutionary legacies? Immunology. 2009 Jan;126(1):18-27. doi: 10.1111/j.1365-2567.2008.03010.x.
8. Kikuchi N, Ishii Y, Morishima Y, Yageta Y, Haraguchi N, Itoh K, Yamamoto M, Hizawa N. Nrf2 protects against pulmonary fibrosis by regulating the lung oxidant level and Th1/Th2 balance. Respir Res. 2010 Mar 18;11(1):31. doi: 10.1186/1465-9921-11-31.
9. Kolb M, Margetts PJ, Anthony DC, Pitossi F, Gauldie J. Transient expression of IL-1beta induces acute lung injury and chronic repair leading to pulmonary fibrosis. J Clin Invest. 2001 Jun;107(12):1529-36. doi: 10.1172/JCI12568.
10. Lekkerkerker AN, Aarbiou J, van Es T, Janssen RA. Cellular players in lung fibrosis. Curr Pharm Des. 2012;18(27):4093-102. doi: 10.2174/138161212802430396.
11. Li J, Zhao L, Zhang Y, Li W, Duan X, Chen J, Guo Y, Yang S, Sun G, Li B. Imbalanced immune responses involving inflammatory molecules and immune-related pathways in the lung of acute and subchronic arsenic-exposed mice. Environ Res. 2017 Nov;159:381-393. doi: 10.1016/j.envres.2017.08.036.
12. Maggi E, Cosmi L, Liotta F, Romagnani P, Romagnani S, Annunziato F. Thymic regulatory T cells. Autoimmun Rev. 2005 Nov;4(8):579-86. doi: 10.1016/j.autrev.2005.04.010.
13. Miyazaki Y, Araki K, Vesin C, Garcia I, Kapanci Y, Whitsett JA, Piguet PF, Vassalli P. Expression of a tumor necrosis factor-alpha transgene in murine lung causes lymphocytic and fibrosing alveolitis. A mouse model of progressive pulmonary fibrosis. J Clin Invest. 1995 Jul;96(1):250-9. doi: 10.1172/JCI118029.

14. Nikota J, Williams A, Yauk CL, Wallin H, Vogel U, Halappanavar S. Meta-analysis of transcriptomic responses as a means to identify pulmonary disease outcomes for engineered nanomaterials. Part Fibre Toxicol. 2016 May 11;13(1):25. doi: 10.1186/s12989-016-0137-5.

15. Nikota J, Banville A, Goodwin LR, Wu D, Williams A, Yauk CL, Wallin H, Vogel U, Halappanavar S. Stat-6 signaling pathway and not Interleukin-1 mediates multi-walled carbon nanotube-induced lung fibrosis in mice: insights from an adverse outcome pathway framework. Part Fibre Toxicol. 2017 Sep 13;14(1):37. doi: 10.1186/s12989-017-0218-0.

16. Ortiz LA, Lasky J, Hamilton RF Jr, Holian A, Hoyle GW, Banks W, Peschon JJ, Brody AR, Lungarella G, Friedman M. Expression of TNF and the necessity of TNF receptors in bleomycin-induced lung injury in mice. Exp Lung Res. 1998 Nov-Dec;24(6):721-43. doi: 10.3109/01902149809099592.

17. Piguet PF, Collart MA, Grau GE, Kapanci Y, Vassalli P. Tumor necrosis factor/cachectin plays a key role in bleomycin-induced pneumopathy and fibrosis. J Exp Med. 1989 Sep 1;170(3):655-63. doi: 10.1084/jem.170.3.655.

18. Redente EF, Keith RC, Janssen W, Henson PM, Ortiz LA, Downey GP, Bratton DL, Riches DW. Tumor necrosis factor-α accelerates the resolution of established pulmonary fibrosis in mice by targeting profibrotic lung macrophages. Am J Respir Cell Mol Biol. 2014 Apr;50(4):825-37. doi: 10.1165/rcmb.2013-0386OC.

19. Venosa A, Malaviya R, Choi H, Gow AJ, Laskin JD, Laskin DL. Characterization of Distinct Macrophage Subpopulations during Nitrogen Mustard-Induced Lung Injury and Fibrosis. Am J Respir Cell Mol Biol. 2016 Mar;54(3):436-46. doi: 10.1165/rcmb.2015-0120OC.

20. Wilson MS, Wynn TA. Pulmonary fibrosis: pathogenesis, etiology and regulation. Mucosal Immunol. 2009 Mar;2(2):103-21. doi: 10.1038/mi.2008.85.

21. Wynn TA. Fibrotic disease and the T(H)1/T(H)2 paradigm. Nat Rev Immunol. 2004 Aug;4(8):583-94. doi: 10.1038/nri1412.

22. Zhang K, Rekhter MD, Gordon D, Phan SH. Myofibroblasts and their role in lung collagen gene expression during pulmonary fibrosis. A combined immunohistochemical and in situ hybridization study. Am J Pathol. 1994 Jul;145(1):114-25.

Relationship: 1706: Activation of Th2 cells leads to Increased cellular proliferation and differentiation

AOPs Referencing Relationship

AOP Name	Adjacency	Weight of Evidence	Quantitative Understanding
Substance interaction with the pulmonary resident cell membrane components leading to pulmonary fibrosis	adjacent	High	Low

Key Event Relationship Description

The wound healing process involves an inflammatory phase, during which the damage tissue/wound is provisionally filled with extracellular matrix (ECM). This phase is characterised by secretion of cytokines/chemokines, growth factors and recruitment of inflammatory cells, fibroblasts and endothelial cells. The activated T helper (Th)1/Th2 response and increased pool of specific cytokines and growth factors such as Interleukin (IL)-1β, IL-6, IL-13, and Transforming growth factor beta (TGF-β), induce fibroblast proliferation. Th type 2 (Th2) cells can directly stimulate fibroblasts to synthesise collagen with IL-1 and IL-13. Th2 cytokines IL-13 and IL-4, known to mediate the fibrosis process induce phenotypic transition of human fibroblasts (Hashimoto et al., 2001). IL-13 is shown to inhibit Matrix metalloproteinases (MMP)-mediated matrix degradation resulting in excessive collagen deposition by downregulating the synthesis and expression of matrix degrading MMPs. IL-13 is also suggested to induce TGF-β1 in macrophages and its absence results in reduced TGF-β1 expression and decrease in collagen deposition (Fichtner-Feigl et al., 2006). These cytokines are suggested to initiate polarization of macrophages to the alternative phenotype (M2). Th2 cells that synthesise IL-4 and IL-13 induce synthesis of Arginase (Arg)-1 in M2 macrophages. The Arg-1 pathway stimulates synthesis of proline for collagen synthesis required for fibrosis (Barron and Wynn, 2011).

Evidence Supporting this KER

The wound healing process involves an inflammatory phase, during which the damage tissue/wound is provisionally filled with extracellular matrix (ECM). This phase is characterised by secretion of cytokines/chemokines, growth factors and recruitment of inflammatory cells, fibroblasts and endothelial cells. The activated T helper (Th)1/Th2 response and increased pool of specific cytokines and growth factors such as Interleukin (IL)-1β, IL-6, IL-13, and Transforming growth factor beta (TGF-β), induce fibroblast proliferation. Th type 2 (Th2) cells can directly stimulate fibroblasts to synthesise collagen with IL-1 and IL-13. Th2 cytokines IL-13 and IL-4, known to mediate the fibrosis process induce phenotypic transition of human fibroblasts (Hashimoto et al., 2001). IL-13 is shown to inhibit Matrix metalloproteinases (MMP)-mediated matrix degradation resulting in excessive collagen deposition by downregulating the synthesis and expression of matrix degrading MMPs. IL-13 is also suggested to induce TGF-β1 in macrophages and its absence results in reduced TGF-β1 expression and decrease in collagen deposition (Fichtner-Feigl et al., 2006). These cytokines are suggested to initiate polarization of macrophages to the alternative phenotype (M2). Th2 cells that synthesise IL-4 and IL-13 induce synthesis of Arginase (Arg)-1 in M2 macrophages. The Arg-1 pathway stimulates synthesis of proline for collagen synthesis required for fibrosis (Barron and Wynn, 2011).

Evidence Supporting this KER

Biological Plausibility

The biological plausibility for this KER is high. There is a widely understood functional relationship between Th2 response related mediators, and their ability to induce proliferation and differentiation of fibroblasts (Shao et al., 2008; Wynn, 2004; Wynn, 2012).

Empirical Evidence

The empirical support for this KER is high. There is a plethora of dose and time response evidence, which show that Th2 cytokines induce the activation and proliferation of fibroblasts (Hashimoto et al., 2001; Lee et al., 2001; additional references can be found in Table 1).

Table 1. Studies providing empirical evidence for the relationship between KE4 (Event 1499) and KE5 (Event 1500). +: Severity of Response. References available in main KER page

Stressor (Reference)	***In vitro/in vivo/ex vivo***	**Species/Cell line**	**Exposure Conditions**	**KE4 (Event 1499) Activation, T helper (Th) type 2 cells**		**KE5 (Event 1500) Increased, fibroblast proliferation, and myofibroblast differentiation**
Silica particles (SiO_2) (Lo Re et al., 2011)	*In vivo/ex vivo*	NMRI, C57BL/6, DBA/2 mice Rag2-/- mice and C57BL/6 wild-type Foxp3-GFP and Foxp3-eGFP/diphtheria toxin receptor (DTR) Depletion of regulatory T cell (DEREG) mice.	2.5 mg/mouse pharyngeal instillation 15 days after instillation, regulatory T cells were purified from Foxp3-GFP transgenic mice. Regulatory T cells were co-culture with mouse lung fibroblast 5, 10, 25, 50, 100 x 10^3 regulatory T cells/well	Increase in expression of PDGF-B and TGF-β1 in purified regulatory T cells PDGF-B: ++ TGF-β1: ++		Fibroblast proliferation 3H-thymidine (48 h co-culture) 5 x 10^3: + 10 x 10^3: + 25 x 10^3: ++ 50 x 10^3: +++ 100 x 10^3: +++
Multi-walled carbon nanotubes (Dong and Ma, 2016)	*In vivo*	Male C57BL/6J mice	40 μg/mouse pharyngeal aspiration. Evaluation: 1, 3, 7, 14 days post-exposure	Increased Th2 cytokines interleukin production IL-4, IL-13, phospho-STAT6 and GATA-3 (mRNA and proteins)		Collagen I deposition
				Day 1+ Day 3 + Day 7: +++ Day 14 +		Day 7: +++
Bleomycin (Cao et al., 2014)	*In vivo*	Male Wistar rats	5 mg/Kg intratracheal instillation Evaluation: 7, 14, 28 days post-exposure	Increased IL-4 content in broncho-alveolar lavage fluid	Increased IFN-γ content in bronchoalveolar lavage fluid	Increased collagen I deposition
				Day 7: +++ Day 14: ++ Day 28: +	Day 7: + Day 14: ++ Day 28: ++	Day 7: + Day 14: ++ Day 28: +++
Wound model and IL-33 (Yin et al., 2013)	*In vivo*	Male BALB/c mice	Skin wounds created on the dorsal skin. Murine recombinant IL-33 (1.0 μg/mouse) intraperitoneal injection once a day from day 0 to day 3 Evaluation: 0 – 14 days post-injury	Alternatively activated macrophages (AAM) increase (vs. PBS) Day 5: ++ mRNA expression of AAM-associated genes increase (vs. PBS) Day 5: ++		% Wound closure increase (vs. PBS): Day 0: Day 3: ++ Day 5: ++ Day 7: ++ Day 10: + Day 14:

						% Reepithelization increase (vs. PBS) Day 1: Day 3: ++ Day 6: ++ Day 14: Collagen deposition increase (vs. PBS) Day 3: Day 5: + Day 7: + Day 14: mRNA expression of extracellular matrix-associated genes increase (vs. PBS) Day 5: ++
IL-4 (Wynes et al., 2004)	*Ex vivo*/*in vitro*	Monolayers of mouse bone marrow-derived macrophages C3H/HeJ mice CCL39 cells	2 ng/ml IL-4 for 26 h (macrophages) CCL39 myofibroblasts were cultured for 24 h with conditioned media from IL-4 treated macrophages	IGF-1 release (IL-4 treated macrophages) +++		CCL39 myofibroblast consumed the macrophage-derived IGF-1 from condition media Caspase-3 activity was reduced in CCL39 myofibroblasts that were protected by macrophage-derived IGF-1 Pro-survival kinases Akt and ERK were activated in CCL39 myofibroblasts by macrophage-derived IGF-1
Radiation (Meziani et al., 2018)	*Ex vivo*/*in vivo*/ Human	Female C57BL/6J mice AMs: Alveolar macrophages IMs: infiltrating macrophages	16 Gray (Gy) single dose locally administered to the whole thorax Evaluation: 0 – 20 weeks post exposure	Differential phenotype of AMs and IMs Day 6: Number of Icam1+ IMs transiently increased on day 6 Week 20: Increased	Activated IMs induced myofibroblastic activation IMs sorted from radiation induced fibrosis tissue 15 weeks post-irradiation were co-cultured with	Week 20: Increased collagen deposition. Increased TGF-β1, PAI-1, and Smad2/3 phosphorylation expressing in lung tissue

				number of CD206+ IMs Week 20: Th1 cytokines decreased and TIMP-1 increased Week 20: IMs expressed Arg-1.	normal fibroblasts: Increased α-SMA and TGF-β1 IMs sorted from normal mouse lung and activated *in vitro* with IL-13/-4 for 24 h: Increased α-SMA expression			
Bleomycin IL-4 and IL-13 (Liu et al., 2011)	*In vivo*/*Ex vivo*/ Human	C57BL/6 mice BALB/c mice GFP-transgenic mice Female fisher 344 rats FIZZ2 knockout mice IL-4 knockout mice IL-4/IL-13 knockout mice STAT6 knockout mice	Bleomycin 2 U/Kg and 10 U/Kg mice Rat alveolar epithelial cells isolated and human primary small airway epithelial cells (PCS-301-010) were treated with 10 ng/ml of rIL-4, rIL-13, rIL-17 or IFN-γ and incubated for 4 h, 8 h Mouse lung fibroblasts were isolated and treated with 2.5 - 100 ng/mL recombinant mouse FIZZ2 for 2, 6, 24 h Evaluation: 0 -21 days post-exposure	FIZZ2 mRNA expression in treated alveolar epithelial cells		Mouse lung fibroblasts treated with FIZZ2		
				IL-4 Treatment: 4 h: ++++ (Rat cells) 8 h: +++ (Rat cells), + (Human cells) IL-13 Treatment: 4 h: ++ (Rat cells) 8 h: ++ (Human cells)		Collagen type I mRNA expression 2 h 10: 25: 6 h 25: +	Abundance of α-SMA protein 24 h 25: + 50: ++ 100: +++	Increased cell proliferation 24 h 10: +++ 25: +++ 50: ++
Bleomycin (Gibbons et al., 2011)	*In vivo*/ Human/ *Ex vivo*	Female C57BL/6 mice	0.05 U intratracheal instillation Evaluation: 0 - 56 days post-exposure	Increase Arg activity and Ym1 expression	Increase Ym1 cells per field	Increased collagen deposition	Increased expression of α-SMA and Col1A1	Increased fibrosis
				Day 25: +++	Day 32: +++	Day 18: ++	Day 25: +++ (α-SMA) ++ (Col1A 1)	Day 32: +++

α-SMA: Alpha-smooth muscle actin.
Akt: Protein kinase B.
Arg: Arginase.
Col1A1: Collagen type I alpha 1 chain.
ERK: Extracellular signal-regulated kinase.
FIZZ2: Found in inflammatory zone 2.
Foxp3: Forkhead box p3.
GATA-3: GATA binding protein 3.
GFP: Green fluorescent protein.
Icam1: Intercellular adhesion molecule 1.
IFN-γ: Interferon gamma.
IGF-1: Insulin-like growth factor 1.
IL: Interleukin.
PAI-1: Plasminogen activator inhibitor 1.
PBS: Phosphate-buffered saline.
PDGF-B: Platelet derived growth factor subunit B.
Rag2: Recombination activating 2.
Smad2/3: SMAD family member (Smad)2/3.
STAT6: Signal transducer and activator of transcription 6.
TGF-β: Transforming growth factor beta.
TIMP: Metalloproteinase inhibitor 1.
Ym1: Chitinase-like protein 3.

A majority of the weight of evidence studies assess collagen synthesis as a proxy to fibroblast proliferation and myofibroblast differentiation. A few studies have shown that Th2 cytokine IL-4 stimulates fibroblast proliferation (Sempowski et al., 1994) and production of ECM components (Postlethwaite et al., 1992). In human studies, the progression of idiopathic pulmonary fibrosis (IPF) is also associated with a sustained IL-4 production (Ando et al., 1999; Wallace and Howie, 1999). Th2 cytokines induce expression and activity of TGF-β1, levels of which are elevated in bronchoalveolar lavage fluid (BALF) of patients suffering from lung interstitial diseases, is a potent inducer of myofibroblast differentiation and collagen synthesis (Kurosaka et al., 1998; Redington et al., 1997). Exposure of Signal transducer and activator of transcription 6 (STAT6) deficient mice to multi-walled carbon nanotubes (MWCNTs), suppressed acute lung inflammation, expression of Th2-mediated gene expression, reduced vimentin positive cells (a marker of fibroblasts), levels of collagen synthesis and reduced the overall fibrotic response to MWCNTs (Nikota et al., 2017). Mice deficient in IL-33r (St2, Th2 response cytokine) or mice treated with anti-IL33 antibody, showed reduced lung inflammation, reduced collagen production and fibrotic pathology induced by bleomycin. IL-33 deficient mice treated with bleomycin showed reduced levels of IL-1 and other pro-inflammatory cytokines. Mice administered exogenously with mature IL-33 enhanced bleomycin-induced lung inflammation, collagen synthesis and fibrotic lesions (Li et al., 2014).

Dose-Response Relationship:

In vivo and *in vitro* studies have demonstrated a dose-response relationship, at the higher dose of the stressor, Th2 cells leads to increased, fibroblast proliferation, and myofibroblast differentiation.

Lo Re et al. (2011) evaluated the role of regulatory T cells (Treg cells) in a mouse model of lung fibrosis induced by silica (SiO_2) particles. SiO_2 particles administered 2.5 mg per mouse by pharyngeal instillation induced an increase in the levels of $CD4^+$Forkhead box p3 $(Foxp3)^+$ regulatory T lymphocytes in lungs after 3 and 15 days of administration. Treg cells, purified from Foxp3-GFP transgenic mice administered with SiO_2, stimulated lung fibroblast proliferation *in vitro* by producing Platelet derived growth factor subunit B (PDGF-B) and TGF-β in a dose-dependent manner. Moreover, these results indicated that the activation of Th2 response (KE4; Event 1499) was needed to activate fibroblast proliferation (KE5; Event 1500). They determined that effector T cells purified from SiO_2-treated mice, in the absence of Treg cells, induced fibrosis by producing IL-4, suggesting that many T cell pathways lead to the fibroproliferative process.

Liu et al. (2011) investigated the role of Found in inflammatory zone 2 (FIZZ2) in pulmonary fibrosis in a rodent bleomycin model and the potential role of FIZZ2 in human fibrotic lung disease. FIZZ2 has been found in pulmonary fibrosis after 14 days of exposure to bleomycin in mice (2 U and 10 U/Kg) and in lung tissue from patients with IPF and nonspecific interstitial pneumonia. The expression was localized mainly to airway epithelial cells and alveolar epithelial cells (AECs), and to a lesser extent in alveolar macrophages and smooth muscle and endothelial cells. AECs were isolated from rats and humans, and they were exposed to 10 ng/ml rIL-4, rIL-13, rIL-17 and Interferon gamma (INF-γ). After 4 h, rIL-4 and rIL-13, induced FIZZ2 mRNA expression in rat lungs. After 8 h, rIL-13 increased FIZZ2 mRNA expression in rat lungs, and rIL-4 and IL-13 induced an expression of FIZZ2 MRNA in human lungs. These results indicate that FIZZ2 mRNA expression is driven by Th2-type cytokines. Mouse lung fibroblasts were isolated and treated with recombinant mouse FIZZ2 at different concentrations. Collagen I deposition was observed at 10 and 25 ng/ml, and Alpha-smooth muscle actin (α-SMA) was induced at 25, 50, and 200 ng/ml; meanwhile, cell proliferation was observed at 10, 25, and 50 ng/ml. These results suggested that FIZZ2 had direct profibrogenic activity. Furthermore,

FIZZ2 acts as a chemoattractant for bone marrow (BM) cells, especially BM-derived $CD11^{c+}$ dendritic cells. In knockout mice treated with bleomycin, a decrease in the FIZZ2 expression was seen, and the adverse effects produced by FIZZ2 decreased. The authors concluded that FIZZ2 is a Th2-associated multifunctional mediator which plays a role in fibroblast proliferation mediated via STAT6 signaling.

Temporal Relationship:

In vitro and *in vivo* studies have demonstrated that Th2 cells are activated prior to fibroblast proliferation and myofibroblast differentiation.

Dong et al. (2016) demonstrated that MWCNTs activated Th2 immune responses. Male C57BL/6J mice were administered with 40 µg/mouse MWCNTs by pharyngeal aspiration. On days 1, 3, and 7 post-exposure, an increase in the expression of Th2 cytokines (IL-4 and IL-3), as well as an induction of STAT6 and GATA Binding Protein 3 (GATA-3) was seen. At day 7, the presence of collagen I fibers was evident.

In another study, male Wistar rats were administered with 5 mg/kg bleomycin by intratracheal instillation. The inflammatory response was evaluated after 7, 14, and 28 days of exposure. Bleomycin increased hydroxyproline levels, total cell counts, and the expression of Nuclear Factor Kappa B (NF-κB) p65 in lung tissue. Collagen type I increased in a time-dependent manner. At day 7, the Th type 1 (Th1) response was suppressed, based on a decrease of Interferon gamma (IFN-γ) and an increase of IL-4 levels. Mice treated with hydrogen sulfide showed less intense effects than mice treated with bleomycin (Cao et al., 2014).

Yin et al. (2013) studied the role of IL-33 in cutaneous wound healing. Male BALB/c mice were injured on the dorsal skin and administered with murine recombinant IL-33 (1.0 µg/mouse). After 5 days of injury, M2 macrophage accumulation and mRNA expression of M2-associated genes increased (fibronectin and collagen). Collagen deposition increased in a time-dependent manner, and the percentage of wound closure and re-epithelization increased over 14 days. This study indicates that macrophage polarization, which is associated with KE4 (Event 1499) preceded the KE5 (Event 1500: fibroblast proliferation). IL-33 is essential for homeostasis and wound healing.

Wynes et al. (2004) evaluated the proliferative response associated with Th2 activation. Insulin-like growth factor-I (IGF-I) is a fibroblast growth and survival factor that has been implicated in the pathogenesis of IPF. The authors observed that mouse BM-derived macrophages from C3H/HeJ mice treated with IL-4 2 ng/ml for 26 h released IGF-I. CCL39 myofibroblasts, cultured with conditioned media from IL-4-treated macrophages, consumed IGF-1 and avoided apoptosis (caspase-3 activity reduced and pro-survival kinases Protein kinase B [Akt] and Extracellular signal-regulated kinase [ERK] were activated). The survival effect was lost when IGF was immunodepleted from macrophage-condition media with IGF-I-specific antibodies. These results indicate that a Th2 response conditions macrophages to release mediators which induce persistence of fibroblasts in a fibrotic setting.

Meziani et al. (2018) studied the role of large doses of radiation in promoting M2 macrophage polarization. In patients with thoracic malignancies and preoperative radiotherapy between 25 and 60 Gray (Gy), an infiltration of CD163+ macrophages was found in fibrotic areas. The pulmonary infiltration was characterized during radiation-induced lung fibrosis in a murine model. Female C57BL/6J mice were locally irradiated at the thorax with a dose rate of 1.08 Gy min^{-1}. A single dose of 16 Gy was locally administered to the whole thorax. Infiltrating macrophages (IMs) and alveolar macrophages were isolated post-irradiation. They observed the number of Intercellular adhesion molecule 1 (Icam1)+ IMs transiently increased at day 6, and an increase number

of CD206+ IMs at week 20 post-irradiation. At this time, Th1 cytokines decreased, and Metalloproteinase inhibitor 1 (TIMP-1) increased. Moreover, IMs express high levels of Arginase (Arg)-1. IMs were co-cultured with normal fibroblasts and increased the expression of α-SMA and TGF-β1. They found that IMs isolated from normal mouse lungs, activated *in vitro* with IL-13 and IL-4 for 24 h, were able to increase α-SMA levels. After 20 weeks, irradiation induced collagen deposition and an increase in the expression of TGF-β1, Plasminogen activator inhibitor 1 (PAI-1), and SMAD family member (Smad)2/3 phosphorylation in lung tissue. Depletion of tissue IMs by anti-Colony stimulating factor 1 receptor (CSF1R) after thoracic irradiation, blocks the observed effects.

Gibbons et al. (2011) studied the role of circulating monocytes and lung macrophages in the pathogenesis of lung fibrosis and the importance of M2 macrophages and Ly6Chi monocyte phenotype. Female C57Bl/6 mice were given 0.05 U bleomycin or $1X10^8$ plaque forming unit (pfu) Adenoviral TGF-β (AdTGF-β) intratracheally. Bleomycin induced early fibrosis at day 18, progressive fibrosis at day 32, or resolving fibrosis at day 56. Bleomycin increased the expression of α-SMA and Collagen type I alpha 1 chain (Col1A1) at day 25. At this time point, they also found an increase in the level of Arg activity and Chitinase-like protein 3 (known as Ym1), and at day 32 an increase in the number of cells per field (markers of M2 macrophages). Macrophages isolated from patients with IPF showed CD163, a human marker of M2 macrophages. AdTGF-β induced an increase in BALF TGF-β at day 5, and collagen deposition at day 14. The administration of liposomal clodronate intratracheally (100 ml) at 10, 21-23 after exposure to bleomycin or AdTGF-β decreased fibrosis, collagen deposition and M2 macrophages. The depletion of circulating monocytes reduced fibrosis and M2 macrophages. It was found that Ly6Chi inflammatory monocytes were the direct precursor of the M2 lung macrophages.

Uncertainties and Inconsistencies

Due to multifarious functions of several cytokines involved in the process of inflammation and repair, the timing of when a pathway is intervened in an experiment is important in the assessment of the KER studies. For example, exposure to pro-fibrotic bleomycin stimulates IL-4 production during the acute inflammatory phase, which is suggested to limit the recruitment of T lymphocytes and production of damaging cytokines such as Tumor necrosis factor alpha (TNF-α), IFN-γ, and nitric oxide, playing a tissue protective role. However, production of IL- 4 during the chronic phase of tissue repair and healing, favors fibrosis manifestation. Treatment of IL4 -/- mice with low doses of bleomycin induced fewer fibrotic lesions compared to IL-4 +/+ mice. However, treatment of high doses of bleomycin induced more lethality in IL-4 -/- mice compared to the wild type mice (Huaux et al., 2003). Moreover, the KEs represented in AOP 173 can function in parallel in a positive feedback loop, perpetuating and magnifying the response at each stage. The resulting microenvironment may contain the same molecules in different proportions exhibiting different functions. Thus, the complexity of the process and the functional heterogeneity of the molecular players involved, makes it nearly impossible to establish KERs using a targeted deletion of one single gene or a pathway in a study, which is how most of the studies are designed.

References

1. Ando M, Miyazaki E, Fukami T, Kumamoto T, Tsuda T. Interleukin-4-producing cells in idiopathic pulmonary fibrosis: an immunohistochemical study. Respirology. 1999 Dec;4(4):383-91. doi: 10.1046/j.1440-1843.1999.00209.x.
2. Barron L, Wynn TA. Fibrosis is regulated by Th2 and Th17 responses and by dynamic interactions between fibroblasts and macrophages. Am J Physiol Gastrointest Liver Physiol. 2011 May;300(5):G723-8. doi: 10.1152/ajpgi.00414.2010.
3. Cao H, Zhou X, Zhang J, Huang X, Zhai Y, Zhang X, Chu L. Hydrogen sulfide protects against bleomycin-induced pulmonary fibrosis in rats by inhibiting NF-κB expression and regulating Th1/Th2 balance. Toxicol Lett. 2014 Jan 30;224(3):387-94. doi: 10.1016/j.toxlet.2013.11.008.
4. Dong J, Ma Q. In vivo activation of a T helper 2-driven innate immune response in lung fibrosis induced by multi-walled carbon nanotubes. Arch Toxicol. 2016 Sep;90(9):2231-2248. doi: 10.1007/s00204-016-1711-1.
5. Fichtner-Feigl S, Strober W, Kawakami K, Puri RK, Kitani A. IL-13 signaling through the IL-13alpha2 receptor is involved in induction of TGF-beta1 production and fibrosis. Nat Med. 2006 Jan;12(1):99-106. doi: 10.1038/nm1332.
6. Gibbons MA, MacKinnon AC, Ramachandran P, Dhaliwal K, Duffin R, Phythian-Adams AT, van Rooijen N, Haslett C, Howie SE, Simpson AJ, Hirani N, Gauldie J, Iredale JP, Sethi T, Forbes SJ. Ly6Chi monocytes direct alternatively activated profibrotic macrophage regulation of lung fibrosis. Am J Respir Crit Care Med. 2011 Sep 1;184(5):569-81. doi: 10.1164/rccm.201010-1719OC.
7. Hashimoto S, Gon Y, Takeshita I, Maruoka S, Horie T. IL-4 and IL-13 induce myofibroblastic phenotype of human lung fibroblasts through c-Jun NH2-terminal kinase-dependent pathway. J Allergy Clin Immunol. 2001 Jun;107(6):1001-8. doi: 10.1067/mai.2001.114702.
8. Huaux F, Liu T, McGarry B, Ullenbruch M, Phan SH. Dual roles of IL-4 in lung injury and fibrosis. J Immunol. 2003 Feb 15;170(4):2083-92. doi: 10.4049/jimmunol.170.4.2083.
9. Kurosaka H, Kurosaka D, Kato K, Mashima Y, Tanaka Y. Transforming growth factor-beta 1 promotes contraction of collagen gel by bovine corneal fibroblasts through differentiation of myofibroblasts. Invest Ophthalmol Vis Sci. 1998 Apr;39(5):699-704.
10. Lee CG, Homer RJ, Zhu Z, Lanone S, Wang X, Koteliansky V, Shipley JM, Gotwals P, Noble P, Chen Q, Senior RM, Elias JA. Interleukin-13 induces tissue fibrosis by selectively stimulating and activating transforming growth factor beta(1). J Exp Med. 2001 Sep 17;194(6):809-21. doi: 10.1084/jem.194.6.809.
11. Li D, Guabiraba R, Besnard AG, Komai-Koma M, Jabir MS, Zhang L, Graham GJ, Kurowska-Stolarska M, Liew FY, McSharry C, Xu D. IL-33 promotes ST2-dependent lung fibrosis by the induction of alternatively activated macrophages and innate lymphoid cells in mice. J Allergy Clin Immunol. 2014 Dec;134(6):1422-1432.e11. doi: 10.1016/j.jaci.2014.05.011.
12. Liu T, Baek HA, Yu H, Lee HJ, Park BH, Ullenbruch M, Liu J, Nakashima T, Choi YY, Wu GD, Chung MJ, Phan SH. FIZZ2/RELM-β induction and role in pulmonary fibrosis. J Immunol. 2011 Jul 1;187(1):450-61. doi: 10.4049/jimmunol.1000964.
13. Lo Re S, Lecocq M, Uwambayinema F, Yakoub Y, Delos M, Demoulin JB, Lucas S, Sparwasser T, Renauld JC, Lison D, Huaux F. Platelet-derived growth factor-producing

CD4+ Foxp3+ regulatory T lymphocytes promote lung fibrosis. Am J Respir Crit Care Med. 2011 Dec 1;184(11):1270-81. doi: 10.1164/rccm.201103-0516OC.

14. Meziani L, Mondini M, Petit B, Boissonnas A, Thomas de Montpreville V, Mercier O, Vozenin MC, Deutsch E. CSF1R inhibition prevents radiation pulmonary fibrosis by depletion of interstitial macrophages. Eur Respir J. 2018 Mar 1;51(3):1702120. doi: 10.1183/13993003.02120-2017.
15. Nikota J, Banville A, Goodwin LR, Wu D, Williams A, Yauk CL, Wallin H, Vogel U, Halappanavar S. Stat-6 signaling pathway and not Interleukin-1 mediates multi-walled carbon nanotube-induced lung fibrosis in mice: insights from an adverse outcome pathway framework. Part Fibre Toxicol. 2017 Sep 13;14(1):37. doi: 10.1186/s12989-017-0218-0.
16. Postlethwaite AE, Holness MA, Katai H, Raghow R. Human fibroblasts synthesize elevated levels of extracellular matrix proteins in response to interleukin 4. J Clin Invest. 1992 Oct;90(4):1479-85. doi: 10.1172/JCI116015.
17. Redington AE, Madden J, Frew AJ, Djukanovic R, Roche WR, Holgate ST, Howarth PH. Transforming growth factor-beta 1 in asthma. Measurement in bronchoalveolar lavage fluid. Am J Respir Crit Care Med. 1997 Aug;156(2 Pt 1):642-7. doi: 10.1164/ajrccm.156.2.9605065.
18. Sempowski GD, Beckmann MP, Derdak S, Phipps RP. Subsets of murine lung fibroblasts express membrane-bound and soluble IL-4 receptors. Role of IL-4 in enhancing fibroblast proliferation and collagen synthesis. J Immunol. 1994 Apr 1;152(7):3606-14.
19. Shao DD, Suresh R, Vakil V, Gomer RH, Pilling D. Pivotal Advance: Th-1 cytokines inhibit, and Th-2 cytokines promote fibrocyte differentiation. J Leukoc Biol. 2008 Jun;83(6):1323-33. doi: 10.1189/jlb.1107782.
20. Wallace WA, Howie SE. Immunoreactive interleukin 4 and interferon-gamma expression by type II alveolar epithelial cells in interstitial lung disease. J Pathol. 1999 Mar;187(4):475-80. doi: 10.1002/(SICI)1096-9896(199903)187:4<475::AID-PATH268>3.0.CO;2-N.
21. Wynes MW, Frankel SK, Riches DW. IL-4-induced macrophage-derived IGF-I protects myofibroblasts from apoptosis following growth factor withdrawal. J Leukoc Biol. 2004 Nov;76(5):1019-27. doi: 10.1189/jlb.0504288.
22. Wynn TA. Fibrotic disease and the T(H)1/T(H)2 paradigm. Nat Rev Immunol. 2004 Aug;4(8):583-94. doi: 10.1038/nri1412.
23. Wynn TA, Ramalingam TR. Mechanisms of fibrosis: therapeutic translation for fibrotic disease. Nat Med. 2012 Jul 6;18(7):1028-40. doi: 10.1038/nm.2807.
24. Yin H, Li X, Hu S, Liu T, Yuan B, Gu H, Ni Q, Zhang X, Zheng F. IL-33 accelerates cutaneous wound healing involved in upregulation of alternatively activated macrophages. Mol Immunol. 2013 Dec;56(4):347-53. doi: 10.1016/j.molimm.2013.05.225.

Relationship: 2652: Increased cellular proliferation and differentiation leads to Accumulation, Collagen

AOPs Referencing Relationship

AOP Name	Adjacency	Weight of Evidence	Quantitative Understanding
Substance interaction with the pulmonary resident cell membrane components leading to pulmonary fibrosis	adjacent	High	High

Key Event Relationship Description

When activated, fibroblasts migrate to the site of tissue injury and build a provisional extracellular matrix (ECM), which is then used as a scaffold for tissue regeneration. Activated fibroblasts in turn produce Interleukin (IL)-13, IL-6, IL-1β and Transforming growth factor beta (TGF-β), propagating the response. In the second phase, which is the proliferative phase, angiogenesis is stimulated to provide vascular perfusion to the wound. During this phase more fibroblasts are proliferated and they acquire Alpha-smooth muscle actin (α-SMA) expression and become myofibroblasts. Thus, myofibroblasts exhibit features of both fibroblasts and smooth muscle cells. The myofibroblasts synthesise and deposit ECM components that eventually replace the provisional ECM. Because of their contractile properties, they play a major role in contraction and closure of the wound tissue (Darby et al., 2014). Apart from secreting ECM components, myofibroblasts also secrete proteolytic enzymes such as metalloproteinases and their inhibitors tissue inhibitor of metalloproteinases, which play a role in the final phase of the wound healing which is scar formation phase or tissue remodelling.

During this final phase, new synthesis of ECM is suppressed to allow remodelling. The wound is resolved with the secretion of procollagen type 1 and elastin, and infiltrated cells including inflammatory cells, fibroblasts and myofibroblasts are efficiently removed by cellular apoptosis. However, in the presence of continuous stimulus resulting in excessive tissue damage, uncontrolled healing process is initiated involving exaggerated expression of pro-fibrotic cytokines and growth factors such as TGF-β, excessive proliferation of fibroblasts and myofibroblasts, increased synthesis and deposition of ECM components, inhibition of reepithelialisation, all of which lead to replacement of the normal architecture of the alveoli and fibrosis (Ueha et al., 2012; Wallace et al., 2007).

Evidence Supporting this KER

Biological Plausibility

The biological plausibility of this KER is high. There is an accepted mechanistic relationship between activated myofibroblasts, and the capacity to secrete collagen (Hinz, 2016a; Hinz, 2016b; Hu and Phan, 2013).

Empirical Evidence

The empirical evidence to support this KER is high. It is generally accepted knowledge that activated myofibroblasts are collagen secreting cells (Blaauboer et al., 2014; Hinz, 2016a; Li et al., 2017; For additional references see Table 1).

Table 1. Studies providing empirical evidence for the relationship between KE5 (Event 1500) and KE6 (Event 68). +: Severity of Response. References available in main KER page

Stressor (Reference)	***In vitro/in vivo/ex vivo***	**Species/Cell line**	**Exposure Conditions**	**KE5 (Event 1500) Increased, fibroblast proliferation, and myofibroblast differentiation**				**KE6 (Event 68) Accumulation, Collagen**
Diphtheria toxin (Osterholzer et al., 2013)	*In vivo*	C57BL/6 mice wild-type Diphtheria toxin receptor (DTR) + mice DTR^{+}/CCR2$^{-/-}$ mice	10.0 µg/kg intraperitoneal injection once/day, 14 days Evaluation: 7, 14, and 21, days after onset of treatment	Exudate macrophages (ExM) increased in DTR+ lungs	Accumulation of ExM and Ly-6C^{high} monocytes in DTR+ lungs	Immunophenotype of ExM and Ly6C^{high} monocytes in DTR+ mice		Lung collagen content in DTR+ mice
				Day 7: +++ Day 14: +++ Day 21: ++	Day 14: ++	Day 14: mRNA or protein expression: Arg, iNOS, IL-13 and TGF-β, CD45+, Col1+ and CCR4.		Day 21: increase hydroxyproline content
Silicon dioxide (SiO_2) (Fang et al., 2018)	*In vivo*	Stock TEK-GFP 287 Sato/JNju (Tie2-GFP) mice	0.5 g/Kg intratracheal instillation Evaluation: 28 days post-exposure	Day 28: GFP localized with α-SMA/Acta2 in lung tissue				Day 28: Sirius red staining (marks collagen I and III) co-localized with GFP signal.
	In vitro	Mouse microvascular lung cells	50 µg/cm^2 for 6, 12, 24, 48 h	Increase protein expression of mesenchymal markers (Col1A1, Acta2)	Decrease protein expression of endothelial markers (Cdh5, PECAM1)	Increase cell proliferation and migration		
				6 h: 12 h: + 24 h: ++ 48 h: +++	6 h: 12 h: + 24 h: + 48 h: ++	6 h: 12 h: 24 h: + 48 h: ++		
	Human	Lung sections from patients	Patients with silicosis					Day 28: Decrease Tie2-GFP and HECTD1 expression
Multi-walled carbon nanotubes (Dong et al., 2017)	*In vivo*	Male C57BL/6J wild-type mice B6.129S4-Timp1tm1Pds/J (Timp1 Knockout) mice	40 µg/mouse pharyngeal aspiration Evaluation: 1, 3, 7, 14 days post-exposure	Timp1 mRNA and protein levels increased in lung, BALF and serum	Increase FN1 protein expression in lungs	Increase FSP protein expression in lungs	Increase Ki67 and PCNA expression levels in lungs	Collagen deposition (Masson's trichrome)

				Day 1: +++ Day 3: +++ Day 7: ++ Day 14: +	Day 1: ++ Day 3: +++ Day 7: +++ Day 14: +	Day 1: + Day 3: +++ Day 7: +++ Day 14: ++	Day 1: + Day 3: ++ Day 7: +++ Day 14: ++	Day 1: + Day 3: ++ Day 7: +++ Day 14: ++
				Day 7: Increase in the levels of Hsp47, vimentin, α-SMA, PDGFR-β, CD63, integrin β1, p-Erk1/2, and genes involved in cell cycle regulation (wild-type and Timp1 knockout)				Day 7: Mice Timp1Knockout showed a significant reduction of fibrosis as compared to wild-type
CeO_2 nanoparticles (Ma et al. 2017)	*In vivo*	Male Sprague-Dawley rats	0.15-7 mg/Kg intratracheal instillation Evaluation: 1 – 28 days post-exposure	Increased soluble collagen in BALF			Increased α-SMA expression in lung tissue	Increases hydroxyproline content in lung tissue
				3.5 mg/Kg Day 3: + Day 28: +++			3.5mg/Kg Day 1: +++ Day 3: ++ Day 28:	Day 28 3.5 mg/Kg: + 7 mg/Kg: +
	Ex vivo	Alveolar Macrophages Fibroblasts ATII cells	Isolated from CeO2 exposed rats 1 - 28 days post-exposure	Increased TGF-β1 (Macrophages)	Decreased proliferation (Fibroblasts)	Increased α-SMA (Fibroblasts & ATII)		
				3.5mg/Kg CeO_2 Day 1: Day 3: ++ Day 10: ++ Day 28: +	Day 28 0.15mg/kg: + 1mg/kg: ++ 3.5mg/kg: +++ 7 mg/Kg: +++	Day 3 (ATII) 3.5mg/kg: +++ Day 28 (Fibroblasts) +++		
Bleomycin (Hu et al., 2015)	*In vivo*	Notch1 conditional knockout (CKO) and wild-type mice	2 U/kg endotracheal injection (wild-type & CKO mice) Evaluation: 7 – 28 days post-exposure	Increased protein expression Jagged-1 and Notch1 in wild-type mouse lungs	Increased expression mRNA α-SMA and Col1, Notch1 protein in isolated wild-type lung fibroblasts	Increased percentage of α-SMA+ cells in lungs		Increased hydroxyproline content in lung tissue

				Jagged1 Day 7: ++ Day 14: ++ Day 21: + Day 28: + Notch1 Day 7: ++ Day 14: + Day 21: - - - - Day 28: - - - -	Day 14 α-SMA (protein & mRNA): +++ Col1 (protein & mRNA): +++ Notch1(protein):	Day 14 Wild-type mice: +++ CKO mice: +	Day 28 CKO mice showed a significant attenuation of collagen deposition as compared to wild-type	
Bleomycin TGF-β (Blaauboer et al., 2014)	*In vivo*	Female C57BL/6 mice	30 μl (1.25 U/ml in phosphate-buffered saline) Bleomycin intratracheal instillation. Evaluation: 1 – 5 weeks post-exposure.	Increased α-SMA protein level on histological staining in lungs			New collagen formation and gene expression	Extracellular matrix proteins Increased protein level on histological staining in lungs
				Week 1: ++ Week 2: +++ Week 3: +			Gene expression of ELN, type V collagen and TNC highly correlated to new collagen formation	ELN Week 1: + Week 2: ++ Week 3: +++ Type V collagen and TNC Week 1: +++ Week 2: ++ Week 4: ++
	In vitro	Primary normal human lung fibroblast Human fetal lung fibroblast	1, 2, 4, 10 ng/mL TGF-β Evaluation: 24, 48 h	Increased mRNA expression 24 h	Increased ELN, COL5A1 mRNA expression 24 h	Increased mRNA expression 48 h, ELN coated surface		

									(10 ng/ml TGF-β)	
				ACTA 1: 2: + 5: ++ 10: +++	COL1A1 1: + 2: ++ 5: ++ 10: +++	ELN 1: + 2: ++ 5: +++ 10: ++++	COL5A1 1: 2: + 5: ++ 10: +++	TNC 1: 2: + 5: + 10: +++	+++ (ACTA2 COL1A1 ELN)	
Radiation (Judge et al., 2015)	Study population/ *In vivo*/*In vitro*	Lung biopsies from patients with thoracic radiation for cancer treatment C57BL/6 mice Primary human lung fibroblast	5 Gray (Gy) total body plus 10 Gy thoracic radiation (mice). Evaluation: 12-26 weeks post-exposure 3, 7 Gy (primary human lung fibroblasts) Evaluation: 5 days post-exposure	Increased LDH expression		Increased extracellular acidification and lactate production (Fibroblasts)		Increased α-SMA protein expression, soluble collagen I, Col1A1, and Col3A1 mRNA levels (Fibroblasts)	TGF-β1 activation (Fibroblasts)	Increased collagen fibers deposition trichrome stain
				Lung biopsies: ++++ Mouse lung: Week 12: Week 16: + Week 18: + Week 26: +++ Fibroblasts: 3 Gy: 7 Gy: +++		Acidification 3 Gy:++ 7 Gy:+++ Lactate: 3 Gy: + 7 Gy: ++		Soluble Collagen 3 Gy: 7 Gy: +++ Col1A1 7 Gy: +++ Col3A1 7 Gy: +++	3 Gy: +++ 7 Gy: ++++	Lung biopsies: +++
Copper oxide nanoparticles (Lai et al., 2018)	*In vivo*	C57BL/6 mice	1, 2.5, 5, 10 mg/Kg intranasal instillation Evaluation: 7, 14, 28 days post-exposure	Increased mRNA levels of CCL-2, CCL-3, IL-4, IL-10, IFN-α, TGF-β1 at day 14.		Cell apoptosis in lung tissue		Increased TGF-β1 content in BALF on day 14	Increased α-SMA on day 28	Increased collagen-I and hydroxyproline content on day 28

				5: +++	Day 14: 1: + 2.5: ++ 5: +++ 5mg/kg: Day 7: ++ Day 14: +++ Day 28: +++	2.5: +++ 5: ++++	2.5: ++ 5: ++++	2.5: ++ 5: +++
Cadmium chloride ($CdCl_2$) (Li et al., 2017)	*In vivo*	C57BL/6 vimentin knockout mice C57BL/6 wild-type mice	0.009, 0.018 mg/Kg intratracheal instillation (once / 2 days; 8 weeks) Evaluation: weeks 1, 2, 4, 8 of exposure.	Increased α-SMA in lung tissue (0.009 mg/Kg)				Increased (0.009 mg/Kg)
				Week 4: +++				Subepithelial thickness Week 4: ++ Airway resistance Week 4: ++ Collagen-I staining Week 4: +++ Picrosirius red Week 4: +++ Collagen content (Sircol assay) Week 1: Week 2: ++ Week 4: ++ Week 8: +++
	In vitro	Primary human fibroblast	5, 10, 20 µM for 3 h. Allowed to recover for 3, 24, 48, 72 h.	Increased α-SMA				Increased
				10 µM $CdCl_2$ for 3 h followed by recovery 3 h: 24 h: 48 h: + 72 h: ++ 20 µM $CdCl_2$ for 3 h followed by recovery 3 h: + 24 h: + 48 h: ++				Soluble collagen (48 h recovery) 5: 10: +++ 20: ++++ Soluble collagen (20 µM $CdCl_2$) 3 h: 24 h: ++++

				72 h: ++	48 h: ++++ 72 h: ++++ Fibronectin and Collagen I (10 and 20 μM $CdCl_2$) 3 h: + 24 h: ++ 48 h: +++ 72 h: +++

Acta2: Actin alpha 2.
Arg: Arginase.
BALF: Bronchoalveolar lavage fluid.
CCL: C-C motif chemokine ligand.
CCR: C-C motif chemokine receptor.
CD: Cluster of differentiation.
Cdh5: Cadherin 5.
Col1: Collagen type I.
COL1A1: Collagen type 1 alpha 1 chain.
Col3A1: Collagen type III alpha 1 chain.
COL5A1: Collagen type V alpha 1 chain.
ELN: Elastin.
ERK: Extracellular signal-regulated kinase.
FN1: Fibronectin 1.
FSP: Fibroblast-specific protein-1.
GFP: Green fluorescent protein.
HECTD1: HECT Domain E3 ubiquitin-protein ligase 1.
Hsp: Heat Shock protein.
IFN: Interferon.
IL: Interleukin.
iNOS: Inducible nitric oxide synthase.
LDH: Lactate dehydrogenase.
Notch1: Neurogenic locus notch homolog protein 1.
PECAM1: Platelet and endothelial cell adhesion molecule 1.
PCNA: Proliferating cell nuclear antigen.
PDGFR-β: Platelet derived growth factor receptor beta.
SMA: Smooth muscle actin.
TGF: Transforming growth factor beta.
Timp1: TIMP metallopeptidase inhibitor 1.
TNC: Tenascin C.

Mice infused subcutaneously with bleomycin showed pronounced lung fibrosis, characterised by elevated levels of TGF-β1 and collagen genes (Hoyt and Lazo, 1988). Radiation induced lung fibrosis was shown to precede high levels of TGF-β1 expression (Yi et al., 1996). Mice lacking TGF-β-receptor II showed resistance to bleomycin induced lung fibrosis (Li et al., 2011). Inhibition of fibroblast proliferation and differentiation by counteracting the activity of TGF-β attenuates bleomycin-induced lung fibrosis (Chen et al., 2013; Guan et al., 2016). Adenoviral vector-mediated gene transfer based transient overexpression of TGF-β1 in lungs of mice induced progressive lung fibrosis (Bonniaud et al., 2004). Targeted inhibition of Wnt/β-catenin signalling by a small molecule drug inhibited the mesenchymal-myofibroblast transition and repressed matrix gene expression leading to attenuated lung fibrosis (Cao et al., 2018).

Dose-Response Relationship:

There are a number of *in vitro* and *in vivo* studies that indicate a dose-response relationship in this KER. At a higher dose of the stressor, an increased in fibroblast proliferation and myofibroblast differentiation leads to increases in ECM deposition.

Ma et al. (2017) studied the role of epithelial-mesenchymal transition (EMT) in cerium oxide (CeO_2) induced fibrosis. Male Sprague-Dawley rats were exposed to 0.15-7 mg/kg CeO_2 via intratracheal instillation and sacrificed at various times post-exposure. At 28 days post-exposure there was a dose-dependent increase in hydroxyproline content in lung tissue. Mice exposed to 3.5 mg/kg showed an increase in soluble collagen levels in bronchoalveolar lavage fluid (BALF) at day 3 and day 28 and an increase in α-SMA expression levels in lung tissue with a peak at day 1 post-exposure. From CeO_2-exposed rats (3.5 mg/kg), macrophages, fibroblast, and alveolar epithelial cells type II (AEC2s) cells were isolated. Macrophages produced TGF-β1 with peaks at day 3 and 10 post-exposure. Fibroblast proliferation decreased in a dose-dependent manner, and an increase in the levels of α-SMA in fibroblasts and AEC2s at day 28 post-exposure. They concluded that CeO_2 exposure affects fibroblast function and induces EMT in AEC2s cells.

Blaauboer et al. (2014) studied the expression of elastin (ELN), type V collagen, and tenascin C (TNC) during the development of lung fibrosis and the effect of myofibroblast differentiation on this expression. Female C57Bl/6 mice were exposed to a single intratracheal instillation bleomycin 30 µl (1.25 U/ml in PBS). Seven days before sacrifice, mice received 35 µl deuterated water (D_2O)/g via intraperitoneal injection to label new collagen. Mice were sacrificed 1, 3, 4 or 5 weeks post-exposure. An increase in the level of α-SMA protein level in histological staining was observed, with a peak after 2 weeks. ECM proteins levels increased (histological staining). Elastin increased in a time-dependent manner with a peak after 4 weeks. Type V collagen and TNC increased after 1 week and decreased over time. They found that gene expression of ELN, type V collagen and TNC highly correlated to new collagen formation. Primary normal human lung fibroblast and human fetal lung fibroblast were exposed to different concentrations of TGF-β1. The expression of Actin assembly-inducing protein (ACTA), Collagen alpha-1(I) chain (COL1A1), ELN, Collagen type V alpha 1 chain (COL5A1) and TNC increased in a dose-response relationship after 24 h. Fibroblast cultured in ELN coatings and stimulated with 10 ng/ml TGF-β1 for 48 h, showed an increase in the levels of ACTA2, COL1A1, and ELN. The *In vitro* study demonstrated that fibrotic changes in the composition of the ECM have a regulatory role during fibrosis development.

Judge et al. (2015) determined that the Lactate dehydrogenase-A (LDHA) enzyme was upregulated in radiation and that lactate is required for radiation-induced myofibroblast differentiation. In lung biopsies obtained from patients who received thoracic radiation for cancer treatment, an overexpression of LDHA and α-SMA by immunostaining was seen, as well as the accumulation of collagen fibers. Mice C57BL/6mice were exposed to 5 Gray

(Gy) total body plus 10 Gy thoracic radiation. They found that LDHA overexpressed in lungs at 26 week, and LDHA mRNA increased over time at 16-26 weeks (post-radiation). Primary human lung fibroblasts were exposed to 3, and 7 Gy. At the highest dose 5 days post-radiation, an increase in the levels of LDHA protein expression, extracellular acidification, lactate levels in supernatants, α-SMA protein expression, soluble collagen I, Col1A1, and Collagen type III alpha 1 chain (Col3A1) mRNA levels, and TGF-β1 bioactivity was seen. LDHA siRNA and an LDH inhibitor, inhibits radiation-induced myofibroblast differentiation.

Lai et al. (2018) studied whether copper oxide (CuO) nanoparticles (NPs) could induce epithelial cell injury, pulmonary inflammation, and fibrosis in C57BL/6 mice. Animals were nasally instilled with 1, 2.5, 5, and 10 mg/kg of CuO NPs, and responses were evaluated at 7, 14, and 28 days post-exposure. In a dose-dependent manner, authors found increased mRNA levels of proinflammatory genes such as C-C motif chemokine ligand (CCL)-2, CCL-3, IL-4, IL-10, Interferon gamma (IFN-α), and TGF-β1 in lung tissue. Cell apoptosis was also increased in a dose-dependent manner at 1, 2.5, and 5 mg/Kg. Also, the increase of TGF-β1 in BALF at day 14 and the increase of α-SMA at day 28 in lung tissue followed a dose-response relationship at 2.5 and 5 mg/Kg. After 28 days of exposure, there was an increase in collagen-I and hydroxyproline content at 2.5 and 5 mg/Kg.

Temporal Relationship:

In vitro and *in vivo* studies highlight the temporal relationship between the two KEs in this KER.

Osterholzer et al. (2013) evaluated local inflammation and fibrosis after a targeted epithelial insult. Wild type (WT) C57BL/6 and transgenic mice expressing the diphtheria toxin (DT) receptor were intraperitoneally injected with DT once daily for 14 days at a dose of 10.0 μg/kg in 100 μl of PBS. Observations were evaluated at various days post-DT initiation. At day 7 and 14, an accumulation of exudate macrophages and Ly-6C^{high} monocytes was observed. The immunophenotype of ExM and Ly-6C^{high} monocytes at day 14 showed an expression of arginase, inducible nitric oxide synthase (iNOs), IL-13, TGF-β, CD45+, Type 1 collagen (Col1)+, and C-C motif chemokine-receptor (CCR)4. CCR2 deficient mice (CCR2-/-) did not show an accumulation of inflammatory cells and fibrosis. Finally, at day 21, lung collagen deposition was evident, as measured by hydroxyproline content.

Fang et al. (2018) studied the EMT characterized by the loss of endothelial specific markers (Cadherine 5 [Cdh5], Platelet and endothelial cell adhesion molecule 1 [PECAM1]), the acquisition of the mesenchymal markers (Col1A1, Acta 2), and the expression of α-SMA and Collagen I and III. Stock TEK-Green fluorescent protein (GFP) 287 Sato/JNiu Tie2-GFP mice were administered with 0.5 g/Kg silicon dioxide (SiO_2) instilled intratracheally in one dose. After 28 days of treatment GFP were localized with α-SMA/Acta2 and the amount of Sirius red (collagen I and III) increased. Mouse microvascular lung cells were exposed to 50 μg/cm^2 for 0, 6, 12, 24, and 48 h. An increase in the level of mesenchymal markers, a decrease in the level of endothelial markers, and an increase in cell proliferation and migration were observed after 12 h in a time-dependent manner. The exposure to SiO_2 increased the expression of circHECTD1 (a circular RNA which regulates the SiO_2-induced EMT) after 1, 3 and 24 h of exposure, and decrease the expression of HECTD1 12, 24 and 48 h post-exposure.

Activated macrophages secrete Metalloproteinase inhibitor 1 (TIMP1) into the ECM to inhibit matrix metalloproteinases and this could promote cell proliferation and inhibit fibroblast apoptosis through CD63/integrin β1 ERK signaling. Dong et al. (2017) characterized TiMP1 expression after multi-walled carbon nanotube (MWCNT) exposure.

Male C57BL/6J WT and B6.129S4-Timp1tm1Pds/J (Timp1 Knockout [KO]) mice were administered with MWCNTs at 40 µg per mouse by pharyngeal aspiration. Lungs were harvested at 1, 3, 7- and 14-days post-exposure. TIMP1 mRNA and protein levels increased in lung, BALF and serum at day 1, and then decreased over time. A similar behavior was observed for Fibronectin 1 (FN1), Fibroblast-specific protein-1 (FSP), Ki67 and Proliferating cell nuclear antigen (PCNA) expression, which are markers of proliferation, with a peak at 7 and 14 days post-exposure. Collagen deposition was observed at 1 day post-exposure with a peak at day 7. At day 7 they also observed an increase in the expression of Heat shock protein (Hsp)47, vimentin, α-SMA, Platelet derived growth factor receptor beta (PDGFR-β), and genes involved in cell cycle regulation (Mitotic checkpoint serine/threonine-protein kinase BUB1 beta [Bub1β], Macrophage-capping protein [Capg], Histone H3-like centromeric protein A [Cenpa], Kinesin-like protein Kif2c, Kinesin-like protein Kif22, Minichromosome maintenance complex component 5 [Mcm5], Polo like kinase 1 [Plk1] and Tubulin alpha-6 chain [Tuba 6]). TIMP1 KO mice displayed reduced responses. The formation of TIMP1/CD63/integrin b1 complex on the cell surface lead to an activation of the extracellular signal-regulated kinases (Erk)1/3 pathway.

Hu et al. (2015) studied the effects of conditional mesenchymal-specific deletion of Neurogenic locus notch homolog protein 1 (Notch1) on pulmonary fibrosis. A conditional KO of Notch1 (CKO) in collagen I-expressing mesenchymal cells was generated (Notch1fl/fl, Col1a2-cre-ER(T)+/0). Col1a2-cre-ER(T)+/0 with WT Notch1 mice and CKO were given daily intraperitoneal injections of tamoxifen for 8 days to induce mesenchymal cell-specific expression of the Cre-ER(T) recombinase and the removal of the floxed Notch1 (Notch1 CKO Mice). Control mice and Notch1 CKO were injected endotracheally with 2 U/Kg Bleomycin. Mice were sacrificed after 7, 14, and 21 days. Jagged1 (Jag-1) and Notch1 protein expression increased with a peak at 7- and 14-days post-exposure. After 14 days of the treatment, an increase in the levels of mRNA and protein of α-SMA and Col1 was seen, as well as an increase in the percentage of α-SMA+ lung fibroblasts. 28 days post-exposure there was an increase in the content of hydroxyproline in lungs. CKO mice showed a significant attenuation of collagen deposition and myofibroblast differentiation.

Li et al. (2017) evaluated whether low-dose cadmium exposure induces peribronchiolar fibrosis through site-specific phosphorylation of vimentin. C57BL/6 mice were exposed to 0.009 or 0.018 mg/kg cadmium chloride ($CdCl_2$) via non-surgical intratracheal instillation in saline every other day for eight weeks. On weeks 1, 2, 4, and 8, mice were sacrificed, and lungs were removed for histology. At week 4, the expression of α-SMA and collagen-I increased. Also, subepithelial thickness and airway resistance increased at this time point. Collagen content was also raised in a time-dependent manner. In a parallel experiment, primary human fibroblasts were incubated with $CdCl_2$ at 5, 10, and 20 µM for 3 h and then allowed to recover for 3, 24, 48, and 72 h. α-SMA protein expression and soluble collagen increased in a dose-dependent manner; meanwhile, α-SMA, fibronectin, and collagen-I increased in a time-dependent manner. These results demonstrated that cadmium induces myofibroblast differentiation and ECM deposition around small airways.

Uncertainties and Inconsistencies

Several studies have shown that inhibition of TGF-β involved in fibroblast activation and collagen deposition results in attenuated fibrotic response in lungs; however, results are inconsistent. More studies are required to support the quantitative KER.

Reference

1. Blaauboer ME, Boeijen FR, Emson CL, Turner SM, Zandieh-Doulabi B, Hanemaaijer R, Smit TH, Stoop R, Everts V. Extracellular matrix proteins: a positive feedback loop in lung fibrosis? Matrix Biol. 2014 Feb;34:170-8. doi: 10.1016/j.matbio.2013.11.002.
2. Bonniaud P, Kolb M, Galt T, Robertson J, Robbins C, Stampfli M, Lavery C, Margetts PJ, Roberts AB, Gauldie J. Smad3 null mice develop airspace enlargement and are resistant to TGF-beta-mediated pulmonary fibrosis. J Immunol. 2004 Aug 1;173(3):2099-108. doi: 10.4049/jimmunol.173.3.2099.
3. Cao H, Wang C, Chen X, Hou J, Xiang Z, Shen Y, Han X. Inhibition of Wnt/β-catenin signaling suppresses myofibroblast differentiation of lung resident mesenchymal stem cells and pulmonary fibrosis. Sci Rep. 2018 Sep 11;8(1):13644. doi: 10.1038/s41598-018-28968-9.
4. Chen YL, Zhang X, Bai J, Gai L, Ye XL, Zhang L, Xu Q, Zhang YX, Xu L, Li HP, Ding X. Sorafenib ameliorates bleomycin-induced pulmonary fibrosis: potential roles in the inhibition of epithelial-mesenchymal transition and fibroblast activation. Cell Death Dis. 2013 Jun 13;4(6):e665. doi: 10.1038/cddis.2013.154.
5. Dong J, Ma Q. TIMP1 promotes multi-walled carbon nanotube-induced lung fibrosis by stimulating fibroblast activation and proliferation. Nanotoxicology. 2017 Feb;11(1):41-51. doi: 10.1080/17435390.2016.1262919.
6. Fang S, Guo H, Cheng Y, Zhou Z, Zhang W, Han B, Luo W, Wang J, Xie W, Chao J. circHECTD1 promotes the silica-induced pulmonary endothelial-mesenchymal transition via HECTD1. Cell Death Dis. 2018 Mar 14;9(3):396. doi: 10.1038/s41419-018-0432-1.
7. Guan R, Wang X, Zhao X, Song N, Zhu J, Wang J, Wang J, Xia C, Chen Y, Zhu D, Shen L. Emodin ameliorates bleomycin-induced pulmonary fibrosis in rats by suppressing epithelial-mesenchymal transition and fibroblast activation. Sci Rep. 2016 Oct 24;6:35696. doi: 10.1038/srep35696.
8. Hinz B. Myofibroblasts. Exp Eye Res. 2016a Jan;142:56-70. doi: 10.1016/j.exer.2015.07.009.
9. Hinz B. The role of myofibroblasts in wound healing. Curr Res Transl Med. 2016b Oct-Dec;64(4):171-177. doi: 10.1016/j.retram.2016.09.003.
10. Hoyt DG, Lazo JS. Alterations in pulmonary mRNA encoding procollagens, fibronectin and transforming growth factor-beta precede bleomycin-induced pulmonary fibrosis in mice. J Pharmacol Exp Ther. 1988 Aug;246(2):765-71.
11. Hu B, Phan SH. Myofibroblasts. Curr Opin Rheumatol. 2013 Jan;25(1):71-7. doi: 10.1097/BOR.0b013e32835b1352.
12. Hu B, Wu Z, Bai D, Liu T, Ullenbruch MR, Phan SH. Mesenchymal deficiency of Notch1 attenuates bleomycin-induced pulmonary fibrosis. Am J Pathol. 2015 Nov;185(11):3066-75. doi: 10.1016/j.ajpath.2015.07.014.
13. Judge JL, Owens KM, Pollock SJ, Woeller CF, Thatcher TH, Williams JP, Phipps RP, Sime PJ, Kottmann RM. Ionizing radiation induces myofibroblast differentiation via lactate dehydrogenase. Am J Physiol Lung Cell Mol Physiol. 2015 Oct 15;309(8):L879-87. doi: 10.1152/ajplung.00153.2015.
14. Lai X, Zhao H, Zhang Y, Guo K, Xu Y, Chen S, Zhang J. Intranasal Delivery of Copper Oxide Nanoparticles Induces Pulmonary Toxicity and Fibrosis in C57BL/6 mice. Sci Rep. 2018 Mar 14;8(1):4499. doi: 10.1038/s41598-018-22556-7.

15. Li M, Krishnaveni MS, Li C, Zhou B, Xing Y, Banfalvi A, Li A, Lombardi V, Akbari O, Borok Z, Minoo P. Epithelium-specific deletion of TGF-β receptor type II protects mice from bleomycin-induced pulmonary fibrosis. J Clin Invest. 2011 Jan;121(1):277-87. doi: 10.1172/JCI42090.

16. Li FJ, Surolia R, Li H, Wang Z, Liu G, Liu RM, Mirov SB, Athar M, Thannickal VJ, Antony VB. Low-dose cadmium exposure induces peribronchiolar fibrosis through site-specific phosphorylation of vimentin. Am J Physiol Lung Cell Mol Physiol. 2017 Jul 1;313(1):L80-L91. doi: 10.1152/ajplung.00087.2017.

17. Ma J, Bishoff B, Mercer RR, Barger M, Schwegler-Berry D, Castranova V. Role of epithelial-mesenchymal transition (EMT) and fibroblast function in cerium oxide nanoparticles-induced lung fibrosis. Toxicol Appl Pharmacol. 2017 May 15;323:16-25. doi: 10.1016/j.taap.2017.03.015.

18. Osterholzer JJ, Olszewski MA, Murdock BJ, Chen GH, Erb-Downward JR, Subbotina N, Browning K, Lin Y, Morey RE, Dayrit JK, Horowitz JC, Simon RH, Sisson TH. Implicating exudate macrophages and Ly-6C(high) monocytes in CCR2-dependent lung fibrosis following gene-targeted alveolar injury. J Immunol. 2013 Apr 1;190(7):3447-57. doi: 10.4049/jimmunol.1200604.

19. Ueha S, Shand FH, Matsushima K. Cellular and molecular mechanisms of chronic inflammation-associated organ fibrosis. Front Immunol. 2012 Apr 10;3:71. doi: 10.3389/fimmu.2012.00071.

20. Wallace WA, Fitch PM, Simpson AJ, Howie SE. Inflammation-associated remodelling and fibrosis in the lung - a process and an end point. Int J Exp Pathol. 2007 Apr;88(2):103-10. doi: 10.1111/j.1365-2613.2006.00515.x.

21. Yi ES, Bedoya A, Lee H, Chin E, Saunders W, Kim SJ, Danielpour D, Remick DG, Yin S, Ulich TR. Radiation-induced lung injury in vivo: expression of transforming growth factor-beta precedes fibrosis. Inflammation. 1996 Aug;20(4):339-52. doi: 10.1007/BF01486737.

Relationship: 1629: Accumulation, Collagen leads to Pulmonary fibrosis

AOPs Referencing Relationship

AOP Name	Adjacency	Weight of Evidence	Quantitative Understanding
Latent Transforming Growth Factor beta1 activation leads to pulmonary fibrosis	adjacent	High	
Substance interaction with the pulmonary resident cell membrane components leading to pulmonary fibrosis	adjacent	High	Low

Evidence Supporting Applicability of this Relationship

Taxonomic Applicability

Term	Scientific Term	Evidence	Links
mouse	Mus musculus	High	NCBI
rat	Rattus norvegicus	High	NCBI
human	Homo sapiens	High	NCBI

Life Stage Applicability

Life Stage	Evidence
Adult	High

Key Event Relationship Description

Fibrosis by definition is the end result of a healing process. It involves a series of lung remodelling and reorganisation events leading to permanent alteration in the lung architecture and a fixed scar tissue or fibrotic lesion (Wallace WA, 2007). Excessive deposition of extracellular matrix (ECM) or collagen is the hallmark of this disease and there is ample evidence to support this KER (Fukuda 1985, Meyer 2017, Richeldi 2017, Thannickal 2004, Zisman 2005).

Evidence Supporting this KER

Biological Plausibility

By definition, pulmonary fibrosis is characterized by excessive deposition of ECM and destruction of native lung architecture (Fukuda 1985, Richeldi 2017, Thannickal 2004). Thus, the plausibility of this association is undisputed.

Empirical Evidence

Excessive ECM deposition is the defining characteristic of pulmonary fibrosis, and the evidence to support this relationship is unequivocal. (Meyer 2017, Thannickal 2004, Zisman 2005).

Reference

1. Fukuda Y, Ferrans VJ, Schoenberger CI, Rennard SI, Crystal RG. Patterns of pulmonary structural remodeling after experimental paraquat toxicity. The morphogenesis of intraalveolar fibrosis. Am J Pathol. 1985 Mar;118(3):452-75.
2. Meyer KC. Pulmonary fibrosis, part I: epidemiology, pathogenesis, and diagnosis. Expert Rev Respir Med. 2017 May;11(5):343-359. doi: 10.1080/17476348.2017.1312346.
3. Richeldi L, Collard HR, Jones MG. Idiopathic pulmonary fibrosis. Lancet. 2017 May 13;389(10082):1941-1952. doi: 10.1016/S0140-6736(17)30866-8.
4. Thannickal VJ, Toews GB, White ES, Lynch JP 3rd, Martinez FJ. Mechanisms of pulmonary fibrosis. Annu Rev Med. 2004;55:395-417. doi: 10.1146/annurev.med.55.091902.103810.
5. Wallace WA, Fitch PM, Simpson AJ, Howie SE. Inflammation-associated remodelling and fibrosis in the lung - a process and an end point. Int J Exp Pathol. 2007 Apr;88(2):103-10. doi: 10.1111/j.1365-2613.2006.00515.x.
6. Williamson JD, Sadofsky LR, Hart SP. The pathogenesis of bleomycin-induced lung injury in animals and its applicability to human idiopathic pulmonary fibrosis. Exp Lung Res. 2015 Mar;41(2):57-73. doi: 10.3109/01902148.2014.979516.
7. Zisman DA, Keane MP, Belperio JA, Strieter RM, Lynch JP 3rd. Pulmonary fibrosis. Methods Mol Med. 2005;117:3-44. doi: 10.1385/1-59259-940-0:003.